4-20-2016 12:00 AM

# Electrokinetic Enhanced Bioremediation of Soils Contaminated with Petroleum Hydrocarbons

Ikrema Abdalla Hassan
*The University of Western Ontario*

Supervisor
Ernest Ynaful
*The University of Western Ontario*

Graduate Program in Civil and Environmental Engineering
A thesis submitted in partial fulfillment of the requirements for the degree in Doctor of Philosophy

# Abstract

Contamination of soil by petroleum hydrocarbons occurs in various operations and activities including exploration, production, transportation of crude and refined oil, and improper management of refinery waste. Very low concentrations of these compounds can threaten human health and the environment. Recent studies have investigated an innovative hybrid approach that utilizes electrokinetics to enhance bioremediation of petroleum hydrocarbon pollution. Nevertheless, the electrolysis reaction byproducts create sharp pH gradient in the soil which endanger the survival of the microorganisms. Electrokinetics can result in an uneven distribution of nutrients and water in the soil. Also, energy consumption increases the overall cost of the hybrid technique and can become a major obstacle restricting wide applications of this technology insitu.

Desorption of phenanthrene resulting from hydraulic flow was compared to desorption driven by electroosmotic flow with a similar flow rate. The power required for the hydraulic flow test was compared with the consumed power in the electrokinetics test. The phenanthrene concentration in effluent samples after desorption by electroosmotic flow was found to be three to four times the concentration after desorption by hydraulic flow. The power required in the hydraulic flow test was three orders of magnitude higher than the power consumed in the electrokinetic flow test.

A novel approach, anode-cathode-compartment (ACC), was proposed to stabilize pH and distribute nutrients in soil in order to enhance electrokinetic bioremediation of soil contaminated with biodegradable compounds. The soil pH and distribution of nutrients in the electrokinetics test employing ACC configuration were examined and compared to the results from the test conducted using conventional anode-cathode (CAC) configuration. The results showed that the soil pH was stabilized during the ACC technique. The nutrients were distributed evenly and the water content in the soil was kept relatively uncharged by electrokinetics.

The ACC technique was applied to investigate electrokinetic bioremediation of soil contaminated with 2 mg phenanthrene per g soil. *Mycobacterium pallens* sp. at a

concentration of $10^8$ colony forming units per mL was used to degrade phenanthrene. Solar energy was used to generate power for the hybrid technique. The results showed bacteria was delivered inside soil in higher intensity in the test conducted with ACC technique compared to CAC test. Also, the amount of phenanthrene degraded was approximately 50% using ACC technique compared to 22% in the CAC test.

Three hundred bacterial strains were isolated from agricultural soil and characterized according to their ability to degrade diesel fuel. Forty five strains able to use diesel fuel as sole carbon and energy source were identified. Three isolates identified as *Acintobacter calcoaceticus*16, *Sphingobacterium multivorum*155, and *Sinorhizobium sp*. B53, respectively, based on their 16S rDNA gene, were selected and subjected to further investigation, including ability to grow in liquid medium at different pH, temperatures, and diesel fuel concentrations, and identification of functional genes. Electrokinetic bioremediation with ACC technique was conducted to mitigate soil contaminated with diesel fuel. A solar panel was used to generate power for electrokinetics. The tests were conducted using the novel bacterial strains AC16, SM155, and SB53. The results showed that the temperature of the soil in the test conducted with ACC was higher than the test control test. Diesel degradation in tests conducted with electrokinetic bioremediation was between 20 and 30%.

Keywords Desorption; Hydraulic flow; Electroosmotic flow; Phenanthrene; pH control; Nutrients; Bioremediation; Petroleum hydrocarbons contamination; Diesel fuel.

# Co-Authorship

This thesis has been prepared in accordance with the regulations for a manuscript format (Integrated-Article) thesis stipulated by the School of Graduate and Postdoctoral Studies at the University of Western Ontario. Dr. Ernest K. Yanful, Dr. Eltayeb Mohamedelhassan, and Dr. Ze-Chun Yuan provided supervision and guidance to the research.

1. **Title:** A review Article: Electrokinetic bioremediation current knowledge and new prospects (Chapter 2)

**Authors:** I. Hassan, E.K. Yanful, E. Mohamedelhassan, and Z-C. Yuan

This paper has been published in the journal of Advances in Microbiology. Volume 6(1): 57-75.

***Contributions*:**

**I. Hassan:** prepared the first draft of the paper

**E.K. Yanful:** reviewed and corrected the paper.

**E. Mohamedelhassan:** reviewed and corrected the paper.

**Z-C Yuan**: reviewed and corrected the paper.

2. **Title:** Sorption of Phenanthrene by Kaolin and Efficacy of Hydraulic Versus Electroosmotic Flow to Stimulate Desorption (Chapter 3)

**Authors:** I. Hassan, E. Mohamedelhassan, E.K. Yanful, and Z-C Yuan

This paper has been published in the journal of Environmental Chemical Engineering. Volume 3(4, Part A): 2301-2310.

***Contributions*:**

**I. Hassan:** designed and performed the laboratory test, analyzed and interpreted the results, and wrote the draft of the paper.

**E. Mohamedelhassan:** assisted in developing the test and the interpretation of the results and reviewed and corrected the paper.

**E.K. Yanful:** reviewed and corrected the paper.

**Z-C Yuan:** reviewed and corrected the paper.

**3. Title:** A new technique for enhancing electrokinetic bioremediation (Chapter 4)

**Authors:** I. Hassan, E. Mohamedelhassan, E.K. Yanful, and W. B. Myint

This paper has been submitted for review and publication in the journal of Environmental Geotechnics

***Contributions*:**

**I. Hassan:** designed and performed the laboratory test, analyzed and interpreted the results, and wrote the draft of the paper.

**E. Mohamedelhassan:** assisted in developing the test and the interpretation of the results and reviewed and corrected the paper.

**E.K. Yanful:** assisted in the interpretation of the results and reviewed and corrected the paper.

**W.B. Myint:** reviewed and corrected the paper.

4. **Title:** Solar power enhancement of electrokinetic bioremediation of phenanthrene (Chapter 5)

**Authors:** I. Hassan, E. Mohamedelhassan, E.K. Yanful, B. Weselowski, and Z-C Yuan

This paper has submitted for review and publication in Chemosphere journal

***Contributions*:**

**I. Hassan:** designed and performed the laboratory test, analyzed and interpreted the results, and wrote the draft of the paper.

**E. Mohamedelhassan:** assisted in developing the test and the interpretation of the results and reviewed and corrected the paper.

**E.K. Yanful:** assisted in the interpretation of the results reviewed and corrected the paper.

**B. Weselowski:** assisted in conducting the laboratory tests.

**Z-C Yuan:** reviewed and corrected the paper.

5. **Title:** Isolation and Characterization of Novel Bacteria in Agricultural Soils for Degradation of Diesel Fuel (Chapter 6)

**Authors:** I. Hassan, E. Mohamedelhassan, E.K. Yanful, B. Weselowski, and Z-C Yuan

This paper has been submitted for review and publication in the journal of Applied and Environmental Microbiology

***Contributions*:**

**I. Hassan:** designed and performed the laboratory test, analyzed and interpreted the results, and wrote the draft of the paper.

**E. Mohamedelhassan:** assisted in developing the test and the interpretation of the results and reviewed and corrected the paper.

**E.K. Yanful:** reviewed and corrected the paper.

**B. Weselowski:** assisted in conducting the laboratory tests and reviewed and corrected the paper**.**

**Z-C Yuan:** assisted in the interpretation of the results reviewed and corrected the paper.

**6. Title:** Solar powered electrokinetic bioremediation of diesel fuel contamination (Chapter 7)

**Authors:** I. Hassan, E. Mohamedelhassan, E. K. Yanful, M. Sumarah, G. Patterson, K. Wang, and Z-C. Yuan

This paper has been submitted for review and publication in the journal of Environmental Science and Technology

***Contributions*:**

**I. Hassan:** designed and performed the laboratory test, analyzed and interpreted the results, and wrote the draft of the paper.

**E. Mohamedelhassan:** assisted the interpretation of the results and reviewed and corrected the paper.

**E.K. Yanful:** assisted the interpretation of the results reviewed and corrected the paper.

**M. Sumarah:** assisted the interpretation of the results**.**

**G. Patterson:** assisted laboratory test and interpretation of the results.

**K. Wang:** assisted laboratory test and interpretation of the results **.**

**Z-C Yuan:** assisted in the interpretation of the results reviewed and corrected the paper.

**7. Title:** Complete Genome Sequence of Arthrobacter sp. LS16, Isolated from Agricultural Soils with Potential for Applications in Bioremediation (Chapter 8)

**Authors:** I. Hassan, A. Eastman, B. Weselowski, E. Mohamedelhassan, E.K. Yanful, and Z-C. Yuan

This paper has been published in ASM journal of Genome Announcements. Volume 4(1): e01586-15.

**I. Hassan:** designed and performed the laboratory test, analyzed and interpreted the results, and wrote the draft of the paper.

**A. Eastman:** assisted in designing laboratory test, analyzed and interpreted the results, and wrote the draft of the paper**.**

**B. Weselowski:** assisted in conducting the laboratory tests

**E. Mohamedelhassan:** assisted in the interpretation and reviewed and corrected the paper.

**E.K. Yanful:** assisted in the interpretation and reviewed and corrected the paper.

**Z-C Yuan:** assisted in the interpretation of the results reviewed and corrected the paper.

# Acknowledgments

I would like to express my deepest gratitude and appreciation to my supervisors Prof. Ernest Yanful and Dr. Eltayeb Mohamedelhassan, for their continuous support, advice and guidance throughout my studies. It would have been impossible to accomplish this achievement without their contributions.

Special thanks go to Dr. Ze-Chun Yuan for his incredible contributions in my research. Without his guidance this dissertation would not have been possible.

I wish to express my sincere thanks to the faculty and staff of the Department of Civil and Environmental Engineering and at Southren Crop Protection and Food Research Centre.

My thanks extend to my dear parents and my brothers and sisters for their continuous prayer to Almighty Allah to bless and give me effort to carry on to my research at best.

I would like to thank my wife for being unfailing source of spiritual power, and my children for putting up with my absentee. Without their encouragement and consistent support, it would not have been possible for me to achieve my academic goals.

# Table of Contents

**CHAPTER 3**
**SORPTION OF PHENANTHRENE BY KAOLIN AND EFFICACY OF HYDRAULIC FLOW VERSUS ELECTROOSMOTIC FLOW TO STIMULATE DESORPTION**

**CHAPTER 4**
**A NOVEL TECHNIQUE FOR pH STABILIZATION FOR ELECTROKINETIC BIOREMEDIATION**



**CHAPTER 5**
**SOLAR POWER ENHANCEMENT OF ELECTROKINETIC BIOREMEDIATION OF PHENANTHRENE**

**CHAPTER 6**
**ISOLATION AND CHARACTERIZATION OF NOVEL BACTERIA STRAINS FROM AGRICULTURAL SOILS FOR THR DEGRADATION OF DIESEL FUEL**

**CHAPTER 7**
**SOLAR POWERED ELECTROKINETIC BIOREMEDIATION OF DIESEL FUEL CONTAMINATION**



**CHAPTER 8**
**COMPLETE GENOME SEQUENCE OF *Arthrobacter* sp. LS16**

# List of Tables

# List of Figures

# CHAPTER 1
# INTRODUCTION

## 1.1 INTRODUCTION

Petroleum hydrocarbons are one of the major energy sources used around the world. However, environmental contamination by petroleum hydrocarbons has become a serious problem threatening human health and creating serious environmental problems. Crude oil drilling, petroleum extraction, and petroleum products delivery by pipelines, rail and tanker trucks inevitably cause oil spills on land. In fact, due to the large amount of accidental oil spills occurs frequently, soil or land remediation becomes more important than ever. A report by Canadian Council of Ministers of the Environment (CCME 2008) indicates that 60% of contaminated sites in Canada involves petroleum hydrocarbons. A report by the Alberta government showed that approximately 29,000 spills occurred between 1975 and 2013. The average oil spill in Alberta is two oil spills per day for the past 37 years (Young 2013). Therefore, it is urgently necessary to develop innovative and cost-effective technology for the mitigation of soils contaminated with petroleum hydrocarbons.

## 1.2 RESEARCH BACKGROUND

Over the years, various remediation methods have been implemented, with varying degrees of success, to mitigate soil contamination. Bioremediation is one of the most cost-effective remediation methods for contaminated soils (Bitchaeva et al. 1997; Chen et al. 2015). There are various bioremediation techniques, including biopile, landfarming, phytoremediation, bioslurry, and bioventing that can be used to degrade pollutants at contaminated sites. Environmental microorganisms, in particular, bacteria, are ubiquitous in nature. Indigenous bacteria have naturally evolved ability to metabolize diverse chemicals including pollutants as food source. This provides a great opportunity to utilize such bacteria in the cleanup of contaminated lands. From the biological and chemical points of view, bioremediation is the employment of indigenous bacteria present in a

contaminated environment to degrade pollutants (Bitchaeva et al. 1997; Chen et al. 2015). The main challenge facing the implementation of conventional in-situ bioremediation techniques is the difficulty of effectively and precisely delivering nutrients to indigenous bacteria, particularly in soils with low hydraulic conductivity. Due to soil heterogeneity and the diverse nature of contamination, the scientific community believes there will not be a single universal remediation method suitable for all types of soils and pollutants; instead, an effective remediation program may involve the collective implementation of two or more methods (Virkutyte et al. 2002).

Many studies have investigated the use of electrokinetics to improve the outcome of bioremediation. Electrokinetic remediation principles can be utilized to deliver nutrients to indigenous bacteria in the soil to stimulate their growth and increase their ability to degrade pollutants (Yeung and Corapcioglu 1994; Alshawabkeh 2009; Reddy and Camesells 2009). This hybrid approach has the potential to restore sites with low hydraulic permeability where conventional bioremediation techniques are deemed ineffective (Yeung et al. 1997). The combination of electrokinetic remediation technology with bioremediation may promote the removal of metal ions that are often inhibitory to bacterial activity, thereby enabling complete remediation of the soil (Chilingar et al. 1997). Unlike pressure-driven flows in which channeling of the fluid through the largest pores is inevitable, electrokinetics permits a more uniform flow distribution and a high degree of control of the direction of flow (Shapiro and Probstein 1993; Chilingar et al. 1997).

Transport phenomena associated with electrokinetics, namely, electroosmotic flow and electromigration, can also be utilized to desorb contaminant from the soil solids and subsequently increase the bioavailability of the contaminant for the bacteria. However, the development of an acidic medium near the anode and an alkaline environment near the cathode by electrolysis reactions, can create unfavorable condition for bacteria (Nyer and Suarez 2002; Luo et al. 2005; Alshawabkeh 2009). In addition, electric current and the associated increase in temperature may affect bacteria survival during the bioremediation

process. Energy consumption is also a major component of the total expenditure of electrokinetic remediation, and sometimes electricity power may not be available in remote areas. Energy consumption increases the overall cost of the bioremediation process and can become a major obstacle restricting wide field applications of this technology.

## 1.3 OBJECTIVES

The main objective of this study is to promote the use of electrokinetic bioremediation to mitigate soil contaminated with petroleum hydrocarbons. To achieve this objective, the following tasks have been undertaken:

1- Investigated the effectiveness of electroosmotic flow in desorption of a polycyclic aromatic hydrocarbon compound (phenanthrene) from contaminated soil and compare it with desorption by hydraulic flow with similar flow rate.

2- Proposed and implemented a novel technique, anode-cathode-compartment (ACC), to stabilize pH and distribute nutrients in soil. The effectiveness of the novel ACC approach in keeping soil pH and water content relatively unchanged during an electrokinetic process was evaluated. The distribution of nutrients in the soil by electrokinetics employing ACC configuration was examined and compared to distribution using conventional anode-cathode (CAC) configuration.

3- Utilized an alternative source of power for electrokinetic bioremediation. The power generated by solar panel was proposed as a sustainable solution to generate the power required for electrokinetic bioremediation to mitigate soil artificially contaminated with phenanthrene.

4- Isolated and characterized bacteria from local site capable of degrading diesel fuel. The environmental conditions that can affect the degradation process including diesel concentration, pH, and temperature were investigated.

5- Employed the isolated strains in electrokinetic bioremediation utilizing ACC technique and using solar panel to generated the power for electrokinetic in an outdoors test.

6- Completed genome sequence for *Arthrobacter* LS16 (environmental bacteria).

## 1.4 SCOPE OF THE STUDY AND OUTLINE OF THESIS

This thesis contains nine chapters. All the chapters are written in the form of technical papers except chapter 1 (Introduction) and chapter 9 (Summary, Conclusions and Recommendations for Future Research). The background information and corresponding references are directly included in each chapter.

Chapter 1 introduces the research topic, objectives and scope of the research and states the contributions of the research to electrokinetic bioremediation applications.

Chapter 2 presents literature review, discusses challenges facing electrokinetic bioremediation, identifies gap of knowledge, and summarizes the new directions.

Chapter 3 investigates sorption of phenanthrene by clay soil and shows the effects of electrokinetics in desorption of phenanthrene. The effect is evaluated by comparing desorption of phenanthrene by electroosmotic flow with desorption by hydraulic flow. The power consumption in each desorption test was computed and compare to the other test.

Chapter 4 proposes a new technique for pH stabilization during electrokinetic bioremediation. Along with the pH, the water content and the nutrients distribution in the soil specimen were determined and compared with those of the test carried out with a conventional electrode configuration.

Chapter 5 presents the use of solar panels to produce the power for electrokinetic bioremediation of phenanthrene using *Mycobacterium Pallens* strain in an outdoors test. Ambient temperatures and the temperatures in the cell were monitored and presented. Voltage generated by solar panel during the test period was monitored and presented. Also,

electric current across the cell are monitored and presented. The concentration of phenanthrene after the test was determined.

Chapter 6 discusses the isolation, characterization of diesel fuel degrading bacteria isolated from agriculture soil. Environmental conditions that can cause stress to indigenous bacteria including diesel concentration, pH, and temperature were investigated and presented.

Chapter 7 presents the application of the ACC technique in an outdoors test to remediate soil contaminated with diesel fuel. The implications of the weather (outdoors temperature) in the voltage gradient across the soil, the current through the soil, and diesel degradation were investigated. Solar panel was used to produce the power for electrokinetic bioremediation. Voltage generated by solar panel during the test period was monitored and presented. Also, electric current across the cell are monitored and presented. Diesel concentration was determined a cross the soil after the test.

Chapter 8 presents complete genome sequencing for *Arthrobacter* LS16 and discusses the potential use of the strain in bioremediation.

Chapter 9 summaries the thesis with the conclusions, and provides suggestions about further research on electrokinetic bioremediation.

## 1.5 CONTRIBUTION TO KNOWLEDGE

The research gave opportunities to:
(1) Prepare a comprehensive literature review that can benefit researches in the electrokinetics bioremediation field. Valuable information is presented and discussed.
(2) Evaluate the effectiveness of the electroosmotic flow in desorption of organic compound. The results provided important information about the possible opportunity of development of a new hybrid technique between natural attenuation and electrokinetics.

(3) Propose and implement a new technique for pH stabilization during the electrokinetic bioremediation. The new technique is suitable for field application because it does not require amendments or extra field work.

(4) Use of solar panels to generate power for electrokinetic bioremediation in a pilot test. Useful information is presented that can help in field applications of electrokinetics bioremediation.

(5) Isolate dozens of bacteria and investigate the capability of bacteria in degrading diesel fuel. Characterized selected novel isolates for diesel fuel degradation.

(6) Conduct electrokinetic bioremediation utilizing novel strains and use the solar power in an outdoors test.

(7) Complete genome sequencing for environmental bacteria (*Arthrobacter* LS16).

## 1.6 RERERENCES

Acar, Y. B. and Alshawabkeh, A. N. (1993). "Principles of electrokinetic remediation."Environmental Science & Technology, **27**(13): 2638-2647.

Alshawabkeh, A. N. (2009). "Electrokinetic soil remediation: Challenges and opportunities." Separation Science and Technology, **44**(10): 2171-2187.

Bitchaeva, O., Ronneau, C. and North Atlantic Treaty organization. Scientific affairs division. (1997). Biotechnology for waste management and site restoration : technological, educational, business, political aspects. Dordrecht ; Boston, Kluwer Academic.

CCME (2008). "Canada-wide standards for petroleum hydrocarbons in soil" Canadian council of ministers of the environment

Chen, M., Xu, P., Zeng, G., Yang, C., Huang, D. and Zhang, J. (2015). Bioremediation of soils contaminated with polycyclic aromatic hydrocarbons, petroleum, pesticides, chlorophenols and heavy metals by composting: Applications, microbes and future research needs, Biotechnol Adv. 2015 May 22. pii: S0734-9750(15)30002-1. doi: 10.1016/j.biotechadv.2015.05.003.

Chilingar, G. V., Loo, W. W., Khilyuk, L. F. and Katz, S. A. (1997). "Electrobioremediation of soils contaminated with hydrocarbons and metals: Progress report." Energy Sources, **19**(2): 129-146.

Luo, Q. S., Zhang, X. H., Wang, H. and Qian, Y. (2005). "The use of non-uniform electrokinetics to enhance in situ bioremediation of phenol-contaminated soil." Journal of Hazardous Materials, **121**(1-3): 187-194.

Nyer, E. K. and Suarez, G. (2002). "Treatment technology: In situ biodegradation is better than monitored natural attenuation." Ground Water Monitoring and Remediation, **22**(1): 30-+.

Reddy, K. R. and Cameselle, C. (2009). Electrochemical remediation technologies for polluted soils, sediments and groundwater. Hoboken, N.J., Wiley**:** xxii, 732 p.

Shapiro, A. P. and Probstein, R. F. (1993). "Removal of Contaminants from Saturated Clay by Electroosmosis." Environmental Science & Technology, **27**(2): 283-291.

Virkutyte, J. and Sillanpaa, M. (2002). "Enhanced electrokinetic remediation of copper and chromium from sand." Abstracts of Papers of the American Chemical Society, **224**: U623-U623.

Virkutyte, J., Sillanpaa, M. and Latostenmaa, P. (2002). "Electrokinetic soil remediation - critical overview." Science of the Total Environment, **289**(1-3): 97-121.

Yeung, A. T. and Corapcioglu, M. (1994). "Electrokinetic flow processes in porous media and their applications." Advances in porous media-volume 2.: 309-395.

Yeung, A. T., Hsu, C. and Menon, R. M. (1997). "Physicochemical soil-contaminant interactions during electrokinetic extraction." Journal of Hazardous Materials, **55**(1-3): 221-237.

Young, L. (2013) "Alberta oil spills: A look over 37 years." Global News.

# CHAPTER 2
# LITERATURE REVIEW[1]

## 2.1 INTRODUCTION

Globally, fossil fuels are among the most important energy sources. Despite efforts to replace fossil fuels with renewable energy sources, it is expected that the market will continue to rely on fossil fuels over the next few decades. Oil spills on land can contaminat soil and create serious environmental problems. Therefore, it is urgently necessary to develop innovative and cost-effective technology for the removal of petroleum hydrocarbons from contaminated soil. Over the years, various remediation methods have been used with varying degrees of success to mitigate soil contamination. Due to soil heterogeneity and the diverse nature of contamination, the scientific community believes that there will not be a single universal remediation method suitable for all types of soils and pollutants; instead, an effective remediation program may involve the collective implementation of two or more methods (Virkutyte et al. 2002). Bioremediation is one of the most cost-effective remediation methods for contaminated soils (Bitchaeva et al. 1997; Chen et al. 2015). There are various bioremediation techniques, including biopile, landfarming, phytoremediation, bioslurry, and bioventing that can be used to degrade pollutants at contaminated sites.

Environmental microorganisms, in particular, bacteria, are ubiquitous in nature. Indigenous bacteria have naturally evolved ability to metabolize diverse chemicals including pollutants as food source in the soil. This provides a great opportunity to utilize such bacteria in the cleanup of contaminated lands. From the biological and chemical points of view, bioremediation is the employment of indigenous bacteria present in a contaminated environment to degrade pollutants (Yeung et al 2011, Chen et al. 2015).

[1]A version of the chapter has been published in the Advances in Microbiology

The type of soil in a contaminated site usually plays an important role in the effectiveness of bioremediation. Current knowledge and advancements in microbiology, such as microbial genomics, metabolism, catalyst, microbial community or soil microbiome, and enzyme secretion can be further manipulated, designed and optimized to enhance the outcome of electrokinetic bioremediation. The main challenge facing the implementation of in-situ conventional bioremediation techniques is the difficulty of effectively and precisely delivering nutrients to indigenous bacteria, particularly in soils with low hydraulic conductivity.

Electrokinetic remediation can be defined as the application of a low level direct current (DC) between a row of positively charged electrodes (anode), and negatively charged electrodes (cathode), placed at the edges of the soil under treatment (Acar et al., 1995). The electric field incites three transport mechanisms, namely: electroosmosis, electromigration, and electrophoresis, plus an electrolysis reaction at the electrodes. Electroosmotic flow is defined as the movement of water in the soil pores from anode to cathode under an applied electrical field. Electroosmotic flow (flow rate, $q_A$ ($m^3/s$)) can be calculated using an empirical formula similar to Darcy's law of hydraulic flow rate, Casagrande (1949) :

$$q_A = k_e E\, A \tag{2.1}$$

where; $k_e$ ($m^2/s.V$) is coefficient of electroosmosis permeability, E (V/m) is the electric field intensity ($-\frac{\Delta E}{\Delta L}$) , and cross-section area, A ($m^2$).

Electromigration is the transport of ions in the pores fluid towards the oppositely charged electrode. The migrational flux ($J_m$) (the ionic movement towards the oppositely charged electrode in soil pore fluid) can be calculated by, (Acar and Alshawabkeh 1993)

$$J_m = c_j u_j \Delta(-E) \tag{2.2}$$

Where effective ion mobility, $u_j$ ($m^2$/ s·V), which is defined as the velocity of the ion in the soil under influence of a unit electric field gradient and can be evaluated by (Koryta, 1982):

$$u_j = \frac{D_j z_j F}{RT} \tau n \tag{2.3}$$

where; $D_j$($m^2$/s) is the diffusion coefficient of ion species j in dilute solution, z, is the valence of ion species j, $F$(96487 C/mol) is the Faraday's constant, $R$ (8.314 J/mol·K) is the universal gas constant, $T$ (K) is the absolute temperature, $\tau$ is the tortuosity factor, and $n$ is the porosity of the soil.

Electrophoresis is the movement of charged colloids under an applied electrical field. Electrolysis reactions produce hydrogen ions at the anode and hydroxyl ions at the cathode (Reed et al., 1996). The hydrogen ions lower the soil pH near the anode and form an acid front, while the hydroxyl ions increase the pH at the cathode vicinity generating a base front. The acid front travels from the anode to the cathode, whereas the base front moves from the cathode to the anode.

Oxidation reaction at the anode:

$$2H_2O - 4e^- \rightarrow 4H^+ + O_2 \tag{2.4}$$

Reduction reaction at the cathode:

$$2H_2O + 4e^- \rightarrow 2OH^- + H_2 \tag{2.5}$$

Electrokinetic remediation is a timely technology that can significantly enhance nutrients delivery to indigenous bacteria, thereby providing a tremendous potential for cleaning contaminated soils including fine-grained soils, which are usually difficult to cleanup using conventional methods (Yeung and Corapcioglu 1994; Alshawabkeh 2009; Reddy and Cameselle 2009). Many studies have investigated the use of electrokinetics to improve the outcome of bioremediation (Yeung et al 2011). The combination of electrochemical technology with bioremediation may promote the removal of metal ions that are often inhibitory to bacterial activity, thereby enabling complete remediation of the soil (Chilingar et al. 1997). Unlike pressure-driven flows in which channeling of the fluid through the largest pores is inevitable, electrokinetics permits a more uniform flow distribution and a high degree of control over the direction of the flow (Shapiro and Probstein 1993; DeFlaun and Condee 1997). Transport phenomena associated with electrokinetics can be utilized to effectively deliver nutrients to indigenous bacteria in the soils, and to enhance bioavailability (electroosmotic flow can enhance desorption).

Figure 2.1 shows the conceptual model where upon a release of petroleum hydrocarbon part of the contaminant evaporates and part moves through soil to contaminate subsurface. Depending on the site environmental conditions, indigenous microorganisms start to adapt and degrade contaminant. In most cases, the biodegradation rate is slow. Electrokinetics can be used to enhance the degradation rate by using the transport mechanisms associated with electrokinetics to deliver nutrients and /or to introduce new bacteria if the indigenous microorganisms are not capable of degrading the contaminant. However, the development of an acidic medium near the anode and an alkaline environment near the cathode by electrolysis reactions can create unfavorable condition for bacteria (Nyer and Suarez 2002; Luo et al. 2005; Alshawabkeh 2009).

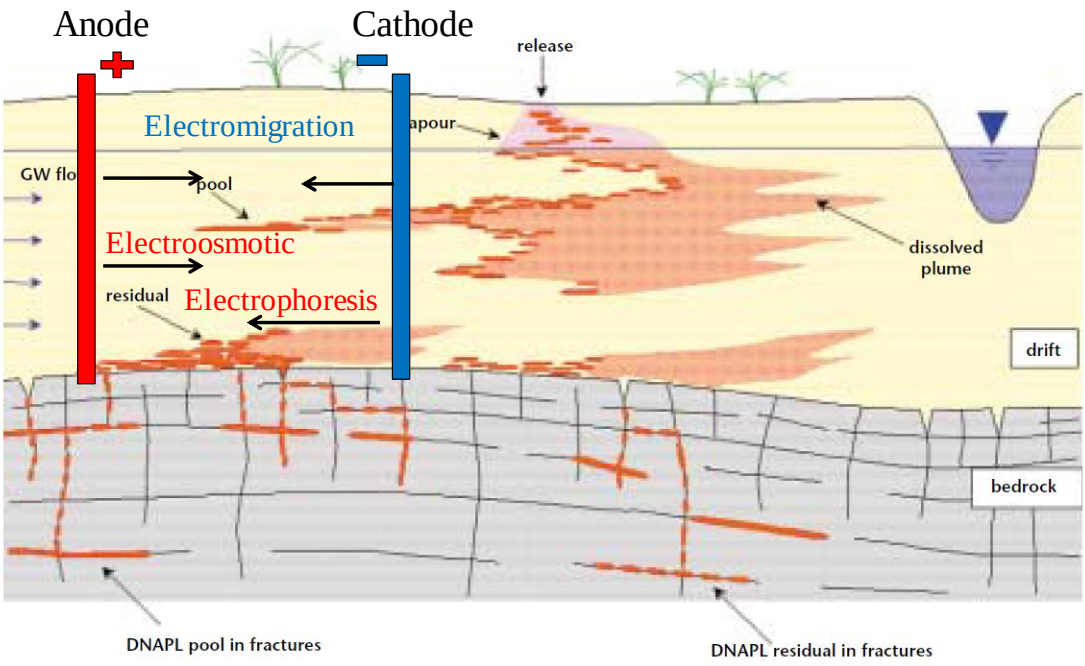


**Figure 2. 1 Conceptual model**

In addition, electric current and the associated increase in temperature may affect the bacteria survival during the bioremediation process. Energy consumption is also a major component of the total expenditure of electrokinetic remediation, and sometimes electricity power may not be available in remote areas. Energy consumption increases the overall cost of the bioremediation process and can become a major obstacle restricting wide field applications of this technology. This paper presents the current knowledge, discusses the major challenges facing field applications of electrokinetic bioremediation, identifies gaps in knowledge, and proposes key research frontiers and areas that future research needs to address. Electrokinetic bioremediation processes can be divided into two main aspects:

• Microorganism related factors such as the existence of nutrients, and the microorganisms' capability of surviving, persisting, and degrading the contaminant.

• Electrokinetic processes; influence of electrokinetic processes include electrolysis reactions, electric current, change in temperature, power for electrokinetics, the availability of power lines near the contamination sites and the cost of electricity. In the following sections, each of the above-mentioned categories will be discussed.

## 2.2 MICROORGANISMS RELATED FACTORS

There are several aspects concerning bacteria or microbes in enhancing the outcome of electrokinetics bioremediation through prolonging the survival of the microbes in soil, or improving bacterial viability and persistence in contaminated soil. This can be divided into two main factors: the soil environment and the characteristics of indigenous bacteria. Survival and persistence of bacteria in the soil environment is affected by changes in soil pH, nutrients, electron acceptors, osmotic stress, temperature (cold or hot weather), UV exposure and chemicals (Inglis and Sagripanti 2006; Locatelli et al. 2013). In addition to soil environment, the characteristics of the indigenous bacteria play a significant role in their existence, for example, some bacteria form biofilms which protects themselves from external stresses (Flemming et al. 2011; Malik et al. 2012). Another mechanism for bacteria to survive is to produce spores (Maldonado and Quintana 2015). In the event of severe weather and nutrient deprivation, bacteria will die eventually producing endospores which have a very hard shell and protect them (McKenney et al. 2013). Typically, under extremely poor living conditions, endspores are in a state of dormancy (sleeping condition); once the environmental conditions improve, the spore will germinate and outgrow (Abel-Santos 2012). There are several strategies that can be explored to manipulate microbes to augment and boost bioremediation as discussed below.

1) Exploring the indigenous bacteria metabolic pathways and using genetic engineering to change or rewire bacterial metabolic pathways to strengthen microorganisms' ability for bioremediation (Qin et al. 2015; Sah et al. 2015). Also, modifying bacterial genes and

regulatory networks to make them tougher to survive and tolerate high contaminant concentration in soils (Kang and Chang 2012).

2) Enhancing bioremediation using a commercially available enzyme which is currently very expensive, but the expected reduction in enzyme prices as the technology continues to improve can significantly reduce the initial cost (McErlean et al. 2006; Karigar and Rao 2011). At some contaminated sites, heavy metals and other chemicals present in soil may denature enzymes which are essentially proteins. Therefore, it will be impractical to use the enzyme directly in bioremediation because such enzyme will be inactivated in the actual soil environment and will not last long. However, microbial genetics can be used to clone, introduce and overexpress exogenous gene or gene clusters in a host bacterial cell so that the bacteria will gain extra ability to continuously produce the enzyme required for bioremediation. However, the enzyme expressed in bacteria has to be delivered or secreted by the bacteria to the environment in order to degrade the contaminant (Brenner et al. 2008). A recent study showed that the use of genetically modified bacterial secretion system can enhance the bioremediation (Schneewind and Missiakas 2012).

3) Exploring metagenomics to enhance electrokinetic bioremediation (Ray et al. 2014). Microbes are a rich source of enzymes and products such as antibiotics. Nevertheless, only less than 5% microbes in nature are culturable and studied so far. Most of these microbes are not culturable in laboratories. Scientists and researchers can harvest the total genomic DNA from soil samples, then chip down the total soil DNA into smaller pieces, and clone it into a vector to make a library. Such a library is called 3D metagenomics DNA library. The cloned library can be introduced into a host bacterium. If such a DNA library contains useful genes or gene clusters that express enzyme capable of degrading contaminants, host bacterium will become more powerful in bioremediation (Yergeau et al. 2012).

4) Characterizing the bacterial metabolism well prior to application for bioremediation. One issue limiting bioremediation is the bacterial production of secondary metabolites that can be more toxic or harmful than the original source contaminants. If we understand bacterial metabolism and the underlying regulatory pathways well, we can change and rewire its metabolism to make them produce less or no toxic products. This area needs to be investigated using the available genetic engineering to reduce the undesired metabolites and enhance the bioremediation outcome.

5) Investigating bacterial activity at the community level, i.e., microbiomes, at contaminated sites. Bacteria rely on some nutrients to enhance their ability at degrading contaminants. Some nutrients or chemical compounds stimulate bacterial growth or promote the growth of bacteria cocktails and survive better at the community level. Bacteria consortia at environmental sites communicate and coordinate behaviors and functionalities at community level using chemicals such as acyl homoserine lactones (AHLs), which is also described as bacterial quorum sensing (QS). QS is well studied for bacterial pathogens as QS regulate bacterial genes and function at the community level so that bacteria collectively act or infect host together, so QS coordinates infection. In addition, bacterial QS can be interfered by chemicals produced by host organisms or already available in nature (Miller and Bassler 2001; Rutherford and Bassler 2012)(Qin et al. 2015; Sah et al. 2015). In nature, QS may help bacteria for better and enhanced bioremediation. However, very few studies have investigated the role of QS in bioremediation (Huang et al. 2013).

6) Isolating and identifying new bacterial strains from nature with enhanced bioremediation abilities, which are resistant to soil and environmental stress conditions and very efficient in bioremediation. The limitation for such isolation is that sometimes these isolates cannot grow in synthetic medium in the laboratory. Therefore, modified medium recipe should be used to allow such bacteria to grow. However, it is really a low chance event, as it is not known which nutrients and components are required to support the growth of such bacteria.

Recently, the authors have isolated dozens of bacterial strains from soil and characterized them according to their ability to degrade diesel efficiently. Three strains have been selected and subjected to further investigation, including identifying functional genes, the ability to grow at different temperatures and pH. This area should be the focus of future research to meet the challenge of bioremediation. In addition, diversifying the samples to isolate such bacteria, i.e., not just focusing on soil, but taking, for instance, samples from the bottom of the sea, forest, hot spring water, or oil field or oil refinery plant may lead to the discovery of novel strains.

## 2.3 BIOSTIMULATION AND BIOAUGMENTATION

Generally speaking, there are three treatment strategies employed for in situ bioremediation: a) natural bioattenuation where the contaminant is transformed to a lesser harmful product, b) biostimulation in which the biodegradation is accelerated by the addition of nutrients, water, electron acceptors or donors, and c) bioaugmentation, which involves the addition of genetically engineered microorganisms or microorganisms with enhanced degradation capabilities to the contaminated zone (Madsen 1991). In the following sections the implementation of electrokinetics in biostimulation and bioaugmentation is discussed.

### 2.3.1 Biostimulation

As bioremediation uses microorganisms to degrade pollutants to harmless products, the success of the technique depends on the growth and reproduction of bacteria. Nutrients and often oxygen are necessary to stimulate the growth and metabolisms of microorganisms. Electrokinetics transports and controls the direction of ion movement inside soil (Yeung 2011). Therefore, when combined with bioremediation, electrokinetics can deliver nutrients to indigenous bacteria in the soil and increase mixing between bacteria and contaminants. Table 2.1 shows some studies that investigated the delivery of nutrients using electrokinetics. The use of electrokinetics for nutrients delivered under controlled pH

conditions was investigated (Kim et al. 2005a). The results showed higher contaminant removal when a polarity exchange technique (bidirectional) is used to deliver the nutrients compared with one direction electric fields (conventional). Under uncontrolled pH environments, the feasibility of effectively transporting two common microorganism nutrients (nitrate and ammonium) by electrokinetics was demonstrated (Schmidt et al. 2007). The results showed that a high amount of nitrate was successfully transported to the anode compared with the ammonium transported to the cathode. The use of the exchange polarity technique to controlled pH resulted in an even distribution of nutrients in the soil compared with one direction electric fields (Xu et al. 2010). The results from electrokinetic bioremediation studies have shown that electrokinetics is successful in delivering nutrients to indigenous bacteria. However, excessive amounts of nutrients in soil exploit the growth and increase the intensity of microorganisms and consequently result in clogging the soil pores causing biofouling (Kim and Han 2003). Therefore, it is important to study and carefully plan for the addition of nutrients. A recent study explored the possibility of providing oxygen to polluted soils by electrokinetics for aerobic bioremediation treatments of the soils (Ramirez et al. 2014). The transported oxygen was generated by electrolysis reaction of water at the anode (see Equation (2.1)). The results showed that oxygen transport occurred in the silty and sandy soils obtaining high dissolved oxygen concentrations between 4 and 9 mg/L which are useful for aerobic biodegradation processes, while transport was not possible in the clay soil.

**Table 2.1** Electrokinetic injections of nutrients

| Soil | Voltage/ current | Nutrient concentration | Highlights/Main outcome | Reference |
|---|---|---|---|---|
| Clay loam | 1 V/cm | 2 g/L $NH_4NO_3$ | Nitrate transport rate 19 cm/d/v | (Xu et al. 2010) |
| | | 2 g/L $KH_2PO_4$ | phosphate results is not presented | |
| Coarse sand | 0.25 V/cm | 1 g/L $NaNO_3$ | Nitrate transported 0.6 cm/h | (Tiehm et al. 2010) |
| Clayey silt | 0.5 V/cm | 2 g/L $NH_4NO_3$ | Nitrate transport rate 5 cm/d/v | (Schmidt et al. 2007) |
| | | 5g/L $KH_2PO_4$ | Phosphate was not transported | |
| Lean clay | 0.85 V/cm | 3.2g/L $NH_4OH$ | 400 mg/kg $NH_4OH$ | (Kim and Han 2003) |
| | | 0.48 $H_2SO_4$ | 200 mg/kg $H_2SO_4$ | |
| Fine sand | 15 $\mu A/cm^2$ | | Nitrate transported 250 mg/L | (Acar et al. 1997) |
| Kaolinite | 123 $\mu A/cm^2$ | | Nitrate transported 250 mg/L | (Acar et al. 1997) |
| Sandy-clay | 0.5 V/cm | 1 g/L $NH_4NO_3$ | Nitrate transported 1.5 mg/kg | (Elektorowicz and Boeva 1996) |
| Kaolinite | 0.4 V/cm | 50 mg/L $NO_3$-N | Nitrate transported | (Segall and Bruell 1992) |
| | | 50 mg/L $PO_4$-P | Phosphorus was not transported | |

### 2.3.2 Bioaugmentation

Introducing new strains of bacteria (bioaugmentation) with superior degradation capabilities can enhance bioremediation outcome. Many researchers have used phenomena associated with electrokinetics to deliver microorganism to contaminated soil (DeFlaun and Condee 1997). For instance, the transport of bacteria in clay and sand by electroosmotic flow and electrophoresis was investigated (Wick et al. 2004). The results showed that 20% of bacteria were transported by electrophoresis. A more recent study showed that microorganisms can be transported by electrokinetics in sand via electrophoresis and the microorganisms remained active and viable after the transport process (Maillacheruvu and Chinchoud 2011). Another study showed that by adding bacteria in the anode and cathode compartment bacteria was transported via electroosmotic flow in clay soil (Mao et al. 2012). However, in general, bioaugmentation studies have not been successful. The lack of success has been attributed to the formation of antibiotics by indigenous bacteria, predation and adaptability of new bacteria to the contaminated soil (Goldstein et al. 1985; Zaidi et al. 1989). For instance, *Pseudomonas* sp. LB400 bacteria were found to be capable of degrading 4-chlorobiphenyl in sterilized soil, but a decrease in their viability was observed when non sterilized soil was used (Blasco et al. 1995; Blasco et al. 1997). Many studies have suggested the use of microbial consortia to mitigate contaminated sites. It is generally known that microbial species do compete one another. Recent reports in microbiology have highlighted the need for an innovative technology that can be used to get rid of or reintroduce certain strains of bacteria (Brenner et al. 2008). In electrokinetic bioremediation, the application of electric current disrupts bacteria membrane by changing the orientation of membrane lipids (Groves et al. 1997). Killing unfavorable bacteria required high pulsed voltages (25 kV cm−1 and 40 - 100 μs pulse duration) and this is related to neither interaction with the products of electrolysis nor with temperature changes but rather a direct effect of the current on the cells (Sale and Hamilton 1967). The effect of direct current application on different strains of bacteria in liquid and slurries has been investigated (Sale and Hamilton 1967; Mizuno and Hori 1988; Jackman et al. 1999). Therefore, electrokinetics has the potential to be that tool. There is a need for further research to be conducted to develop this area.

Recent advancement in biotechnology and molecular tools has enhanced the production and recovery of enzymes. Many authors have suggested the use of enzyme (Biocatalysis) in bioremediation instead of microorganism (Alcalde et al. 2007; Peixoto et al. 2011). The use of enzyme in bioaugmentation can result in avoiding the competition between indigenous bacteria and the new strains. The advantages of using enzymes in bioaugmentation are enzymes can simplify the process (they do not generate by-products), it is easier to work with enzymes than with the whole microorganism, enzyme capabilities can be improved at the production stage. However, the cost of enzyme production is high. Also there is an issue about shelf life and stability of the enzymes. The use of enzymes has not been investigated in electrokinetic bioremediation (Peixoto et al. 2011). Enzyme delivery via electrokinetics transport mechanisms is a new research area and there is a need to investigate the efficiency of electrokinetic in delivery of enzymes to contaminated zones.

## 2.4 ELECTROKINETIC PROCESSES

Phenomena associated with the application of electrokinetics (electrolysis reactions, electromigration, electroosmotic flow, electrophoresis) can alter the physiochemical properties of the soil matrix and pore fluid (Alshawabkeh 2009; Kim et al. 2010). These changes, including the development of pH and voltage gradients, formation of zones with different current density, variation of electric current and voltage gradient, and an increase in temperature of the soil, can play a significant role in the outcome of the electrokinetic bioremediation processes. Electroosmotic flow can enhance bioavailability by stimulating desorption of contaminants from the soil (Shi 2008a).

### 2.4.1 pH gradient

The electrolysis reactions of water occur at the electrodes in an electrokinetic process and result in oxidation reduction reactions. Oxidation takes place at the anode, which generates

hydrogen ions (acid front $H^+$) and liberates oxygen gas. On the other hand, reduction occurs at the cathode, which produces hydroxyl ions (base front $OH^-$) and disperses hydrogen gas. The acid front (i.e. $H^+$) moves towards the cathode by electroosmotic flow, diffusion, and electromigration and lowers the pH of the soil along its path. The hydroxide ions form the base front travel towards the anode by electromigration and diffusion and elevate the pH of the soil in the vicinity of the cathode. The drastic change in soil pH (acidic near the anode and alkaline near the cathode) plays a very important role in the outcome of the removal of heavy metals and other contaminants from soil by electrokinetic remediation and in the degradation of contaminants by an electrokinetic bioremediation process. Most of the heavy metals are soluble at a pH less than 7 and precipitate at a pH higher than 7. Typically, the soil pH in electrokinetic remediation near the anode is in the range 2 - 3.5 and near the cathode between 8 - 11 (Page and Page 2002). For example, copper and cobalt are found in solutions in the pH range between 4 and 6 while they precipitate (for example, as insoluble hydroxides) at pH higher than 7. Thus, the decrease in soil pH (near the anode) is favorable for heavy metal dissolution and hence removal. However, the increase in soil pH can cause precipitation of heavy metals and render the technique ineffective in removing contaminants in the vicinity of the cathode. On the other hand, in electrokinetic bioremediation there is an optimum pH at which the capability of bacteria in degradation of a particular contaminant is optimum. Most bacteria can live in a pH range between 6 and 8. Special strains of bacteria can tolerate extreme pH values. Bacteria can adapt the cytoplasm pH to the surrounding environment by controlling the exchange of H+ (internal proton concentration) through the cell wall. However, the abrupt change in pH gradient across cell membrane has an adverse effect on growth and metabolism of bacteria (Cotter and Hill 2003; Padan et al. 2005; Krulwich et al. 2011)

To address the challenges caused by the pH gradient, researchers have previously implemented conventional and innovative techniques to control pH during electrokinetic remediation. The conventional techniques include the use of an ion selective membrane such as cation-exchange membrane, which prevents the transport of the hydroxide ions from the cathode to the soil as shown in Figure 2.1 (Hansen et al. 1997), continuous

changing/removing of the solution in the electrode compartments (Niqui-Arroyo et al. 2006), addition of chemical conditioning agents such as ethylenediaminetetraacetic (EDTA) (Reed et al. 1995; Wong et al. 1997), acetic acid (Acar and Alshawabkeh 1993), and nitric acid (Denisov et al. 1996). Innovative techniques on the other hand include a stepwise moving anode (Chen et al. 2006; Rajic et al. 2012), polarity exchange (Luo et al. 2005; Pazos et al. 2006), circulation of an electrolyte (anolyte and catholyte) solution in the electrode compartments (see Figure 2.2) (Kim and Han 2003; Mao et al. 2012; Wu et al. 2012), and the two anodes technique (TAT) (see Figure 2.3) which has investigated the control of the advancement of the acid and the base fronts (Hassan et al. 2015a). The soil type (mostly buffer capacity) and the presence of anions which contribute to the buffer capacity (besides carbonates, hydrocarbonates and hydroxides): borates, phosphates, silicates and organic acids anions influence the pH changes and should be taken into account when choosing the right pH-regulation technique (Rajic et al. 2012).

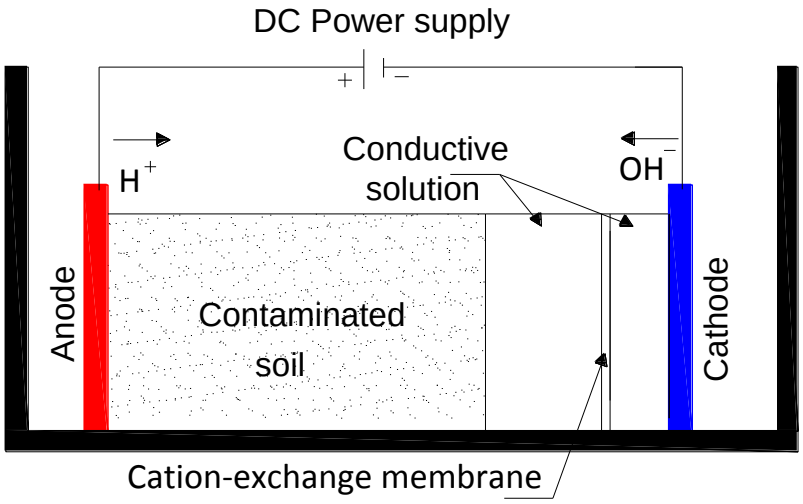


**Figure 2. 2** Electrokinetic remediation with ion selective membrane (after Li and Neretniek, 1999)

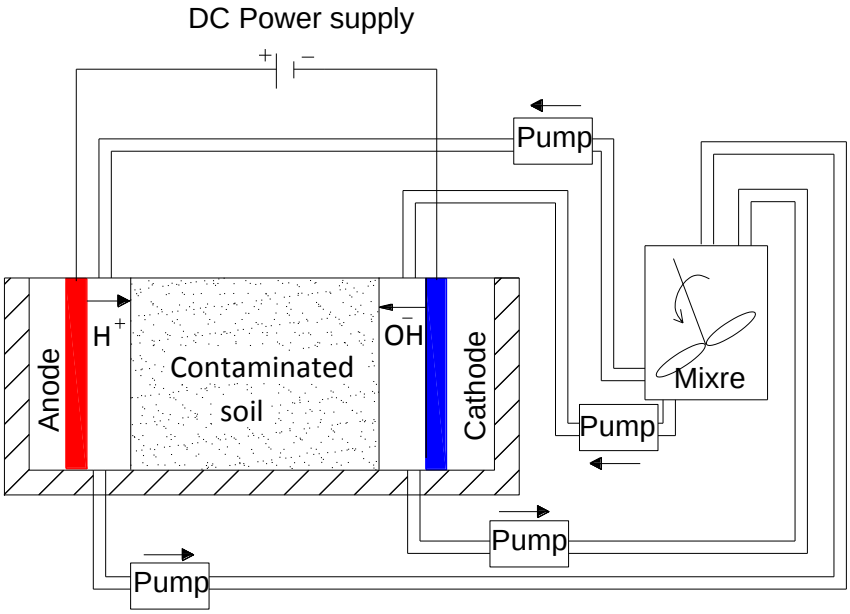


**Figure 2. 3** Electrokinetic remediation cell with electrolyte solution circulation technique (after Wu et al. 2012)

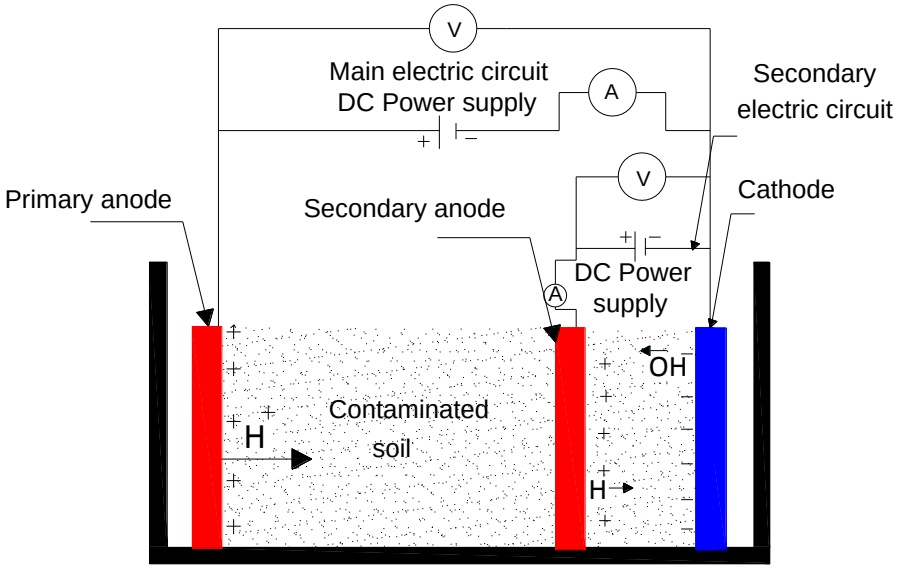


**Figure 2. 4** Two anode technique (TAT) (after Hassan et al. 2015a)

Many researchers have investigated the effect of pH on electrokinetic bioremediation using conventional methods. For instance, the use of electrokinetic bioremediation to mitigate creosote-polluted clay soil was investigated (Niqui-Arroyo et al. 2006). In this study, the soil pH was kept relatively unchanged by continuously changing/removing the solution in the electrode compartments. This technique not only involves additional cost but might not be suitable for field applications. Moreover, the practice of replacing the electrolyte solution produces a polluted solution that requires treatment before being released into the environment. The addition of a chemical conditioning agent is not favorable because it generates by-products that may be toxic and harmful. Furthermore, the use of acid to control pH can acidify the contaminated soil, which is very difficult (if not impossible) to restore to its previous condition (Hassan and Mohamedelhassan 2014). The innovative techniques that have been proposed to overcome the negative impact of the pH gradient are either costly or not suitable for electrokinetic bioremediation in field applications. The step moving anode involves extra field work, as the anode should be advanced (relocated several times) towards the cathode during the process. Also, the technique is only suitable for electrokinetic remediation of heavy metals because the advancement of the anode creates an acidic environment all through the contaminated soil ($pH \leq 5$) which results in desorption of heavy metals from soil but is not recommended for bioremediation. Likewise, the two anode technique is not suitable for electrokinetic bioremediation.

In electrokinetic bioremediation, the low pH has a detrimental effect on bacteria. The polarity exchange technique relies mainly on the preciseness of pH measurement during the treatment and the current intensity. The soil pH and water content of phenol-contaminated soil were controlled using the polarity reversal technique (Luo et al. 2005). This technique can be suitable for electrokinetic bioremediation, however, continuous pH monitoring is required which is challenging and increases the overall cost of the process. Kim and Han (Kim and Han 2003) implemented the circulation of electrolyte solution as shown in Figure 2.2. This technique can be effective and suitable for electrokinetic bioremediation; however, the field application can be costly because of the need for continuous pumping operation. Therefore, the circulation of electrolyte solution (anolyte

and catholyte) in the electrode compartments is a troublesome technique for field application. In electrokinetic bioremediation applications, the control of soil pH is crucial for successful treatment. Methods presented in recent literature show great advancements in the effort to control pH during electrokinetics application. However, more research is needed to improve existing methods and to develop new or innovative techniques to control the pH during electrokinetic bioremediation application, in particular.

The authors have investigated a new technique to stabilize pH and to distribute nutrients uniformly during electrokinetic bioremediation. The new technique uses an anode and a cathode at the same water compartment. The hypothesis is that the coexistence of an anode and a cathode in the same water compartment will result in the hydrogen ions generated at the anode neutralizing the hydroxyl ions produced at the cathode and thereby forming water. In accordance with Equations (2.4) and (2.5), the proposed novel configuration is assumed to generate equivalent numbers of hydrogen ions and hydroxide ions with all the ions reacting to form water. Therefore, the new technique overcomes the shortcomings of other pH stabilization techniques by stabilizing the pH without the need for pumping or amendments while maintaining electroosmotic and electromigration movement in one direction.

### 2.4.2 Electric current density and voltage gradient

In general, the application of electric current through specific medium can cause direct and/or indirect effects on existing microorganisms. An example of direct effect is a rupture in the cell membrane due to a voltage gradient greater than 0.4 V across the cell wall (Mizuno and Hori 1988; Sperelakis 1995). Indirect effects include the generation of by-products that are harmful to the microorganisms such as corrosion products introduced by metallic electrodes, which dissolve due to electrolysis reactions (Roberge 2008). Much of the research has been conducted to investigate the effect of electric current on viability of bacteria for disinfection purposes and in the food industry (Katsuki et al. 2000; Schoenbach

et al. 2000). For instance, the use of high pulse DC current to kill yeast and bacteria investigated (Sale and Hamilton 1967). It was concluded that DC current, and not temperature or products of electrolysis, caused the death/inactivation of living organisms. Over the last decade, researchers have investigated the influence of electric current on electrokinetic bioremediation treatment.

Table 2.2 summarizes the results of studies that investigated the effects of electrical current on survival/transport of microorganisms during electrokinetic remediation. The effect of fixed applied electric current on different intensities of bacteria suspended on liquid and soil slurry was investigated (Jackman et al. 1999). It was found that electric current had a detrimental effect on low cell densities, however, high cell densities survived despite the applied electric field intensities and the controlled current environment. The use of electrokinetic bioremediation to remove pentadecane from a kaolinite soil showed that the optimum pollutant removal was achieved using an intermediate electric current density of 0.63 $mA/cm^2$ compared with the higher and lower current densities of 3.13 and 1.88 $mA/cm^2$ , respectively (Kim et al 2005). Another study showed that using optimum electric field in electrokinetic bioremediation not only removes pollutants but also retains the most microorganisms (Wan et al. 2011). The results showed 37% of total petroleum hydrocarbons were removed from the area near the anode with an optimum electric field of 2 V/cm.

**Table 2.2** Effects of electrical current

| Medium | Current intensity or voltage gradient used | Highlights/Main outcome | Reference |
|---|---|---|---|
| Liquid | 20 mA/cm$^2$ | High cell density survive | (Jackman et al. 1999) |
| Soil (kaolinite) | 0.31,0.63,1.88,3.13 mA/cm$^2$ | Optimum current 0.63 mA/cm$^2$ | (Kim et al. 2005a) |
| Liquid | 0.04,4,8,12,14 mA/cm$^2$ | Optimum electric field density 100 kJ/L | (Tiehm et al. 2009) |
| Liquid | 10.2 mA/cm$^2$ | No effect on cell activity | (Shi et al. 2008b) |
| Glass beads | 1.8 mA/cm$^2$ | Low level DC has no effect of cell viability | (Shi et al. 2008a) |
| Clay and silt | 0.314 mA/cm$^2$ | pH changes near the anode is major factor affecting the microbial communities | (Lear et al. 2004) |
| Soil | 1.0 mA/cm$^2$ | no negative effect on indigenes bacteria | (Wick et al. 2010) |
| hide-soak liquors | 2 A | Deactivated bacteria | (Birbir et al. 2008) |
| Activated sludge | 0.5- 1.5 mA/cm$^2$ | pH or direct contact caused bacterial inhibition | (Li et al. 2001) |
| Fine grained soil | 2 V/cm | The population of bacteria increased near the cathode | (Wan et al. 2011) |
| Sandy loam | 0.46 v/cm | Rate of transport is 0.11 cm/h<br>Microorganisms are active after the transport process | (Maillacheruvu and Chinchoud 2011) |
| Tap water | 0.28-1.4 v/cm | Optimum voltage intensity is between 0.28 and 1.4 v/cm | (Alshawabkeh et al. 2004) |

In a recent study, it was observed that microorganisms were capable of degrading organic matter after being transported under an electric field (Maillacheruvu and Chinchoud 2011). Very few studies investigated the effect of the electrode materials on the electrokinetic bioremediation. For instance, the results of an experimental study (Tiehm et al. 2009) showed that the electrochemical reactions between the electrode material and the soil medium products significantly affected the activities of the microbial community. Although that study highlighted the importance of the electrode material in the process, the possible chemical reactions and the by-products were not detected. That study also concluded that the combined effect of applied current intensity and duration is the crucial factor affecting living organisms rather than the current intensity alone. The effect of electrode materials in electrokinetic applications using different materials for anode and cathode including steel, copper, and carbon with different combination (anode-cathode) was investigate (Mohamedelhassan and Shang 2001). The results showed that using a particular material as anode and another as cathode or vice versa can result in considerable differences in the electrode performance (efficiency). Therefore, there is a real need for research to be conducted to address the effect of electrode materials in electrokinetic bioremediation.

### 2.4.3 Temperature

Microorganisms can live in a wide range of temperature (thermophile 45˚C to 120˚C, mesophile 20˚C to 45˚C, or psychrophile −20˚C to 10˚C). However, microorganisms growth rate in general increases with increase in temperature and the microorganism optimum degradation capability occurs at temperature between 25˚C and 40˚C (Nyer and Suarez 2002; Van Hamme et al. 2003). Many researchers have reported an increase in temperature during electrokinetic processes. For example, a study showed that soil temperature increased between 5˚C and 20˚C with the maximum increase reported in the soil near the anode (Mohamedelhassan and Shang 2008). An increase in temperature up to 90$^{o}$C during field application of electrokinetic remediation of trichloroethylene was reported (Ho et al. 1999a; Ho et al. 1999b). Although, it is well documented that

electrokinetic processes can generate heat and elevate the temperature of the soil in the treatment zone, however, the effect of temperature on electrokinetic bioremediation has not been fully investigated. Investigators tend to attribute the increase in biodegradation to nutrient delivery by electrokinetic (Kim et al. 2010a). Few reports have discussed the effect of temperature increase during electrokinetic bioremediation. For instance, the delivery of nutrients and oxygen to microorganisms in the soil was investigated (Suni et al. 2007). It was suggested that the increase in temperature associated with the applied electric field has a positive impact on microbial activities. On the other hand, continuous application of electrokinetic remediation using high applied voltage for long duration can elevate the temperature inside the soil being treated. The high temperature has an adverse effect on the viability of microorganisms. Intermittent current was used to avoid the adverse impact of the high temperature (Ho et al. 1999b). The use of current intermittence not only controls the increase in temperature, but also enhances the outcome of the electrokinetic application (Mohamedelhassan and Shang 2001).

### 2.4.4 Bioavailability

Bioavailability can be defined as the quantity of contaminants present in soil pore fluid at a given time with respect to metabolism of the soil biota (Wick et al. 2007). Bioavailability is also sometimes defined as the fraction of contaminants that is ready to be consumed by microorganisms (Semple et al. 2004). Upon the release of pollutants into a soil matrix, depending on environmental conditions, sorption of the pollutants by the soil matrix takes place. In the subsurface, the only mechanisms for desorption of contaminants from the soil matrix is back-diffusion. Therefore, desorption is the major factor controlling the bioavailability of contaminants. There are two schools of thought on bioavailability. Some researchers believe that bacteria can degrade a contaminant, even if it is attached to the soil matrix (Singh et al. 2003). Other researchers consider desorption of contaminants from soil as a prerequisite (contaminants to be desorbed first from the soil matrix before bacteria can degrade it) (Harms and Zehnder 1995; Shelton and Doherty 1997). Electroosmotic flow creates flow within the double layer, therefore, can enhance desorption of contaminants (Shi et al. 2008a). Recently, the authors have investigated the effectiveness of the

electroosmotic flow compared to hydraulic flow in stimulating desorption of organic contaminants (Hassan et al. 2015b). It was found that the concentration of the contaminant in the effluent after desorption tests using electroosmotic flow is three to four times higher than the concentration in the hydraulic flow tests. Also, the power consumption during the hydraulic flow tests was three orders of magnitude higher than the power consumed during the electroosmotic flow tests

### 2.4.5 Available power sources for electrokinetics

Energy consumption is a major component of the total cost of electrokinetic remediation. High energy consumption increases the overall cost of the remediation process and can become a major obstacle restricting wide field applications of this technology. Although, the cost of energy represents 30% of the total cost of an electrokinetic remediation process (Alshawabkeh et al. 1999), very few research projects have addressed the high energy cost (Yuan et al. 2009). Solar energy, a renewable energy source with no adverse environmental impact, is a novel power option for electrokinetics and can be economically viable, in particular, for remote sites without active power lines (Yuan et al. 2009).

In the last decade solar energy has gained the attention of scientists and the general public, leading to a multitude of beneficial applications. According to Solar Buzz report (SolarBuzz 2010), more than 70% of the photovoltaic (PV) resources have been installed in northern countries including Germany, Japan, USA, and Canada. More importantly, it has been observed that more electricity can be generated by PV panels during the wintertime because of sunlight reflection off snow, the albedo effect (Andrews et al. 2013). Although, solar cells can be an excellent candidate for power supply in electrokinetics, there is little or no published research that has investigated their use in electrokinetic bioremediation or the effect of the night-time off power cycle on the microorganisms. The use of solar cells as a source of power can reduce the electricity transmission expenses and eliminate power losses in the transmission lines. Furthermore, the power produced by solar

cells is environmentally friendly. Also, solar panels produce DC electric field that is usable in electrokinetic applications without alteration (i.e. without the need for DC transformer). The expected reduction in solar cell prices as the technology continues to improve can significantly reduce the initial cost of a solar power system. The power generated by solar cell panel depends on the time of day and the weather conditions. This can cause fluctuations in the power supply during the day and intervals of zero voltage at night, especially in the northern latitudes with little day light during winter.

The application of an electric field in electrokinetics results in ion orientation in the double layer against the electric current, which reduces the efficiency of the remediation process. Interruption of the electric field allows the restoration of original ions orientation, which can enhance the remediation process. It is suggested that the fluctuation of the power generated from solar panels during the day and the diminishment of electric field during the night would stimulate the remediation process. Many studies have proven that current intermittence is beneficial to the outcome of an electrokinetic process (Mohamedelhassan and Shang 2001; Hansen and Rojo 2007). In a previous study, the authors have used solar panels to generate power for the electrokinetic remediation of clay soil contaminated with copper (Hassan and Mohamedelhasan 2012; Hassan et al. 2015a). Three solar panels were used to generate 41, 27 and 13.5 V. The results showed that solar panels can be used successfully to produce enough power for electrokinetic remediation of heavy metal-contaminated soils. In recent work, the authors used solar panels to generate power for the electrokinetic bioremediation of clay soil contaminated with phenanthrene. The results showed that solar panels can be used successfully to produce enough power for electrokinetic bioremediation of petroleum hydrocarbons. Moreover, the intervals of zero voltage at night can decrease soil temperature in field applications, which is a benefit.

## 2.5 FIELD APPLICATIONS

Electrokinetic remediation has been in use for a while to clean up sites contaminated with heavy metals as well as for ground improvement in laboratory and field scale. For instance, previous study showed the effectiveness of electrokinetic remediation, field application, in the removal of copper from a contaminated site, the average removal was 85% of the initial copper (Chung 2009). Many researchers have conducted laboratory tests using electrokinetic bioremediation (Table 2.3). On the other hand, field applications are very limited. For example, Lasagna technique was used to remove trichloroethylene (TCE) from a contaminated site, in Paducah, Kentucky (Ho et al. 1999b). At this site, electrokinetics was successful in cleaning up TCE form clay soil with removal between 95% and 99%. However, very few field studies have been conducted in electrokinetic bioremediation. The first field application of electrokinetic bioremediation was conducted in Denmark in 2012 to degrade perchloroethylene (PCE) from clay soil. The dimensions of the site investigated were 1.8 × 3 × 2.7 to 7.2 m in width, length and depth, respectively. The results showed that electrokinetics can be used successfully to deliver microorganisms capable of degrading perchloroethylene (PCE).

**Table 2.3** Laboratory tests using different contaminants

| Medium | Contaminant | Contaminant concentration | Highlights/Main outcome | Reference |
|---|---|---|---|---|
| Fine soil (from a contaminated site) | Petroleum hydrocarbon | 78600 mg/kg | 37% reduction | (Wan et al. 2011) |
| Sand | Diesel | 6800 mg/kg | 60% reduction | (Kim et al. 2010) |
| Clayey soil | Phenanthrene | 200 mg/kg | 65% removal | (Xu et al. 2010) |
| Coarse sand/sand | Creosote | 50, 200, 500, 900, 6800 mg/kg | 50, 68, 80% reduction | (Suni et al. 2007) |
| Sandy loam | Phenol | 180 mg/kg | 58% reduction | (Luo et al. 2006) |
| Clay | Creosote | 1300 mg/kg | 35% reduction | (Niqui-Arroyo et al. 2006) |
| Kaolinite | Pentadecane | 1000, 5000, 10000, 20000 mg/kg | 77.6% reduction | (Kim et al. 2005a) |
| Sandy loam | phenol | 200 mg/kg | 49, 60, 67% reduction | (Luo et al. 2005) |

## 2.6 FUTURE RESEARCH

The Electrokinetic bioremediation can be an effective remediation technique suitable for field applications, provided that the process cost can be reduced and the pH gradient is controlled. High energy consumption increases the overall cost of the remediation process and may become a major factor restricting the field application of the technology. There are very few studies in the available literature that have investigated the cost of energy in electrokinetic bioremediation, which is a major contributor to the total cost of the process. Research to date has shown a low to moderate percentage of contaminant removal using electrokinetic bioremediation. Future research should pay more attention to optimize the removal efficiency by electrokinetic bioremediation. In addition, current research tends to address the pH issue using two different approaches, either by using conventional techniques, in which chemical compounds are added to control the pH, or by conservative techniques, such as using a pump to circulate the anode and cathode compartment fluids in an attempt to neutralize the pH. Both techniques can result in a further increase in the overall cost of remediation. Moreover, the effect of the increase in temperature associated with electrokinetic bioremediation has not been fully investigated.

Advanced technologies, in particular, biotechnology and synthetic biology provide great opportunities for enhancing electrokinetic bioremediation with reduced cost. This may involve several research components including, prolonging the survival and function of the microbes in contaminated sites, identifying new bacterial strains with better performance in bioremediation, enhancing the metabolic ability of indigenous bacteria through microbial genetic engineering, exploring the rich microbial sources for powerful contaminant degrading enzymes using metagenomics, and designing smart engineering tools for efficient bioremediation. It is anticipated that, with intense research efforts, electrokinetic bioremediation would become a viable technology in the near future.

## 2.7 REFERENCES

Abel-Santos, E. (2012). Bacterial spores: current research and applications. Norfolk, UK, Caister Academic Press.

Acar, Y. B. and Alshawabkeh, A. N. (1993). "Principles of electrokinetic remediation." environmental science & Technology, **27**(13): 2638-2647.

Acar, Y. B., Rabbi, M. F. and Ozsu, E. E. (1997). "Electrokinetic injection of ammonium and sulfate ions into sand and kaolinite beds." Journal of Geotechnical and Geoenvironmental Engineering, **123**(3): 239-249.

Alcalde, M., Ferrer, M. and Plou, F. J. (2007). "Environmental biocatalysis: From remediation with enzymes to novel green processes." Biocatalysis and Biotransformation, **25**(2-4): 113-113.

Alshawabkeh, A. N. (2009). "Electrokinetic soil semediation: challenges and opportunities." Separation Science and Technology, **44**(10): 2171-2187.

Alshawabkeh, A. N., Shen, Y. P. and Maillacheruvu, K. Y. (2004). "Effect of dc electric fields on COD in aerobic mixed sludge processes." Environmental Engineering Science, **21**(3): 321-329.

Alshawabkeh, A. N., Yeung, A. T. and Bricka, M. R. (1999). "Practical aspects of in-situ electrokinetic extraction." Journal of Environmental Engineering-Asce, **125**(1): 27-35.

Andrews, R. W., Pollard, A. and Pearce, J. M. (2013). "The effects of snowfall on solar photovoltaic performance." Solar Energy, **92**: 84-97.

Birbir, Y., Ugur, G. and Birbir, M. (2008). "Inactivation of bacterial population in hide-soak liquors via direct electric current." Journal of Electrostatics, **66**(7-8): 355-360.

Bitchaeva, O., Ronneau, C. and North Atlantic Treaty Organization. Scientific Affairs Division. (1997). Biotechnology for waste management and site restoration : technological, educational, business, political aspects. Dordrecht ; Boston, Kluwer Academic.

Blasco, R., Mallavarapu, M., Wittich, R. M., Timmis, K. N. and Pieper, D. H. (1997). "Evidence that formation of protoanemonin from metabolites of 4-chlorobiphenyl degradation negatively affects the survival of 4-chlorobiphenyl-cometabolizing microorganisms." Applied and Environmental Microbiology, **63**(2): 427-434.

Blasco, R., Wittich, R. M., Mallavarapu, M., Timmis, K. N. and Pieper, D. H. (1995). "From xenobiotic to antibiotic, formation of protoanemonin from 4-chlorocatechol by enzymes of the 3-Oxoadipate pathway." Journal of Biological Chemistry, **270**(49): 29229-29235.

Brenner, K., You, L. C. and Arnold, F. H. (2008). "Engineering microbial consortia: a new frontier in synthetic biology." Trends in Biotechnology, **26**(9): 483-489.

CCME (2008). "Canada-wide standards for petroleum hydrocarbons in soil." Canadian council of ministers of the environment

Chen, M., Xu, P., Zeng, G., Yang, C., Huang, D. and Zhang, J. (2015). Bioremediation of soils contaminated with polycyclic aromatic hydrocarbons, petroleum, pesticides, chlorophenols and heavy metals by composting: Applications, microbes and future research needs, Biotechnol Adv. 2015 May 22. pii: S0734-9750(15)30002-1. doi: 10.1016/j.biotechadv.2015.05.003.

Chen, X. J., Shen, Z. M., Yuan, T., Zheng, S. S., Ju, B. X. and Wang, W. H. (2006). "Enhancing electrokinetic remediation of cadmium-contaminated soils with stepwise moving anode method." Journal of Environmental Science and Health Part a-Toxic/Hazardous Substances & Environmental Engineering, **41**(11): 2517-2530.

Chilingar, G. V., Loo, W. W., Khilyuk, L. F. and Katz, S. A. (1997). "Electrobioremediation of soils contaminated with hydrocarbons and metals: Progress report." Energy Sources, **19**(2): 129-146.

Chung, H. I. (2009). "Field Applications on Electrokinetic Reactive Pile Technology for Removal of Cu from In-situ and Excavated Soils." Separation Science and Technology, **44**(10): 2341-2353.

Cotter, P. D. and Hill, C. (2003). "Surviving the acid test: Responses of gram-positive bacteria to low pH." Microbiology and Molecular Biology Reviews, **67**(3): 429-+.

DeFlaun, M. F. and Condee, C. W. (1997). "Electrokinetic transport of bacteria." Journal of Hazardous Materials, **55**(1-3): 263-277.

Denisov, G., Hicks, R. E. and Probstein, R. F. (1996). "On the kinetics of charged contaminant removal from soils using electric fields." Journal of Colloid and Interface Science, **178**(1): 309-323.

Elektorowicz, M. and Boeva, V. (1996). "Electrokinetic supply of nutrients in soil bioremediation." Environmental Technology, **17**(12): 1339-1349.

Flemming, H.-C., Wingender, J. and Szewzyk, U. (2011). Biofilm Highlights. Dordrecht, Springer.

Goldstein, R. M., Mallory, L. M. and Alexander, M. (1985). "Reasons for possible failure of inoculation to enhance biodegradation." Applied and Environmental Microbiology, **50**(4): 977-983.

Groves, J. T., Boxer, S. G. and McConnel, H. M. (1997). "Electric field-induced reorganization of two-component supported bilayer membranes." Proceedings of the National Academy of Sciences of the United States of America, **94**(25): 13390-13395.

Hansen, H. K., Ottosen, L. M., Kliem, B. K. and Villumsen, A. (1997). "Electrodialytic remediation of soils polluted with Cu, Cr, Hg, Pb and Zn." Journal of Chemical Technology and Biotechnology, **70**(1): 67-73.

Hansen, H. K. and Rojo, A. (2007). "Testing pulsed electric fields in electroremediation of copper mine tailings." Electrochimica Acta, **52**(10): 3399-3405.

Hassan, I., and Mohamedelhasan, E. (2014). "Sorption, desorption, remediation, and fertility characteristics of clay soil." Journal of Civil Engineering and Architecture, **8**: 1274-1284.

Hassan, I. and Mohamedelhasan, E. (2012). "Electrokinetic remediation with solar power for a homogeneous soft clay contaminated with copper." International Journal of Environmental Pollution and Remediation (IJEPR) **1**(1): 67-74.

Hassan, I., Mohamedelhassan, E. and Yanful, E. K. (2015a). "Solar powered electrokinetic remediation of Cu polluted soil using a novel anode configuration." Electrochimica Acta, **181**: 58-67.

Hassan, I., Mohamedelhassan, E., Yanful, E. K. and Yuan, Z.-C. (2015b). "Sorption of phenanthrene by kaolin and efficacy of hydraulic versus electroosmotic flow to stimulate desorption." Journal of Environmental Chemical Engineering, **3**(4, Part A): 2301-2310.

Harms, H. and Zehnder, A. J. B. (1995). "Bioavailability of Sorbed 3-Chlorodibenzofuran." Applied and Environmental Microbiology, **61**(1): 27-33.

Ho, S. V., et al. (1999a). "The lasagna technology for in situ soil remediation. 1. Small field test." Environmental Science & Technology, **33**(7): 1086-1091.

Ho, S. V., et al. (1999b). "The Lasagna technology for in situ soil remediation. 2. Large field test." Environmental Science & Technology, **33**(7): 1092-1099.

Huang, Y. L., Zeng, Y. H., Yu, Z. L., Zhang, J., Feng, H. and Lin, X. C. (2013). "In silico and experimental methods revealed highly diverse bacteria with quorum sensing and aromatics biodegradation systems - A potential broad application on bioremediation." Bioresource Technology, **148**: 311-316.

Inglis, T. J. J. and Sagripanti, J. L. (2006). "Environmental factors that affect the survival and persistence of Burkholderia pseudomallei." Applied and Environmental Microbiology, **72**(11): 6865-6875.

Jackman, S. A., Maini, G., Sharman, A. K. and Knowles, C. J. (1999). "The effects of direct electric current on the viability and metabolism of acidophilic bacteria." Enzyme and Microbial Technology, **24**(5-6): 316-324.

Kang, A. and Chang, M. W. (2012). "Identification and reconstitution of genetic regulatory networks for improved microbial tolerance to isooctane." Molecular Biosystems, **8**(4): 1350-1358.

Karigar, C. S. and Rao, S. S. (2011). "Role of microbial enzymes in the bioremediation of pollutants: A review." Enzyme Research, (1): 1-11.

Katsuki, S., et al. (2000). "Inactivation of Bacillus stearothermophilus by pulsed electric field." Ieee Transactions on Plasma Science, **28**(1): 155-160.

Kim, D. K., Kim, D., Kim, S. J. and Park, S. J. (2010a). "Effect of ionic mobility of working electrolyte on electrokinetic energy conversion in sub-micron channels." International Journal of Thermal Sciences, **49**(7): 1128-1132.

Kim, K. J., Cho, J. M., Baek, K., Yang, J. S. and Ko, S. H. (2010b). "Electrokinetic removal of chloride and sodium from tidelands." Journal of Applied Electrochemistry, **40**(6): 1139-1144.

Kim, S. H., Han, H. Y., Lee, Y. J., Kim, C. W. and Yang, J. W. (2010c). "Effect of electrokinetic remediation on indigenous microbial activity and community within diesel contaminated soil." Science of the Total Environment, **408**(16): 3162-3168.

Kim, S. J., Park, J. Y., Lee, Y. J., Lee, J. Y. and Yang, J. W. (2005). "Application of a new electrolyte circulation method for the ex situ electrokinetic bioremediation of a laboratory-prepared pentadecane contaminated kaolinite." Journal of Hazardous Materials, **118**(1-3): 171-176.

Kim, S. S. and Han, S. J. (2003). "Application of an enhanced electrokinetic ion injection system to bioremediation." Water Air and Soil Pollution, **146**(1-4): 365-377.

Krulwich, T. A., Sachs, G. and Padan, E. (2011). "Molecular aspects of bacterial pH sensing and homeostasis." Nature Reviews Microbiology, **9**(5): 330-343.

Lear, G., et al. (2004). "The effect of electrokinetics on soil microbial communities." Soil Biology & Biochemistry, **36**(11): 1751-1760.

Li, X. G., Cao, H. B., Wu, J. C. and Yu, K. T. (2001). "Inhibition of the metabolism of nitrifying bacteria by direct electric current." Biotechnology Letters, **23**(9): 705-709.

Locatelli, A., Spor, A., Jolivet, C., Piveteau, P. and Hartmann, A. (2013). "Biotic and Abiotic Soil Properties Influence Survival of Listeria monocytogenes in Soil." Plos One, **8**(10).

Luo, Q. S., Wang, H., Zhang, X. H., Fan, X. Y. and Qian, Y. (2006). "In situ bioelectrokinetic remediation of phenol-contaminated soil by use of an electrode matrix and a rotational operation mode." Chemosphere, **64**(3): 415-422.

Luo, Q. S., Zhang, X. H., Wang, H. and Qian, Y. (2005). "The use of non-uniform electrokinetics to enhance in situ bioremediation of phenol-contaminated soil." Journal of Hazardous Materials, **121**(1-3): 187-194.

Madsen, E. L. (1991). "Determining Insitu Biodegradation - Facts and Challenges." Environmental Science & Technology, **25**(10): 1663-1673.

Maillacheruvu, K. Y. and Chinchoud, P. R. (2011). "Electrokinetic transport of aerobic microorganisms under low-strength electric fields." Journal of Environmental Science and Health Part a-Toxic/Hazardous Substances & Environmental Engineering, **46**(6): 589-595.

Maldonado, L. A. and Quintana, E. T. (2015). "Unexpected Properties of Micromonosporae from Marine Origin." Advances in Microbiology, **5**: 452-456.

Malik, A., Grohmann, E. and SpringerLink (2012). Environmental Protection Strategies for Sustainable Development. Dordrecht, Springer Science+Business Media B.V.

Mao, X. H., et al. (2012). "Electrokinetic-enhanced bioaugmentation for remediation of chlorinated solvents contaminated clay." Journal of Hazardous Materials, **213**: 311-317.

McErlean, C., Marchant, R. and Banat, I. M. (2006). "An evaluation of soil colonisation potential of selected fungi and their production of ligninolytic enzymes for use in soil bioremediation applications." Antonie Van Leeuwenhoek International Journal of General and Molecular Microbiology, **90**(2): 147-158.

McKenney, P. T., Driks, A. and Eichenberger, P. (2013). "The Bacillus subtilis endospore: assembly and functions of the multilayered coat." Nature Reviews Microbiology, **11**(1): 33-44.

Miller, M. B. and Bassler, B. L. (2001). "Quorum sensing in bacteria." Annual Review of Microbiology, **55**: 165-199.

Mizuno, A. and Hori, Y. (1988). "Destruction of Living Cells by Pulsed High-Voltage Application." Ieee Transactions on Industry Applications, **24**(3): 387-394.

Mohamedelhassan, E. and Shang, J. (2001). "Effects of electrode materials and current intermittence in electro-osmosis." Proceedings of the ICE-Ground Improvement, **5**(1): 3-11.

Mohamedelhassan, E. and Shang, J. Q. (2008). "Electrokinetic cementation of calcareous sand for offshore foundations." International Journal of Offshore and Polar Engineering, **18**(1): 73-80.

Niqui-Arroyo, J. L., Bueno-Montes, M., Posada-Baquero, R. and Ortega-Calvo, J. J. (2006). "Electrokinetic enhancement of phenanthrene biodegradation in creosote-polluted clay soil." Environmental Pollution, **142**(2): 326-332.

Nyer, E. K. and Suarez, G. (2002). "Treatment technology: In situ biodegradation is better than monitored natural attenuation." Ground Water Monitoring and Remediation, **22**(1): 30-+.

Padan, E., Bibi, E., Ito, M. and Krulwich, T. A. (2005). "Alkaline pH homeostasis in bacteria: New insights." Biochimica Et Biophysica Acta-Biomembranes, **1717**(2): 67-88.

Page, M. M. and Page, C. L. (2002). "Electroremediation of contaminated soils." Journal of Environmental Engineering-Asce, **128**(3): 208-219.

Pazos, M., Sanroman, M. A. and Cameselle, C. (2006). "Improvement in electrokinetic remediation of heavy metal spiked kaolin with the polarity exchange technique." Chemosphere, **62**(5): 817-822.

Peixoto, R. S., Vermelho, A. B. and Rosado, A. S. (2011). "Petroleum-degrading enzymes: Bioremediation and new prospects." Enzyme Research, **2011**(1): 475193-7.

Qin, J. F., et al. (2015). "Modular pathway rewiring of Saccharomyces cerevisiae enables high-level production of L-ornithine." Nature Communications, **6**.

Rajic, L., Dalmacija, B., Dalmacija, M., Roncevic, S. and Perovic, S. U. (2012). "Enhancing electrokinetic lead removal from sediment: Utilizing the moving anode technique and increasing the cathode compartment length." Electrochimica Acta, **86**: 36-40.

Ramirez, E. M., Camacho, J. V., Rodrigo, M. A. R. and Canizares, P. C. (2014). "Feasibility of electrokinetic oxygen supply for soil bioremediation purposes." Chemosphere, **117**: 382-387.

Ray, D., Mohandass, S. N. and Roy, P. (2014). "Molecular Phylogeny of Arctic Microbes Using Metagenomic Approach." Advances in Microbiology, **4**: 1278-1284.

Reddy, K. R. and Cameselle, C. (2009). Electrochemical remediation technologies for polluted soils, sediments and groundwater. Hoboken, N.J., Wiley**:** xxii, 732 p.

Reed, B. E., Berg, M. T., Thompson, J. C. and Hatfield, J. H. (1995). "Chemical Conditioning of Electrode Reservoirs during Electrokinetic Soil Flushing of Pb-Contaminated Silt Loam." Journal of Environmental Engineering-Asce, **121**(11): 805-815.

Roberge, P. R. (2008). Corrosion engineering: principles and practice. New York, McGraw-Hill.

Rutherford, S. T. and Bassler, B. L. (2012). "Bacterial Quorum Sensing: Its Role in Virulence and Possibilities for Its Control." Cold Spring Harbor Perspectives in Medicine, **2**(11).

Sah, S., Aluri, S., Rex, K. and Varshney, U. (2015). "One-Carbon Metabolic Pathway Rewiring in Escherichia coli Reveals an Evolutionary Advantage of 10-Formyltetrahydrofolate Synthetase (Fhs) in Survival under Hypoxia." Journal of Bacteriology, **197**(4): 717-726.

Sale, A. J. H. and Hamilton, W. A. (1967). "Effects of High Electric Fields on Microorganisms .I. Killing of Bacteria and Yeasts." Biochimica Et Biophysica Acta, **148**(3): 781-&.

Schmidt, C. A. B., Barbosa, M. C. and de Almeida, M. D. S. (2007). "A laboratory feasibility study on electrokinetic injection of nutrients on an organic, tropical, clayey soil." Journal of Hazardous Materials, **143**(3): 655-661.

Schneewind, O. and Missiakas, D. M. (2012). "Protein secretion and surface display in Gram-positive bacteria." Philosophical Transactions of the Royal Society B-Biological Sciences, **367**(1592): 1123-1139.

Schoenbach, K. H., Joshi, R. P., Stark, R. H., Dobbs, F. C. and Beebe, S. J. (2000). "Bacterial decontamination of liquids with pulsed electric fields." Ieee Transactions on Dielectrics and Electrical Insulation, **7**(5): 637-645.

Segall, B. A. and Bruell, C. J. (1992). "Electroosmotic Contaminant-Removal Processes." Journal of Environmental Engineering-Asce, **118**(1): 84-100.

Semple, K. T., Doick, K. J., Jones, K. C., Burauel, P., Craven, A. and Harms, H. (2004). "Defining bioavailability and bioaccessibility of contaminated soil and sediment is complicated." Environmental Science & Technology, **38**(12): 228a-231a.

Shapiro, A. P. and Probstein, R. F. (1993). "Removal of Contaminants from Saturated Clay by Electroosmosis." Environmental Science & Technology, **27**(2): 283-291.

Shelton, D. R. and Doherty, M. A. (1997). "A model describing pesticide bioavailability and biodegradation in soil." Soil Science Society of America Journal, **61**(4): 1078-1084.

Shi, L., Harms, H. and Wick, L. Y. (2008a). "Electroosmotic flow stimulates the release of alginate-bound phenanthrene." Environmental Science & Technology, **42**(6): 2105-2110.

Shi, L., Muller, S., Harms, H. and Wick, L. Y. (2008b). "Effect of electrokinetic transport on the vulnerability of PAH-degrading bacteria in a model aquifer." Environmental Geochemistry and Health, **30**(2): 177-182.

Shi, L., Muller, S., Loffhagen, N., Harms, H. and Wick, L. Y. (2008c). "Activity and viability of polycyclic aromatic hydrocarbon-degrading Sphingomonas sp LB126 in a DC-electrical field typical for electrobioremediation measures." Microbial Biotechnology, **1**(1): 53-61.

Singh, N., et al. (2003). "Bioavailability of an organophosphorus pesticide, fenamiphos, sorbed on an organo clay." Journal of Agricultural and Food Chemistry, **51**(9): 2653-2658.

SolarBuzz (2010). "Solarbuzz Reports World Solar Photovoltaic " Marketbuzz.

Sperelakis, N. (2012). Cell physiology sourcebook: essentials of membrane biophysics. Amsterdam;Boston;, Elsevier/Academic Press.

Sperelakis, N. (1995). Cell physiology source book. San Diego, Academic Press.

Suni, S., Malinen, E., Kosonen, J., Silvennoinen, H. and Romantschuk, M. (2007). "Electrokinetically enhanced bioremediation of creosote-contaminated soil: Laboratory and field studies." Journal of Environmental Science and Health Part a-Toxic/Hazardous Substances & Environmental Engineering, **42**(3): 277-287.

Tiehm, A., Augenstein, T., Ilieva, D., Schell, H., Weidlich, C. and Mangold, K. M. (2010). "Bio-electro-remediation: electrokinetic transport of nitrate in a flow-through system for enhanced toluene biodegradation." Journal of Applied Electrochemistry, **40**(6): 1263-1268.

Tiehm, A., Lohner, S. T. and Augenstein, T. (2009). "Effects of direct electric current and electrode reactions on vinyl chloride degrading microorganisms." Electrochimica Acta, **54**(12): 3453-3459.

Van Hamme, J. D., Wong, E. T., Dettman, H., Gray, M. R. and Pickard, M. A. (2003). "Dibenzyl sulfide metabolism by white rot fungi." Applied and Environmental Microbiology, **69**(2): 1320-1324.

Virkutyte, J. and Sillanpaa, M. (2002). "Enhanced electrokinetic remediation of copper and chromium from sand." Abstracts of Papers of the American Chemical Society, **224**: U623-U623.

Virkutyte, J., Sillanpaa, M. and Latostenmaa, P. (2002). "Electrokinetic soil remediation - critical overview." Science of the Total Environment, **289**(1-3): 97-121.

Wan, C. L., Du, M. A., Lee, D. J., Yang, X., Ma, W. C. and Zheng, L. N. (2011). "Electrokinetic remediation and microbial community shift of beta-cyclodextrin-dissolved petroleum hydrocarbon-contaminated soil." Applied Microbiology and Biotechnology, **89**(6): 2019-2025.

Wang, E., Mohr, R. K., Buechele, A. C. and Pegg, I. L. (1996). "Current density effects on the corrosion of ceramic and metallic electrode materials in waste glasses." Scientific Basis for Nuclear Waste Management Xix, **412**: 173-180.

Wick, L. Y., et al. (2010). "Responses of soil microbial communities to weak electric fields." Science of the Total Environment, **408**(20): 4886-4893.

Wick, L. Y., Mattle, P. A., Wattiau, P. and Harms, H. (2004). "Electrokinetic transport of PAH-degrading bacteria in model aquifers and soil." Environmental Science & Technology, **38**(17): 4596-4602.

Wick, L. Y., Shi, L. and Harms, H. (2007). "Electro-bioremediation of hydrophobic organic soil-contaminants: A review of fundamental interactions." Electrochimica Acta, **52**(10): 3441-3448.

Wong, J. S. H., Hicks, R. E. and Probstein, R. F. (1997). "EDTA-enhanced electroremediation of metal-contaminated soils." Journal of Hazardous Materials, **55**(1-3): 61-79.

Wu, X. Z., Gent, D. B., Davis, J. L. and Alshawabkeh, A. N. (2012). "Lactate injection by electric currents for bioremediation of tetrachloroethylene in clay." Electrochimica Acta, **86**: 157-163.

Xu, W., Wang, C. P., Liu, H. B., Zhang, Z. Y. and Sun, H. W. (2010). "A laboratory feasibility study on a new electrokinetic nutrient injection pattern and bioremediation of phenanthrene in a clayey soil." Journal of Hazardous Materials, **184**(1-3): 798-804.

Yergeau, E., Sanschagrin, S., Beaumier, D. and Greer, C. W. (2012). "Metagenomic analysis of the bioremediation of diesel-contaminated Canadian high actic soils." Plos One, **7**(1).

Yeung, A. T. and Corapcioglu, M. (1994). "Electrokinetic flow processes in porous media and their applications." Advances in porous media-volume 2.: 309-395.

Yeung, A. T. and Gu, Y. Y. (2011). "A review on techniques to enhance electrochemical remediation of contaminated soils." Journal of Hazardous Materials, **195**: 11-29.

Young, L. (2013) "Alberta oil spills: A look over 37 years." Global News.

Yuan, S. H., Zheng, Z. H., Chen, J. and Lu, X. H. (2009). "Use of solar cell in electrokinetic remediation of cadmium-contaminated soil." Journal of Hazardous Materials, **162**(2-3): 1583-1587.

Zaidi, B. R., Murakami, Y. and Alexander, M. (1989). "Predation and Inhibitors in Lake Water Affect the Success of Inoculation to Enhance Biodegradation of Organic-Chemicals." Environmental Science & Technology, **23**(7): 859-863.

# CHAPTER 3
# SORPTION OF PHENANTHRENE BY KAOLIN AND EFFICACY OF HYDRAULIC FLOW VERSUS ELECTROOSMOTIC FLOW TO STIMULATE DESORPTION[1]

## 3.1 INTRODUCTION

In the industrial era, the environment has been heavily affected by improper disposal of waste from petroleum extraction and anthropogenic activities. Polycyclic aromatic hydrocarbons (PAHs) are an important group of pollutants because some of them have been identified as mutagenic, carcinogenic, and/or teratogenic (Tsai et al. 2001; Reddy et al. 2006). PAHs are characterized by their polarity and low solubility in water, both of which hinder their removal from soils (Hatheway 2002; Connell 2005). The risk assessment and the evaluation of the fate of the contamination source are solely dependent on understanding the sorption and desorption characteristics of the pollutant. Sorption of a certain contaminant in the environment is commonly described by the distribution coefficient between sorbent (e.g. soil) and sorbate (e.g. aqueous phase), assuming the process is linear. The partition coefficient depends on the environment and can be estimated by the product of contaminant and organic carbon partition coefficient ($K_{oc}$) and organic carbon fraction in the sorbent ($f_{oc}$). In the literature, reported values of $K_{oc}$ vary over a wide range. For instance, log $K_{oc}$ for phenanthrene ranges from 3.97 to 6.12, i.e. a variation of more than two orders of magnitude in $K_{oc}$ (Kayal and Connell 1990). Recent studies have shown that not only does the fraction of organic carbon in the sorbent control the sorption, but also the type of organic carbon (humin, humic acid, and fluvic acid) and the environmental conditions play a dominant role in the sorption partitioning phenomenon (Celis et al. 2006; Pan et al. 2006).

[1]A version of this chapter has been published in Environmental Chemical Engineering

For example, Terashima et al. (2003) demonstrated that the presence of high molecular weight humic acids results in high sorption of polycyclic aromatic hydrocarbons (PAHs). A study by Pan et al. (2006) has shown that humin (HM) is responsible for slow sorption of PAH, whereas, fulvic and humic acids are predominant in the initial sorption stage. The findings of the aforementioned researchers are in agreement with the concept of biphasic sorption, which has been discussed extensively in the literature (Weber and Huang 1996; Huang and Weber 1998; Chai et al. 2006). There are several well established methods for determining $f_{oc}$, such as wet oxidation and dry oxidation (Carter and Gregorich 2008). Although the values of $K_{oc}$ and $f_{oc}$ can be determined by any of the aforementioned techniques, the test can result in under or over estimation of the sorption process. This is because soils' organic matter fractions and organic matter types play a crucial role in the sorption and desorption capacity of the soil to petroleum hydrocarbons. Therefore, determining the sorption coefficient is essential to understand the behaviour of contaminant and interaction between the contaminant 'sorbate' and the matrix 'sorbent' when the contaminant released in the environment.

In the last two decades, desorption of organic contaminants from soil has gained considerable attention in the literature as it is the key factor governing the bioavailability and consequently the biodegradation (Kan et al. 1994; Cornelissen et al. 1997; Cornelissen et al. 1998; Burgos et al. 1999; Shi et al. 2008; Gao et al. 2010). Many research studies have shown that batch desorption tests can result in less than 100% of the sorbate recovery; a phenomenon called hysteresis. For example, Kan et al. (1994) research study has shown that because of the hysteresis between sorption and desorption for hydrocarbon organic contaminants, only 30-50% of sorbed PAHs was recoverable after a batch desorption test. At contaminated sites, desorption mechanism is slow and depends on many factors including: (i) sorbate concentration gradient inside the sorbent, which develops during the sorption phase with higher sorbate farther inside the sorbent, (ii) thickness of the double layer, (iii) sorbate chemical properties, and (iv) sorbent physico-chemical properties. It has

been shown that PAHs partitioned into clay soil is highly susceptible to mobilization by groundwater and degradation by soil-microorganisms (Talley et al. 2002).

Desorption of contaminants from the sorbent by the effect of ground water flow has a fundamental role in mitigation of contaminated sites (Khan and Husain 2003). For instance, natural attenuation remediation technique depends solely in desorption by ground water flow as a major mechanism for degradation of the contaminants (Khan et al. 2004). In this method the concentration of the contaminant in soils and ground water is monitored in a source zone and in contaminated plume. Due to the fact that the groundwater flow rate is very slow, the decrease in contaminant concentration by desorption (the effect of groundwater) may take centuries until it reaches the regulatory requirements or the standards (Thornton et al. 2001; Grathwohl et al. 2002). Electroosmotic flow, associated with electrokinetics, creates flow within the stern layer in the double layer. The stern layer is next to the soil matrix (sorbent) where the sorption of organic contaminants takes place. The electroosmotic flow in this region can enhance back diffusion of the contaminant from the soil matrix to the pore fluid and accelerate desorption of the contaminant, which can result in reducing the amount of time required for mitigation of contaminated sites. According to the Helmholtz-Smoluchowski model, the most commonly used theory to describe electroosmosis, the width of the electroosmotic flow tube in a soil mass extends beyond the free water to the interface between the fixed and mobile parts of the electrical double layer (Yeung and Corapcioglu 1994). In contrast, the hydraulic flow takes place in the zone of the free water alone. Since adsorbed PAH compounds are held very close to the surface of the soil, a flow generated within the electrical double layer may facilitate desorption of these compounds. Furthermore, electrokinetic remediation has a high potential for generating electroosmotic flow in fine-grained soils in which the groundwater flow rate is very slow so these soils are difficult to cleanup using conventional methods (Yeung et al. 1997). From the above discussion, the potential of electrokinetics in promoting desorption of contaminants by electroosmotic flow makes the technique a suitable candidate to be coupled with natural attenuation to enhance the outcome of natural attenuation. Electrokinetics requires a direct current (DC) power supply to produce the

necessary power for the process, which arguably can increase the cost of the hybrid technique (electrokinetics natural attenuation). Studies by Yuan et al. (2009) and Souza et al. (2016) have shown that solar panels can be used to generate enough power for electrokinetics remediation processes with the former study finding the cost of power by the solar panels to be less than that from the grid in China. This makes the hybrid technique, if successful, an excellent option to be used in contaminated sites at remote areas where electrical power lines are not abundant or absent.

Recent review articles by Yeung and Gu (2011) and Gill et al. (2014) have discussed various techniques to enhance electrokinetic remediation along with electrokinetics coupled with other remediation techniques. None of the aforementioned articles, however, has discussed the coupling of electrokinetics with natural attenuation. Desorption of PAH by electroosmotic flow to enhance natural attenuation has not been well studied. In fact, there are very few articles in the available literature that have studied the role of electroosmotic flow in desorption of PAHs from soil (Shi et al. 2008; Lopez-Vizcaino et al. 2014). A study by Shi et al. (2008) has shown that desorption of phenanthrene from glass beads by electroosmotic flow is more efficient than desorption by hydraulic flow.

In the present study, phenanthrene is selected as a model polycyclic aromatic hydrocarbon, and its sorption by kaolinite clay soil is investigated. Desorption of the sorbate (phenanthrene) resulting from hydraulic flow is compared to desorption driven by electroosmotic flow. One application of this study would be coupling electrokinetic remediation with natural attenuation. To the best of the authors' knowledge, this is one of the first studies that has compared the effectiveness of electroosmotic and hydraulic flows in desorption of PAH from a clay soil.

## 3.2 MATERIALS AND METHODS

Inorganic kaolinite clay soil, 96-99.9% kaolinite (EPK case number 1332-58-7), purchased from (EdgarMinerals, Florida, US) was used as the sorbent in the experiments. Table 3.1 shows the physical and chemical properties of the soil. Atterberg limits (liquid and plastic limits) were determined following the procedure D4318-10 (D4318 2010) described by American society for testing and materials (ASTM). The maximum and the minimum void ratios were determined. Maximum void ratio ($e_{max}$) is the void ratio (that is, volume of voids divided by the volume of solids) of the soil in its loosest state. It was determined by allowing a soil sample to settle by gravity in a graduated cylinder, cover the cylinder with latex sheet and turn the cylinder upside down slowly, and then the soil volume is measured (Venkatramaiah 1995; Yamamuro and Lade 1997; Wood 2003). The minimum void ratio ($e_{min}$) is the void ratio of the soil in its densest state, and was determined by measuring the volumes of soil voids and solids after compaction using the modified Proctor test (Venkatramaiah 1995; Wood 2003; Bradshaw and Baxter 2007). Five water contents, 0.14, 0.18, 0.30, 0.35, and 0.48 were used in the compaction test. Sieve analysis on the soil revealed that all the particle sizes were less than 0.075 mm (passed No. 200 sieve). Accordingly, hydrometer analysis was conducted to obtain particle size distribution, in accordance with ASTM D422-63 (D422-63 2007). Total organic carbon analyzer (TOC-$V_{CPN}$, SHIMADZU, Kyoto, Japan) was used to determine the organic carbon fraction ($f_{oc}$) in the soil.

Soil pH was determined using ASTM D4972-13 (D497 2013). For the cation exchange capacity, ammonium acetate and potassium chloride were used as extractants to obtain first the soluble cations and then bound or exchangeable cations. Inductively coupled plasma-optical emission spectroscopy (ICP-OES, VARIAN, USA) was used to determine the cation concentrations in solution. The specific surface area of the kaolinite clay was determined using surface area analyser (Micromeritics, Gemini instrument, USA). The specific area is estimated using Brunauer, Emmett and Teller (BET Method) method. In this method the surface area is calculated from the amount of nitrogen gas adsorbed by the soil particles measured at the boiling point of nitrogen and atmospheric pressure.

Sorption of phenanthrene by kaolinite clay was investigated using batch tests. Kinetics sorption tests were carried out to determine the rate of phenanthrene sorption by the soil. Desorption of phenanthrene from the soil was investigated using three techniques: batch testing, hydraulic flow, and electroosmotic flow measurements. The procedures followed in the sorption and desorption experiments are outlined in the next sections.

**Table 3.1** Soil physicochemical properties

| Soil property | Measured value |
|---|---|
| Liquid limit | 64% |
| Plastic limit | 35% |
| $e_{max}$ | 3.1 |
| $e_{min}$ | 0.92 |
| Organic carbon content ($f_{oc}$) | 0.45% |
| pH | 4.2 |
| Cation exchange capacity | 3.75 meq/100g of soil |
| Specific surface area | 28.75 $m^2/g$ |

## 3.3 SORPTION TESTS

Batch tests were carried out at room temperature (22$^o$C) to investigate the sorption characteristics of phenanthrene (97%, from Sigma-Aldrich) as a model polyaromatic hydrocarbon (PAH) compound, using kaolinite clay as sorbent. Stock solution with a concentration of 1.0 g/L was prepared by mixing phenanthrene with acetonitrile in a 1.0 L amber glass bottle. The solution was shaken by a table top shaker for 24 h. Two liters of background solution was prepared using de-ionized water irradiated with UV for the

purpose of disinfection. The following compounds were added per liter of background solution: 100 mg sodium azide ($NaN_3$) to suppress microorganisms, 5 mg $NaHCO_3$ to control solution pH, and 0.554 g calcium chloride to provide solution strength. A 200 mL of six solutions containing 300, 400, 500, 600, 700, and 800 µg/L of phenanthrene were prepared using the stock solution and the background solution. From each of the prepared solutions, 50 mL were measured and added to 0.5 g of kaolinite clay that had been weighed into conical flasks. Each flask was sealed with glass cap, parafilm, and covered with aluminum foil (this was done to prevent or minimize degradation by photo-oxidation). The flasks were shaken for 15 days in a table shaker. The solutions were transferred to heavy duty glass centrifuge tubes (35 mL, Kimble). Each glass centrifuge bottle was sealed with a screw cap and the cap was covered with silver foil to prevent the loss of phenanthrene to the cap materials. The tubes were centrifuged at 4000 rpm (equivalent to 1920 g force) for 20 min in a Sorvall RC-5B Refrigerated Superspeed Centrifuge (Thermo Scientific, USA). A sample of supernatant (750 µL) was recovered from each tube and analyzed for phenanthrene using reverse-phase high-performance liquid chromatography (HPLC, Agilent, USA). The tests were conducted in triplicate.

## 3.4 DESORPTION TESTS

The sorbate (phenanthrene) desorption from the kaolinite was investigated using batch test, hydraulic flow tests, and electroosmotic flow tests. Following the batch sorption test, the supernatant was discarded from each flask and replaced with 50 mL of the background solution (free of phenanthrene). The flasks were sealed as described in the sorption test and shaken by a table shaker for 15 days. At the end of the desorption tests, the supernatants were collected and analyzed using the procedure described in the sorption test above.

Desorption of phenanthrene from the clay matrix by hydraulic flow and electroosmotic flow were compared using kaolinite artificially contaminated with phenanthrene. Six concentrations, 500, 1000, 2000, 3000, 4000, and 5000 mg phenanthrene/kg of dry

kaolinite, were used in desorption tests. The concentrations used in the study were selected based on our review of concentrations used in the published literature and to cover a wide range of contaminant concentrations (Niqui-Arroyo et al. 2006; Delille et al. 2008). The samples were prepared as follows: 1 kg of soil and the corresponding amount of phenanthrene were weight. Phenanthrene was dissolved in methanol and then mixed with soil (to ensure uniform distribution of phenanthrene in the soil), and the soil was placed under fume hood over night for methanol evaporation to take place (in dark). Background solution was prepared using de-ionized water irradiated with UV for the purpose of disinfection. The following compounds were added per liter of background solution: 100 mg sodium azide ($NaN_3$) to suppress microorganisms, 5 mg $NaHCO_3$ to control solution pH, and 0.554 g calcium chloride to provide solution strength. Following, the soil was mixed with the background solution to a water content of 60%.

Desorption of sorbate by hydraulic flow can be investigated using a fixed wall permeameter where a steel mold is used to host the soil specimen. Alternatively, the test can be conducted using flexible wall apparatus in which a polymeric membrane is used to contain the soil sample. In this study, the fixed wall apparatus was selected over the flexible wall because of concerns over possible reaction(s) between the hydrophobic organic compound (phenanthrene) and the flexible wall membrane. Figure 3.1 shows a schematic of the fixed wall hydraulic permeability test apparatus that was used to apply hydraulic flow through the soil specimen in the present study. A saturated soil specimen, 54 mm in diameter and 20 mm long with a corresponding mass of 74.9 g was placed in the fixed wall permeability stainless steel mold. The water content, void ratio and pore volume of the soil specimen were 60%, 1.6, and 28.2 mL, respectively. The background solution, pH of 7.45, was loaded in the syringe and used as permeant. The tests were conducted in triplicate. Glass bottles were used to collect the effluent. The pressure transducer was connected to a data logger and a computer where pressure was recorded periodically during the test using GEN2000 software. Wattmeter (KiLL WaTT$^{TM}$) was used to measure the power consumption during the tests. The flow rate was kept constant and the test was terminated after three pore volumes were collected. The Darcy's velocity and volumetric flow are

found to be $6.45 \times 10^{-7}$ m/s and $1.48 \times 10^{-9}$ $m^3$/s, respectively. A custom-designed electrokinetic cell was used to carry out desorption by electroosmotic flow tests. Figure 3.2 shows the schematic of the electrokinetic desorption cell. The cell is composed of anode, cathode compartment, and a middle section that connects to the two

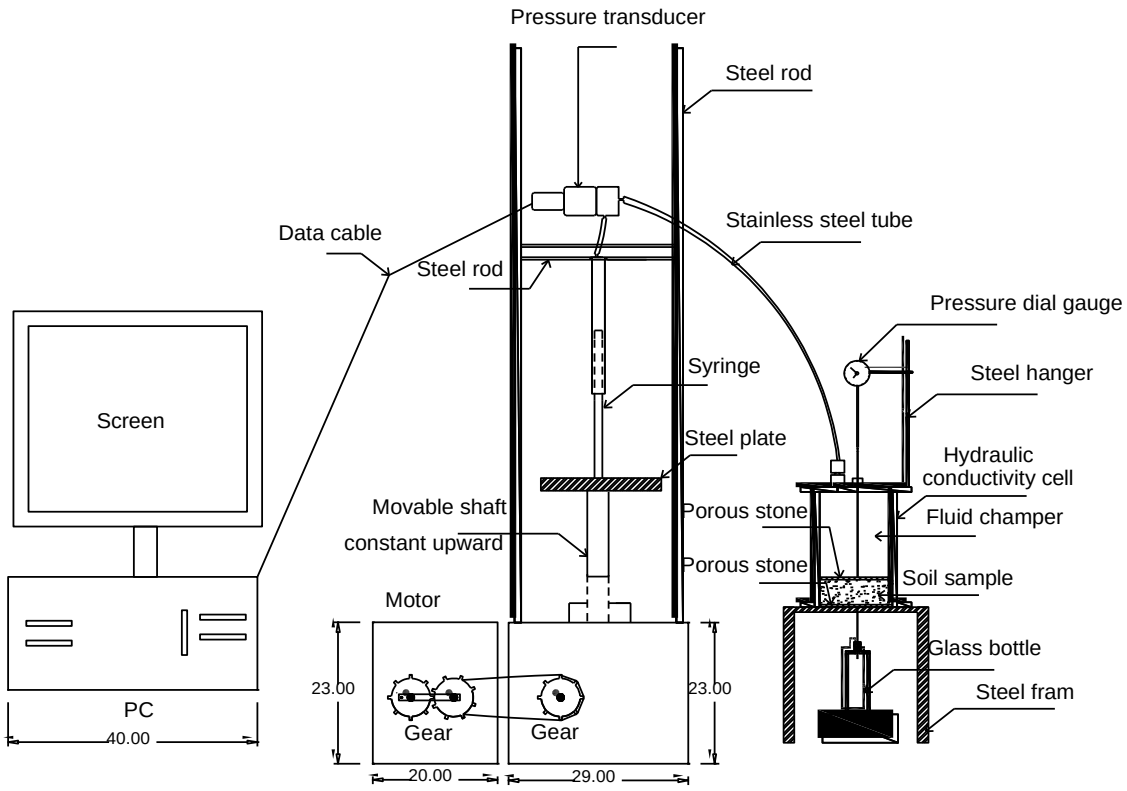


**Figure 3.1** Schematic of fixed wall hydraulic permeameter test apparatus (dimensions in cm)

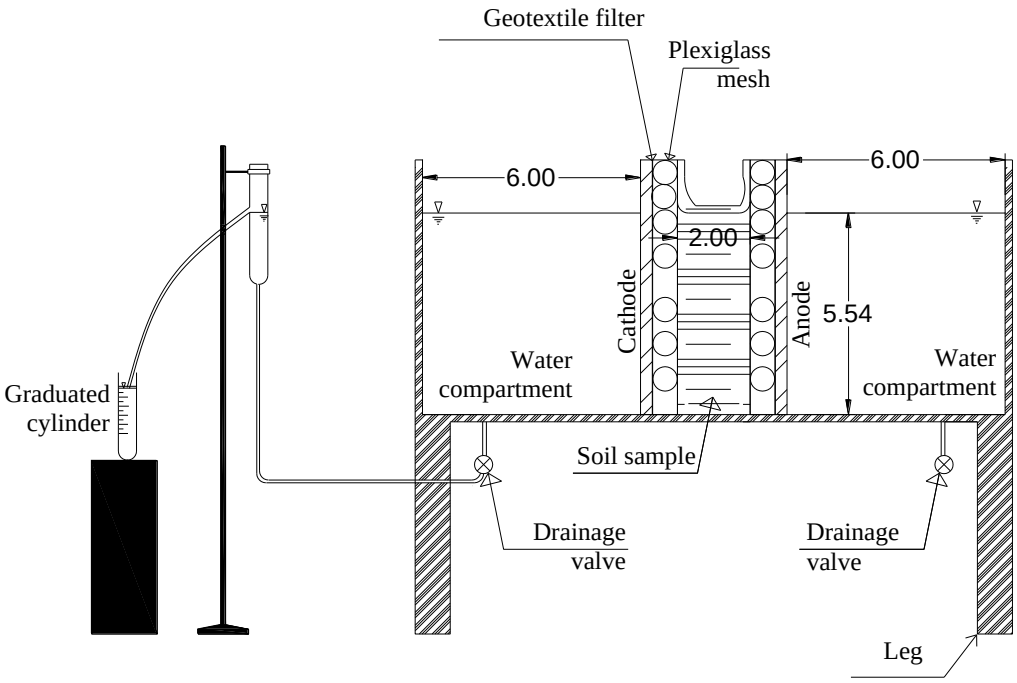


**Figure 3.2** Schematic of electrokinetic desorption cell (dimensions in cm)

electrode compartments. The middle section's shape and dimensions are identical to those of the fixed wall stainless steel mold (diameter 54 mm and length 20 mm). The middle section houses the soil sample. During the tests, pH at the anode and cathode compartments was controlled by the addition of hydrochloric acid to the cathode compartment and sodium hydroxide to the anode compartment as needed. The applied voltage was varied from 6 to 14 V to obtain corresponding current values of 0.3 to 0.43 mA/cm$^2$ during the test. The electroosmotic flow during the test was 1.4 to 1.5 x $10^{-9}$ m$^3$/s, which is similar to the volumetric flow rate in the hydraulic flow tests. Permeant was collected at the cathode compartment and the volume was measured every hour. Both hydraulic test and electrokinetic test were terminated after (5.2 hours) collection of three pore volumes of flow.

## 3.5 KINETICS

Kinetics test was conducted to investigate the phenanthrene sorption rate using a phenanthrene concentration of 500 µg/L (prepared as described before) at room temperature. From the prepared solutions, 50 mL were measured and added to 0.5 g of kaolinite clay that had been weighed into the Erlenmeyer flasks. For phenanthrene analysis, samples from the flasks were collected after 0.5, 1, 3, 7, and 9 h. The test protocol and analysis procedure developed and described in the sorption test section was followed in the kinetics test.

## 3.6 ANALYSIS

At the end of the batch sorption and desorption tests, a sample (750 µL) from the supernatant was transferred to 2.0 mL amber screw vial where 750 µL acetonitrile was then added to the vial. Phenanthrene concentration in solution was determined using reverse-phase HPLC. The HPLC method was developed using Agilent ZORBAX Eclipse XDB-C18 HPLC column (4.6x150 mm, 5 µm). Acetonitrile and distilled water irradiated with UV (using UV ultrapure water system, Barnstead) were used as the mobile phase in a ratio 0.7 acetonitrile /0.3 distilled water (volume/volume). The chromatographic conditions used were as follow: column temperature 30$^{o}$C, injection volume 100 µL, flow rate 1.5 mL/min, Diode array detector (DAD) set at 260 nm, reference 400 nm, and Fluorescence detector (FLD) set at UV wavelength of 254 nm and fluorescence emission of 380 nm. Standard solutions, with known concentrations, were used to obtain a seven-point calibration curve.

## 3.7 RESULTS AND DISCUSSION

Initial phenanthrene concentration ($C_i$) in the liquid phase, equilibrium concentrations in the liquid phase ($C_e$), and concentration in the soil at equilibrium ($S_s$) after the test were determined. All the tests were conducted in triplicate. The results are discussed in the following sections.

### 3.7.1 Sorption and desorption batch tests

Phenanthrene as a nonpolar compound tends to segregate from water to soil and binds to soil organic matter (SOM). There are two mechanisms by which the sorption can takes place, physical or chemical. The physical sorption occurs if the force of attraction between adsorbate and adsorbent are Van de Waal's forces (very weak forces). The chemical adsorption is due the chemical pond (very strong cannot be easily reversed). Sorption of petroleum hydrocarbons is dependent on the amount of SOM in soil. Also, part of the phenanthrene sorption takes place in soil minerals (Celis et al. 2006). The SOM for the clay used in this study is 0.45%. A study by Celis et al. (2006) showed that sorption cannot be predicted or calculated from the knowledge of soil organic matter alone. Therefore, in this study, batch sorption tests were conducted to determine the sorption parameters of the soil used in this study. Freundlich and Langmuir isotherms were fitted to the present experimental data. Freundlich isotherm, shown in Figure 3.3, was found to best represent the results. Freundlich equation can be expressed logarithmically as (Watts 1998):

$$Log(S_s) = Log\left(K_f\right) + nLog(C_e) \quad (3.1)$$

Where: $S_s$ is phenanthrene concentration in soil (μg/g), $C_e$ is the equilibrium concentration of solution (g/L), and $K_f$ and n are constants.

After the sorption tests, the equilibrium concentration of solution in the flasks ($C_e$) were determined using the method described above and the phenanthrene concentration in soil ($S_s$) was back calculated from the initial and equilibrium aqueous phase concentrations. The values of the constants $K_f$ and n, determined by using Equation 3.1 and the Freundlich isotherms in Figure 3.3, are presented in Table 3.2.

**Table 3.2** Freundlich isotherm model fitting results

| Temp. | Regression equation | $K_f$ $(\mu g L^n/g^{(1+n)})^n$ | n | $R^2$ | $R^{'}$ | SEE $10^{-3}$ | F $10^{-3}$ |
|---|---|---|---|---|---|---|---|
| $22^O$ C | $Log(S_s)$ = 0.848 log $(C_e)$-0.876 | 0.133 | 0.848 | 0.95 | 0.93 | 32 | 4 |

Where: $R^2$ is the coefficient of determination; $R^{'}$ is the adjusted R square, SEE standard error of estimate, and F is the significant of the regression

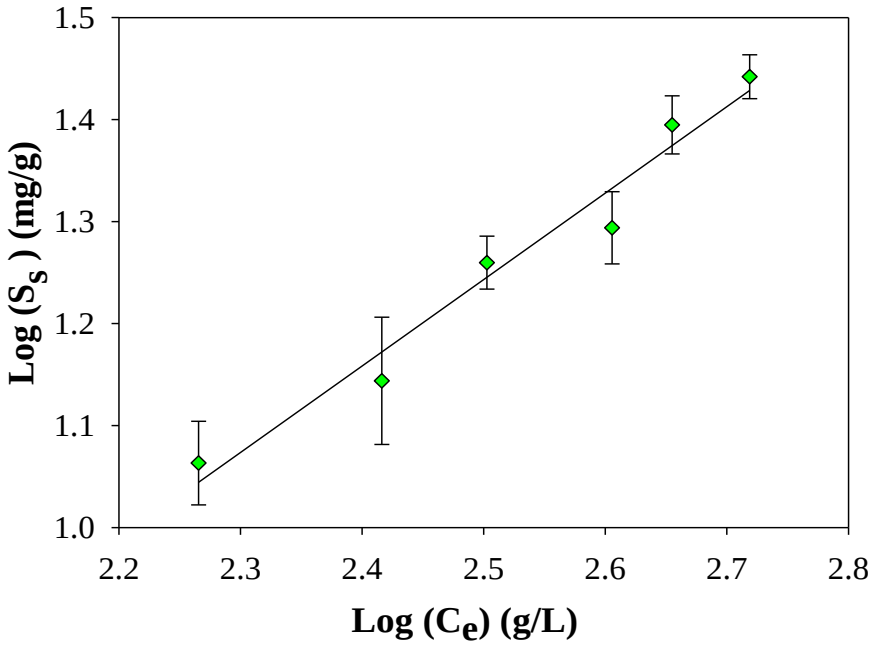


**Figure 3.3** Freundlich sorption isotherm

The overall regression accuracy of Freundlich isotherm model is presented by the coefficient of determination R square and adjusted R square. The standard error of estimate (SEE) is calculated as to indicate the agreement between the calculated and observed values. The probability that the regression output is not random is presented by the significance of regression (F).

In contaminated sites, it is important to estimate the amount of phenanthrene partitioned to the soil and that dissolved in water. The partition coefficient depends on the environment and can be estimated by the product of contaminant and organic carbon partition coefficient ($K_{oc}$) and organic carbon fraction in the sorbent ($f_{oc}$). In the literature, reported values of $K_{oc}$ phenanthrene vary over more than two fold measure (Kayal and Connell 1990). Recent studies have shown that the fraction of organic carbon and the type of organic carbon play a dominant role in the sorption partitioning phenomenon (Celis et al. 2006; Pan et al. 2006). The determination of the values of $K_{oc}$ and $f_{oc}$ experimentally can result in under or over estimation of sorption partition coefficient. This is because not only does the soil organic matter fraction play a crucial role in the sorption capacity of the soil, but also, more importantly, the type of organic matter in the contaminated soil. Therefore, the determination of the sorption model constant is essential to understanding the behavior of phenanthrene and the interaction between the phenanthrene and the kaolinite when the phenanthrene released in the environment.

After the batch sorption tests, the samples were centrifuged and the supernatants were decanted, and phenanthrene free solution was added to the soil in each flask and shaken on a table shaker for another 15 days. Phenanthrene equilibrium concentrations, after desorption tests, are depicted in Figure 3.4. The test results showed that not all the sorbed phenanthrene by the soil matrix can be desorbed. The results showed that the percentage of phenanthrene desorbed from soil samples with high amounts of sorbed phenanthrene is less than that desorbed from soil samples with low amounts of sorbed phenanthrene. However, the difference between the percentages of desorbed phenanthrene in the aforementioned cases is not significant. The highest desorption percentage reported is 81% at the low sorbed amount and the lowest is 76% at the high sorbed amount. These findings are in agreement with the results from Huang et al. (Huang et al. 1998).

Many research studies have shown that batch desorption tests can result in less than 100% recovery of the sorbate; a phenomenon called hysteresis. For instance, a study by Kan et

al. (1994) has shown that because of the hysteresis between sorption and desorption for hydrocarbon organic contaminants, only 30-50% of sorbed PAHs was recoverable after a batch desorption test. As per the present study results, for clay soil contaminated with phenanthrene at the range of concentrations tested, the use of conventional soil flushing technique with solution 10 times the mass of the soil can remove 76% of the initial phenanthrene. Obviously, this will be a very expensive and impractical for full scale applications. Therefore, this study investigated two other alternatives desorption of phenanthrene by hydraulic flow and electroosmotic flow.

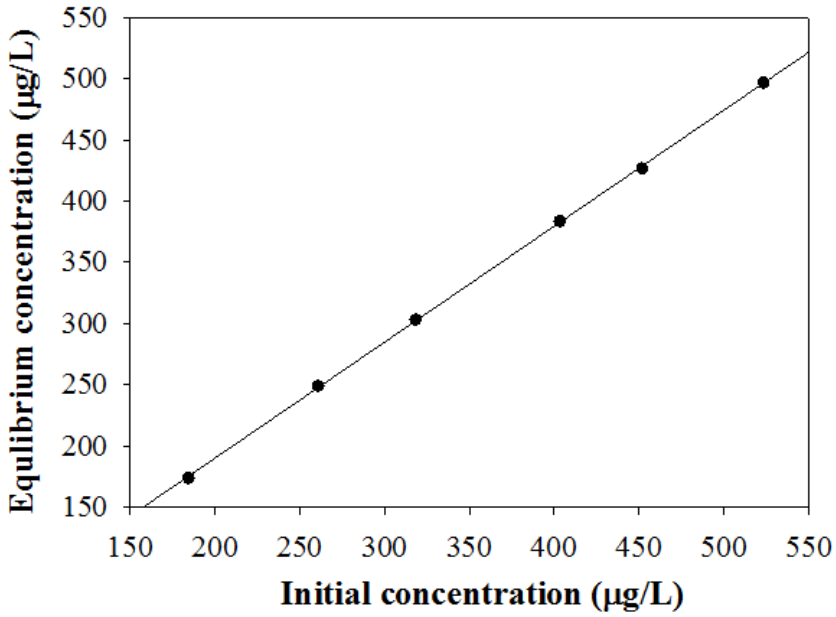


**Figure 3.4** Phenanthrene desorption in batch tests

Kinetics test was conducted to investigate the phenanthrene sorption rate using phenanthrene concentration of 500 µg/L. Figure 3.5 shows the sorption rate increases rapidly between points a and b, increased slightly between point c and d, and there is no change in the sorption amount between point d and f suggesting that most of the sorption took place in the first three hours.

The kinetics test is conducted for better understanding of the sorption process with time. The results from the kinetics were necessary in conducting the subsequent tests in the study, for example, to decide on the spiked period for the soil in preparation for desorption test.

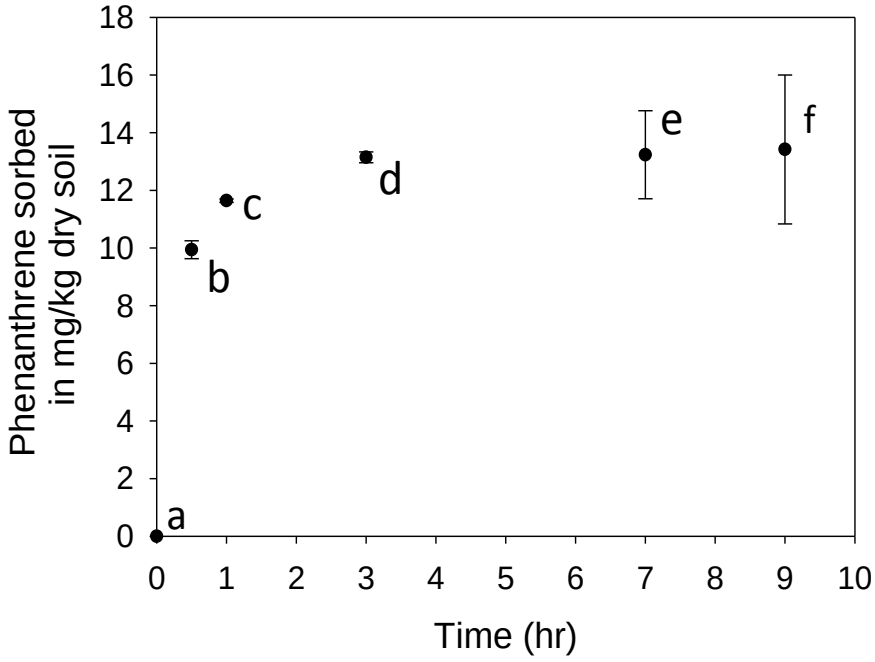


**Figure 3.5** Phenanthrene sorption rate

## 3.7.2 Desorption by electroosmotic flow and by hydraulic flow

Desorption of phenanthrene from clay soil was investigated using hydraulic flow and electroosmotic flow. Concentrations of 500, 1000, 2000, 3000, 4000 and 5000 mg phenanthrene per kg of dry soil were used in the investigation and the results are shown in Figures 3.6 to 3.11.

At low concentration the amount of phenanthrene desorbed from soil specimen increased with an increase in the number of pore volumes. This trend is found to be common to both

desorption of phenanthrene by electroosmotic and hydraulic flow (see Figure 3.6 (a)). The results show that the phenanthrene removal by electroosmotic flow is one to two times higher than the removal by hydraulic flow. The high and low energy binding sites in soil specimen are distributed between SOM and soil minerals. Normally, the SOM hosts the high energy binding while soil minerals include the low energy binding sites (Gunasekara and Xing 2003). Usually, the sorbate binds to the high energy binding sites first. Therefore, high energy is required to desorb bound sorbate from sorbent. Figure 3.6 (b) shows that the pressure needed to generate hydraulic flow is increased at the first two hours and then remains steady until three pore volumes were obtained. This is found to be the same for all tests with different phenanthrene concentrations. The consumption by electric motor (hydraulic flow driving force) is computed as 0.35 kWh per pore volume. The energy consumption for electrokinetics is determined as $0.5 \times 10^{-3}$ kWh in the first pore volume. The energy consumption required for desorption by electroosmotic flow (see Figure 3.6 (a)) is decreased as the number of pore volumes is increased. The energy consumption in the hydraulic test is three orders of magnitude higher than the energy consumption in the electrokinetics test.

The thickness of the double layer, as widely described in literature by Equation 3.2, is directly proportional to the permittivity and inversely proportional to the valence and concentration of the pore fluid (Shang et al. 1994)

$$\frac{1}{k} = \sqrt{\frac{\varepsilon_o K_m R T}{2 z^2 F^2 C_o}} \tag{3.2}$$

where: $\frac{1}{k}$ is the thickness of the double (m), $\varepsilon_o$ is the permittivity of vacuum $C^2/(J\text{-}m)$, $K_m$ is the relative permittivity of pore fluid, $F$ is the Faraday constant = $9.6487 \times 10^4$ C/mol, $R$ is the gas constant = 8.314 J/(mol-K), $T$ is the absolute temperature (K), $C_o$ is the molarity of ions in solution ($mol/m^3$), and $z$ is the valence of cations and anions.

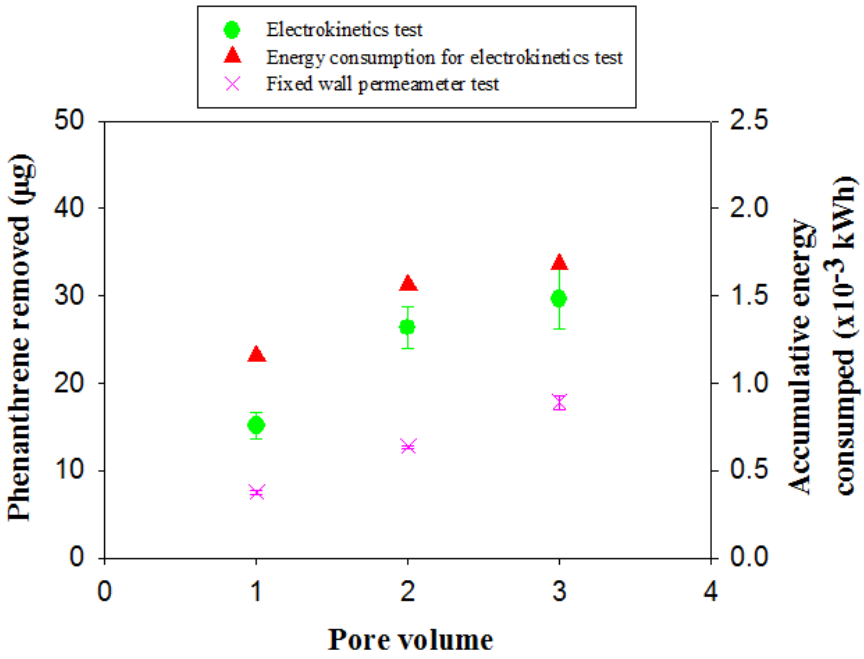


(a) Phenanthrene removal per pore volume and energy consumption for electrokinetic test

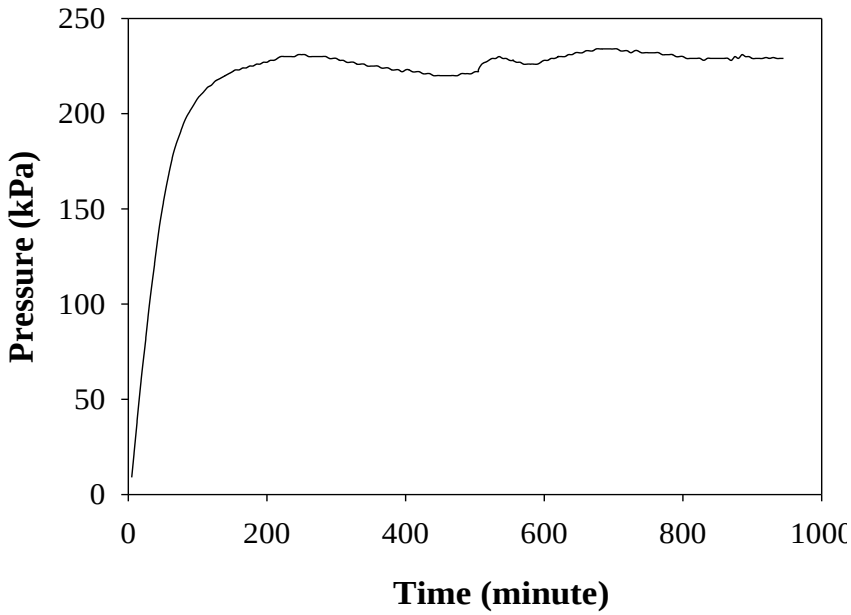


(b) Pore water pressure during fixed wall hydraulic permeability test

**Figure 3.6** Phenanthrene concentration 500 mg/kg

In the present study the chemical composition of permeant fluid and pore fluid is the same, except that the pore fluid contains phenanthrene desorbed from soil matrix, therefore the valence and the concentration of the pore fluid are constant. The permittivity is influenced by phenanthrene concentration and the pore water. Shang et al. (1994) suggested the permittivity of water in stern layer can be taken as 6 and in the Gouy layer as 80, whereas the permittivity of organic compound in Stern and Gouy layers can be consider to be equal (≈2) because their polarization is not affected by the charge in the clay minerals.

Desorption by hydraulic flow at phenanthrene concentration of 1000 mg/kg of dry soil follow similar trend as discussed above (see Figure 3.7). At concentration of 2000 mg/kg of dry soil (Figure 3.8) there is no variation in the amount desorbed by hydraulic flow after the second and the third pore volume. However, at higher concentrations 3000, 4000, and 5000 mg/kg of dry soil (Figures 3.9, 3.10, and 3.11) there is no variation in desorbed amount between the first, second, and third pore volume. It can be concluded that, as the concentration increased, there were no changes in the amount of phenanthrene desorbed with each successive pore volume. Desorption by electroosmotic flow showed no changes between the removal after the second and the third pore volume at concentration of 1000 mg/kg and no changes between the mount desorbed with the increase in the number of pore volumes at concentration of 2000 mg/kg. At higher concentrations, 3000, 4000, and 5000 mg/kg of dry soil, the amount desorbed by the first pore volume is higher than the amount desorbed by the second and third pore volumes. The high amount of phenanthrene removed in the first pore volume can be attributed to the saturation of both SOM sorption sites and soil mineral sorption sites. The results show higher desorption can be achieved by electroosmotic flow than by hydraulic flow, however, the comparison is limited because desorption by hydraulic flow is not feasible in the field.

The tests setup in this study was designed to investigate six various phenanthrene concentrations to be desorbed over three pore volumes. In the published literature, similar studies have been conducted using three pore volumes (Hardcastle and Mitchell 1974;

Fernandez and Quigley 1985; Yong et al. 1992). Three pore volumes are enough to displace the original resident pore fluid and provide an assessment of the effect of phenanthrene concentrations. Moreover, the tests were conducted in triplicates and the results showed that there is a trend.

Typically, the Darcy's velocity for ground water in kaolinite clay is around $2x10^{-9}$ m/s and there is no control over the direction of the flow of ground water. Electrokinetics can be used to generate electroosmotic flow with a velocity higher than ground water flow. Moreover, the direction of electroosmotic flow can be controlled by the orientation of electrodes.

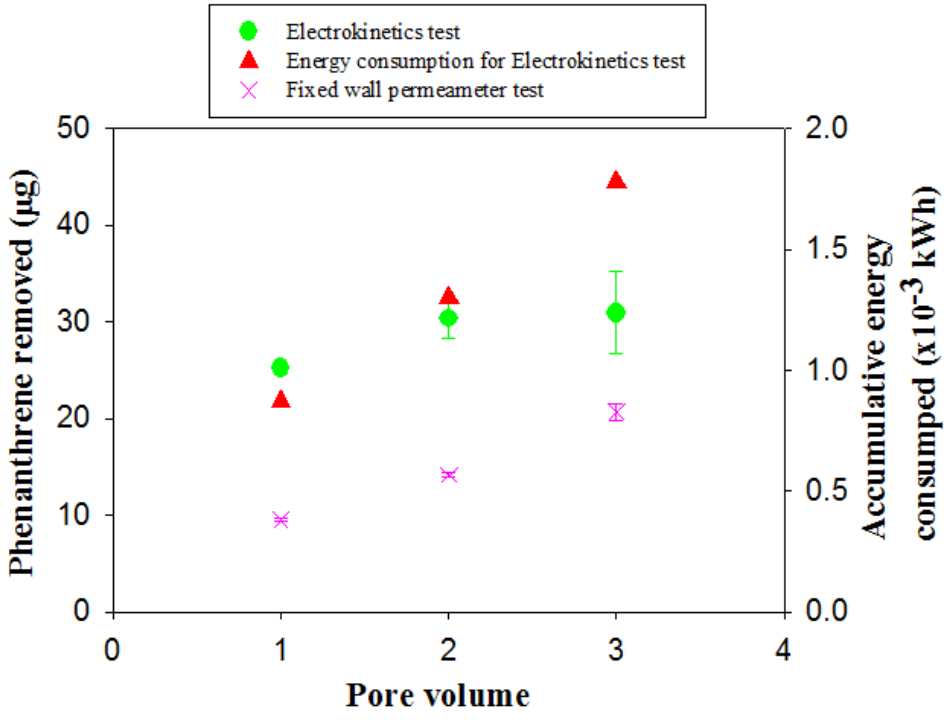


**Figure 3.7** Phenanthrene concentration 1000 mg/kg

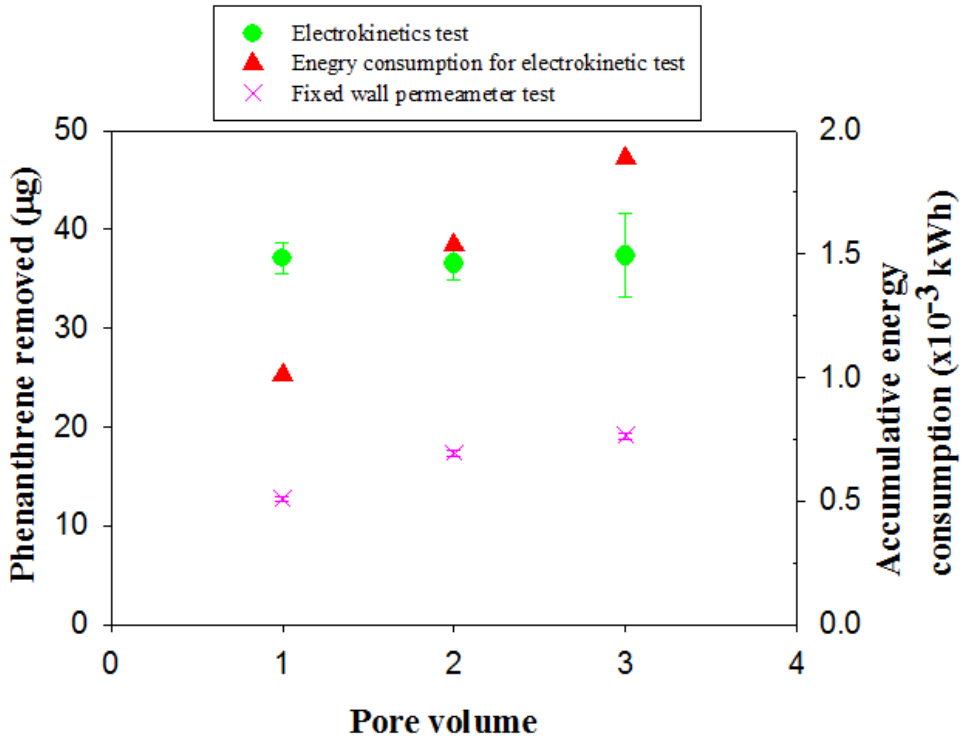


**Figure 3.8** Phenanthrene concentration 2000 mg/kg

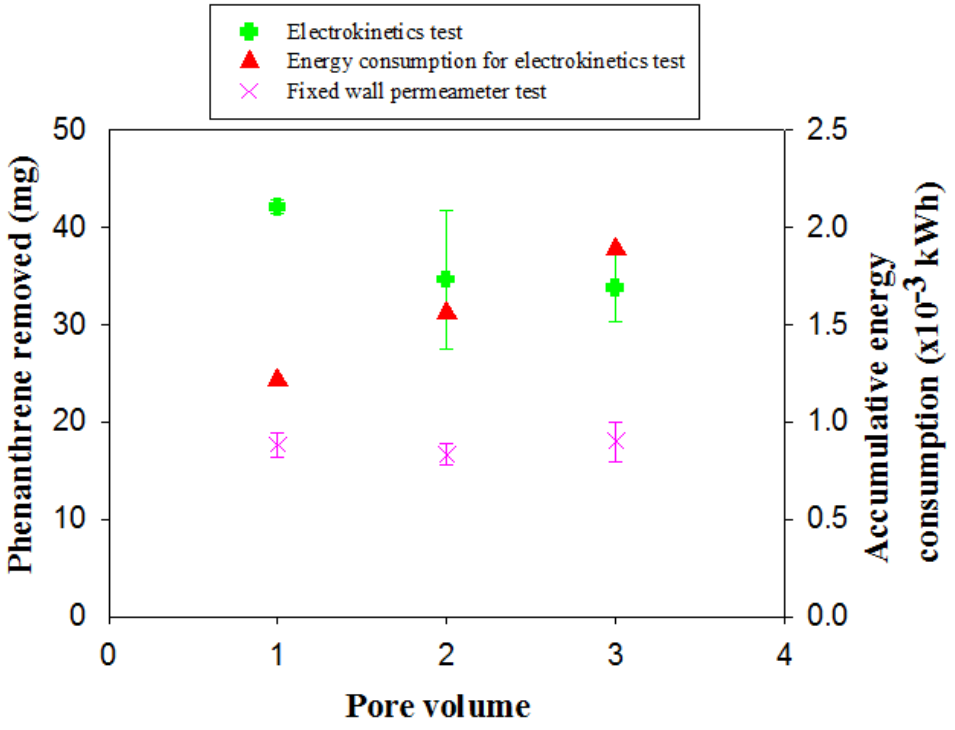

**Figure 3.9** Phenanthrene concentration 3000 mg/kg

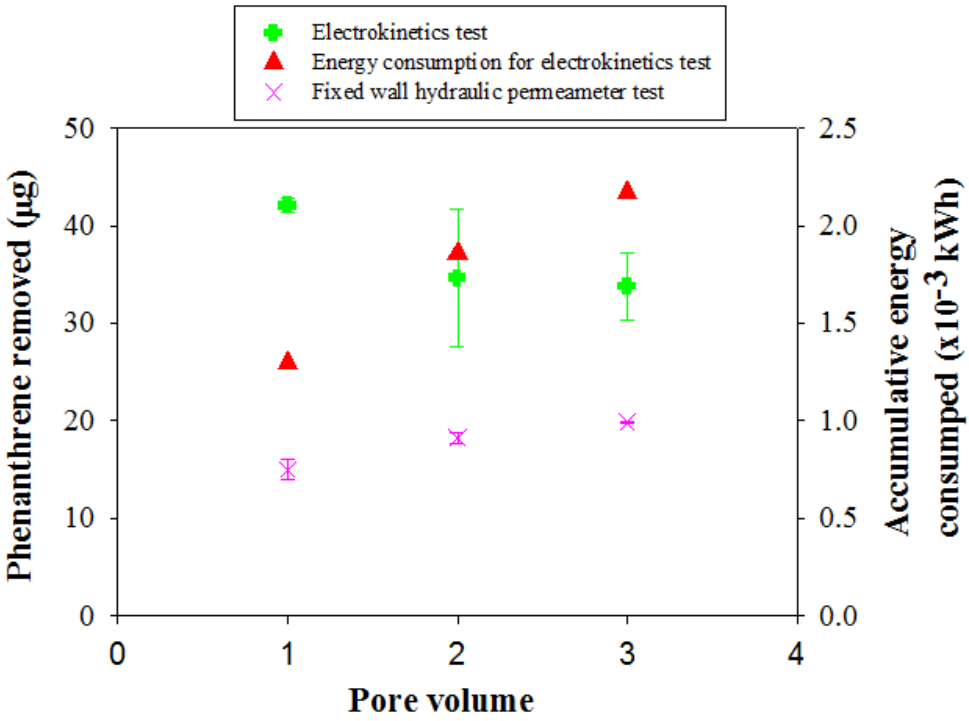


**Figure 3.10** Phenanthrene concentration 4000 mg/kg

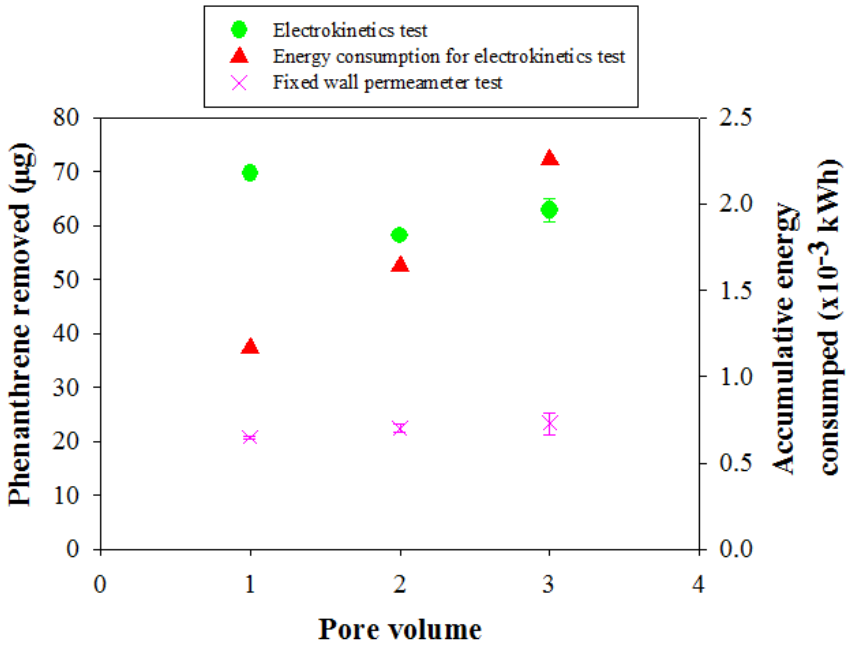


**Figure 3.11** Phenanthrene concentration 5000 mg/kg

The addition of ground phenanthrene and water to the soil sample can result in four possible partitioning phases including soluble (aqueous) phase, sorbed phase, vapour phase, and insoluble phase. The maximum amount of phenanthrene ($C^T$ mg/kg) that can be present in soil without the presence of insoluble phase can be calculated using Equation 3.3.

$$C^T = \frac{C_i}{\rho_b}(K_d\rho_b + \theta_w + H'\theta_a) \quad (3.3)$$

where $C_i$ is the solubility (mg/L), $\rho_b$, is the soil bulk density (g/cm$^3$), $\theta_w$ is the water-filled porosity, $H'$ unit less Henry's constant, and $\theta_a$ is the air-filled porosity. The sorption partition coefficient $K_d$ indicates how much phenanthrene dissolved in water and the amount that sorbed to the soil matrix. The solubility of phenanthrene in water is very low 800-1500 µg/L (Mackay 2006). Therefore, in real contaminated sites, most of the phenanthrene will partition to the soil until the soil sorption sites are saturated and the balance will present as non-aqueous phase (Feenstra et al. 1991). The hydraulic flow and electroosmotic flow can contribute to the mobilization of each of these partition phases with different efficiency. Desorption test is designed to investigate the effectiveness of the hydraulic flow and electroosmotic flow in reducing the concentration of phenanthrene in the soil matrix.

In the present study, the soil sample was saturated with water to eliminate phenanthrene vapour phase. The hydraulic flow can mobilize the phenanthrene in aqueous phase that exist outside the double layer boundary (see Figure 3.12). For a specific medium, the hydraulic conductivity depends on the permeability of the medium, and is directly proportional to permeant density, and inversely proportional to permeant dynamic viscosity. The pressure required to generate a flow of $1.48\text{x}10^{-3}$ mL/s through the soil sample was found to be 260 kPa (equivalent to water head of 26.5 m). In the fixed wall hydraulic test, the energy consumption by the electric motor (hydraulic flow driving force) is computed as 0.325 kWh per pore volume. The energy consumption for each

electrokinetics test is determined by the voltage and the current recorded during that test. It was found that the energy is increased from $1.68x10^{-3}$ to $1.78x10^{-3}$ to $1.89x10^{-3}$ to $2.01x10^{-3}$ to $2.17x\ 10^{-3}$, and to $2.26x10^{-3}$ kWh with the phenanthrene concentrations of 0.5, 1, 2, 3, 4, and 5 g phenanthrene per kg of dry soil, respectively. This can be attributed to the fact that the thickness of the double layer is decreased with a decrease in pore fluid permittivity, and is directly proportional to the concentration of organic compound in the Stern and Gouy layers (Fernandez and Quigley 1985; Shang et al. 1994). Figure 3.12 shows the double layer around the sorbent and the orientation of sorbate molecules at the kaolinite and SOM surface (Thompson and Goyne 2012; Casagrande and Shannon 1952; Letterman 1999; Maurice et al. 2009). As the thickness of the double layer decreases, the cross section of the free permeant flow is increased resulting in high hydraulic or electroosmotic flow. Nevertheless, desorption by electroosmotic flow results in three to four times higher removal of phenanthrene than by hydraulic flow. There is a significant difference in the energy consumption between the hydraulic and electrokinetic tests. The energy consumption in the fixed wall hydraulic test is four orders of magnitude higher than the energy consumption in the electrokinetics test. Therefore, it can be concluded that the electroosmotic flow when used to remove phenanthrene from kaolinite is more efficient and less costly than hydraulic flow. Shi et al. (2008) reported 1.4 to 1.8 times higher removal of phenanthrene from Alginate beads by electroosmotic flow than by hydraulic flow. Although, in the present study a particular soil was used in the tests, the findings are in general agreement with results reported by Shi et al. (2008). (See Appendices A Table A.1 to Table A.6 for detailed calculations)

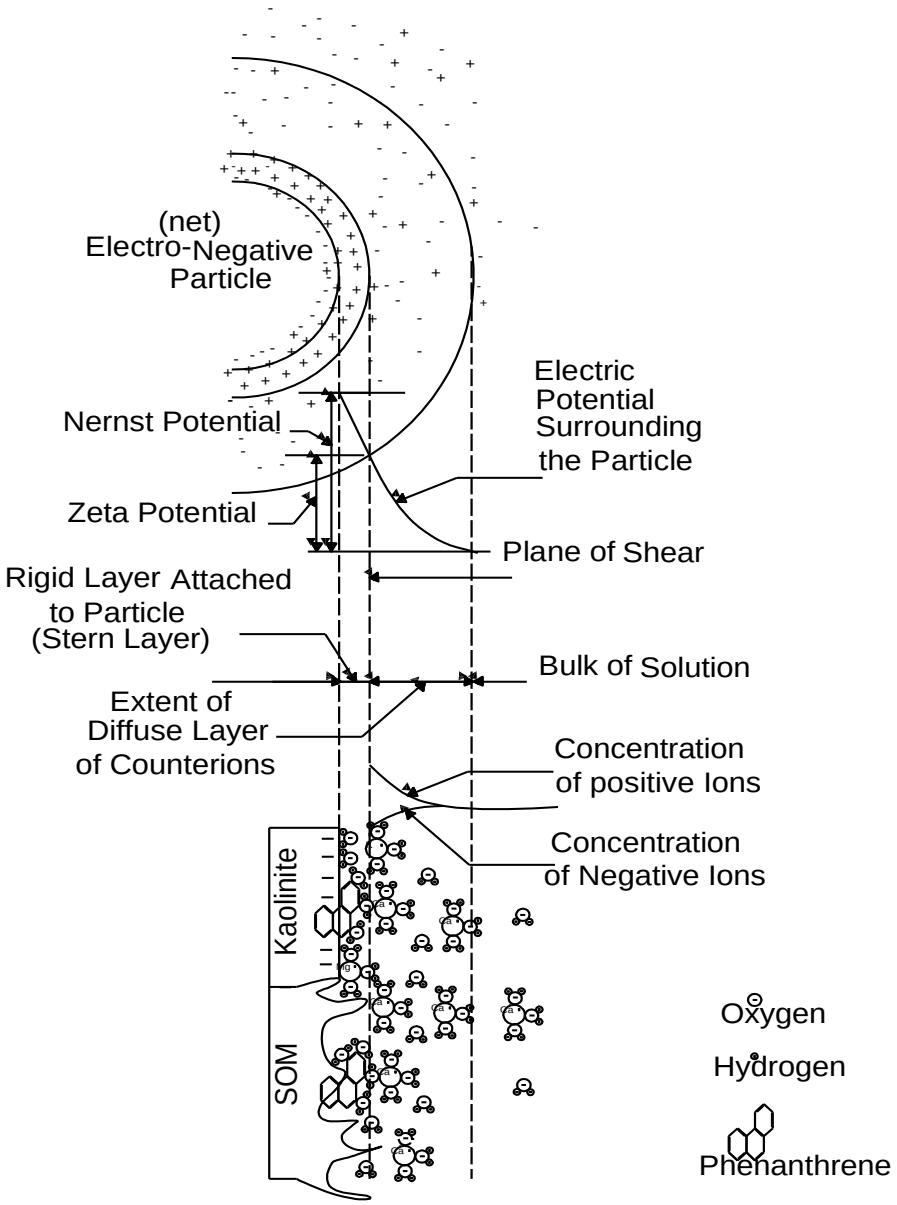


**Figure 3.12** Schematic diagram for double layer and Phenanthrene orientation at the sorbent surface (Modified from Casagrande (Casagrande and Shannon 1952), Letterman (Letterman 1999), Maurice (Maurice et al. 2009), and Thompson and Goyne (Thompson and Goyne 2012))

## 3.8 CONCLUSIONS

PAH contaminants adhere to soils when they are released into the environment. Desorption of a PAH contaminant from the soil is essential for a successful remediation process. Three tests were carried out to investigate sorption and desorption kinetics for phenanthrene as a representative PAH compound and kaolinite as a soil matrix. The data from the batch sorption test was fitted by the Freundlich and Langmuir isotherms where the Freundlich isotherm was found to best represent the results. Desorption test results, after the batch sorption tests, showed that not all the sorbed phenanthrene by the soil matrix can be desorbed. The highest desorption percentage reported in the batch tests is 81% and the lowest is 76%. Desorption of phenanthrene by electroosmotic flow in all the tests was found to be significantly higher than desorption caused by hydraulic flow. For example, in the soil specimen with an initial phenanthrene concentration of 4000 mg/kg, the phenanthrene removed after one pore volume of electroosmotic flow was about four times the amount removed after one pore volume of hydraulic flow. Phenanthrene desorption by hydraulic flow increased approximately linearly with the number of pore volumes in soil specimens with concentrations of 500, 1000, and 2000 mg phenanthrene/kg of soil, whereas desorption by electroosmotic flow was approximately linear for phenanthrene concentrations of 500 and 1000 mg/kg of soil.

Typically, the Darcy's velocity for ground water in kaolinite clay is around $2x10^{-9}$ m/s and there is no control over the direction of the flow of ground water. Electrokinetics can be used to generate electroosmotic flow with a velocity higher than ground water flow. Moreover, the direction of electroosmotic flow can be controlled by the orientation of electrodes. The results of this study showed that desorption of phenanthrene can be promoted by the use of electroosmotic flow. The removal of the phenanthrene from contaminated soil using electroosmotic flow was three to four times higher than in soil samples treated with hydraulic flow desorption. Moreover, the power required in the hydraulic test was found to be three orders of magnitude higher than the power requirement in the electrokinetic test.

## 3.9 REFERENCES

Bradshaw, A. S. and Baxter, C. D. P. (2007). "Sample preparation of silts for liquefaction testing." Geotechnical Testing Journal, **30**(4): 324-332.

Burgos, W. D., Munson, C. M. and Duffy, C. J. (1999). "Phenanthrene adsorption-desorption hysteresis in soil described using discrete-interval equilibrium models." Water Resources Research, **35**(7): 2043-2051.

Carter, M. R., Gregorich, E. G. (2008).Soil sampling and methods of analysis.Canadian Society of Soil Science. Boca Raton, FL, CRC Press.

Casagrande, A. and Shannon, W. (1952). "Base course drainage for airport pavements." American Society of Civil Engineers Transactions.

Celis, R., De Jonge, H., De Jonge, L. W., Real, M., Hermosin, M. C. and Cornejo, J. (2006). "The role of mineral and organic components in phenanthrene and dibenzofuran sorption by soil." European Journal of Soil Science, **57**(3): 308-319.

Chai, Y. Z., Kochetkov, A. and Reible, D. D. (2006). "Modeling biphasic sorption and desorption of hydrophobic organic contaminants in sediments." Environmental Toxicology and Chemistry, **25**(12): 3133-3140.

Connell, D. W. (2005). Basic concepts of environmental chemistry. Boca Raton, FL, CRC/Taylor & Francis.

Cornelissen, G., Rigterink, H., Ferdinandy, M. M. A. and Van Noort, P. C. M. (1998). "Rapidly desorbing fractions of PAHs in contaminated sediments as a predictor of the extent of bioremediation." Environmental Science & Technology, **32**(7): 966-970.

Cornelissen, G., Rigterink, H., Ferdinandy, M. M. A. and vanNoort, P. C. M. (1997). "Rapidly desorbing fractions of PAHs in contaminated sediments predict bioremediation results." Abstracts of Papers of the American Chemical Society, **214**: 168-ENVR.

D422-63 (2007). "Standard Test Method for Particle-Size Analysis of Soils." Annual Book of American Society for Testing and Materials (ASTM) Standards, **04.08**.

D4318-10e1 (2010). "Standard Test Methods for Liquid Limit, Plastic Limit, and Plasticity Index of Soils" Annual Book of American Society for Testing and Materials (ASTM) Standards **04.08**.

D4972-13 (2013). "Standard Test Method for pH of Soils." Annual Book of American Society for Testing and Materials (ASTM) Standards **04.08**.

Delille, D., Duval, A. and Pelletier, E. (2008). "Highly efficient pilot biopiles for on-site fertilization treatment of diesel oil-contaminated sub-Antarctic soil." Cold Regions Science and Technology, **54**(1): 7-18.

Feenstra, S., Mackay, D. M. and Cherry, J. A. (1991). "A Method for Assessing Residual Napl Based on Organic-Chemical Concentrations in Soil Samples." Ground Water Monitoring and Remediation, **11**(2): 128-136.

Fernandez, F. and Quigley, R. M. (1985). "Hydraulic Conductivity of Natural Clays Permeated with Simple Liquid Hydrocarbons." Canadian Geotechnical Journal, **22(**2): 205-214.

Gao, Y. Z., Ren, L. L., Ling, W. T., Gong, S. S., Sun, B. Q. and Zhang, Y. (2010). "Desorption of phenanthrene and pyrene in soils by root exudates." Bioresource Technology, **101**(4): 1159-1165.

Gill, R. T., Harbottle, M. J., Smith, J. W. N. and Thornton, S. F. (2014). "Electrokinetic-enhanced bioremediation of organic contaminants: A review of processes and environmental applications." Chemosphere, **107**: 31-42.

Grathwohl, P., Klenk, I. D., Maier, U. and Reckhorn, S. B. F. (2002). "Natural attenuation of volatile hydrocarbons in the unsaturated zone and shallow groundwater plumes: scenario-specific modelling and laboratory experiments." Groundwater Quality: Natural and Enhanced Restoration of Groundwater Pollution, (275): 141-146.

Gunasekara, A. S. and Xing, B. S. (2003). "Sorption and desorption of naphthalene by soil organic matter: Importance of aromatic and aliphatic components." Journal of Environmental Quality, **32**(1): 240-246.

Hardcastle, J. H and Mitchell, J. K. (1974). "Electrolyte Concentration-Permeability Relationships in Sodium Illite-Silt Mixtures." Clays and Clay Minerals, **22**(2): 143-154.

Hassan, I., Mohamedelhassan, E. and Yanful, E. K. "Solar powered electrokinetic remediation of Cu polluted soil using a novel anode configuration." Electrochimica Acta , **181**: 58-67.

Hatheway, A. W. (2002). "Geoenvironmental protocol for site and waste characterization of former manufactured gas plants; worldwide remediation challenge in semi-volatile organic wastes." Engineering Geology, **64**(4): 317-338.

Huang, W. L. and Weber, W. J. (1998). "A distributed reactivity model for sorption by soils and sediments. 11. Slow concentration dependent sorption rates." Environmental Science & Technology, **32**(22): 3549-3555.

Huang, W. L., Yu, H. and Weber, W. J. (1998). "Hysteresis in the sorption and desorption of hydrophobic organic contaminants by soils and sediments - 1. A comparative analysis of experimental protocols." Journal of Contaminant Hydrology, **31**(1-2): 129-148.

Kan, A. T., Fu, G. M. and Tomson, M. B. (1994). "Adsorption-Desorption Hysteresis in Organic Pollutant and Soil Sediment Interaction." Environmental Science & Technology, **28**(5): 859-867.

Kayal, S. I. and Connell, D. W. (1990). "Partitioning of Unsubstituted Polycyclic Aromatic-Hydrocarbons between Surface Sediments and the Water Column in the Brisbane River Estuary." Australian Journal of Marine and Freshwater Research, **41**(4): 443-456.

Khan, F. I. and Husain, T. (2003). "Evaluation of a petroleum hydrocarbon contaminated site for natural attenuation using 'RBMNA' methodology." Environmental Modelling & Software, **18**(2): 179-194.

Khan, F. I., Husain, T. and Hejazi, R. (2004). "An overview and analysis of site remediation technologies." Journal of Environmental Management, **71**(2): 95-122.

Letterman, R. D. (1999). Water quality and treatment: a handbook of community water supplies, McGraw-hill New York.

Lopez-Vizcaino, R., et al. (2014). "Removal of phenanthrene from synthetic kaolin soils by electrokinetic soil flushing." Separation and Purification Technology, **132**: 33-40.

Mackay, D. (2006). Handbook of physical-chemical properties and environmental fate for organic chemicals. Boca Raton, FL, CRC/Taylor & Francis.

Maurice, P. A., Haack, E. A. and Mishra, B. (2009). "Siderophore sorption to clays." Biometals, **22**(4): 649-658.

Niqui-Arroyo, J. L., Bueno-Montes, M., Posada-Baquero, R. and Ortega-Calvo, J. J. (2006). "Electrokinetic enhancement of phenanthrene biodegradation in creosote-polluted clay soil." Environmental Pollution, **142**(2): 326-332.

Pan, B., et al. (2006). "Distribution of sorbed phenanthrene and pyrene in different humic fractions of soils and importance of humin." Environmental Pollution, **143**(1): 24-33.

Reddy, K. R., Ala, P. R., Sharma, S. and Kumar, S. N. (2006). "Enhanced electrokinetic remediation of contaminated manufactured gas plant soil." Engineering Geology, **85**(1-2): 132-146.

Shang, J. Q., Lo, K. Y. and Quigley, R. M. (1994). "Quantitative-Determination of Potential Distribution in Stern-Gouy Double-Layer Model." Canadian Geotechnical Journal, **31**(5): 624-636.

Shi, L., Harms, H. and Wick, L. Y. (2008). "Electroosmotic flow stimulates the release of alginate-bound phenanthrene." Environmental Science & Technology, **42**(6): 2105-2110.

Souza, F. L., SaÃ©z, C., Llanos, J., Lanza, M. R. V., CaÃ±izares, P. and Rodrigo, M. A. (2016). "Solar-powered electrokinetic remediation for the treatment of soil polluted with the herbicide 2,4-D." Electrochimica Acta, **190**: 371-377.

Talley, J. W., Ghosh, U., Tucker, S. G., Furey, J. S. and Luthy, R. G. (2002). "Particle-scale understanding of the bioavailability of PAHs in sediment." Environmental Science & Technology, **36**(3): 477-483.

Terashima, M., Tanaka, S. and Fukushima, M. (2003). "Distribution behavior of pyrene to adsorbed humic acids on kaolin." Journal of Environmental Quality, **32**(2): 591-598.

Thompson, A. and Goyne, K (2012). "Introduction to the sorption of chemical constituents in soils." Nature Education Knowledge, **4 (7) (2012)** :15.

Thornton, S. F., Lerner, D. N. and Tellam, J. H. (2001). "Attenuation of landfill leachate by clay liner materials in laboratory columns: 2. Behaviour of inorganic contaminants." Waste Management & Research, **19**(1): 70-88.

Tsai, P. J., Shieh, H. Y., Lee, W. J. and Lai, S. O. (2001). "Health-risk assessment for workers exposed to polycyclic aromatic hydrocarbons (PAHs) in a carbon black manufacturing industry." Science of the Total Environment, **278**(1-3): 137-150.

Venkatramaiah C. Geotechnical Engineering (1995), Scond edition, New Age International publishers, New Delhi, India.

Wang, B. Y. (2007). Environmental biodegradation research focus, Nova Science Publishers

Watts, R. J. (1998). "Hazardous wastes: sources, pathways, receptors."

Weber, W. J. and Huang, W. L. (1996). "A distributed reactivity model for sorption by soils and sediments .4. Intraparticle heterogeneity and phase-distribution relationships under nonequilibrium conditions - Response." Environmental Science & Technology, **30**(10): 3130-3131.

Wood, D. M. (2004) Geotechnical Modelling, Spon Press, London and New York, Taylor&Francis Group.

Yamamuro, J. A. and Lade, P. V. (1997). "Static liquefaction of very loose sands." Canadian Geotechnical Journal, **34**(6): 905-917.

Yeung, A. T. and Corapcioglu, M. (1994). "Electrokinetic flow processes in porous media and their applications." Advances in porous media-volume 2.: 309-395.

Yeung, A. T. and Gu, Y. Y. (2011). "A review on techniques to enhance electrochemical remediation of contaminated soils." Journal of Hazardous Materials, **195**: 11-29.

Yeung, A. T., Hsu, C. and Menon, R. M. (1997). "Physicochemical soil-contaminant interactions during electrokinetic extraction." Journal of Hazardous Materials, **55**(1-3): 221-237.

Yong, R. N., Mohamed, A.-M. O. and Warkentin, B. P. (1992). Principles of contaminant transport in soils. Amsterdam ; New York, Elsevier.

Yuan, S. H., Zheng, Z. H., Chen, J. and Lu, X. H. (2009). "Use of solar cell in electrokinetic remediation of cadmium-contaminated soil." Journal of Hazardous Materials, **162**(2-3): 1583-1587.

# CHAPTER 4
# A NOVEL TECHNIQUE FOR pH STABILIZATION FOR ELECTROKINETIC BIOREMEDIATION[1]

## 4.1 INTRODUCTION

Contamination of soil and groundwater by petroleum hydrocarbons occurs in various operations including exploration and production of oil, transportation of crude and refined oil, and improper management of refinery waste. Petroleum hydrocarbons (PHCs) exist in the subsurface as separate phase liquids immiscible with both water and air, referred to as Non-Aqueous Phase Liquids (NAPLs). Very low concentrations of these compounds can threaten human health and the environment. Over the years, many remediation methods have been used with various degrees of success to mitigate petroleum hydrocarbon pollution. Among these methods, recent studies have investigated an innovative hybrid technique that joins electrokinetics and bioremediation. The aim of this hybrid approach is to accelerate the natural biodegradation of contaminants by increasing the opportunities for interaction between microorganisms and contaminants and activating the existing microbial community in the subsurface by delivering nutrients required to promote microbial growth (Acar et al. 1997; Budhu et al. 1997). In a bioremediation process, there is an optimum pH range at which the capability of specific microorganisms to degrade a particular contaminant is maximized. Most bacteria can live in a pH range between 6 and 8; however, special kind of bacteria can tolerate extreme pH values (<2 or >10). Although bacteria can adapt the cytoplasm pH to the surrounding environment by controlling the exchange of hydrogen ions (internal proton concentration) through the cell wall, the abrupt change in pH gradient across bacterial membrane has an adverse effect on bacterial growth and metabolism (Cotter and Hill 2003; Padan et al. 2005; Krulwich et al. 2011). In electrokinetic remediation, the electric field incites three transport mechanisms, namely: electroosmosis, electromigration, and electrophoresis along with electrolysis reaction at the electrodes.

[1]A version of this chapter has been submitted to Environmental Geotechnics

Electroosmosis is the movement of liquid in soil pores relative to a stationary charged soil particle under an applied electrical field. Electromigration is the transport of ions in the pores fluid towards the oppositely charged electrode whereas electrophoresis is the movement of charged colloids under an applied electrical field (Acar and Alshawabkeh 1993). Electrolysis reactions occur at the electrodes in an electrokinetic process and result in oxidation-reduction reactions (Alshawabkeh 2009). Oxidation takes place at the anode, which generates hydrogen ions (acid front) and liberates oxygen gas. On the other hand, reduction occurs at the cathode, which produces hydroxyl ions (base front) and disperses hydrogen gas (Acar and Alshawabkeh 1993).

Oxidation reaction at the anode:

$$2H_2O - 4e^- \rightarrow O_2(g) + 4H^+(aq) \quad (4.1)$$

Reduction reaction at the cathode:

$$4H_2O + 4e^- \rightarrow 2H_2(g) + 4OH^-(aq) \quad (4.2)$$

Where: $O_2$ (g) is oxygen in the gaseous phase, $H^+$(aq) is hydrogen in the aqueous phase, $H_2$ (g) is hydrogen in the gaseous phase, and $OH^-$(aq) is hydroxyl ions in the aqueous phase.

The acid front (i.e. $H^+$) moves towards the cathode by electromigration, electroosmotic flow, and diffusion and lowers the pH of the soil along its path. The hydroxide ions that form the base front travel towards the anode by electromigration and diffusion and elevate the pH of the soil in the vicinity of the cathode (Acar and Alshawabkeh 1993). The drastic change in soil pH (acidic near the anode and alkaline near the cathode) plays a very important role in the outcome of the mitigation of petroleum hydrocarbons by electrokinetic bioremediation (Alshawabkeh 2009). The development of pH gradient in the soil by electrolysis reactions of water is detrimental to the existence of bacteria and can subsequently decrease the effectiveness of electrokinetic bioremediation. For example,

Kim et al. (2010) observed that changes in soil pH during electrokinetics had reduced microbial cell number and microbial diversity.

Much research has investigated means to neutralize soil pH during electrokinetic remediation. This includes the use of ion selective membranes (Hansen et al. 1997); addition of chemical conditioning agents such as ethylenediaminetetraacetic (EDTA) (Reed et al. 1995; Wong et al. 1997), acetic acid and nitric acid (Denisov et al. 1996); continuous changing, removal and circulation of the solution in the electrode compartments (Niqui-Arroyo et al. 2006); polarity reversal (Luo et al. 2005; Pazos et al. 2006); and configurations of electrodes and electrical fields (e.g. unidirectional, bidirectional and rotational operations) (Luo et al. 2006). The practice of replacing the electrolyte solution results in solution pollution that requires treatment before release into the environment. The addition of a chemical conditioning agent is not favorable because it generates undesirable by-products and adds additional expense. Furthermore, the use of acids to control the pH level can acidify the contaminated soil which makes it very difficult, if not impossible, to restore soil to its previous condition (Hassan and Mohamedelhassan 2014).

Although polarity exchange may result in a neutral soil pH during electrokinetic bioremediation, the technique requires continuous pH monitoring which can be challenging and increase the overall cost of the process. Polarity exchange also results in bidirectional (i.e. the direction is reversed with polarity change) movement of the pore fluid, nutrients, and bacteria (Luo et al. 2005). The technique can increase bioavailability provided the time before polarity exchange is sufficient to cause the bidirectional movement. However, a long duration before polarity exchange increases the pH at the cathode and decreases the pH at the anode which is not favorable to the bioremediation process. For example, Kim et al. (2005a) stated that “it is not feasible to control the pH using the polarity exchange technique”. In a study by Pazos et al. (2006), it was found that the low pH environment induced at specific compartment when the electrode is used as an anode had not increased when the specific electrode used as a cathode. This provides

evidence that the polarity exchange technique can not be used to keep the pH at the electrode compartment to remain unchanged. Research by Kim and Han (2003) implemented the circulation of electrolyte solution in order to keep the pH at the electrode compartments neutral, an approach that can be effective and suitable for electrokinetic bioremediation treatment. However, the circulation of electrolyte solution (anolyte and catholyte) in a field application can be difficult and costly due to the need for continuous pumping during the treatment.

As the goal of bioremediation is to use microorganisms to degrade pollutants to less harmful products, the success of the technique would depend on the growth and reproduction of microorganisms. Often, nutrients are necessary to stimulate microbial growth and metabolism. Electrokinetics transports ions through the soil and allows for the control of the direction and magnitude of movement. Therefore, when combined with bioremediation, electrokinetics can deliver nutrients to indigenous bacteria in the soil and increase mixing between bacteria and contaminants. Many studies have investigated the delivery of nutrients using electrokinetics. For example, Schmidt et al. (2007) demonstrated the feasibility of transporting two common microorganism nutrients (nitrate and ammonium) by electrokinetics in a tropical clayey soil. The results, however, showed nonuniform nutrients distribution with a higher amount of nitrate transported to the soil in the vicinity of the anode compared with the ammonium transported to the soil near the cathode. Xu et al. (2010) observed that in electrokinetics bioremediation tests using polarity exchange to control pH, a relatively even distribution of nutrients in the soil was achieved compared with tests that used one direction electric fields. The results from electrokinetic bioremediations studies have shown that electrokinetics is successful in delivering nutrients to indigenous bacteria. However, excessive amounts of nutrients in soil can exploit microbial growth and increase the population of microorganisms and consequently lead to clogging of soil pores and, eventually, fouling (Kim and Han 2003). Therefore, it is important to study and carefully plan for the addition of nutrients. The implementation of the aforementioned approaches in field applications increases the complexity of the process and needs either the addition of chemical compounds or

provision of extra personnel supervision/intervention or both. Thus, the overall cost of the remediation process increases regardless of the improvement in the effectives of the process.

In electrokinetic bioremediation applications, the control of soil pH is crucial for a successful treatment. The methods presented to date in the literature show great advancements in the effort to control pH during electrokinetic applications. However, more research should be conducted to further improve existing methods and to develop new and innovative techniques to control the pH during the electrokinetic bioremediation applications. To date, no innovative low cost pH control techniques have yet been investigated.

The present study proposes a novel approach, anode-cathode-compartment (ACC), to stabilize pH and distribute nutrients in soil in order to enhance electrokinetic bioremediation of soil contaminated with biodegradable compounds. The goal of the study is to demonstrate the effectiveness of the novel ACC approach in keeping soil pH and water content relatively unchanged during an electrokinetic process. The distribution of nutrients in the soil by electrokinetics employing ACC configuration was examined and compared to distribution using conventional anode-cathode (CAC) configuration. The new proposed ACC technique overcomes the shortcomings of other pH stabilization techniques by stabilizing the pH without the need for pumping or amendments while maintaining the resultant electroosmotic and electromigration movement in one direction.

## 4.2 EXPERIMENTAL PROGRAM

Inorganic kaolinite clay soil, 96-99.9% (by mass) kaolinite (EPK case number 1332-58-7), purchased from EdgarMinerals, Florida, US, was used in the experiments. Sieve analysis on the soil revealed that all particle sizes were less than 0.075 mm (passed No. 200 sieve).

Accordingly, hydrometer analysis was conducted in accordance with ASTM D422-63 (D422-63 2007) to obtain the particle size distribution. Atterberg limits (liquid and plastic limits) were determined following ASTM D4318-10e1 (D4318 2010). Soil pH was determined in accordance with ASTM D4972-13 (D4972-13 2013). Cation exchange capacity was determined using ammonium acetate and potassium chloride as extractants in order to obtain first soluble cations and then bound or exchangeable cations. Inductively coupled plasma-optical emission spectroscopy (ICP-OES) was used to determine the cations concentration in solution. The specific surface area of the kaolinite clay was determined using Micromeritics Gemini instrument. The physico-chemical and geotechnical properties of the kaolinite clay are presented in Table 4.1.

**Table 4.1** Soil physicochemical properties

| Soil property | Measured value |
|---|---|
| Liquid limit | 64% |
| Plastic limit | 35% |
| $e_{max}$ | 3.1 |
| $e_{min}$ | 0.92 |
| Organic carbon content ($f_{oc}$) | 0.45% |
| pH | 4.2 |
| Cation exchange capacity | 3.75 meq/100g of soil |
| Specific surface area | 28.75 $m^2/g$ |

In general, there are two separate water compartments in a conventional electrokinetic (conventional anode cathode CAC) remediation setup. One compartment houses the anolyte solution and the anode electrode where hydrogen ions (i.e. acid front) are produced by electrolysis reactions. The other compartment hosts the cathode and catholyte solution and in this compartment the base front (hydroxyl ions) is generated. This study proposes a

novel configuration (anode-cathode compartment ACC) in which the electrokinetic cell is divided into two water compartments and a soil specimen chamber in between. Each water compartment houses an anode and a cathode, as shown in Figure 4.1. The first water compartment hosts Anode $A1^{+}$ and Cathode $A2^{-}$ and the second compartment contains Anode $A2^{+}$ and Cathode $A1^{-}$. In the first electrokinetic cell, the electrodes are connected to the power supply using two electric circuits, electric circuit 1 was between Anode $A1^{+}$ and Cathode $A1^{-}$, and electric circuit 2 was connecting Anode $A2^{+}$ to Cathode $A2^{-}$ (in the second and third electrokinetic cells electric circuits 1 was between $B1^{+}$ and $B1^{-}$ and $C1^{+}$ and $C1^{-}$ and electric circuit 2 connected $B2^{+}$ to $B2^{-}$ and $C2^{+}$ to $C2^{-}$). The hypothesis is that the coexistence of an anode and a cathode in the same water compartment will result in the hydrogen ions generated at the anode neutralizing the hydroxyl ions produced at the cathode and thereby forming water. In accordance with equations (4.1) and (4.2), the proposed novel configuration is assumed to generate equivalent numbers of hydrogen ions and hydroxide ions with all the ions reacting to form water.

In the present study, an Electrokinetic Voltage Controller (EKVC) device (Figure 4.1) was designed and manufactured to switch the electric potential between the two electric circuits such that at any given time there is only one electric current running through either electric circuit 1 or 2 in the electrokinetic cell. The EKVC takes an input of dc voltage of up to 50 V and has six output ports and a programmable timer. These output ports are arranged in two groups of three outputs. For each output port, there are four switched voltage points. Three of the voltage points are used to monitor the voltage distribution across the soil and one to record the electric current. These points are switched to three groups of a four data acquisition points. The voltage distribution profile (at three points) across the soil under treatment and the electric current through the soil are monitored using the voltage points connected to data acquisition terminals (National Instruments). A computer code has been written using the software Labview 2013 to connect the data acquisition terminals with a PC and record the data.

The EKVC alternates the voltage between outputs groups at a set programmable time. The timer can be set to alternate the voltage between the two electric circuits for intervals from thirty seconds to six minutes in thirty second steps. The EKVC can be connected to up to three electrokinetic cells. For instance, EKVC can be connected to electrokinetic cell such that A1+ and A1- form the first electric circuit and the second electric circuit is connected between A2+ and A2-. Also, the EKVC controls the duration time of the electric current delivered through the electric circuits. In this study the EKVC is set to control the current through the two electric circuits in a complete cycle of nine minutes. First, the current is delivered through the first electric circuit (between anode A1+ and cathode A1-) for three minutes. The current is then delivered through the second electric circuit (between anode A2+ and cathode A2-) for three minutes followed by an off period of three minutes for both circuits. The EKVC can be set for any desired time setup. The off time (three minute) has been selected based on preliminary tests that were conducted to determine the time required for neutralization of hydrogen and hydroxyl ions in the water compartments. In the preliminary tests, the pH was measured at five locations (V, W, X, Y, and Z in Figure 4.3) in the electrodes compartment. At the beginning, the test was conducted with 1 min on and 1 min off. It was found that the off period is not enough for the pH probe reading to be stabilized. The EKVC was then set to 2 min on and 2 min off. The pH probe readings showed that the pH in the water compartment varied in the five locations (see Figure 4.4). The pH in the water compartment was stabilized when the time was set to 3 min on and 3 min off (see Figure 4.5). The off time needed for pH neutralization may vary depending on the properties of the soil and electrolyte solutions as well as the voltage gradient and electrode material.

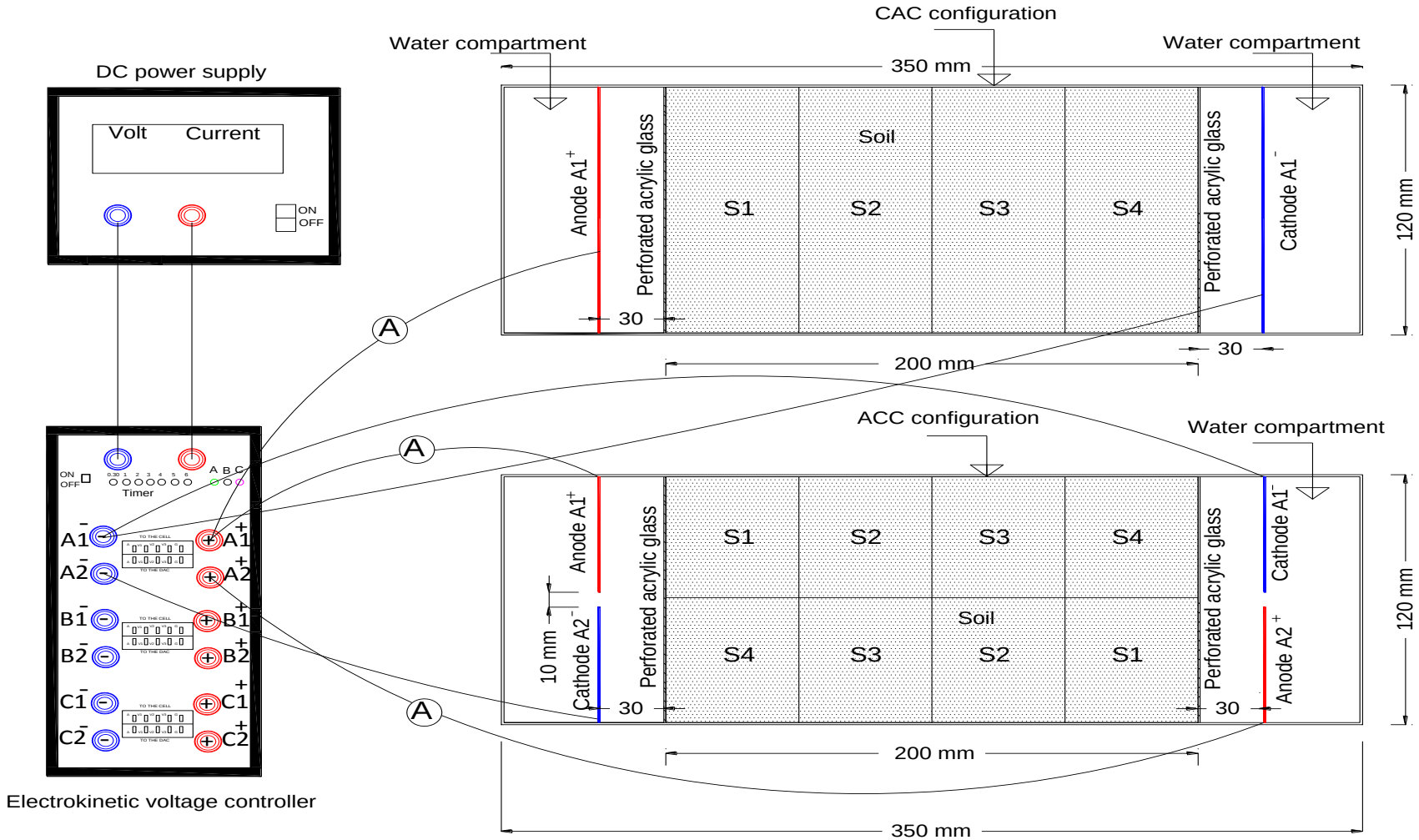


**Figure 4.1** Schematic of the experimental setup CAC and ACC electrode configuration (top view)

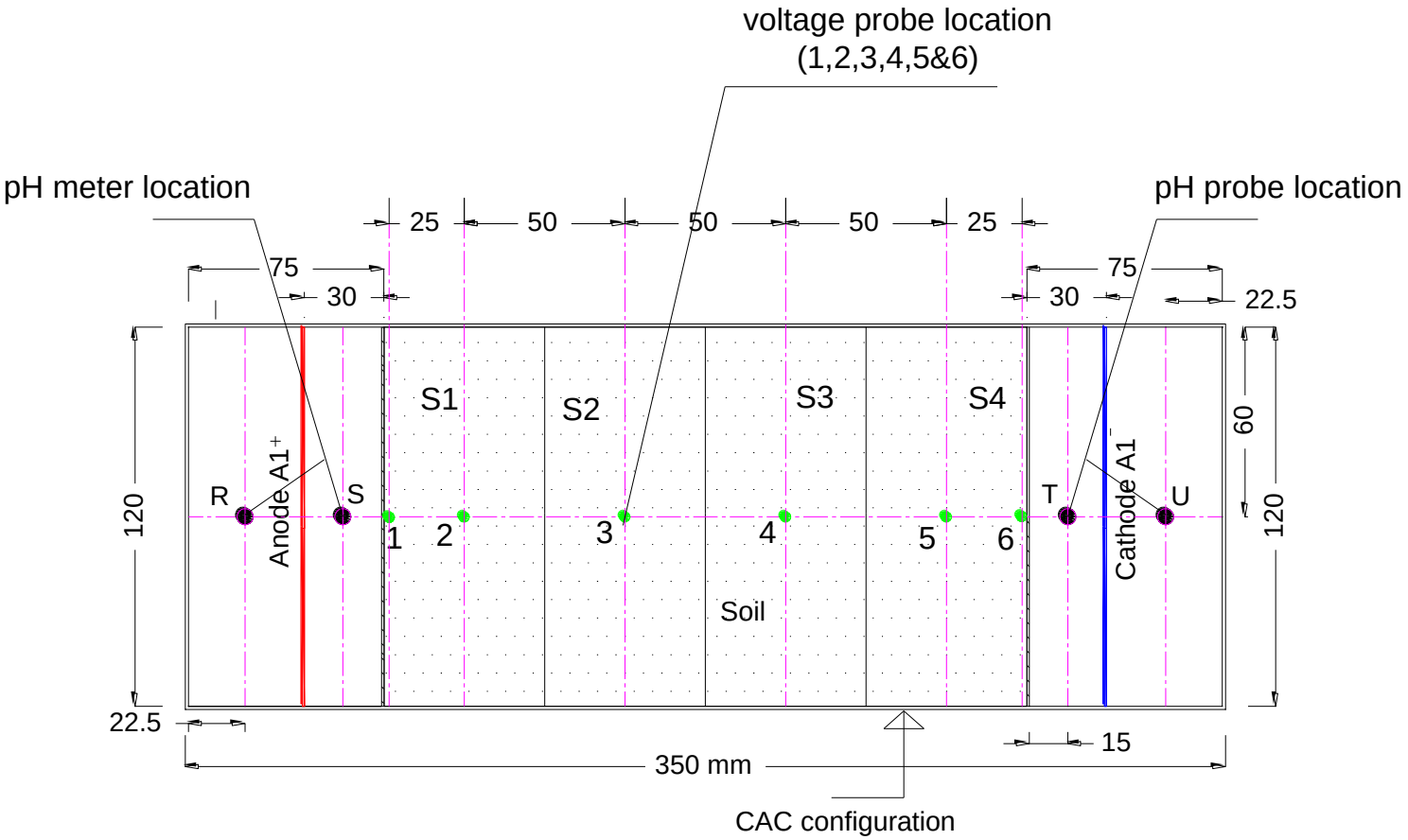


**Figure 4.2** Soil sections after the test, voltage probes, and pH meter position in CAC configuration tests

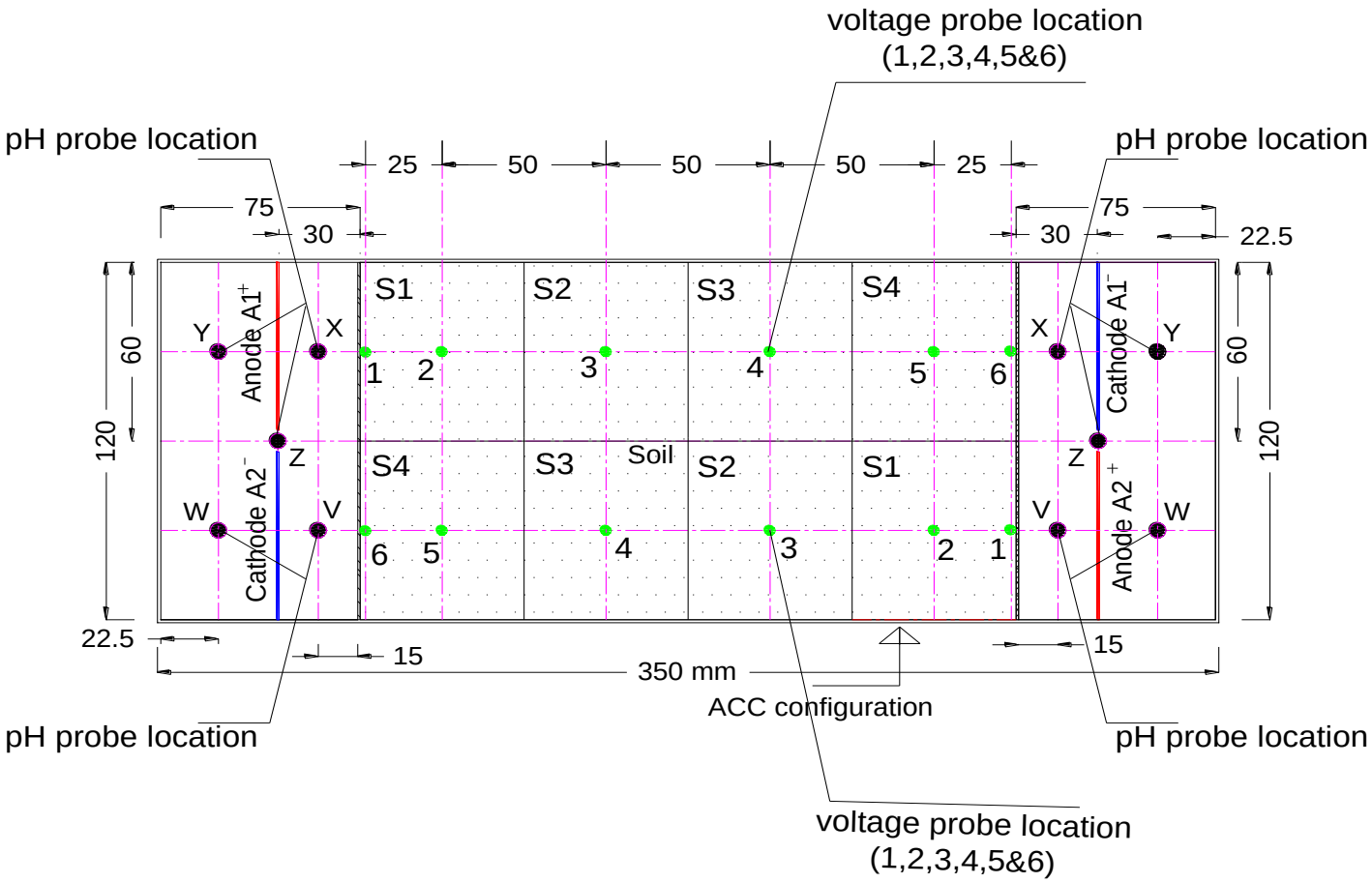


**Figure 4.3** Soil sections after the test, voltage probes, and pH meter position in ACC configuration tests

The experimental equipment consisted of six identical electrokinetic remediation cells, a soil pore fluid squeezer, digital multimeter (U1241A Agilent), and a DC power supply. The electrokinetic remediation cell, constructed from clear Plexiglas plates 12 mm in thickness, has inner dimensions of 350 mm × 120 mm × 100 mm (length × width × height), as shown in Figure 4.1. The cell is composed of upper part, base, cover, and two movable rectangular perforated Plexiglas (120 mm × 100 mm). The upper part forms the outer boundaries that accommodate the soil specimen. One side of the upper part is detachable to allow for easy recovery and minimum disturbance of soil samples used for subsequent parametric studies after an electrokinetic test. The cover has four small holes located at equal distances to make provision for four voltage probes used to monitor the voltage gradient across the soil specimen during the test. The soil pore fluid squeezer cell is composed of steel cylinder, steel piston, and a grooved base with porous plate and a drainage line. The steel cylinder inner dimensions are 50 mm in diameter and 100 mm long. The multimeter was used to measure the voltage at probe location 1 and 6 as shown in Figure 4.3.

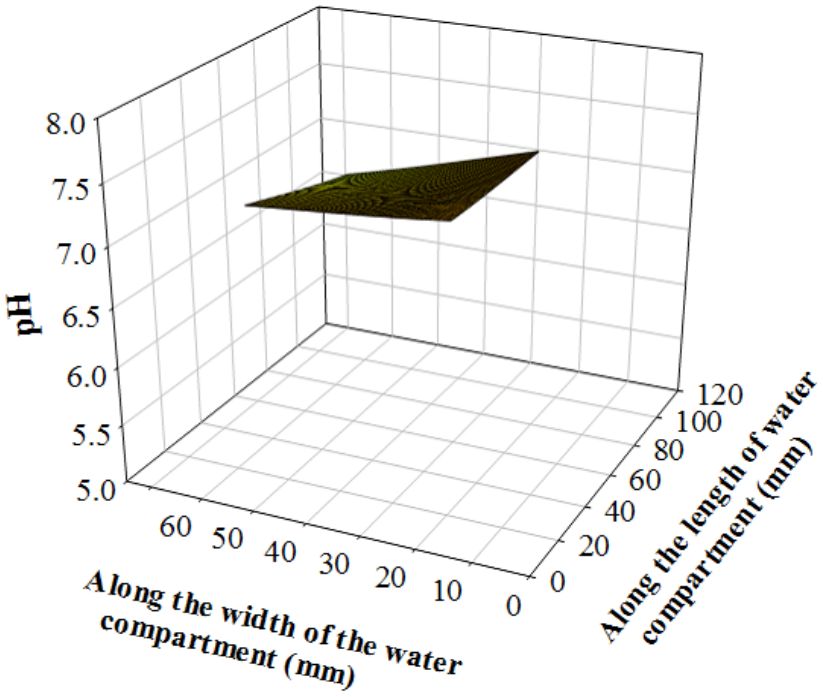


**Figure 4.4** pH for ACC test operating at 2 min on and 2 min off

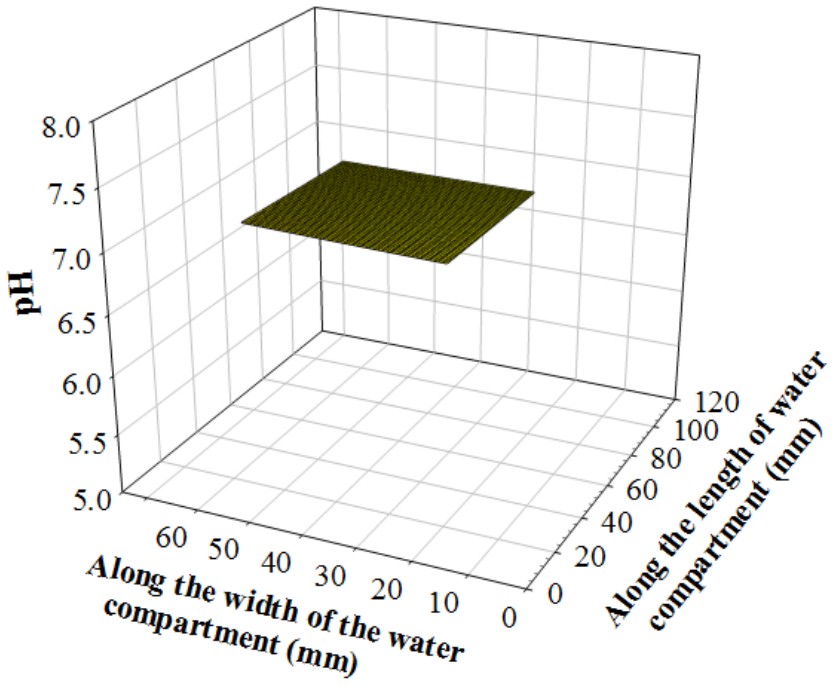


**Figure 4.5** pH for ACC test operating at 3 min on and 3 min off

Prior to preparing the soil specimen, a dry soil sample was autoclaved at 120$^{o}$C for 30 min and de-ionized water was irradiated with UV for the purpose of disinfection. The autoclaved soil was weighed and the volume of de-ionized water required for a water content of 60% (similar to the liquid limit) was measured and poured in a container. Mercury chloride ($HgCl_2$) 5g/kg dry soil and 100 mg/L sodium azide ($NaN_3$) were added to suppress the growth of microorganisms as described by previous researchers (Ishikawa et al. 2006; Suni et al. 2007). Electrokinetics cells were washed using 70% ethanol and placed in a biosafety cabinet under a UV light over night to kill any microorganisms. The soil specimen was prepared by thoroughly mixing the clay soil with water using a mechanical mixer. In the ACC, the electric field was applied using four stainless steel electrodes, each 76 x 55 x 1.5 mm (length × width × thickness), that were placed in the water compartments where one pair of electrodes served as the anodes and the other pair as the cathodes. The two electrodes for each pair were placed 10 mm from each other as

shown in Figure 4.1. Whereas for CAC, the electric field was applied using two stainless steel electrodes, each 76 x 110 x 1.5 mm (length × width × thickness), that were placed in the water compartments where one electrode served as the anode and the other as the cathodes as shown in Figure 4.1. A geotextile filter was wetted by water and situated between the electrodes and the perforated acrylic glass. The soil was placed into the electrokinetic cell in three layers for a total height of 60 mm. Each layer was rodded (tamped) using steel rod to prevent the entrapment of air pockets and to produce soil specimens with similar densities. The high water content of the soil and the thorough rodding (tamping) during placement in the cell insured that the soil specimen was nearly, if not fully, saturated. Sodium nitrate, $NaNO_3$ 1 g/L, solution was prepared and used as anolyte and catholyte. Other electrolyte compositions due to clay contact with water are shown in Table 4.2.

Two set of tests were conducted in triplicates (see Table 4.3). The first set represents the conventional anode-cathode (CAC) electrode configuration in electrokinetics and serves as a control. The proposed novel anode-cathode-compartment (CAC) technique includes two electric circuits and two electrodes in each water compartment.

Electric current, voltage across the soil, and pH in the water compartments were monitored and recorded during the tests. Voltage across the soil was recorded using the data acquisition and the multimeter. At the end of each test, the soil was extruded from the cell and divided into four equal sections in the CAC test; S1, S2, S3, and S4 (see Figure 4.2) and eight similar sections in the ACC test, S1 to S4 in circuit 1 and circuit 2 (see Figure 4.3). The water content and pH were determined for each section. Part of the soil from each section was squeezed and the pore fluid was collected. The pH and electrical conductivity of the pore fluid were determined using pH and electrical conductivity probes. Also, nitrate ($NO_3$) concentration was determined using high pressure liquid ion chromatograph.

**Table 4.2** Composition of electrolyte

| Ions | mg /L |
|---|---|
| $Ca^{2+}$ | 0.94 |
| $K^{+}$ | 0.32 |
| $Mg^{2+}$ | 0.19 |
| $Na^{+}$ | 270.12 |
| $Al^{3+}$ | 0.13 |
| $Ba^{+}$ | 0.02 |
| $Fe^{3+}$ | 0.01 |
| $NO_3^{-}$ | 729.00 |
| $Cl^{-}$, $SO_4^{-2}$, $PO_4^{3-}$ (under detection limit)* | |

**Table 4.3** ACC and CAC tests layout

| Cell | Applied voltage (V/cm) | Electrode in first water compartment | Electrode in second water compartment | Test duration (h) | Current interval min | electric circuits |
|---|---|---|---|---|---|---|
| CAC test 1 | 2 | Anode | Cathode | 312 | 3 min on 6 min off | Circuit 1 |
| CAC test 2 | 2 | Anode | Cathode | 312 | 3 min on 6 min off | Circuit 1 |
| CAC test 3 | 2 | Anode | Cathode | 312 | 3 min on 6 min off | Circuit 1 |
| AAC test 1 | 2 | Anode A1 | Cathode A1 | 312 | 3 min on 3min off | Circuit 1 |
| | | Cathode A2 | Anode A2 | | | Circuit 2 |
| AAC test 2 | 2 | Anode B1 | Cathode B1 | 312 | 3 min on 3min off | Circuit 1 |
| | | Cathode B2 | Anode B2 | | | Circuit 2 |
| AAC test 3 | 2 | Anode C1 | Cathode C1 | 312 | 3 min on 3 min off | Circuit 1 |
| | | Cathode C2 | Anode C2 | | | Circuit 2 |

# 4.3 RESULTS AND DISCUSSION

## 4.3.1 pH

In the electrokinetics tests with conventional-anode-cathode configuration (CAC test 1, CAC test 2, and CAC test 3), electrolysis reactions of water at the electrodes decreased the pH in the anode compartment from 7.5 to around 2 and increased the pH in the cathode compartment from 7.6 to approximately 11. In the tests with the novel anode-cathode-compartment configuration (ACC test 1, ACC test 2, and ACC test 3), the pH of the water in the two compartments remained relatively unchanged (7.5 to 7.6 before the test and 7.7 to 7.8 after the test).

Figure 4.6 shows the profile of soil pore fluid pH after electrokinetic treatment with CAC and ACC configurations. In agreement with the change in pH in the water compartment caused by electrolysis reactions and the movements of the acid and base frons in tests with CAC configuration, Figure 4.6 shows that the pH in section S1 (near the anode) decreased to 2.5 and the pH in section S4 (close to the cathode) increased to 6.5 compared to an original pH of 4.2 before the test. Figure 4.6 indicates that the pH of the pore fluid in sections S2 and S3 remain relatively close to the original pH. In an electrokinetic bioremediation treatment, a low pH environment (observed in soil pore fluid near the anode) has a detrimental effect on microorganisms. Likewise, pore fluid of high pH (found in the soil near the cathode) results in unfavorable conditions and reduces the chance for microbial growth.

The novel anode-cathode-compartment (ACC) configuration allows the hydrogen ions generated by electrolysis reactions at the anode to neutralize the hydroxyl ions formed at the cathode and produce water. Unlike the tests performed with CAC configuration, the pH values obtained after tests carried with ACC configuration varied narrowly between 3.8 and 4.5. This clearly shows the effectiveness of the novel technique in keeping the pH of

the soil unchanged during an electrokinetic bioremediation treatment. The relatively unchanged pH of the water compartment and of the soil pore fluid confirms our hypothesis. Microorganisms may tolerate a low or high pH environment by controlling the exchange of hydrogen ions through their cell membrane. However, the abrupt change in pH as seen in tests with CAC configuration (Figure 4.6) has a very negative impact on the growth and metabolism of the microorganisms. The novel ACC configuration achieves the goal of keeping the pH of the entire soil pore fluid uniform.

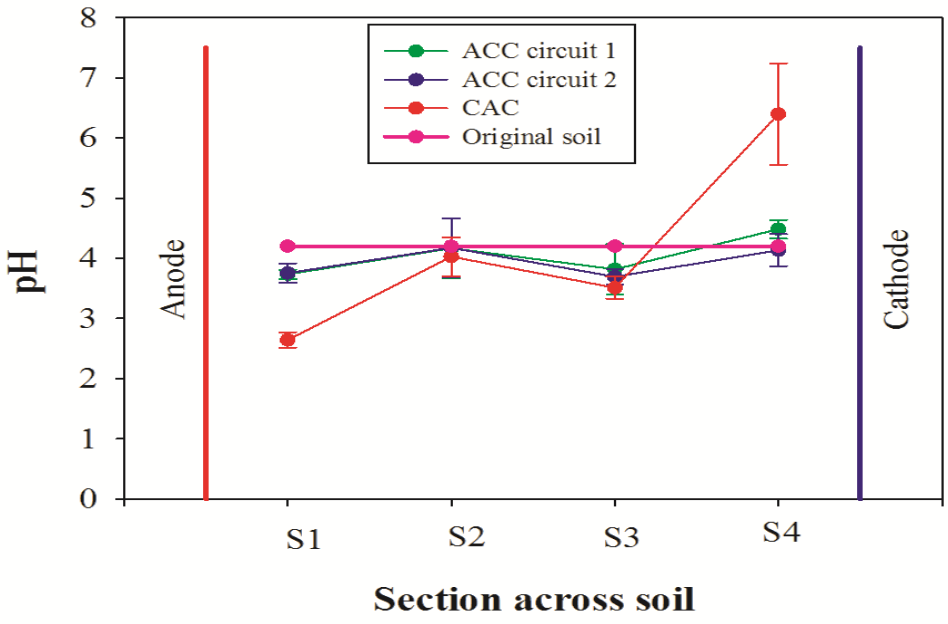


**Figure 4.6** pH of original soil, soil pore fluid in control CAC tests, and ACC for electric circuit 1 and circuit 2

## 4.3.2 Electric current and voltage gradient

Figure 4.7 shows the current density during the conventional anode-cathode (CAC) configuration tests (CAC test 1, CAC test 2, and CAC test 3) and the tests carried with novel anode-cathode-compartment (ACC) configuration (ACC test 1, ACC test 2, and ACC test 3). The results showed that the current had decreased drastically during the three

CAC tests and reach only 25% on the initial current density at the end of the test. The decrease in electric current directly resulted from a decreased in the electrical conductivity of the soil. The bulk electrical conductivity of a soil mass is a product of the electrical conductivity of the soil pore fluid and the soil solids with the conductivity of the former generally being much higher. As a result of the changes in the pore fluid chemistry (i.e. precipitation of ionic species due to changes in pH) and quantity (i.e. reduction in water content of the soil) during an electrokinetic process, the electrical conductivity of the soil and subsequently the electric current in the soil generally decrease with time (Mohamedelhassan 2009). The decrease in current is also due to the meeting of the acid and basic fronts into the soil since it yielded $H_2O$ and removed ions that transport charge (Pazos et al. 2006). The change in the pore fluid chemistry induces shrinkage of the double layer and consequently a higher charges concentration in the diffuse layer resulting a potential reduction between the stern and diffuse layer and as a drop in the electric current (Reddy and Cameselle 2009). Thus, the change in the pore fluid pH plays a primary role in the decay of the electric current, in particular if water is provided at the anode and the change in the water content of the soil is not drastic, during an electrokinetic process.

Contrary to the CAC test, Figure 4.7 shows that in ACC tests the current density slightly increased during the first 48 h of the test and then remained relatively unchanged afterward. The current density marginally increased again after 216 h. In general however, the current density during most of the test was 0.01 $mA/mm^2$ ±15%, showing a small variation in comparison with the CAC tests. Since the pH of the pore remained relatively unchanged, the slight increase in the current can be attributed to the increase in the electrical conductivity of the soil caused by the transposition of the $NaNO_3$ from the electrode compartment into the pores of the soil (presented in section 4.3.4).

The more stable electrical current in ACC tests is favourable for an electrokinetic bioremediation process as it will enhance the nutrients delivery and uniformity into the

soil. It worth noting the low current density used in this study was chosen to avoid the adverse effect of high current on indigenous bacteria as report by Tiehm et al. (2009).

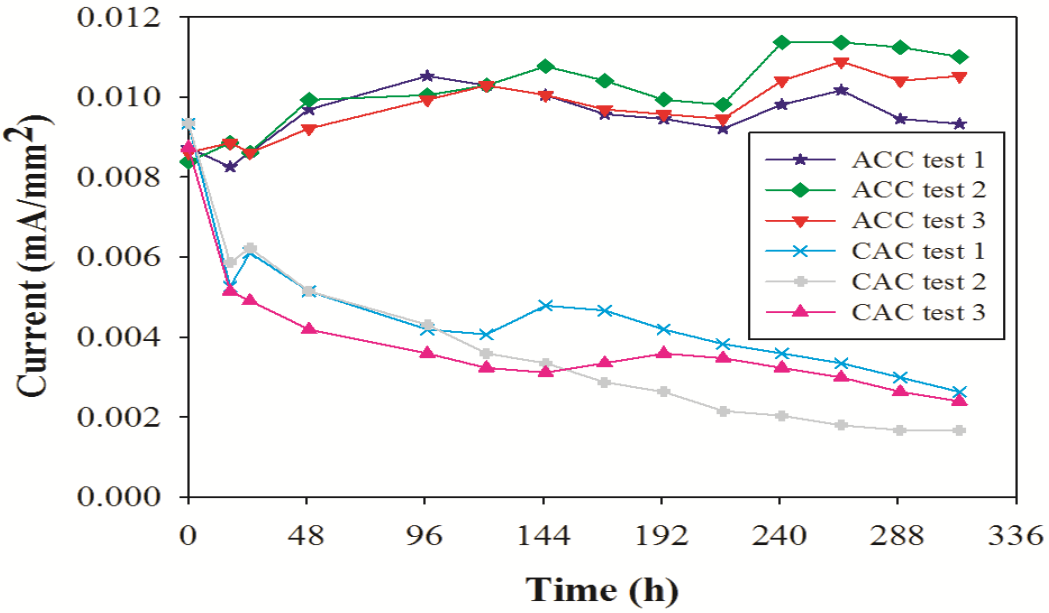


**Figure 4.7** Electric current density during electrokinetic tests

As ACC with a constant applied voltage is shown to be successful in keeping the pH of the soil pore fluid to remain relatively unchanged, it had kept the electrical conductivity of the soil approximately the same. This was evidence by the small changes in the current density during the test. This research is a part of a bigger project aimed at promoting the use of solar energy as the source of electricity for electrokinetic bioremediation as recent studies have shown that inexpensive solar panels can generate enough energy for electrokinetics (Yuan et al. 2009, Hassan and Mohamedelhassan 2012). The goal is to introduce an integrated solar electrokinetic bioremediation system with an economically viable initial cost and a low running cost that is independent of power from the grid. The solar panels will be connected directly to the electrodes in the bioremediation system without the need for DC transformers. The voltage generated by a solar cells panel is predictable and fairly stable during most of the daytime hours. The effectiveness of novel ACC configuration in

controlling the pH of the pore fluid using a constant voltage is very promising for using ACC with solar cell panels.

The voltage gradient during the ACC and CAC is presented in Figure 4.8. The drop in the voltage at the anode-soil interface was high in the CAC test compared to the ACC test. This means that an electrokinetic treatment using ACC can be more efficient than with CAC. Moreover, the electric potential across the soil in ACC test is higher than in CAC test, that suggests more favorable ion transportation by electromigration with ACC configuration.

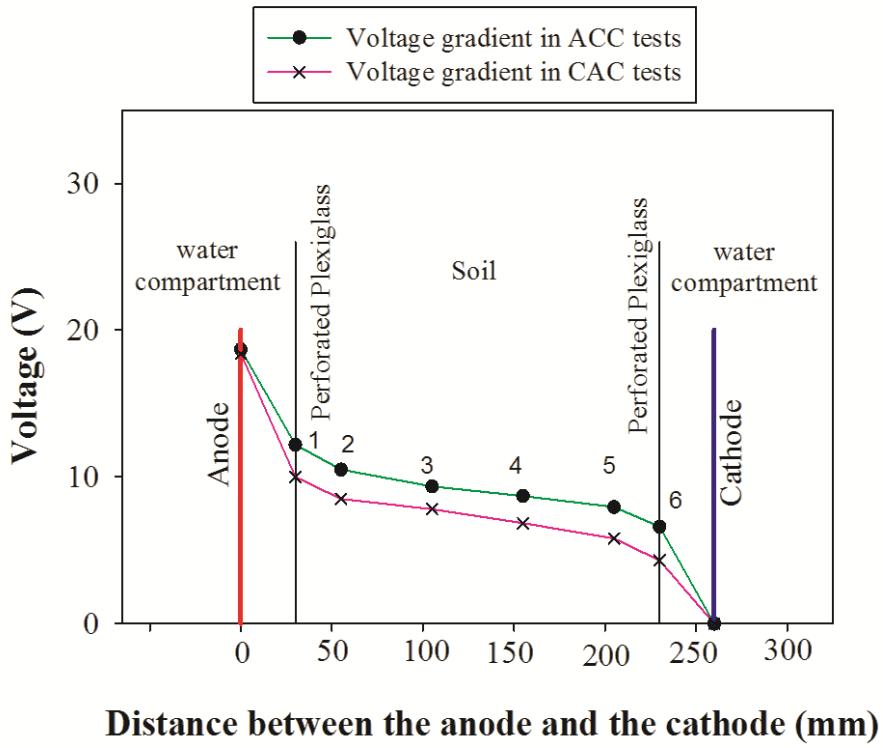


**Figure 4.8** Voltage gradients during CAC and ACC tests

### 4.3.3 Water content

The water content of a contaminated soil plays a dominant role in the outcome of a bioremediation process. For instance, the presence of the pore fluid is crucial to provide the medium necessary for the interchange and transport of the nutrients in subsurface. But the more important aspect is the dissolved oxygen in the pore fluid which is vital for aerobic bioremediation process (Ribeiro et al. 2015). Figure 4.9 shows the water content across the soil specimen after CAC and ACC tests. The water content varies across the CAC cell with higher water content in section S1 (near the anode) and lower water content near the cathode (section S4). In bioremediation applications when the soil dries out, the indigenous bacteria form spores. In contrast, the water content in the soil sections after the test with the novel ACC configuration were fairly uniform. The presence of uniform water content across the soil yields a uniform dissolved oxygen concentration which would be beneficial for the growth of microorganisms present in the soil (Ribeiro et al. 2015).

In an electrokinetic process, the water in the pores of a negatively charged soil such as kaolinite is transported by electroosmotic flow from the anode to the cathode. In a system that provides water to anode compartment to replace water drained at the cathode, similar to this experimental setup in this study, the water content of the soil is expected to remain relatively unchanged provided that the electroosmotic flow in the soil is uniform and there is no change in the soil temperature. Figure 4.9 shows the water content of the soil generally decreased in both ACC and CAC tests compared with the original water content with the decrease in the former being more uniform. The decreased in water content is likely caused by a non-uniform electroosmotic flow in the soil and/or the heating effect associated with electrokinetics. Mohamedelhassan et al. (2005) showed that the temperature of the soil increased by up to $15^{o}$ C in electrokinetic tests with a voltage gradient and a current density comparable to this study.

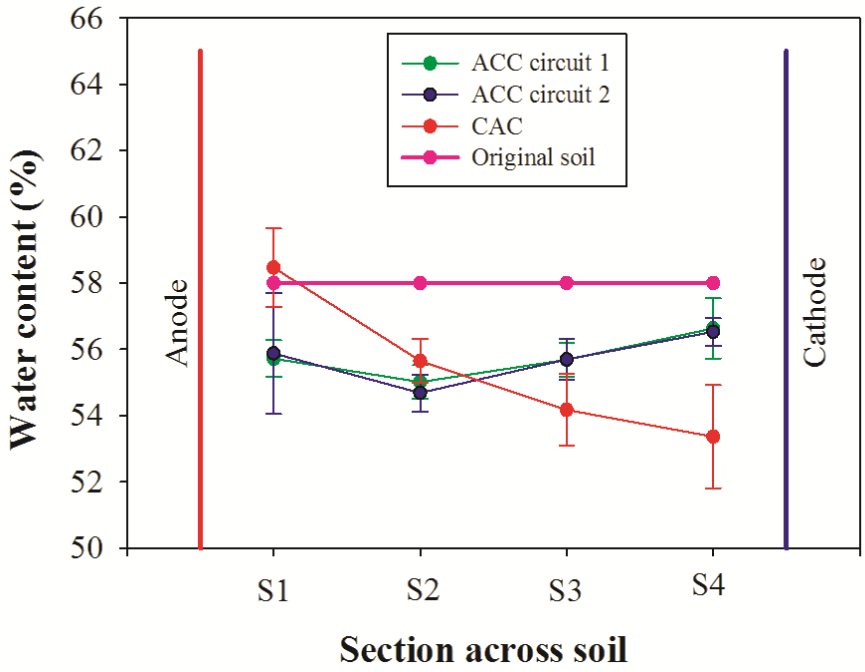


**Figure 4.9** Water content in original soil, control CAC, and ACC electric circuit 1 and circuit 2

In Helmholtz-Smoluchowski model, widely accepted by researchers to quantify electroosmotic flow, the flow rate is proportional to the zeta potential (Mitchell and Soga 2005). Studies have shown that the zeta potential of a clay soil is very sensitive to the pH of the pore fluid. For example, the study by Vane and Zang (1997) has shown that the zeta potential for a kaolinite soil ranged from +0.7 mV at pH of 2 to -54 mV at pH of 10. Also, it found that the coefficient of electro-osmotic permeability to be three times greater at pH of 5 than at pH of 3. The non-uniform change in the water content of the CAC tests is likely due to the non-uniform electroosmotic flow in the soil caused by the changes in the pH of the pore fluid (Figure 4.6) and the subsequent change in the zeta potential. This can be qualitatively illustrated by comparing Figures 4.6 and 4.9. As shown in the figures, the highest pH and the lowest water content were in section S4 which is consistent with the Helmholtz-Smoluchowski model since the highest zeta potential and the highest water

drained from soil by electroosmosis is expected in S4. Likewise, the lowest pH and highest water content was found in section S1. The relatively uniform decrease of the water content in the ACC tests is likely caused the heating of the soil by electrokinetics as the pH of the pore fluid (Figure 4.6) remained fairly uniform suggesting a more uniform electroosmotic flow. Luo et al. (2005) presented that the water content in electrokinetic test with polarity exchange varied by 5% across the soil. The water content of the soil after electrokinetic with electrolyte circulation to control the pH has not been discussed in the available literature (Kim and Han 2003; Kim et al. 2005a; Mao et al. 2012; Wu et al. 2012). As far as we know this is one of the first studies that presented the water content of the soil when the pH was kept relatively the same during an electrokinetic process.

### 4.3.4 Nutrient distribution

Nitrate is required for the growth and metabolism of microorganisms that are capable of degrading petroleum hydrocarbons contaminants. In an electrokinetic bioremediation process, the nitrate is transported from the electrode compartment to the soil pores by electroosmotic and electro migration. Figure 4.10 shows the nitrate distribution after the tests with CAC and ACC configuration. As seen in the figure, in the CAC tests the highest nitrate concentration was found in section S1 near the anode and that the concentration decreased drastically in the subsequent sections toward the cathode (sections S2, S3, and S4). For example, while a nitrate concentration of 2700 mg/L was reported at S1 a significantly lower nitrate concentration of 105 mg/L was found in S4. The nitrate concentration profile is in agreement with previous studies by Tiehm et al. (2010) and Xu et al. (2010). It has been reported in the literature that a high concentration of nitrate near the anode has an adverse effect on the remediation process because microorganisms in the soil tend to consume the nitrate and grow rapidly causing biofouling and clogging of the soil voids (Rabbi et al. 2000; Kim and Han 2003). The drastically uneven distribution of nitrate concentrations in the soil indicates that the conventional anode–cathode (CAC) configuration in electrokinetic bioremediation may be not only ineffective in nutrients delivery but, it may also introduce biofouling and clogging of soil pores.

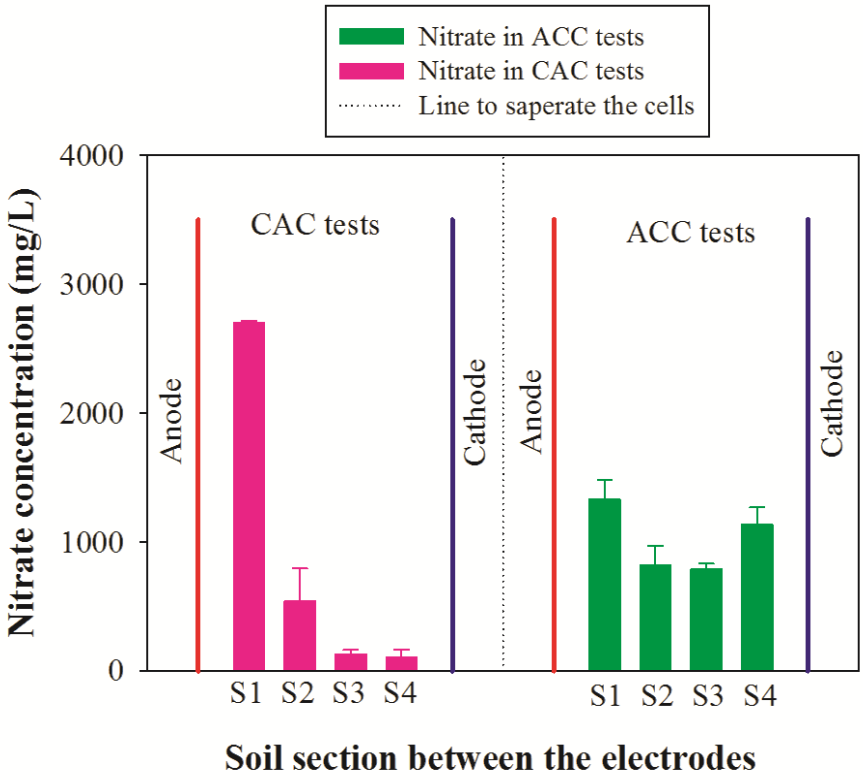


**Figure 4.10** Nitrate concentrations in the pore fluid after the CAC and ACC tests

On the other hand, the tests conducted using the novel anode-cathode-compartment (ACC) showed a more uniform nutrients distribution across the soil specimen (see Figure 4.10) with maximum and minimum nitrate concentrations of 1300 mg/L and 800 mg/L. Table 4.2 shows that nutrients distribution in the soil sections. The results show that total amount of $NaNO_3$ delivered by ACC (854 mg) is comparable to that delivered by CAC (754 mg) (The data in Table 4.4 is calculated using the water content in the soil sections and the mass of soil in each section). The recovery was 97% and 96% in the test conducted with ACC and CAC, respectively. The success of ACC in the more even nutrients delivery can be attributed to the more uniform pore fluid pH and electroosmotic flow and the steady electric current, as discussed before.

These results demonstrate the superiority of ACC over other conventional anode cathode configurations and other pH stabilization techniques in delivering more uniform nutrients into the soil. For instance, the polarity exchange technique can neutralize the pH across the soil section, but it also generates bidirectional electroosmotic flow and consequently a non-uniform nutrients distribution (Pazos et al. 2006). In this study one dimensional electrode configuration was used where electrode surface area covered most of the cross sectional area of the soil under treatment. Decreasing the spacing between the electrodes (opposite polarity) in the same compartment minimizes the area of inactive electric field, but increases the overall cost of the treatment (Alshawabkeh et al. 1999). The ACC technique can be further optimized by changing the distance between the electrodes in the same compartment.

**Table 4.4** Nutrients distribution (mass balance)

| | $NaNO_3$ (mg) | |
|---|---|---|
| | ACC | CAC |
| S1 | 278.60 | 592.70 |
| S2 | 168.90 | 113.80 |
| S3 | 165.60 | 26.60 |
| S4 | 241.00 | 21.10 |
| Electrolyte solutions | 197.90 | 292.50 |
| Total | 1052.00 | 1046.70 |

(Initial $NaNO_3$ in water compartments 1092 mg)

This study addresses application of new innovative approach to solving an existing challenge. The development of acid and base fronts by electrolysis reactions of water is considered a major drawback for using electrokinetic assisted bioremediation. This research proposed and investigated a new electrode configuration to stabilize the pore fluid pH during electrokinetics bioremediation. The results showed that the technique was

successful in keeping the pH of the water in the electrode compartments and consequently the pH of the pore fluid approximately unchanged. More importantly, the nutrients were distributed somewhat evenly across the soil under treatment and the water content of the soil between the electrodes was fairly uniform. The new technique is easy to implement and can be used in field applications of electrokinetic bioremediation. The main advantage is the ability to stabilize the pH and to evenly distribute the nutrients in the soil without the need for amendments or extra fieldwork. The technique can contribute to advancing the knowledge and application of electrokinetic bioremediation.

## 4.4 CONCLUSIONS

In electrokinetics, electrolysis reactions form a pH gradient in soil. A pH gradient has an adverse effect on the microbial existence in the soil. The success of an electrokinetic bioremediation treatment relies mainly on the microbial performance. Therefore, controlling the pH during an electrokinetic bioremediation treatment is crucial for its success. This study demonstrates the effectiveness of the novel ACC technique in keeping the pH in the soil to remain relatively unchanged by electrokinetics contrary to the conventional configurations where a zone of high pH was developed near the cathode and an acidic zone was created at the anode. The change in water content of the soil was also found to less drastic than in the tests with conventional configuration. More important, the novel ACC configuration succeeded in delivering nutrients to the entire clay soil specimen at a relatively uniform concentration, whereas most of the nutrients was found to accumulate near the anode in the test with the conventional configuration. The novel techniques succeeded in delivering the nutrient to the entire soil utilizing a low current density despite the very low hydraulic conductivity of the clay soil which would require a very high hydraulic pressure to deliver nutrients by a hydraulic flow. The ACC technique has the potential to enhance the outcome of the electrokinetic bioremediation process by eliminating the pH gradient, decreasing the change in water content and distributing the nutrient to the entire soil. However, more research is required to optimize the setup and scale up the tests before field applications.

## 4.5 REFERENCES

Acar, Y. B. and Alshawabkeh, A. N. (1993). "Principles of Electrokinetic Remediation." Environmental Science & Technology, **27**(13): 2638-2647.

Acar, Y. B., Rabbi, M. F. and Ozsu, E. E. (1997). "Electrokinetic injection of ammonium and sulfate ions into sand and kaolinite beds." Journal of Geotechnical and Geoenvironmental Engineering, **123**(3): 239-249.

Alshawabkeh, A. N. (2009). "Electrokinetic Soil Remediation: Challenges and Opportunities." Separation Science and Technology, **44**(10): 2171-2187.

Alshawabkeh, A. N., Gale, R. J., Ozsu-Acar, E. and Bricka, R. M. (1999). "Optimization of 2-D electrode configuration for electrokinetic remediation." Journal of Soil Contamination, **8**(6): 617-635.

Budhu, M., Rutherford, M., Sills, G. and Rasmussen, W. (1997). "Transport of nitrates through clay using electrokinetics." Journal of Environmental Engineering-Asce, **123**(12): 1251-1253.

Cotter, P. D. and Hill, C. (2003). "Surviving the acid test: Responses of gram-positive bacteria to low pH." Microbiology and Molecular Biology Reviews, **67**(3): 429-453.

D422-63 (2007). "Standard Test Method for Particle-Size Analysis of Soils." Annual Book of American Society for Testing and Materials (ASTM) Standards, **04.08**.

D4318-10e1 (2010). "Standard Test Methods for Liquid Limit, Plastic Limit, and Plasticity Index of Soils " Annual Book of American Society for Testing and Materials (ATSM)Standards **04.08**.

D4972-13 (2013). "Standard Test Method for pH of Soils." Annual Book of American Society for Testing and Materials (ASTM) Standards **04.08**.

Denisov, G., Hicks, R. E. and Probstein, R. F. (1996). "On the kinetics of charged contaminant removal from soils using electric fields." Journal of Colloid and Interface Science, **178**(1): 309-323.

Hansen, H. K., Ottosen, L. M., Kliem, B. K. and Villumsen, A. (1997). "Electrodialytic remediation of soils polluted with Cu, Cr, Hg, Pb and Zn." Journal of Chemical Technology and Biotechnology, **70**(1): 67-73.

Hassan, I., E. Mohamedelhasan (2014). "Sorption, Desorption, Remediation, and Fertility characteristics of clay soil." Journal of Civil Engineering and Architecture, **8**: 1274-1284.

Hassan, I. and Mohamedelhasan, E. (2012). "Electrokinetic Remediation with Solar Power for a Homogeneous Soft Clay Contaminated with Copper." International Journal of Environmental Pollution and Remediation (IJEPR) **Volume 1**(Issue 1): 67-74.

Ishikawa, T., Zhu, B. L. and Maeda, H. (2006). "Effect of sodium azide on the metabolic activity of cultured fetal cells." Toxicology and Industrial Health, **22**(8): 337-341.

Kim, S. H., Han, H. Y., Lee, Y. J., Kim, C. W. and Yang, J. W. (2010). "Effect of electrokinetic remediation on indigenous microbial activity and community within diesel contaminated soil." Science of the Total Environment, **408**(16): 3162-3168.

Kim, S. J., Park, J. Y., Lee, Y. J., Lee, J. Y. and Yang, J. W. (2005). "Application of a new electrolyte circulation method for the ex situ electrokinetic bioremediation of a laboratory-prepared pentadecane contaminated kaolinite." Journal of Hazardous Materials, **118**(1-3): 171-176.

Kim, S. S. and Han, S. J. (2003). "Application of an enhanced electrokinetic ion injection system to bioremediation." Water Air and Soil Pollution, **146**(1-4): 365-377.

Krulwich, T. A., Sachs, G. and Padan, E. (2011). "Molecular aspects of bacterial pH sensing and homeostasis." Nature Reviews Microbiology, **9**(5): 330-343.

Luo, Q. S., Wang, H., Zhang, X. H., Fan, X. Y. and Qian, Y. (2006). "In situ bioelectrokinetic remediation of phenol-contaminated soil by use of an electrode matrix and a rotational operation mode." Chemosphere, **64**(3): 415-422.

Luo, Q. S., Zhang, X. H., Wang, H. and Qian, Y. (2005). "The use of non-uniform electrokinetics to enhance in situ bioremediation of phenol-contaminated soil." Journal of Hazardous Materials, **121**(1-3): 187-194.

Mao, X. H., et al. (2012). "Electrokinetic-enhanced bioaugmentation for remediation of chlorinated solvents contaminated clay." Journal of Hazardous Materials, **213**: 311-317.

Mitchell, J. K. and Soga, K. i. (2005). Fundamentals of soil behavior. Hoboken, N.J., John Wiley & Sons.

Mohamedelhassan, E. (2009). "Electrokinetic strengthening of soft clay." Ground Improvement, **162**(4): 157-166.

Mohamedelhassan, E., Shang, J. Q., Ismail, M. A. and Randolph, M. F. (2005). "Electrochemical cementation of calcareous sand for offshore foundations." International Journal of Offshore and Polar Engineering, **15**(1): 71-79.

Niqui-Arroyo, J. L., Bueno-Montes, M., Posada-Baquero, R. and Ortega-Calvo, J. J. (2006). "Electrokinetic enhancement of phenanthrene biodegradation in creosote-polluted clay soil." Environmental Pollution, **142**(2): 326-332.

Nyer, E. K. and Suarez, G. (2002). "Treatment technology: In situ biodegradation is better than monitored natural attenuation." Ground Water Monitoring and Remediation, **22**(1): 30-39.

Padan, E., Bibi, E., Ito, M. and Krulwich, T. A. (2005). "Alkaline pH homeostasis in bacteria: New insights." Biochimica Et Biophysica Acta-Biomembranes, **1717**(2): 67-88.

Pazos, M., Sanroman, M. A. and Cameselle, C. (2006). "Improvement in electrokinetic remediation of heavy metal spiked kaolin with the polarity exchange technique." Chemosphere, **62**(5): 817-822.

Rabbi, M. F., et al. (2000). "Electrokinetic injection of nutrients in layered clay/sand media for bioremediation applications." Emerging Technologies in Hazardous Waste Management 8: 29-38.

Reddy, K. R. and Cameselle, C. (2009). Electrochemical remediation technologies for polluted soils, sediments, and groundwater. Hoboken, N.J., Wiley.

Reed, B. E., Berg, M. T., Thompson, J. C. and Hatfield, J. H. (1995). "Chemical Conditioning of Electrode Reservoirs during Electrokinetic Soil Flushing of Pb-Contaminated Silt Loam." Journal of Environmental Engineering-ASCE, **121**(11): 805-815.

Ribeiro, A. B., Mateus, E. P. and Couto, N. (2015). Electrokinetics Across Disciplines and Continents: New Strategies for Sustainable Development, Springer.

Schmidt, C. A. B., Barbosa, M. C. and de Almeida, M. D. S. (2007). "A laboratory feasibility study on electrokinetic injection of nutrients on an organic, tropical, clayey soil." Journal of Hazardous Materials, **143**(3): 655-661.

Suni, S., Malinen, E., Kosonen, J., Silvennoinen, H. and Romantschuk, M. (2007). "Electrokinetically enhanced bioremediation of creosote-contaminated soil: Laboratory and field studies." Journal of Environmental Science and Health Part a-Toxic/Hazardous Substances & Environmental Engineering, **42**(3): 277-287.

Tiehm, A., Augenstein, T., Ilieva, D., Schell, H., Weidlich, C. and Mangold, K. M. (2010). "Bio-electro-remediation: electrokinetic transport of nitrate in a flow-through system for enhanced toluene biodegradation." Journal of Applied Electrochemistry, **40**(6): 1263-1268.

Tiehm, A., Lohner, S. T. and Augenstein, T. (2009). "Effects of direct electric current and electrode reactions on vinyl chloride degrading microorganisms." Electrochimica Acta, **54**(12): 3453-3459.

Vane, L. M. and Zang, G. M. (1997). "Effect of aqueous phase properties on clay particle zeta potential and electro-osmotic permeability: Implications for electro-kinetic soil remediation processes." Journal of Hazardous Materials, **55**(1-3): 1-22.

Wong, J. S. H., Hicks, R. E. and Probstein, R. F. (1997). "EDTA-enhanced electroremediation of metal-contaminated soils." Journal of Hazardous Materials, **55**(1-3): 61-79.

Wu, X. Z., Gent, D. B., Davis, J. L. and Alshawabkeh, A. N. (2012). "Lactate injection by electric currents for bioremediation of tetrachloroethylene in clay." Electrochimica Acta, **86**: 157-163.

Xu, W., Wang, C. P., Liu, H. B., Zhang, Z. Y. and Sun, H. W. (2010). "A laboratory feasibility study on a new electrokinetic nutrient injection pattern and bioremediation of phenanthrene in a clayey soil." Journal of Hazardous Materials, **184**(1-3): 798-804.

Yuan, S. H., Zheng, Z. H., Chen, J. and Lu, X. H. (2009). "Use of solar cell in electrokinetic remediation of cadmium-contaminated soil." Journal of Hazardous Materials, **162**(2-3): 1583-1587.

# CHAPTER 5
# SOLAR POWER ENHANCEMENT OF ELECTROKINETIC BIOREMEDIATION OF PHENANTHRENE[1]

## 5.1 INTRODUCTION

Polycyclic aromatic hydrocarbon (PAH) compounds are found in crude oil, coal and tar deposits. Polycyclic aromatic hydrocarbons are released into the environment via accidental spills, leakage from underground storage tanks and pipelines, and industrial and agricultural activities. PAH compounds are known to be toxic, mutagenic, teratogenic, and/or carcinogenic (Reddy and Saichek 2003; Reddy and Cameselle 2009). Thus, when released to the environment, PAHs become a health hazard to human and ecological receptors. In the present study, phenanthrene has been selected as a model compound to represent hydrocarbon contaminants for many reasons. It is one of the sixteen PAH compounds listed by United States environmental protection agency (EPA) as priority pollutants (Bouvrette et al. 2006; Andersson and Achten 2015). Phenanthrene, composed of three fused benzene rings, is also known as a parent compound because it is dominant in many PAHs. Many recalcitrant heavy hydrocarbons contain four benzene rings or more, and they can be degraded via co-metabolic degradation. For instance, microorganisms can use phenanthrene (three benzene rings) as their sole carbon and energy source and can produce enzymes that can degrade other hydrocarbon compounds, such as fluorine (Boldrin et al. 1993; Puglisi et al. 2007; Coppotelli et al. 2010). Many researchers have used phenanthrene because it is the simplest compound that contains both bay region and k region (Cerniglia 1984; Boldrin et al. 1993; Zhao et al. 2009). The bay and k regions are used to determine the relative carcinogenetic properties of the PAH compounds (Puglisi et al. 2007). Many techniques have been developed and implemented to mitigate contaminated sites. These include, pump and treat, thermal desorption, aeration, biopiles, bioremediation, electrokinetics, soil vapour extraction, soil washing, soil flushing.

[1]A version of the chapter has been submitted to Chemosphere- Journal-Elsevier

Among these methods, bioremediation technology stands out for its low cost and minimal negative impact on the environment (Moody et al. 2001). Bioremediation can be an effective remediation technique. Recent studies have investigated an innovative hybrid technique that joins electrokinetics and bioremediation (Yeung and Gu 2011; Gill et al. 2014). The aim of this hybrid approach is to accelerate the natural biodegradation of contaminants by increasing the opportunities for interaction between microorganisms and contaminants and activating the existing microbial community in the subsurface by delivering nutrients required to promote microbial growth (Acar et al. 1997; Budhu et al. 1997). Many bacterial strains from genus *Mycobacterium* were identified as capable of degrading phenanthrene including, s *Mycobacterium vandaalenii* PYR-1, *Mycobacterium* sp. LB501T, CABI (Boldrin et al. 1993; Moody et al. 2001; Kim et al. 2005b; Seo et al. 2009). Among these isolates, *Mycobacterium pallens* sp. was first isolated from contaminated soil from Hawaii, US. The isolate was identified as capable of degrading phenanthrene (Hennessee et al. 2009). *Mycobacterium pallens* sp. was deposited at American Type Culture Collection (ATCC).

The operating systems of site remediation techniques require energy to execute their processes. The energy consumption varies from one technique to another. In general, high-energy consumption increases the overall cost of the remediation process and can become a major obstacle restricting wide field applications of the technology. The majority of these techniques use fossil fuel products as the source of energy. Fossil fuels are not only a depleting source of energy, but the use of fossil fuels can contribute to soil, water, and air pollution (Bona et al. 2011; Dias et al. 2012; Sutton et al. 2013). Thus, some of the available remediation techniques contribute to the environmental pollution. In the last decade, the need for finding economical alternative sources of power to replace the power from the grid has become urgent. An alternative source of power to fossil fuels can be the energy generated by the sun. Solar panels produce a DC electric field that is acceptable in electrokinetic applications without alteration (i.e. without the need for a DC transformer). The use of power generated by solar panels with other remediation techniques requires the conversion of DC to AC (alternating current). Therefore, electrokinetics can be considered

as the best candidate that can use the power generated by solar panels because there is no need for the conversion process.

Solar energy, a renewable energy source with no adverse environmental impact, is a novel power option for electrokinetic bioremediation and can be economically viable, in particular, for remote sites without active power lines (Yuan et al. 2009; Hassan et al. 2015; Hassan et al. 2016; Souza et al. 2016). A study by Alshawabkeh et al. (1999) showed that the energy cost of an electrokinetic remediation process represented 30% of the total cost. In the last decade solar energy has gained the attention of scientists and the general public, leading to a multitude of beneficial applications. According to a SolarBuzz report (SolarBuzz 2010), more than 70% of photovoltaic (PV) resources have been installed in northern hemisphere countries including Germany, Japan, USA, and Canada. The use of solar cells as a sole source of power can also reduce electricity transmission expenses and eliminate power loss in transmission lines. Although solar cells can be an excellent candidate for power supply in remediation techniques, there is little to no research in the available literature that has investigated their use in electrokinetic bioremediation or the effect of the off power cycle (during darkness) on microorganisms.

The present study investigated the use of electrokinetic bioremediation to mitigate kaolinite clay artificially contaminated with phenanthrene. A solar panel was used to generate the power for electrokinetic bioremediation. *Mycobacterium pallens* was used to degrade phenanthrene. A new technique to stabilize the pH during electrokinetic bioremediation was used in this study. The efficieny of the new technique in delivering nutrients and bacteria was investigated and compared to the conventional anode cathode configuration.

# 5.2 MATERIALS AND METHODS

## 5.2.1 Clay, phenanthrene, bacteria

Inorganic kaolinite clay, 96-99.9% kaolinite (EPK case number 1332-58-7, supplier EdgarMinerals, Florida, US), was used for the tests. Phenanthrene, 99.7% purity was purchased from Fisher Scientific, Canada. All solvents were HPLC grade and purchased from Sigma Aldrich, Canada. *Mycobacterium pallens* ATCC 1372 (freeze dry) was purchased from Cedarlane, Canada (supplier ATCC, US). The broth media 7H9 and agar media 7H10 were purchased from VWR, Canada. *Mycobacterium pallens* (ATCC® BAA-1372™) was first reactivated (or revived) using 1395 medium following the procedure described by the supplier (American type culture collection (ATCC)). The medium (1395 medium) was prepared using 4.7 g Middlebrook 7H9 broth, 2.0 mL glycerol, and 900 mL deionized water. The broth was sterilized at 121$^{o}$C for 20 minutes and 100 mL of ADC enrichment was aseptically added to the broth. The pellet was rehydrated in the broth tube and incubated for one week at 30$^{o}$C in a rotary drum. Pellets for stock were washed two times using normal saline (NaCl) 0.85% (w/v) and resuspended in 0.85% (w/v) NaCl and 15% (v/v) Glycerol and then stored at -80°C.

## 5.2.2 Apparatus

The experimental equipment consisted of three custom-made electrokinetic remediation cells (Sabic polymershapes, London, ON, Canada), custom-made electrokinetics voltage controller (EKVC) (Electronic Shop, University of Western Ontario), pore fluid squeezer, data acquisition system (USB-6008 National Instruments, US), portable data logging system (Omega 320, UK), Eppendorf centrifuge 5810R 15amp version (Hamburg, Germany), Bio-RAD Smart Spec™Plus (California, US), gas chromatography-mass spectrometer (GC/MS) (Agilent Technologies, US). Solar cell panel was used to generate the power for the electrokinetic bioremediation. Cell dimensions are 1590 mm × 820 mm. The maximum current, and maximum power of the cell are 3.40 A, and 200 W, respectively.

The electrokinetic remediation cells, constructed from clear Plexiglas plates 12 mm in thickness, has inner dimensions of 350×120×100 mm (length × width × height), as shown in Figure 5.1. Each cell is composed of upper part, base, cover, and two movable rectangular perforated Plexiglas (120 mm ×100 mm). The cell is divided, by the rectangular perforated Plexiglas, into two water compartments and a soil specimen chamber in between. Each water compartment houses an anode and a cathode, as shown in Figure 5.1. The first water compartment hosts Anode $A1^+$ and Cathode $A2^-$ and the second compartment contains Anode $A2^+$ and Cathode $A1^-$. In each electrokinetic cell, the electrodes are connected to the solar panel using two electric circuits (Figure 5.1): circuit 1 between Anode $A1^+$ and Cathode $A1^-$, and circuit 2 between Anode $A2^+$ and Cathode $A2^-$ (in the second and third electrokinetic cells electric circuits 1 between $B1^+$ and $B1^-$ and $C1^+$ and $C1^-$ and electric circuit 2 connected $B2^+$ to $B2^-$ and $C2^+$ to $C2^-$). The hypothesis of the electrodes placement is that the coexistence of an anode and a cathode in the same water compartment will result in the hydrogen ions generated at the anode neutralizing the hydroxyl ions produced at the cathode, thereby forming water and keeping the pH unchanged.

The Electrokinetics Voltage Controller (EKVC) device (Figure 5.1) was designed to switch the electric potential between the two electric circuits at predetermined intervals and such that at any given time there is only one electric current running through either electric circuit 1 or 2 in the electrokinetic cell. The EKVC takes maximum current of 1 A and an input of DC voltage of up to 70 V, and has six output ports and a programmable timer. A computer code has been written using Labview 2013 to connect the data acquisition terminals and EKVC with a PC for real time data recording. The EKVC alternates voltage between outputs groups at a set programmable time. HyperWare software (included with Omega-320 System) was used to develop a program, Program Net, for communications between the Omega-320 and the PC. The Program Net provided instruction for Omega-320 including which channels to sample, when to sample, and how to process the incoming signals. Via HyperComm, collected data was displayed and downloaded.

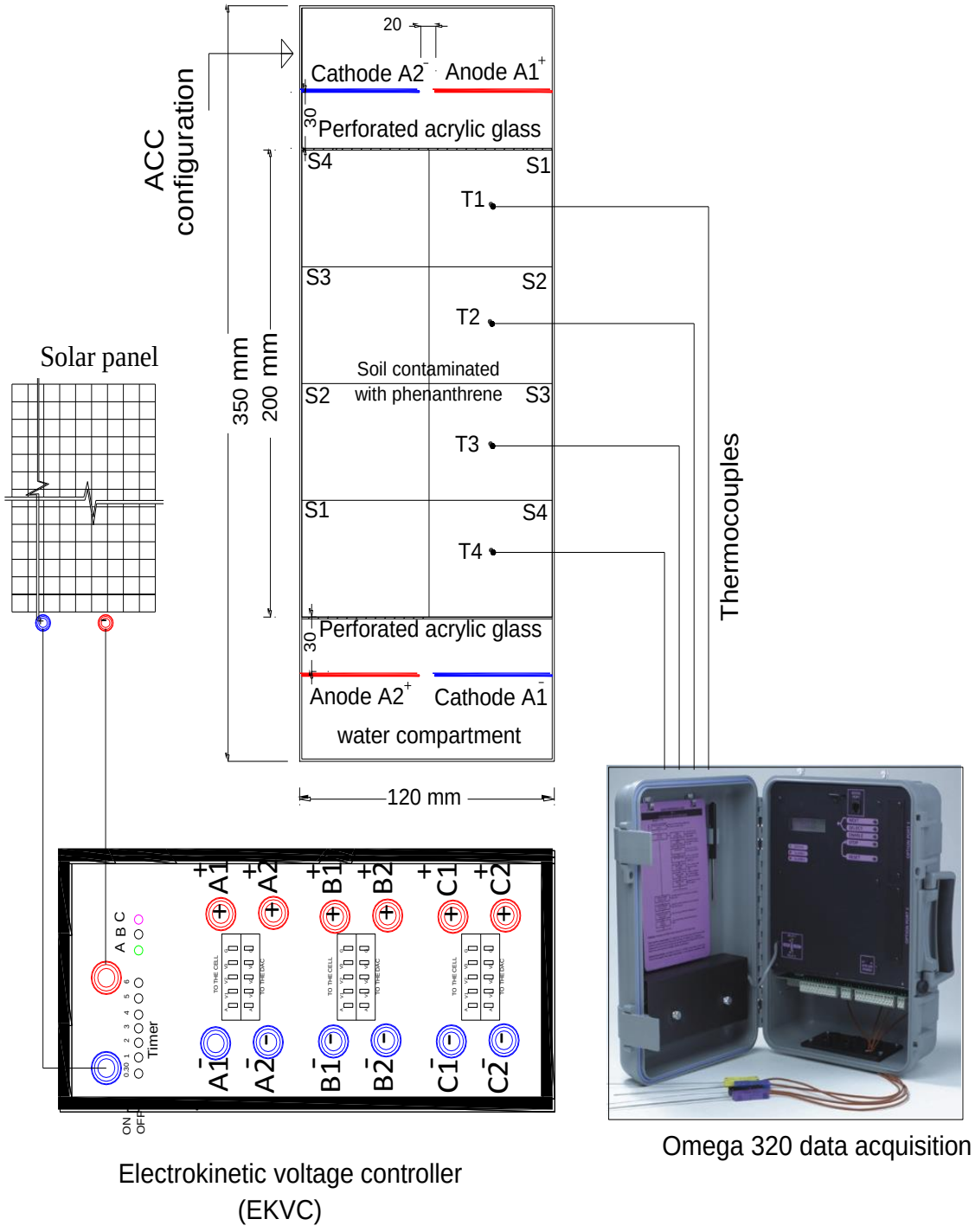


**Figure 5.1** Schematic diagram off the electrokinetic remediation cell, EKVC, Omega 320, and solar panel

## 5.2.3 Test procedure

(a) Preliminary tests

Preliminary tests were conducted to investigate the ability of *Mycobacterium pallens* in degrading phenanthrene. Middlebrook 7H10 medium was sterilized then OADC enrichment was added, the mixture was poured into Petri plates (≈10 mL in a 10 cm plate) and left open under biosafety cabinet to solidify. Phenanthrene was dissolved in dimethyl sulfoxide (DMSO) as stock solution at concentration of 100 mg/mL. Under the biosafety cabinet, 100 µL from stock solution was spread over the solid 7H10 medium in the Petri plates, to form opaque layer, and left under the biosafety cabinet to evaporate the DMSO. *Mycobacterium pallens* (ATCC® BAA-1372™) from stock (prepared above) was grown in 1395 medium at 30ºC for 7 days, pelleted at 10000 rpm, washed with 5 ml sterile 0.85% (w/v) NaCl twice (to remove the nutrients) and resuspended in 0.85% (w/v) NaCl and the optical density ($OD_{600}$) of the solution was adjusted to 1. Inocula (20 µL) from this solution were added in the center of the Petri plates prepared above (7H10 solid medium supplemented with a layer of phenanthrene). Then the Petri plates were incubated at 30º C and monitored for clearing zone around the drop.

Batch tests were conducted to investigate the growth of *Mycobacterium pallens* sp at different temperatures. *Mycobacterium pallens* sp was added in separate 250 mL Erlenmeyer flasks contain 50 mL minimal medium (the minimal medium consists of $NH_4SO_4$- 1 g/L, $KH_2PO_4$ - 0.5 g/L, $K_2HPO4$ - 0.5 g/L, $MgSO_4$- 0.1 g/L, NaCl - 6 g/L, $CaCL_2$ - 0.1 g/L, and MES Hydrate- 1 g/L) with 0.3% (v/v) glycerol as a sole carbon source. Solutions optical density was adjusted at $OD_{600}$ of 0.5. Two flasks were incubated aerobically at incubated shakers (150 rpm) adjusted at different two temperatures 48ºC, and 18ºC for 15 days. The test was conducted in triplicates. After the test, 5 µL from each flask was strike in a Petri plate supplemented with soil 7H10 medium and incubated at 30ºC in and the growth was monitored

Batch tests were conducted to investigate the growth of *Mycobacterium pallens* sp at different pHs. Minimal medium solution was prepared and placed in two 250 mL Erlenmeyer flasks (each contain 50 mL). Then, pHs in the flasks were adjusted to pH 12 and pH 2 and the solutions were sterilized. Glycerol (sterile) was added to the flasks to 0.3% (v/v) as a sole carbon source. *Mycobacterium pallens* sp was added to the solution in the flasks ($OD_{600}$ of 0.5) and incubated aerobically at 30$^{o}$ C in a shaker (150 rpm) for 15 days. The test was conducted in triplicates. After the test, 5 µL from each flask was strike in Petri plate supplemented with soil 7H10 medium and incubated at 30$^{o}$ C in and the growth was monitored.

(b) Electrokinetic bioremediation tests

The physical and chemical properties of the inorganic kaolinite clay soil were presented in Table 5.1. Soil samples with a phenanthrene concentration of 2 mg/g dry soil were prepared as follows: the soil sample was sterilized for 24 h at 120$^{o}$C in a dry oven. To verify that the sample was sterile soil, 1 g of soil was mixed with 10 mL of sterile 0.85% NaCl, left to settle by gravity, and then the supernatant was plated on Luria broth (LB) agar plates. The sterile soil and the corresponding amount of phenanthrene (phenanthrene was dissolved in methanol) were thoroughly mixed under biosafety cabinet using a mechanically rotating rod. The mixture was placed under a biosafety cabinet overnight for methanol evaporation to take place. Stock solutions, 1g/L of NaCl, $NaNO_3$, and $KH_2PO_4$, were prepared to be added later in the water compartment. Four sets of tests were conducted. Table 5.2 shows the details of the test setups.

The first set of tests (test 1 and 2) was designed to compare the efficiency of a new anode cathode compartment (ACC) electrode configuration and a conventional anode-cathode (CAC) electrode configuration in delivering bacteria to the clay soil. The sterilized kaolinite was saturated using sterilized deionized water (water content 60%) and placed in electrokinetic cells' soil chamber (Cell X, and Cell Y) in three layers for a total height of

60 mm. Each layer was tamped using rectangular Plexiglass plate and a pestle to prevent the entrapment of air pockets and to produce soil specimens with similar densities. *Mycobacterium pallens* ($10^8$ CFU/mL) (from the Glycerol stock), was suspended in a solution of 0.1% (w/v) $NaNO_3$ and 0.1% (w/v) $KH_2PO_4$ and loaded in the water compartments. The new ACC electrode configuration was used in Cell X. CAC configuration was used in Cell Y.

The second set of tests (tests 3 and 6) represents biostimulation (supplementation of the contaminated soil with nutrients to enhance the growth and metabolism of indigenous bacteria). In test 3 (Cell A with ACC configuration), the soil was artificially contaminated with phenanthrene 2 mg/g (as described above). The water content of the soil was adjusted to 60% using *Mycobacterium pallens* ($10^8$ CFU/mL) suspended in 0.1% (w/v) NaCl solution. The soil sample was placed in the soil chamber in layers (as described above). The water compartments were filled with a solution of 0.1% (w/v) $NaNO_3$, and 0.1% (w/v) $KH_2PO_4$. The control test for this configuration was test 6 (Cell H), where no electric field was applied.

The third set (tests 4 and 7) was designed to represent a bioaugmentation scenario (introduction of bacterial strains with superior capabilities). In test 4 (Cell B with ACC configuration), soil was artificially contaminated with phenanthrene 2 mg/g and thoroughly mixed with a solution of 0.1% (w/v) of $NaNO_3$ and 0.1% (w/v) $KH_2PO_4$ to a water content of 60%. The soil sample was placed in the soil chamber in layers (as described above). *Mycobacterium pallens* ($10^8$ CFU/mL) suspended in 0.85% NaCl (w/v) was added to the water compartments. Cell F (test 7) represented the control for the third set of tests where no electric field was applied.

The fourth set (tests 5 and 8) was designed to simulate a contaminated site where the indigenous bacteria lacked the ability to degrade the contaminant and the nutrients were

not sufficient for bacterial growth. In test 5 (Cell C with ACC configuration), the soil was artificially contaminated with phenanthrene (2 mg/g) and placed in the soil chamber (as described above). *Mycobacterium pallens* (CFU $10^8$/mL) suspended in a solution of 0.1% (w/v) of $NaNO_3$, and 0.1% (w/v) $KH_2PO_4$ was added to the water compartments. The control for this set of tests was Cell G (test 8).

The soil was placed into the electrokinetic cell in three layers for a total height of 60 mm. Each layer was tamped using rectangular Plexiglass plate and a pestle to prevent the entrapment of air pockets and to produce soil specimens with similar densities. In each cell, four voltage probes were connected to EKVC which was connected to a data acquisition system. The temperature of the soil during the test was monitored by four thermocouples placed at equal distance inside the soil and connected to Omega data acquisition system.

The tests were conducted at the Southern Crop Protection and Food Research Center (SCPFRC), Agriculture and Agri-Food Canada, London, Ontario, Canada. The electrokinetic cells, EKVC, a PC, Omega 320, and the data acquisition system were placed inside two cabinets placed in a microplot field area (open yard) at SCPFRC. The latitude and the longitude of London, Ontario are 42.98 and -81.24, respectively. The solar panel was placed near the cabinets in the microplots and for optimum sun exposure, the solar panel was tilted to an angle $28^o$ and faced south. The solar panel was connected to the EKVC in the cabinets via electrical wires

The voltage output of the solar panel, voltage gradient across the electrokinetic cell, temperature inside the cell, and the electric current through the cell were monitored and recorded regularly during the test using real time data acquisition systems (described above). After the tests, the soil samples in the cells were divided into four sections, S1 to S4, between the anode and the cathode and phenanthrene concentration was determined for each section (Figures 5.3 (a) and (b)). Part of the soil from each section was squeezed and the pore fluid was collected. Nitrate ($NO_3$) concentration in the pore fluid was determined using high pressure liquid ion chromatograph. *Mycobacterium pallens* CFU in each section was determined using standard plate count method.

### 5.2.4 Procedures for phenanthrene extraction and determination

Phenanthrene in soil samples before and after the tests were first extracted and then the concentrations was determined using GC-MS. Phenanthrene was extracted using a sonicating water bath for 4 h at room temperature. After the test, soil sample from each section, 1.0 g, was weighed in 35 mL heavy duty glass tubes and 20 mL of a 1:1 Acetone : Dichloromethane solution was added to the tube and placed in the sonicator for 2 h and then the solution was replaced by fresh solution and sonicated for another 2 hr. After sonication the solution was replaced for the second time by fresh 20 mL solution and the tube was placed in a shaker table (150 rpm) overnight. The solutions were then combined together (60 mL), and a Kuderna-Danish apparatus was used to reduce the volume to 5 mL. The extraction method was validated by the addition of 0.5, 1, 2, 3, 4, 5 mg of phenanthrene to 1 g of sterial dry soil and then extract the phenanthrene. Figure 5.2 shows that the results fit the regression line with R-squared = 0.98. The extraction tests show recovery between 97% at phenanthrene concentration 2mg/g. Column chromatography backed with alumina and anhydrous sodium sulphate was used to filter the analyte and the final solution was filtered using 25 µm filters. GC-MS was used to determined phenanthrene concentration. The GC-MS method used gas chromatography column HP-MS (length 30 m, internal diameter 250 µm, film thickness 0.25 µm), with helium as a carrier gas, injected volume of 1 µL, initial temperature of 150$^{o}$C held for 2 min, and then ramped at 10$^{o}$C per min up to 280$^{o}$C and held for 2 min.

**Table 5.1** Soil physiochemical properties

| Soil property | Measured value |
|---|---|
| Liquid limit | 60 (±2) |
| Plastic limit | 34 (±1) |
| $e_{max}$ | 3.1 (± 0.4) |
| $e_{min}$ | 0.92 (±0.03) |
| pH | 4.2 (±0.1) |
| Cation exchange capacity | 3.75 (±0.10) meq/100 g of soil |
| Specific surface area | 28.75 (± 1.5) $m^2/g$ |

The values between the brackets are the range of errors

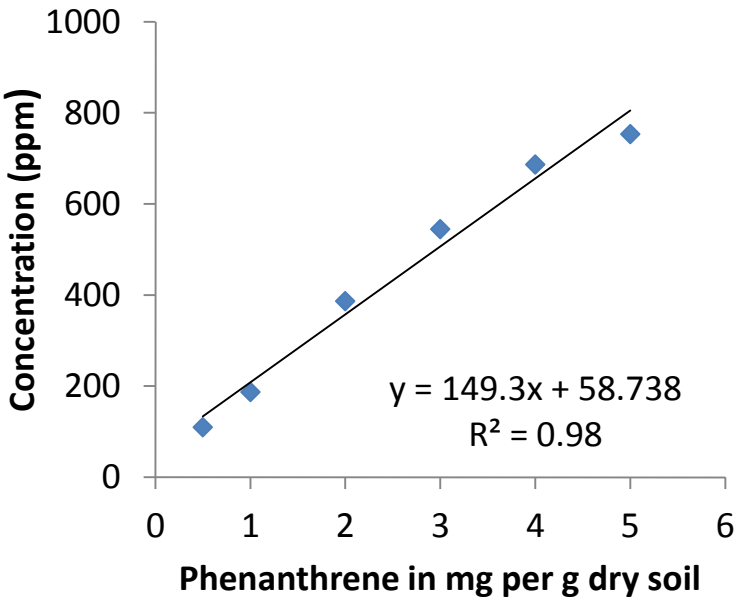


**Figure 5.2 Phenanthrene extraction**

**Table 5.2** Set of tests

| Test | Cell | Soil compartment | Water compartment | Configuration |
|---|---|---|---|---|
| 1 | Cell X | Uncontaminated sterile soil | *Mycobacterium pallens* (FCU $10^8$/mL) | EK (ACC) |
| 2 | Cell Y | Uncontamined sterile soil | *Mycobacterium pallens* (FCU $10^8$/mL) | EK (CAC) |
| 3 | Cell A | 2mg/g phenanthrene, *Mycobacterium pallens* $NaNO_3$ solution (FCU $10^8$/mL) | 1 g/L of $NaNO_3$ and $KH_2PO_4$ solution | EK (ACC) |
| 4 | Cell B | 2mg/g phenanthrene and 1 g/L of $NaNO_3$, and $KH_2PO_4$ | *Mycobacterium pallens* (FCU $10^8$/mL) in 0.85% NaCl | EK (ACC) |
| 5 | Cell C | 2mg/g phenanthrene | *Mycobacterium pallens,* (FCU $10^8$/mL) in solution of 1 g/L of $NaNO_3$ and $KH_2PO_4$ | EK (ACC) |
| 6 | Cell D control | 2g/L phenanthrene, *Mycobacterium pallens* NaNO3 solution (FCU $10^8$/mL) | 1 g/L of $NaNO_3$, and $KH_2PO_4$ | No |
| 7 | Cell E control | 2g/L phenanthrene and 1 g/L of $NaNO_3$, and $KH_2PO_4$ | *Mycobacterium pallens* (FCU $10^8$/mL) in solution of 0.85% NaCl | No |
| 8 | Cell F control | 2g/L phenanthrene | *Mycobacterium pallens* (FCU $10^8$/mL) In solution of 1 g/L of $NaNO_3$, and $KH_2PO_4$ | No |

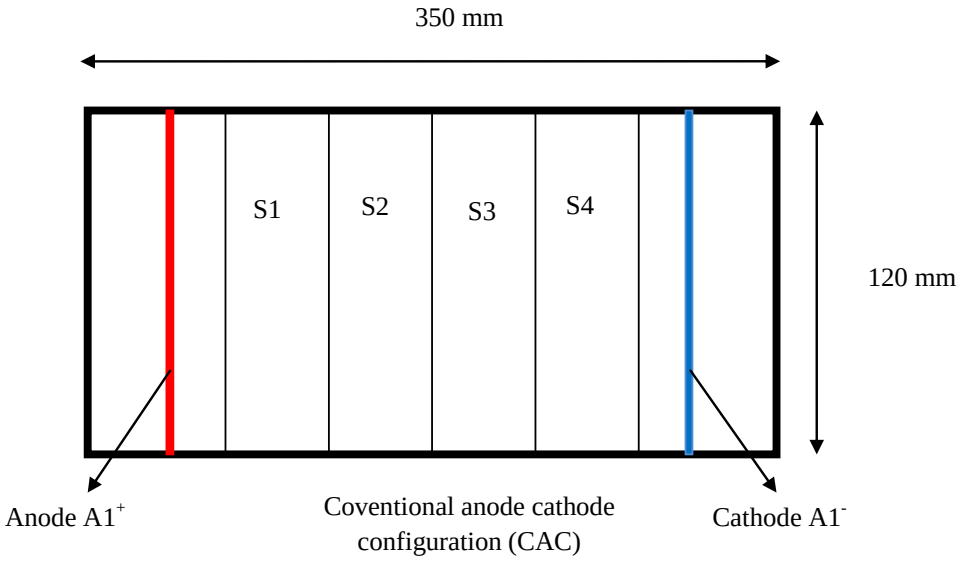


**Figure 5.3 (a)** Soil sections in the conventional anode cathode configuration (CAC)

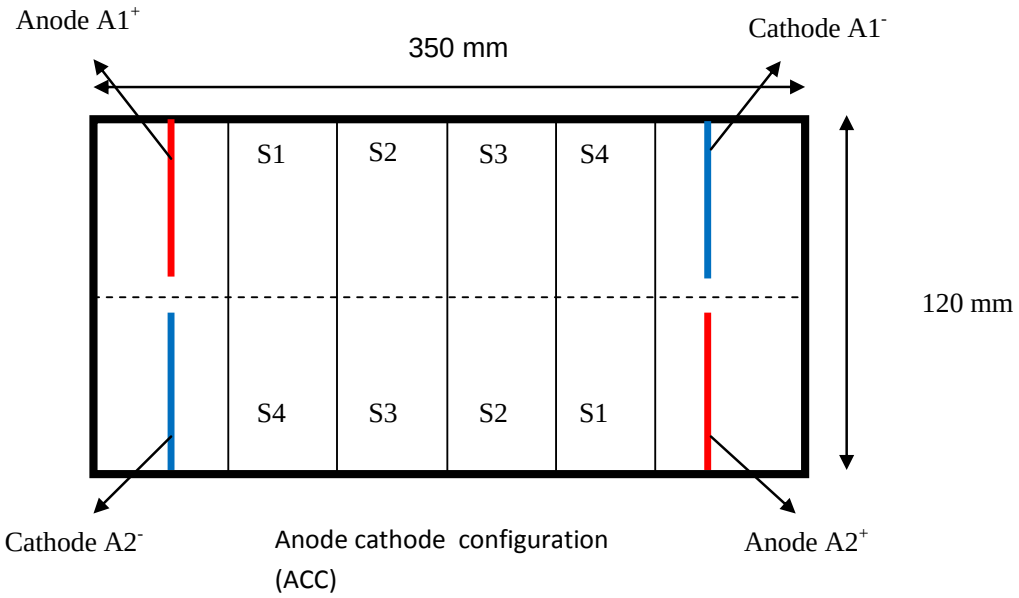


**Figure 5.4 (b)** Soil sections in the anode cathode configuration (ACC)

# 5.3 RESULTS AND DISCUSSION

## 5.3.1 Voltage generated by solar panel

The voltage generated by the solar panel and the electric current through the cells were recorded in real-time by the data acquisition system. The power generated by solar cell panels depends on the duration of the day and the weather conditions. This can cause fluctuations in the power supply during the day and intervals of zero voltage at night, especially in the northern hemisphere with low daylight in the winter months. Figure 5.4 shows the average voltage generated by the solar during the tests period of 30 days. The figure shows that in general the voltage generated increased from zero before sunrise to maximum of 57 V around 9:00 AM. Between 9:00 AM and 4:00 PM the generated voltage raged between 52 V to 57 V. The generated voltage started to decrease rapidly around 7:00 PM and reached zero at sunset.

Figure 5.4 shows fluctuation of the voltage generated from the solar panel during the day and the diminishment of electric field during the night. Analogous to the positive effect of intermittent current in electrokinetic application as reported in previous researchers (Mohamedelhassan and Shang 2001; Reddy and Saichek 2004; Hansen and Rojo 2007; Reddy and Cameselle 2009), the fluctuation of the voltage generated from the solar panel can be beneficial to the remediation process. This is because the application of an electric field in electrokinetics results in ions orienting in the double layer against the electric current, which reduces the efficiency of the remediation process. The fluctuation of the electric field allows for the restoration of the original ion orientation, which can enhance the remediation process (Mohamedelhassan and Shang, 2001).

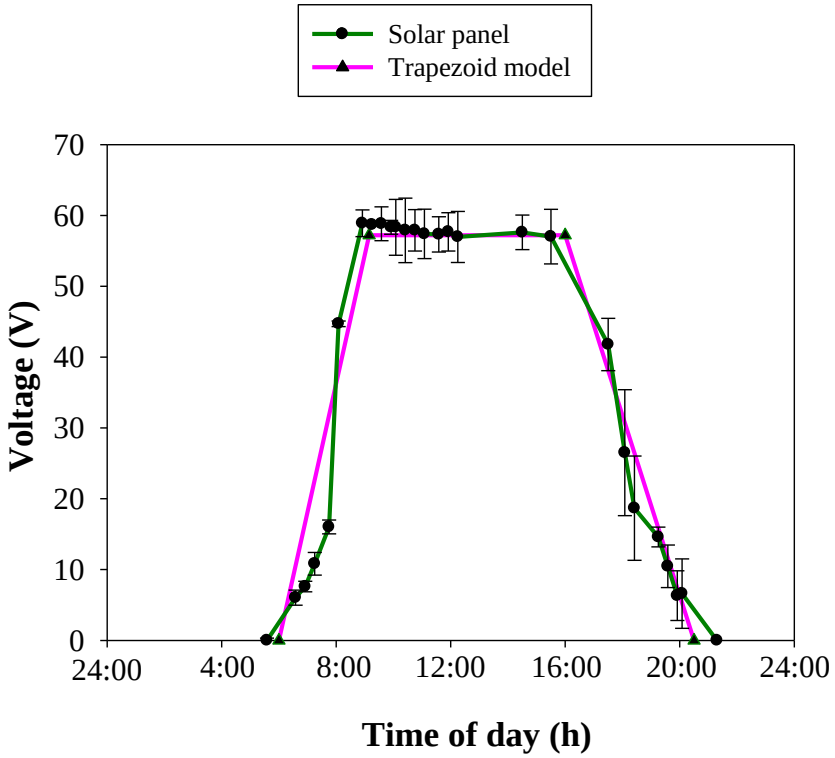


**Figure 5.5** Voltage generated by solar panel

The profile of the voltage generated by the solar panel shows that the solar panel generate voltage in the range of <1 V/cm in the first hour and a half after the sun rise and at the last hour and a half before the sun set. The solar panel generate 2 V/cm during the rest of the day (soil sample length 30cm, maximum voltage from solar 60V) which enough for electrokinetic bioremediation (Reddy and Cameselle 2009). The distribution of generated voltage as shown in Figure 5.4 is in agreement with trapezoidal model described by Zhang and Smith (2008) where the daylight hours represent the bottom base of the trapezoid and the noon hours represent the upper base of the trapezoid. The height of the trapezoid is the maximum irradiance during the day. The results from this study showed that the power generated by solar energy is not only sufficient for electrokinetic bioremediation, but can also be monitored and evaluated using the trapezoidal model.

### 5.3.2 Electric current

The electrical current during the test, in Cell A, Cell B, and Cell C, as shown in Figure 5.5, varied between 0.68 A and 0.11 A during the daytime and diminish to zero during the night. As expected, the current was directly proportional to the variation in voltage generated by solar panel. In general, the profile of the current during the day can be divided into five intervals. In the first interval, the current started with a low magnitude at sunrise and increase gradually until about 8:00 AM. The second interval showed a rapid increase (exponentially) in current values between 8:00 and 9:00 AM. The figure shows stable current values in the third interval between 9:00 AM and 6:00 PM. A rapid decrease in the current was observed in the fourth interval between 6 and 7 PM, as well as a gradual decrease in the fifth interval between 7:00 PM and sunset. From the figure, the current values are somewhat the same in the cells A, B, and C during the first and the fifth interval. The figure, however, shows differences in the current values in the cells during the second and the fourth intervals. A significant difference in the current values in the cells is obvious during the third interval. In the third interval, the current in Cell A (0.68 A) was high compared to the currents in Cell B (0.4 A) and Cell C (0.11 A). The differences between the current values in the cells can be attributed to the initial constituents of the matrix in the cell. Whereas the contaminated soil in Cell A was mixed with bacteria, the soil in Cell B was mixed with nutrients, and in Cell C nothing was added to the contaminated soil. Electrical current in Cell A is directly proportional to electrical conductivity. The existence of nutrients and bacteria can increase electrical conductivity (see Table 5.3). Therefore, the high current in Cell A can be attributed to higher electrical conductivity.

**Table 5.3** Electrical conductivity

| Liquid composition | Electrical conductivity ms/cm (live bacteria) | Electrical conductivity ms/cm (live bacteria) |
|---|---|---|
| NaCl (sterile) | 14.90 | 14.90 |
| NaCl+*Mycobacterium pallens* | 15.70 | 15.53 |
| Minimal medium (sterile) | 13.25 | 13.12 |
| MM+*Mycobacterium pallens* | 13.32 | 12.9 |

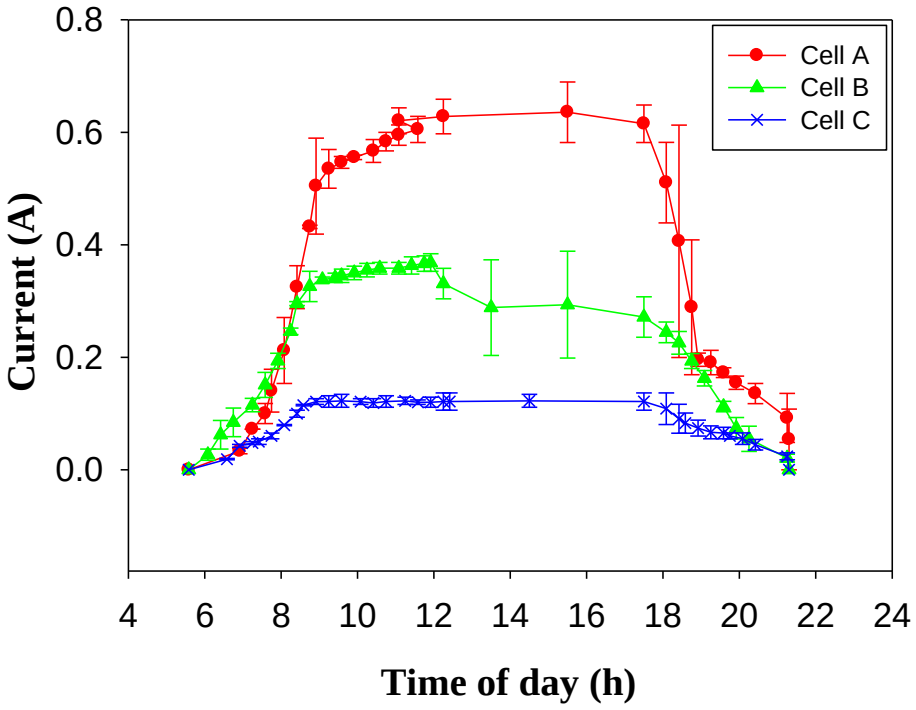


**Figure 5.6** The current during the tests in Cell, A, B, and C

The power during treatment is presented in Figure 5.6. As seen in the figure and in agreement with the electric current during the test, the highest power was 530 W reported in Cell A compared with the highest value of 400 W in cell B and 150 W in cell C. The total energy consumption during the thirty days, period of the test for Cell A, Cell B, and Cell C was 7650, 5100, 1800 Wh, respectively. The energy consumption during electrokinetics tests is a major contributor to the overall cost of the process. In general, the cost of the energy generated by solar panel is estimated to be less than five cents per kilowatt-hour (Lacey 2015).

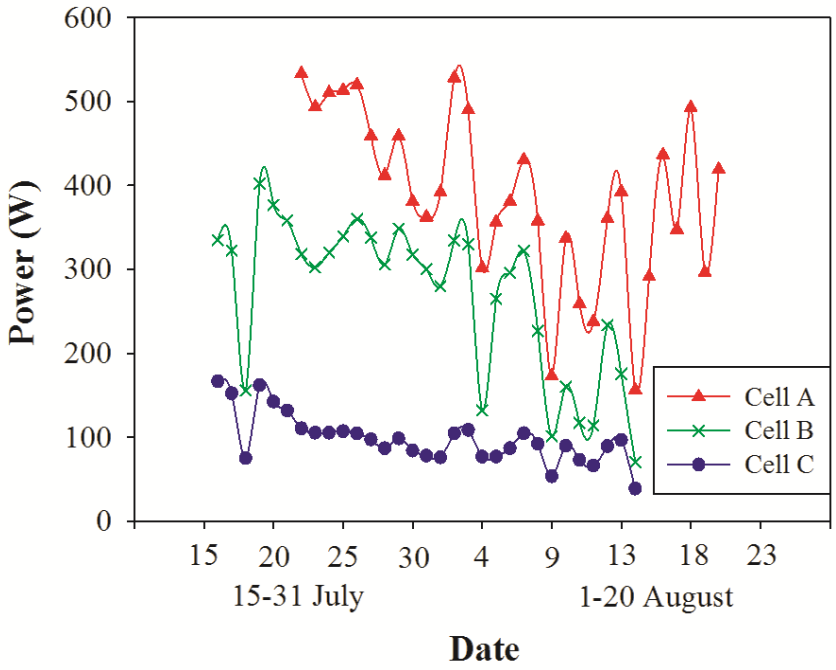


**Figure 5.7** The power during the tests in Cell A, B and C

The price of the solar panel, used in this study, was one hundred and fifty Canadian dollars and the expected life span is twenty-five years. The current price of grid electricity in London, Ontario, Canada, varies between 8 and 16 cent per kWh off peak and on peak, respectively. The current from the grid is an alternating current and cannot be used in electrokinetic bioremediation, which requires direct current, unless converted to a direct current. The average price of the DC power supply (needed to convert the alternating current to a direct current) is 200 Canadian dollars. The total cost of energy in the case of

using solar panel to generate the power is 150 Canadian Dollars (the price of the solar panel) whereas the total cost of energy from the gird can be calculated from the following equation (5.1):

Total cost of energy = Price of the DC power supply + Cost of energy used

$$=200 \text{ Canadian Dollars} + (\text{energy consumed in kWh/m}^3) \times (\text{rate 8-16 cen/kWh}) \quad (5.1)$$

The total cost of power in case of the use of solar panel is equal to the initial cost of the solar panel and dose not depend on the power consumed (there no charges for the power generated by solar panel). On the other hand, the cost of power in the case of the use of the electricity from the grid depends on cost of power kWh and increase with the increase in power consumption. Therefore, the cost of energy from the grid is higher than the cost of energy when the solar panel is used to generate the power. The cost of energy known to be a major component of the overall cost of the remediation processes (Reddy and Cameselle 2009). Thus, the reduction in the energy cost will have a significant impact on the decrease of the overall cost of the process.

### 5.3.3 Temperature inside electrokinetic cell compared to ambient temperature

Part of the energy used during the treatment process transformed into heat and resulted in elevating the temperature of the soil. Few reports have discussed the effect of temperature increase during electrokinetic bioremediation. In this study, the minimum, median, and maximum ambient temperatures for London, Ontario, Canada, obtained from Environment Canada were compared with the soil temperature in the cell. There was no prominent difference between the soil minimum temperatures in Cell A, Cell B, and Cell C. The ambient temperature was 2 to 5$^{o}$C lower than the minimum temperature in the cells (see Figure 5.7). The increase in soil temperature in the cells was due to the transformation of energy (flow of the electrical current through the soil) into heat. The median temperatures of the soil in the cells were higher than the median ambient temperature (Figure 5.8). There

is a significant difference between the maximum temperatures in the cells (Figure 5.9), with the highest temperature occurring in Cell A, followed by Cell B and then in Cell C. The electrical current (Figure 5.5) was highest in Cell A compared to Cell B and Cell C, showing a direct correlation between the current and the temperature. The results from this study provide the evidence that the application of electric current in electrokinetics can cause an increase in soil temperature.

The batch tests showed that *Mycobacterium pallens* sp. can survive and grow at 18$^{o}$C, however, at 48$^{o}$ there was no growth reported. Despite the fluctuation of temperature (18$^{o}$C-48$^{o}$C) during the outdoors test, *Mycobacterium pallens* sp. CFU after the test was between $3x10^{5}$-$5x10^{5}$ CFU in the soil sections after ACC tests (Cell A, Cell B, Cell C). Therefore, it can be concluded that the variation of the temperature during the test contributed to the *Mycobacterium pallens* sp. survival.

The results for the current study are in a general agreement with previous studies. For example, a study by Mohamedelhassan and Shang (2008) showed that soil temperature increased between 5$^{o}$C and 20$^{o}$C with the maximum increase reported in the soil near the anode. Ho et al. (1999) reported an increase in temperature up to 90$^{o}$C during field application of electrokinetic remediation of trichloroethylene. In the study, the increase in temperature was reduced by using an intermittent current (periods of zero power). The present study showed that the fluctuation of the power generated by the solar panel during the day and the period of zero power during the night played an important role in reducing soil temperature.

The conventional electrokinetics methods using power from the grid can result in an increase in temperature, but this increase is constant during the day and could have a negative impact on the indigenous bacteria. The use of intermittent current was

implemented by the researches to a void the adverse effect of the temperature (Ho et al. 1999).

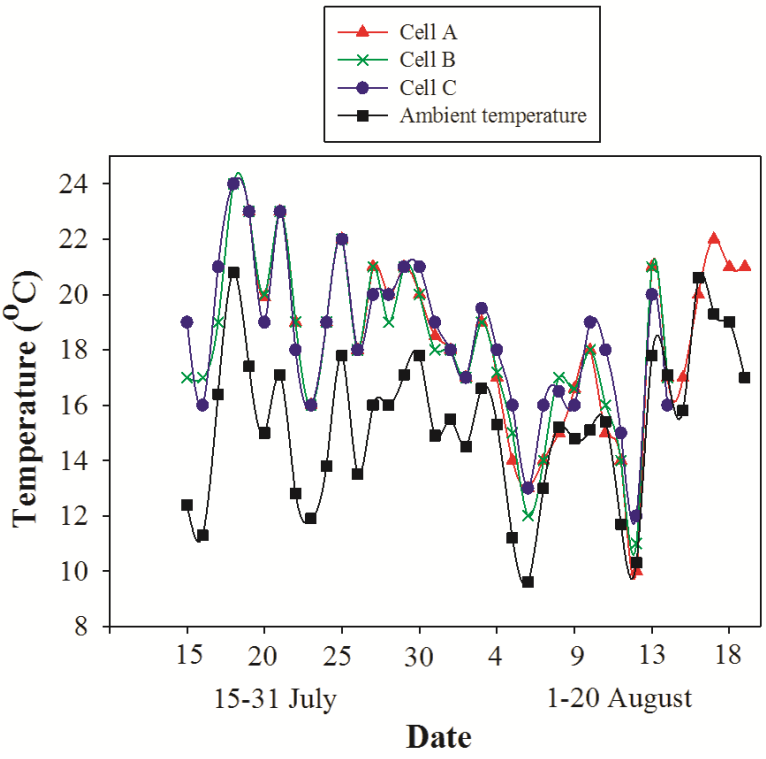


**Figure 5.8** The minimum temperature in Cell A, Cell B, and Cell C during the tests

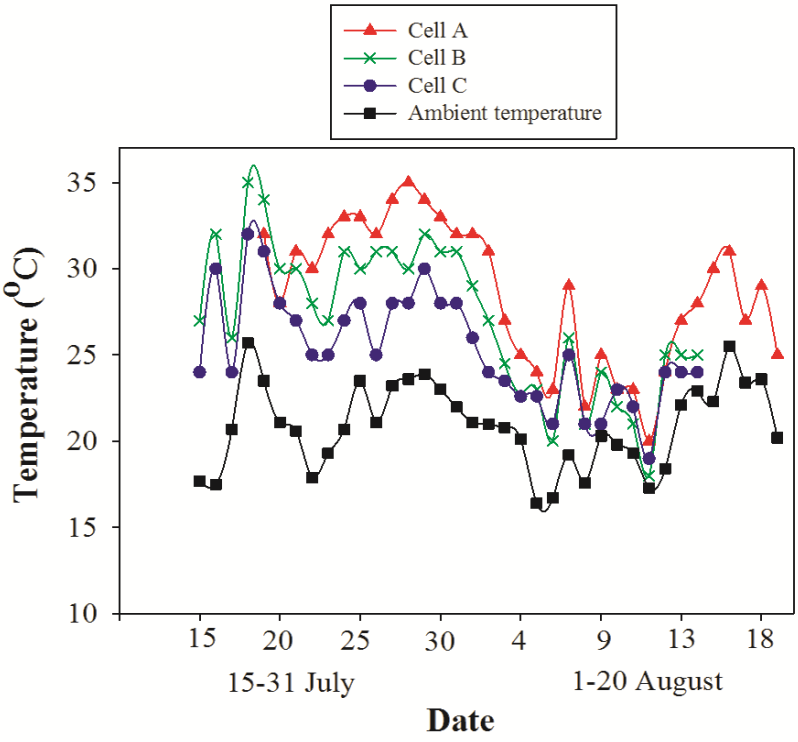


**Figure 5.9** The median temperature in Cell A, Cell B, Cell C during the tests

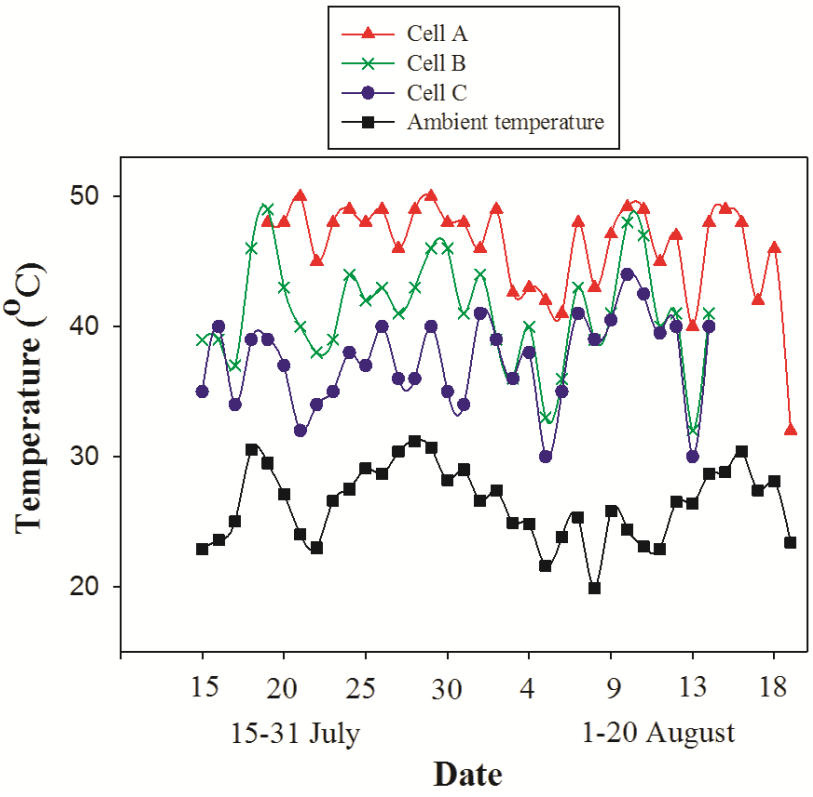


**Figure 5.10** The maximum temperature in Cell A, Cell B, Cell C during the tests

### 5.3.4 Bacterial movement

The efficacy of the new ACC configuration in delivering bacteria was compared to that of the CAC configuration. The standard plate count method was used to enumerate the colony forming units (CFU/g of soil) of *Mycobacterium pallens* sp. in the soil sections after the test. Figure 5.10 shows the distribution of *Mycobacterium pallens* sp. after the tests. As seen in Figure 5.10, CFU/g of soil in the test carried out with ACC technique varied between $1.6x10^5$ and $2.5x10^5$ CFU/g of soil compared to only $1x10^3$ CFU/g of soil near the anode and $2.3x10^3$ CFU/g of soil near the cathode in the test carried with CAC. In the test conducted using ACC, the figure shows that the CFU are somewhat evenly distributed, which clearly illustrates the effectiveness of ACC in delivering bacteria into the pores of kaolinite compared with CAC. In the test conducted using CAC configuration, the low number of colony forming units of $1x10^3$ at the anode compared to the $2.3x10^3$ CFU/g of soil at the cathode can be attributed to the low and pH environment caused by the electrolysis reaction. The pH in the anode and cathode compartments was monitored during the test. The pH decreased from 7 to approximately 2 at the anode and increased to about 11 at the cathode which is in agreement with typical pH changes near the electrodes (Page and Page 2002). The pH batch tests showed that *Mycobacterium pallens* sp. cannot survive the low pH 2 and the high pH 12.

In bioremediation processes the capability of bacteria to degrade a particular contaminant is optimum at a certain pH range. Most bacteria can live in a pH range between 6 and 8. Special strains of bacteria can tolerate extreme pH values (<2 or >10). Bacteria can adapt their cytoplasmic pH to the surrounding environment by controlling the exchange of H+ (internal proton concentration) through the cell wall or by the production of acids/bases in the cytoplasm (Booth 1985). However, the abrupt change in pH gradient across the cell membrane has an adverse effect on the growth and metabolism of bacteria (Cotter and Hill 2003; Padan et al. 2005; Krulwich et al. 2011).

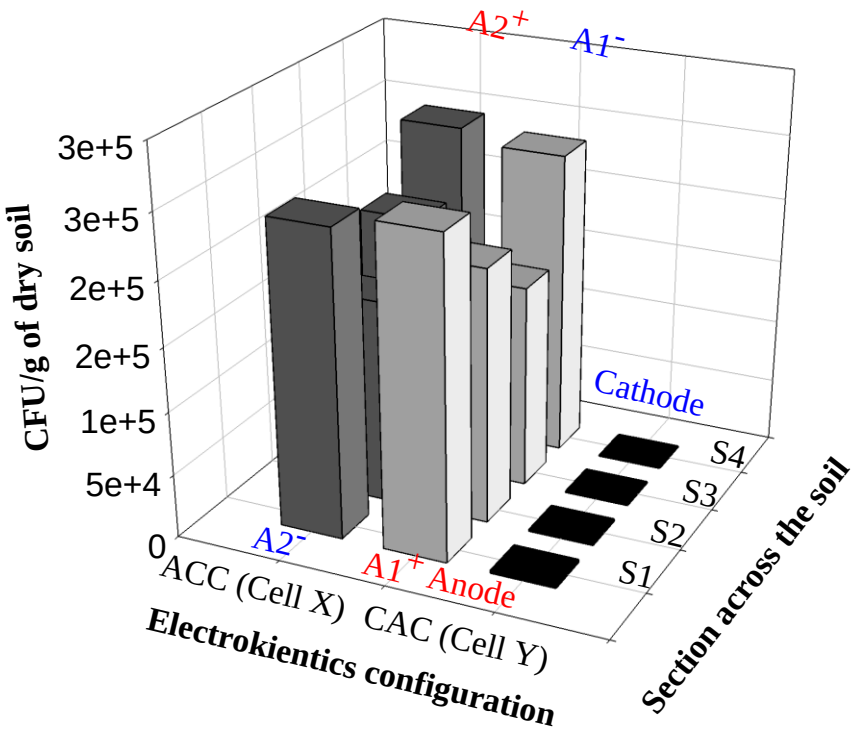


**Figure 5.11** Distribution of *Mycobacterium pallens* sp. after the tests in Cell X (ACC) and Cell Y (CAC).

In the CAC test, the investigation revealed that after six days the bacteria count (CFU) at the anode diminished which can be attributed to the low pH environment. In addition, the solution level in the anode compartment became very low after ten days; the test with CAC configuration was therefore terminated. The decrease in the solution level at the anode can be attributed to the transport of water from the anode to the cathode by electroosmotic flow and evaporation. In the test conducted with ACC configuration, the CFU value was the highest at the edge of the soil adjacent to the water compartments and relatively low at the middle section. These results provide proof that the ACC configuration is efficient in delivering bacteria. The success of the ACC configuration can be attributed to the stabilization of pH of the electrode water compartments which remained close to 7. The distribution of bacteria in the soil after the tests support our hypothesis that the ACC configuration can result in electroosmotic flow from anode $A1^{+}$ to cathode $A1^{-}$ and from anode $A2^{+}$ to cathode $A2^{-}$.

### 5.3.5 Nutrient delivery

The water compartments were filled with a nutrient that contain $NaNO_3$ (source of nitrogen) and $KH_2PO_4$ (source of potassium and phosphoorus). The results showed (see Figure 5.11) that $NaNO_3$, concentration higher than 100 mg/L, was delivered and distributed evenly in Cell A by electrokinetics with ACC configuration. However, the results showed that $KH_2PO_4$ was not transported. This is in agreement with previous studies that showed phosphorus was not transported into the soil but rather precipitated at the water compartment (Segall and Bruell 1992; Schmidt et al 2007; Xu et al. 2010). The success of the ACC configuration in delivering $NaNO_3$ can be attributed to two inherent characteristics of the ACC configuration. The first characteristic is the intermittent current which enhances electroosmotic flow as has been widely discussed in the literature (e.g. Mohamedelhassan and Shang 2001; Reddy and Camesselle 2009). The second characteristic is the control of pH. In Helmholtz-Smoluchowski model, widely accepted by researchers to quantify electroosmotic flow, the flow rate is proportional to the zeta potential (Mitchell and Soga 2005). Studies have shown that the zeta potential of a clay soil is very sensitive to the pH of the pore fluid. For example, the study by Vane and Zang (1997) has shown that the zeta potential for a kaolinite soil ranged from +0.7 mV at pH of 2 to -54 mV at pH of 10. Also, it found that the coefficient of electro-osmotic permeability to be three times greater at pH of 5 than at pH of 3. The non-uniform nutrients distribution in CAC tests is likely due to the non-uniform electroosmotic flow in the soil caused by the changes in the pH of the pore fluid and the subsequent change in the zeta potential. The relatively uniform nutrients distribution in the ACC tests is likely due to the pH of the pore fluid remained fairly uniform suggesting a more uniform electroosmotic flow.

Also, ACC technique maintains the resultant polarity between the electrodes in one direction and hence results in a net flow of ions in one direction.

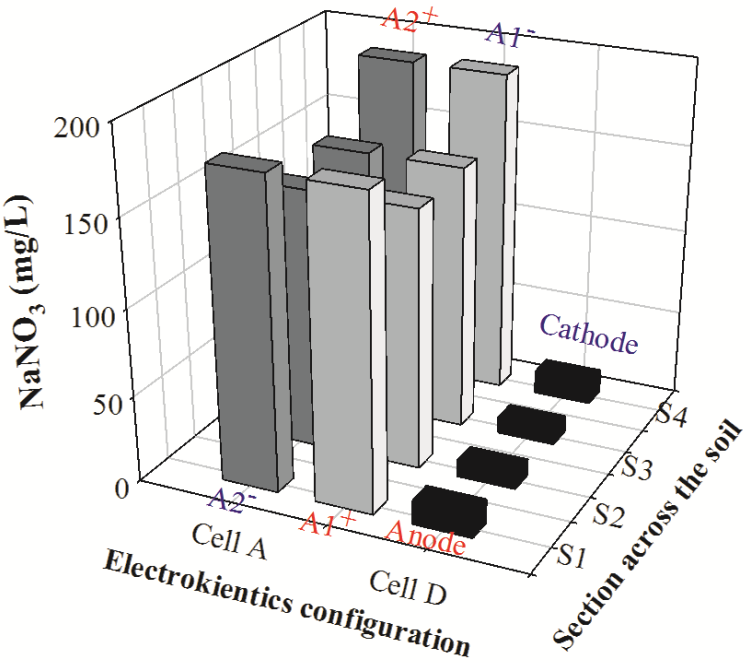


**Figure 5.12** Sodium Nitrate ($NaNO_3$) concentration in soil pore fluid after the tests in Cell A and Cell D.

### 5.3.6 Phenanthrene degradation

In electrokinetic bioremediation with a conventional DC power supply, researchers either use a constant current or a constant applied voltage. Both methods result in an increase in temperature, but not fluctuate during the day. The application of electrokinetics bioremediation using power generated by a solar panel added a unique effect to the degradation process. The fluctuation of the current during the day and the associated change in temperature is a unique phenomenon in this type of application. The effect of this phenomenon on the degradation efficiency has, to date, not been reported in the literature. The high temperature and high current can have a detrimental effect on indigenous bacteria. In the current study, the test setups resulted in different current in each cell and consequently different temperature. Phenanthrene degradation was found to be

different from one cell to another and was directly proportional to the current and the temperature. In the cell with the highest current and temperature and ACC configuration (Cell A), the degradation of phenanthrene was higher compared to the degradation in the other cells (Figure 5.12). After the test, the phenanthrene concentrations in Cell A were 50%, 75, 75%, and 47% in sections 1, 2, 3, and 4, respectively. In Cell D (the control), a high amount of phenanthrene, 80%, 88%, 90%, and 78% remained after the tests in sections 1, 2, 3, and 4. The high phenanthrene degradation in Cell A can be attributed to the effect of high current (the control Cell D has no current) which generated high temperature that enhanced the bioavailability of phenanthrene.

The concentration of phenanthrene in soil sections in Cell B after the tests were 61.5% 75%, 73%, and 64% of the initial concentration in section 1, 2, 3, and 4 respectively (Figure 5.13). It was observed that the phenanthrene concentration at the end of the test in Cell B is higher than in Cell A. This can be explained by the fact that in Cell B the current was used to deliver only bacteria into the soil, whereas in Cell A both nutrients and bacteria were applied to the soil. Lower amounts of phenanthrene were degraded in Cell C, which had low current and low temperature (Figure 5.14). In Cell C the remaining phenanthrene concentrations in soil sections 1, 2, 3, and 4 were 62%, 80%, 82% and 72.5% of the initial concentration, respectively. In Cell F (the control), the phenanthrene degradation was only 2 - 5%. In Cell F the phenanthrene contaminated soil was placed in the middle compartment and the solution contained bacteria was placed in the water compartment. The main mechanism of bacterial transport in the soil was diffusion. The clay soil has very low porosity that contributed to limiting the transport of bacteria in the soil. The higher degradation in Cell C compared to Cell F can be attributed to the fact that electric current was used to deliver bacteria and nutrients to soil.

The results show high phenanthrene degradation in Cell A compared to Cell B and Cell C. The main different between the tests is the soil composition. In Cell A soil was mixed with phenanthrene, bacteria, and nutrients. In Cell B the soil was mixed with phenanthrene and nutrients. In Cell C the soil was mixed with phenanthrene only. The test in Cell A is

designed to mimic a contaminated site where both bacteria and nutrients are existing. While, in Cell B the contaminant and bacteria are present in the site but there is lack of nutrients. The test in Cell C represents a contaminated site that lack both bacteria and nutrients. The high current in Cell A can be attribute to the higher electrical conductivity. The electrical current resulted in high temperature. Both current and temperature can contribute to the degradation enhancement (Wan et al. 2011, Kim et al 2005, Nyer and Suarez 2002, Van Hamme et al. 2003). Also, an indirect effect, the high current which generated high temperature that enhanced the bioavailability of phenanthrene. It was observed that the phenanthrene concentration at the end of the test in Cell B is higher than in Cell A. This can be explained by the fact that in Cell B the current was used to deliver only bacteria into the soil, whereas in Cell A both nutrients and bacteria were applied to the soil. Lower amounts of phenanthrene were degraded in Cell C, which had low current and low temperature.

In Canada, the regulatory guidelines for maximum level of phenanthrene in freshwater is 0.4 µg/L and 41 µg/kg in sediments (Canadian council of ministers of the environment (CCME 2010)). In the present study the initial concentration of phenanthrene was 2mg/kg, the test was conducted for 30 days. The degradation rate was between 33 µg/kg per day and 8 µg/kg per day. The degradation rate in this study is in an agreement with previous studies. For example, phenanthrene degradation was presented as 12.9 mg/day g dry cell (Yang et al. 2014). Study by Grosser et al. (2000) showed that, in the presence of surfactant, the phenanthrene degradation rate was 71 µg/L per day.

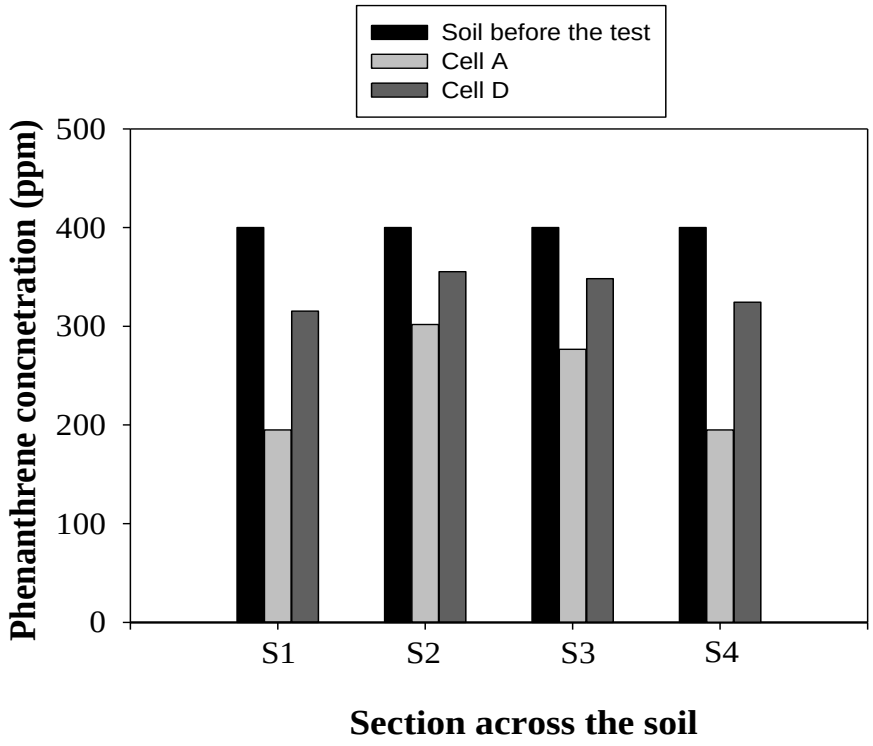


**Figure 5.13** Phenanthrene concentration in the soil after the tests in Cell A and Cell D

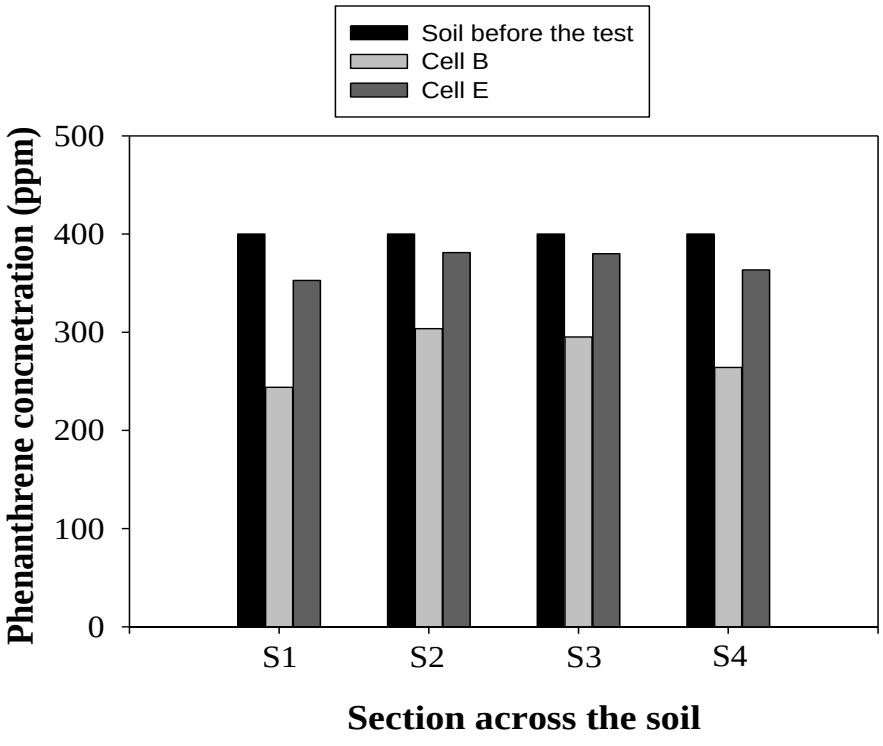


**Figure 5.14** Phenanthrene concentration in the soil after the tests in Cell B and Cell E

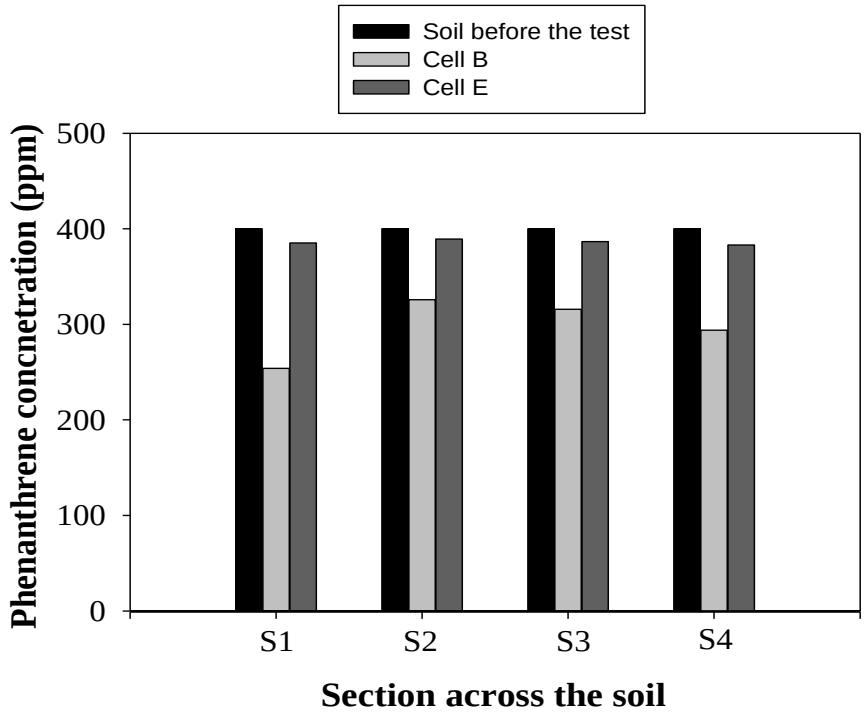


**Figure 5.15** Phenanthrene concentration in the soil after the tests in Cell C and Cell F

## 5.4 CONCLUSIONS

The results showed that temperature is a major factor in the outcome of electrokinetic bioremediation. The degradation of phenanthrene was directly related to the current and temperature, and the highest phenanthrene degradation was observed in the cell with that had the highest current and temperature. The results showed that the power generated by solar panel increased from zero volt at sunrise to a maximum of 60 V after 4 hours. The power then stabilized around the maximum, with minor fluctuation depending on weather conditions, for the next eight hours. Finally, the power started to decrease in the last three hours to zero volt at sunset. It is clear that solar panels can be a source of substantial power for electrokinetic bioremediation. The use of solar power can reduce the total cost of the process, and the added benefits would include temperature fluctuation during the day. The zero voltage intervals during the night result in lowering of the soil temperature and therefore contribute to the success of the process. It was observed that the current generated in the cell is directly related to the composition of the soil in the electrokinetic cell. The results showed that the ACC configuration is effective in delivering bacteria and nutrients.

The success of the ACC configuration can be attributed to the stabilization of the pH at the water compartments which remained close to 7. It was observed that the nutrients were somewhat evenly distributed inside the cells treated with ACC. Application of electrokinetic bioremediation to mitigate soil contaminated with hydrocarbons has a tremendous capacity to be a highly efficient degradation method.

## 5.5 REFERENCES

Acar, Y. B., Rabbi, M. F. and Ozsu, E. E. (1997). "Electrokinetic injection of ammonium and sulfate ions into sand and kaolinite beds." Journal of Geotechnical and Geoenvironmental Engineering, **123**(3): 239-249.

Alshawabkeh, A. N., Yeung, A. T. and Bricka, M. R. (1999). "Practical aspects of in-situ electrokinetic extraction." Journal of Environmental Engineering-ASCE, **125**(1): 27-35.

Andersson, J. T. and Achten, C. (2015). "Time to say goodbye to the 16 EPA PAH? Toward an up-to-date Use of PACs for environmental purposes." Polycyclic Aromatic Compounds, **35**(2-4): 330-354.

Boldrin, B., Tiehm, A. and Fritzsche, C. (1993). "Degradation of phenanthrene, fluorene, fluoranthene, and pyrene by a mycobacterium Sp." Applied and Environmental Microbiology, **59**(6): 1927-1930.

Bona, C., de Rezende, I. M., Santos, G. D. and de Souza, L. A. (2011). "Effect of soil contaminated by diesel oil on the germination of seeds and the growth of schinus terebinthifolius raddi (Anacardiaceae) eeedlings." Brazilian Archives of Biology and Technology, **54**(6): 1379-1387.

Booth, I. R. (1985). "Regulation of Cytoplasmic Ph in Bacteria." Microbiological Reviews, **49**(4): 359-378.

Bouvrette, P., Hrapovic, S., Male, K. B. and Luong, J. H. T. (2006). "Analysis of the 16 Environmental Protection Agency priority polycyclic aromatic hydrocarbons by high performance liquid chromatography-oxidized diamond film electrodes." Journal of Chromatography A, **1103**(2): 248-256.

Budhu, M., Rutherford, M., Sills, G. and Rasmussen, W. (1997). "Transport of nitrates through clay using electrokinetics." Journal of Environmental Engineering-Asce, **123**(12): 1251-1253.

Canadian Council of Ministers of the Environment (2010). Canadian Soil Quality Guidelines CARCINOGENIC AND OTHER POLYCYCLIC AROMATIC HYDROCARBONS (PAHs) (Environmental and Human Health Effects) Scientific Criteria Document (revised) PN 1445 ISBN 978-1-896997-94-0.

Cerniglia, C. E. (1984). "Microbial-Metabolism of Polycyclic Aromatic-Hydrocarbons." Advances in Applied Microbiology, **30**: 31-71.

Coppotelli, B. M., Ibarrolaza, A., Dias, R. L., Del Panno, M. T., Berthe-Corti, L. and Morelli, I. S. (2010). "Study of the Degradation Activity and the Strategies to Promote the Bioavailability of Phenanthrene by Sphingomonas paucimobilis Strain 20006FA." Microbial Ecology, **59**(2): 266-

Cotter, P. D. and Hill, C. (2003). "Surviving the acid test: Responses of gram-positive bacteria to low pH." Microbiology and Molecular Biology Reviews, **67**(3): 429-+.

Dias, R. L., et al. (2012). "Bioremediation of an aged diesel oil-contaminated Antarctic soil: Evaluation of the "on site" biostimulation strategy using different nutrient sources." International Biodeterioration & Biodegradation, **75**: 96-103.

Gill, R. T., Harbottle, M. J., Smith, J. W. N. and Thornton, S. F. (2014). "Electrokinetic-enhanced bioremediation of organic contaminants: A review of processes and environmental applications." Chemosphere, **107**: 31-42.

Grosser, R. J., Friedrich, M., Ward, D. M. and Inskeep, W. P. (2000) Effect of model sorptive phases on phenanthrene biodegradation: Different enrichment conditions influence bioavailability and selection of phenanthrene-degrading isolates. Applied and Environmental Microbiology **66(7)**:2695-2702.

Hansen, H. K. and Rojo, A. (2007). "Testing pulsed electric fields in electroremediation of copper mine tailings." Electrochimica Acta, **52**(10): 3399-3405.

Hassan, I., Mohamedelhassan, E. and Yanful, E. K. (2015). "Solar powered electrokinetic remediation of Cu polluted soil using a novel anode configuration." Electrochimica Acta, **181**: 58-67.

Hassan, I., Mohamedelhassan, E., Yanful, E. K. E. and Yuan, Z.-C. (2016). "A Review Article: Electrokinetic Bioremediation Current Knowledge and New Prospects." Advances in Microbiology, **6**(1): 57-75.

Ho, S. V., et al. (1999). "The Lasagna technology for in situ soil remediation. 2. Large field test." Environmental Science & Technology, **33**(7): 1092-1099.

Krulwich, T. A., Sachs, G. and Padan, E. (2011). "Molecular aspects of bacterial pH sensing and homeostasis." Nature Reviews Microbiology, **9**(5): 330-343.

Lacey, S. (2015). "Cheapest Solar Ever: Austin Energy Gets 1.2 Gigawatts of Solar Bids for Less Than 5 Cents." GTM the leading information services provider for the next-generation electricity system., SOLAR PROJECTS.

Mitchell, J. K. and Soga, K. i. (2005). Fundamentals of soil behavior. Hoboken, N.J., John Wiley & Sons

Mohamedelhassan, E. and Shang, J. (2001). "Effects of electrode materials and current intermittence in electro-osmosis." Proceedings of the ICE-Ground Improvement, **5**(1): 3-11.

Mohamedelhassan, E. and Shang, J. Q. (2008). "Electrokinetic cementation of calcareous sand for offshore foundations." International Journal of Offshore and Polar Engineering, **18**(1): 73-80.

Moody, J. D., Freeman, J. P., Doerge, D. R. and Cerniglia, C. E. (2001). "Degradation of phenanthrene and anthracene by cell suspensions of Mycobacterium sp strain PYR-1." Applied and Environmental Microbiology, **67**(4): 1476-1483.

Page, M. M. and Page, C. L. (2002). "Electroremediation of contaminated soils." Journal of Environmental Engineering-Asce, **128**(3): 208-219.

Padan, E., Bibi, E., Ito, M. and Krulwich, T. A. (2005). "Alkaline pH homeostasis in bacteria: New insights." Biochimica Et Biophysica Acta-Biomembranes, **1717**(2): 67-88.

Puglisi, E., Cappa, F., Fragoulis, G., Trevisan, M. and Del Re, A. A. M. (2007). "Bioavailability and degradation of phenanthrene in compost amended soils." Chemosphere, **67**(3): 548-556.

Reddy, K. R. and Cameselle, C. (2009). Electrochemical remediation technologies for polluted soils, sediments and groundwater. Hoboken, N.J., Wiley**:** xxii, 732 p.

Reddy, K. R. and Saichek, R. E. (2003). "Effect of soil type on electrokinetic removal of phenanthrene using surfactants and cosolvents." Journal of Environmental Engineering-Asce, **129**(4): 336-346.

Reddy, K. R. and Saichek, R. E. (2004). "Enhanced electrokinetic removal of phenanthrene from clay soil by periodic electric potential application." Journal of Environmental Science and Health Part a-Toxic/Hazardous Substances & Environmental Engineering, **39**(5): 1189-1212.

Schmidt, C. A. B., Barbosa, M. C. and de Almeida, M. D. S. (2007). "A laboratory feasibility study on electrokinetic injection of nutrients on an organic, tropical, clayey soil." Journal of Hazardous Materials, **143**(3): 655-661.

Segall, B. A. and Bruell, C. J. (1992). "Electroosmotic Contaminant-Removal Processes." Journal of Environmental Engineering-Asce, **118**(1): 84-100.

SolarBuzz (2010). "Solarbuzz Reports World Solar Photovoltaic " Marketbuzz.

Souza, F. L., SaÃ©z, C., Llanos, J., Lanza, M. R. V., CaÃ±izares, P. and Rodrigo, M. A. (2016). "Solar-powered electrokinetic remediation for the treatment of soil polluted with the herbicide 2,4-D." Electrochimica Acta, **190**: 371-377.

Sutton, N. B., et al. (2013). "Impact of Long-Term Diesel Contamination on Soil Microbial Community Structure." Applied and Environmental Microbiology, **79**(2): 619-630.

Vane, L. M. and Zang, G. M. (1997). "Effect of aqueous phase properties on clay particle zeta potential and electro-osmotic permeability: Implications for electro-kinetic soil remediation processes." Journal of Hazardous Materials, **55**(1-3): 1-22.

Xu, W., Wang, C. P., Liu, H. B., Zhang, Z. Y. and Sun, H. W. (2010). "A laboratory feasibility study on a new electrokinetic nutrient injection pattern and bioremediation of phenanthrene in a clayey soil." Journal of Hazardous Materials, **184**(1-3): 798-804.

Yang, H. Y., Jia, R. B., Chen, B. and Li, L. (2014) Degradation of recalcitrant aliphatic and aromatic hydrocarbons by a dioxin-degrader Rhodococcus sp strain p52. Environmental Science and Pollution Research **21(18)**:11086-11093.

Yeung, A. T. and Gu, Y. Y. (2011). "A review on techniques to enhance electrochemical remediation of contaminated soils." Journal of Hazardous Materials, **195**: 11-29.

Yuan, S. H., Zheng, Z. H., Chen, J. and Lu, X. H. (2009). "Use of solar cell in electrokinetic remediation of cadmium-contaminated soil." Journal of Hazardous Materials, **162**(2-3): 1583-1587.

Zhang, Y. and Smith, S. J. (2008). "Long-Term Modeling of Solar Energy: Analysis of Concentrating Solar Power (CSP) and PV Technologies " Report to US Department of Energy.

Zhao, H. P., Wu, Q. S., Wang, L., Zhao, X. T. and Gao, H. W. (2009). "Degradation of phenanthrene by bacterial strain isolated from soil in oil refinery fields in Shanghai China." Journal of Hazardous Materials, **164**(2-3): 863-869.

# CHAPTER 6
# ISOLATION AND CHARACTERIZATION OF NOVEL BACTERIA STRAINS FROM AGRICULTURAL SOILS FOR THR DEGRADATION OF DIESEL FUEL[1]

## 6.1 INTRODUCTION

The significant increase in the human population in the last 50 years has resulted in high demand for food supplies and agricultural products (Zinkina and Korotayev 2014). Current agricultural practices rely heavily on heavy machinery, raising the potential for soil contamination. Diesel is the primary fuel for agriculture machineries (Jokiniemi et al. 2012). Diesel fuel spills from leaking storage tanks and pipelines are common. Recently, large volumes of accidental oil spills have occurred in Canada and US. For instance, at Lac-Megantic, Quebec, Canada, rail disaster in July 2013 (Transportation-Safety-Board-of-Canada 2014), the oil train explosion near Casselton, N.D. Dec 2013, and the largest crude oil spill on land which occurred in a farmer land due to a rupture in a pipeline in North Dakota, US (Golgowski 2013). Bioremediation is a cost-effective method for the removal of petroleum hydrocarbons from soil (Yergeau et al. 2009; Yeung and Gu 2011; Gill et al. 2014). Diesel fuel is composed of aliphatic hydrocarbons (64%), alkenes (1-2%), and aromatic hydrocarbons(35%) (Yergeau et al. 2009). Understanding the behavior of indigenous microorganisms is essential for the development of successful bioremediation treatment for diesel fuel spills (Singh and Tripathi 2007; Bona et al. 2011; Sutton et al. 2013). Suitable bacteria consorti capable of producing enzymes necessary for complete diesel fuel degradation are needed for remediation of diesel fuel (mixture of aliphatic and aromatic hydrocarbons) spills. Therefore, isolating and identifying new bacterial strains from nature with enhanced bioremediation abilities, which are resistant to soil and environmental stress conditions is crucial for efficient bioremediation.

[1]A version of this chapter has been submitted to Applied and Environmental Microbiology

Bacteria start degrading less complex hydrocarbons (for example, alkanes), and then aromatic hydrocarbons which are recalcitrant compounds (Whyte et al. 2002). Depending on the genera, the aerobic degradation of alkane is known to be catalysed by different genes including monooxygenases *alk*B gene, alkane hydroxylases (alkM), soluble electron transfer proteins rubredoxin (rubA), and rubredoxinreductase (rubB), xcpR gene (Yergeau et al. 2009). Also, the behavior of prospective diesel degrading bacteria under various environmental conditions is essential for the survival of the microorganisms and the effectiveness of the bioremediation process. High concentrations of some contaminants are lethal to bacteria and can prevent certain metabolic reactions (Talley 2006). Therefore, it is critically to identify the toxicity level of the contaminant to bacteria. The optimal temperature and pH conditions for bacterial growth vary from one bacterial strain to another. However, low and high temperature and/or pH environments can be harmful to most types of bacteria (Cotter and Hill 2003; Padan et al. 2005).

This study presents isolation of dozens of bacterial strains and the characterization of them based on their capability of degrading diesel fuel. The genes expressed in the diesel degradation process were investigated.

## 6.2 MATERIALS AND METHODS

Three hundred bacterial strains were isolated from corn and canola roots. Serial dilutions were plated on Luria broth (LB) agar plates and incubated at 28$^{o}$C for 24 h. Each strain was purified three (single colony) times prior to further analysis. Diesel fuel degradation assays were conducted using the strains. Figure 6.1 shows the protocol followed to identify isolates capable of degrading diesel fuel. Single colonies were streaked on Petri-dishes with minimal medium mixed with 2% diesel fuel as a sole carbon source and incubated in the dark at 28$^{o}$C and bacterial growth was monitored for 5 days. The minimal medium consists of $NH_4SO_4$- 1 g/L, $KH_2PO_4$ - 0.5 g/L, $K_2HPO4$ - 0.5 g/L, $MgSO_4$- 0.1 g/L, NaCl - 6 g/L, $CaCl_2$ - 0.1 g/L, and MES Hydrate- 1 g/L. Strains that showed growth were further

investigated. They were streaked on Petri-dishes with minimal medium, and Petri-dishes with carbon dioxide. Furthermore, strains that showed growth only in minimal medium with diesel were again streaked in Petri-dishes with minimal medium mixed with 2% diesel fuel to determine the growth of bacteria. Forty five strains were identified as capable of degrading diesel fuel. Genomic DNA of these strains was isolated using Sigma-Aldrich GenElute Bacterial Genomic DNA Kit (Product No. NA2120) following the manufacturers protocol. The quality of the product was determined using Nanodrop 2000 (Thermo Scientific). Polymerase chain reactions (PCR) were conducted using the DNA of the strains as a template in reactions and the 16sRNA forward primer and reverse primer. The PCR reaction was carried out with the Bio-Rad T1000 Thermal Cycler (Bio-Rad): one initial denaturation cycle at 98 ºC for 5 min, followed by 30 cycles of denaturation for 30 s at 98 °C, annealing for 30 s at 55 °C, and extension for 60 s at 72 °C, with the final overall extension for 10 min at 72 ºC. PCR products were visualized by gel electrophoresis using a 1% TAE Gel stained with ethidium bromide. The 16sRNA PCR products were purified using QIAquick PCR Purification Kit (Qiagen) and sent for sequencing using an Applied Biosystems 3730 Analyzer at Eurofins Genomics (Louisville, KY). Basic local alignment search tool (BLAST) algorithm was used to identify closest/similar strains using the sequences of the PCR products (http//www.ncbi.nlm.nih.gov). Nineteen of these strains were identified by 16sRNA sequence analysis. Three isolates *Acinetobacter calcoaceticu-16* (AC16), *Sinorhizobium sp. B84-53* (SB53), and *Sphingobacterium multivorum-155* (SM155) were selected for further investigations. The following tests were conducted using the three isolates:

1- The isolates were grown in liquid minimal medium, pH 5.75, with diesel as sole carbon source to assess the ability of isolates to degrade diesel fuel. Isolates were grown in separate 250 mL Erlenmeyer flasks with total volume of 50 mL of minimal media supplemented with seven different diesel fuel concentrations 6%, 5%, 4%, 3%, 2%, 1%, and 0.5% (v/v) as carbon and energy source. The diesel was sterilized using 25 µm membrane filters (Whatman). The isolates were grown for two days at 28$^{o}$C in Luria broth (LB), washed two times with 0.85% NaCl and the washed cells were used to prepare initial solutions of $OD_{600}$ of 0.5 of the isolates. Flasks were incubated aerobically at 28$^{o}$C in a

shaker (150 rpm) for 15 days. The growth of the isolates was monitored by optical density at 600 nm ($OD_{600}$) and recorded during the test period of 15 days.

2-The isolates were grown in separate 250 mL Erlenmeyer flasks contain 50 mL minimal medium with 2% (v/v) diesel fuel as sole carbon source. Flasks were incubated aerobically in incubator shakers (150 rpm) adjusted at four different temperatures 48$^{o}$C, 38$^{o}$C, 28$^{o}$C, and 18$^{o}$C for 15 days. The initial solutions contain isolates of $OD_{600}$ of 0.5. The optical density of 600 nm ($OD_{600}$) of each isolate was monitored and recorded during the test period.

3-The isolates were grown in separate 250 mL Erlenmeyer flasks contain 50 mL minimal medium with 2% (v/v) diesel fuel at six different pH 12, 10, 8, 6, 4, and 2. Flasks containing strains were incubated aerobically at 28$^{o}$C in a shaker (150 rpm) for 15 days. Initial solutions contain isolates at $OD_{600}$ of 0.5. The $OD_{600}$ of each isolate was monitored during the test period of 15 days.

4-Seven solutions containing the isolates at $OD_{600}$ of 0.5 were prepared. (i) Each isolate was grown in a separate 35 mL heavy duty glass tube with a total volume of 15 mL of minimal medium supplemented with 2% (v/v) diesel fuel. Then, 1 g of soil was added into the tubes. (ii) Three solutions (15 mL each) containing minimal medium and 2% diesel fuel and 1 g soil were prepared using each of the isolate with the other two (iii) The three isolates were added to a solution (15 mL) containing minimal media and 2% diesel fuel and 1 g soil. Three tubes containing minimal medium and 2% diesel were prepared to serve as control. The seven solutions and the controls were grown in an incubator shaker at 28$^{o}$C for 15 days. Diesel fuel concentration was determined using GC/MS after 15 days. The soil used in the experiments was obtained from a local site in London, Ontario, Canada. Tests were carried out in accordance with the American Society of Testing and Materials standard procedures to determine the physical and chemical properties of the soil. Tests carried out included particle-size distribution analysis, Hydrometer, Atterberg limits,

specific gravity, cation exchange capacity, and total organic carbon. Most of the tests were carried out in triplicate and the results are shown in Table 6.1. According to the Unified Soil Classification System (USCS), the group symbol of soil is SC and the group name is Clayey sand.

5- Polymerase chain reaction (PCR) was conducted using DNAs' of the three isolates as a template in reactions to confirm the existence of selected seventeen genes, known to be active in diesel fuel degradation. The isolates were grown for two days at 28$^{o}$ C in Luria broth (LB) agar plate. Pure colonies were picked up and dissolved in 1 mL ultrapure water (milli-Q water). Genomic DNAs for the three isolates AC16, SB53, and SM155 were extracted from the pellet using GenElute Bacterial Genomic DNA Kit from Sigma-Aldrich according to manufacturer's instructions. The primers of the genes of interest were acquired from Eurofins MWG Operon (see Table 6.1). PCR run as shown above and varied annealing temperature were used depending on $T_m$ of the primers pair for 45 s.

**Table 6.1** Soil properties

| Soil property | Measured value |
|---|---|
| Liquid limit | 25 (±2) |
| Plastic limit | 18 (±1) |
| Uniformity coefficient ($C_u$) | 5.3 |
| Coefficient of gradation | 1.5 |
| Electrical conductivity | 869 μS/cm |
| pH | 7.0 (±0.1) |
| Cation exchange capacity | 16.75 (±0.10) meq/100 g of soil |
| Organic carbon content | 2.3% (±0.05) |

The values between the brackets are the range of errors.

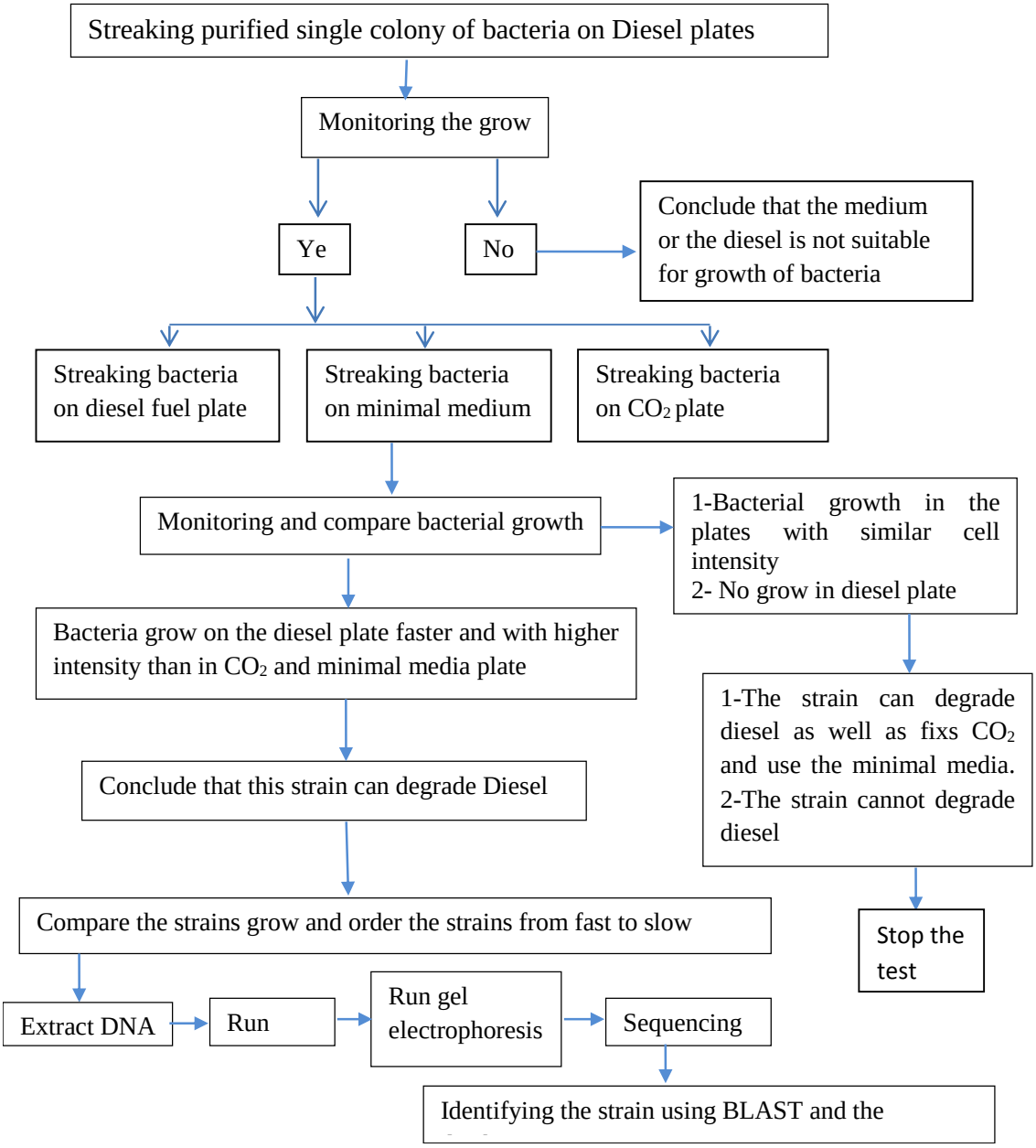


**Figure 6.1** Flow chart for identifying strains capable of degrading diesel fuel

**Table 6.2** The primers for the genes

| Seq Name (primer) | Seq 5’ to 3’ | Reference |
|---|---|---|
| 16S RNA F | GTAGCGGGTCGAGAGGATG | (Lin et al. 2013) |
| 16S RNA R | GCCTCCTCCTCGCTTAAAGT | (Lin et al. 2013) |
| LipB F | CCAACCCTAGCAGCATCATT | (Lin et al. 2013) |
| LipB R | TGCAACAAGCTCTGCTTCAG | (Lin et al. 2013) |
| 1698F | CAACATCGGTTTGATCAAC | (Powell et al. 2006) |
| 2041R | CGTTGCATGTTGGTACCCAT | (Powell et al. 2006) |
| LipA F | CTTCCGTTTCAACGATTGGT | (Lin et al. 2013) |
| LipA R | TATACGCTGCACCGACAGAG | (Lin et al. 2013) |
| rubA F | GATTTATGATGAAGCCGAAGG | (Lin et al. 2013) |
| rubA R | GTCAGGGCAAGTCCAGTCAT | (Lin et al. 2013) |
| P450 F | GTGGGCGGCAACGACACGAC | (Maier et al. 2001) |
| P450 R | GCAGCGGTGGATGCCGAAGCCTAA | (Maier et al. 2001) |

6- Real-time polymerase chain reaction (RT-PCR) was conducted to identify the genes that expressed in the three isolates during diesel fuel degradation tests. The selected isolates were grown in minimal medium, pH 5.75, with diesel as sole carbon source. Isolates were grown in separate Erlenmeyer flasks with total volume of 50 mL of minimal medium supplemented with 2% (v/v) diesel fuel concentrations. Control tests consisted of isolates grown in separate Erlenmeyer flasks containing 50 mL of minimal medium supplemented with 0.5% (v/v) glycerol. The flasks were incubated aerobically at 28$^{o}$C in a shaker (150 rpm) for 15 days. After 3 and 7 days, 1 mL from each flask was obtained and centrifuged at 15000 rpm for 1 min, which resulted in a pellet and a cell-free supernatant. Bacterial RNA from each of the three isolates in the tests and in the control were extracted using Presto$^{TM}$ Mini RNA Bacteria Kit (Geneaid) according to manufacturer's instructions and used in the RT-PCR. The RNA purity and yield was determined using Nanodrop 2000 (Thermo Scientific). cDNA libraries of the control and diesel treatments were prepared using a SensiFAST™ cDNA Synthesis Kit .according to the manufacturer's protocol using 500ng of RNA as starting template. RT-PCR was performed in 20uL volumes using the SsoFast™EvaGreen Supermix (Bio-Rad) according to the manufacturer's instructions on a CFX96 Touch™ Real-Time PCR Detection System (Bio-Rad).

Diesel in liquid medium was extracted using liquid-liquid extraction method. The liquid was transfer, after the tests, into a separator funnel and 20 mL of solvents (mixture of Acetone and Dichloromethane (1:1)) was added, the mixture was shaken for one minute and left in a vertical position for two-phase separation to take place. The extraction was repeated two times and volumes were combined. The combined volume was reduced to 10 mL using a Kuderna-Danish apparatus.

Extraction of diesel fuel from soil samples in tests (4) above was conducted as follows: the solution (15 mL) was removed after centrifugation (2300 g) of the tubes for 40 min. Liquid liquid extraction was used to extract the diesel fuel from the liquid sample. Solvent, Acetone and Dichloromethane mixture 1:1 (20 mL) was added and the tube was placed in

the sonicator for 2 h and then the solution was replaced with a fresh solvent (1:1) and sonicated again for 2 h. After sonication the solution was replaced for the second time with 20 mL of fresh solvent and the tube was placed in a table shaker (150 rpm) overnight. The solutions were then combined together (60 mL), and a Kuderna-Danish apparatus was used to reduce the volume to 10 mL.

Diesel concentrations in the samples were determined using GC/MS. Column chromatography backed with alumina and anhydrous sodium sulphate was used to remove water and filter the analyte. Final solutions were filtered using 25 µm TPF filters. The GC-MS method used a gas chromatography column HP-MS (length 30 m, internal diameter 250 µm, film thickness 0.25 µm), helium as a carrier gas, injected volume of 1 µL, initial temperature of 70$^{o}$C held for 2 min, and then ramped at 5$^{o}$C per min up to 300$^{o}$C and held for 5 min.

## 6.3 RESULTS AND DISCUSSION

### 6.3.1 Effect of diesel fuel concentration

The growth of the isolates was monitored over a period of 15 days and determined by optical density ($OD_{600}$). Figures 6.2, 6.3, and 6.4 present the results. It was observed that AC16 growth rate increased with increase in diesel fuel concentration between 0.5% and 2%. At a diesel fuel concentration of 0.5% isolate AC16 started to grow in the first 24h. The short lag time suggests that AC16 can consume diesel fuel at a concentration of 0.5% without the need for adaptation time. The lag time for AC16 growth was more than 24 h at a diesel fuel concentration of 1%. This can be attributed to the time needed by AC16 to adapt to the environment. At higher concentrations between 2% and 6%, bacteria required 48 h to adapt to the diesel fuel. The maximum growth occurred after 14 days at a diesel concentration of 2%. It was observed that bacterial growth decreased as the concentration

increased from 3% to 6%. The slow growth at high concentrations (3%-6%) can be attributed to the possibility that high diesel concentration had an adverse effect on the growth of bacteria (Virkutyte et al. 2002).

In general, the results showed that strain AC16 has tolerance to diesel fuel concentration up to 6%. For SM155, bacteria growth increased with an increase of diesel fuel concentration between 0.5 and 1%. At higher concentrations, growth decreased with an increase in concentration. In general, SM155 shows growth trends in diesel fuel similar to that of AC16. For SB53, the lag period was 48 h for diesel fuel concentrations of 0.5, 1, 2, and 3%. The growth curves for SB53 are similar at diesel concentrations of 0.5 and 1%. The highest growth was observed at a diesel concentration of 2%. The growth behavior is moderate at higher concentrations (3% and 4%) in the first seven days and increased afterwards. At higher concentrations 5% and 6% the growth curve shows that the lag time for SB53 was seven days.

The isolates showed a capability of degrading diesel but different growth behavioral patterns in using diesel fuel as a sole carbon source. For AC16, the $OD_{600}$ increased rapidly in the first 9 days of incubation and then remained somewhat constant until the end of the test. SM155 shows steep growth rate curve for the first six days of incubation and then lower proficiency in the utilization of diesel fuel. Figures 6.2, 6.3, and 6.4 show that the lag phase of bacterial growth is different between the isolates with the shortest lag phase reported in the test conducted using AC16 followed by SM155 and then SB53. The longest lag phase was found in the test with SB53.

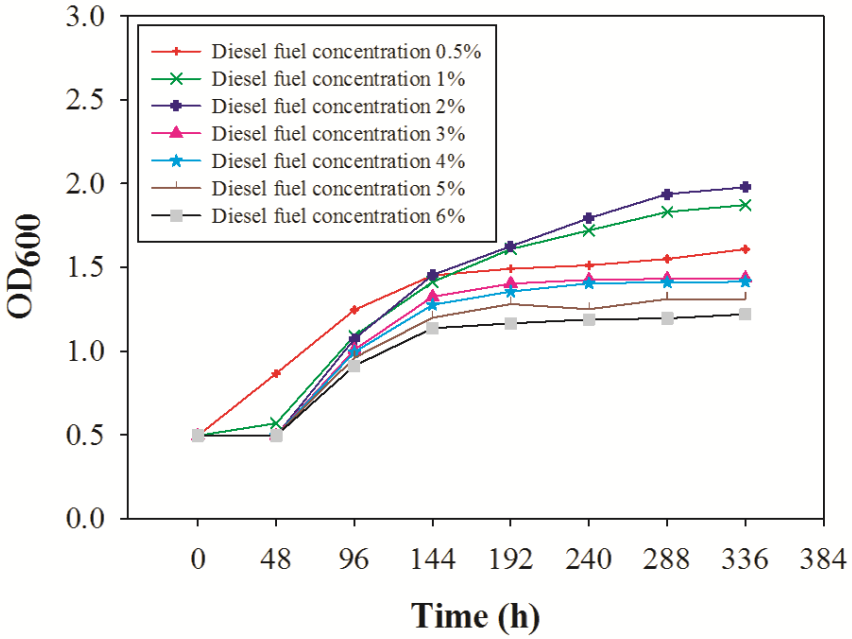


**Figure 6.2** Degradation of different diesel concentration by strain AC16

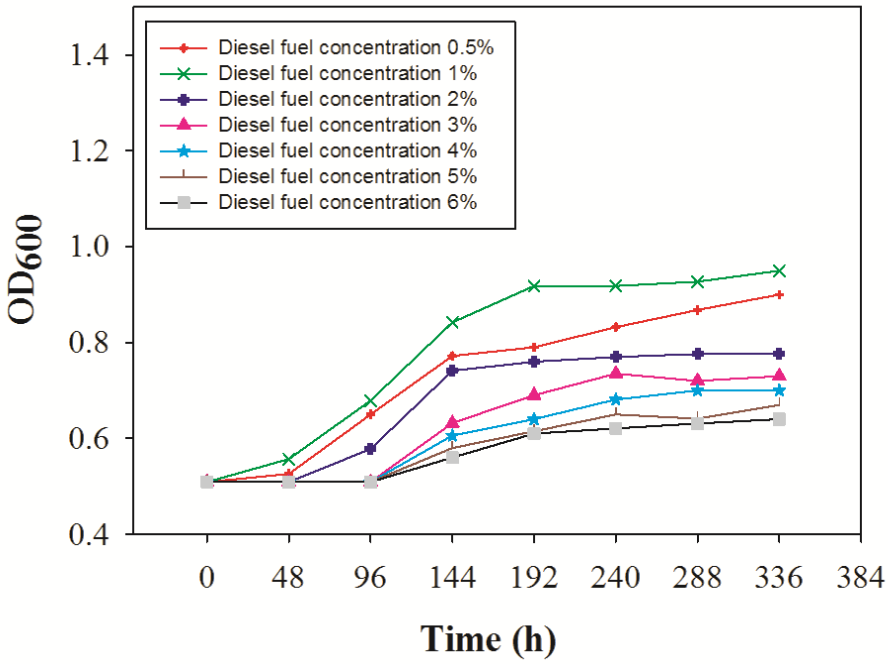


**Figure 6.3** Degradation of different diesel concentration by strain SM155

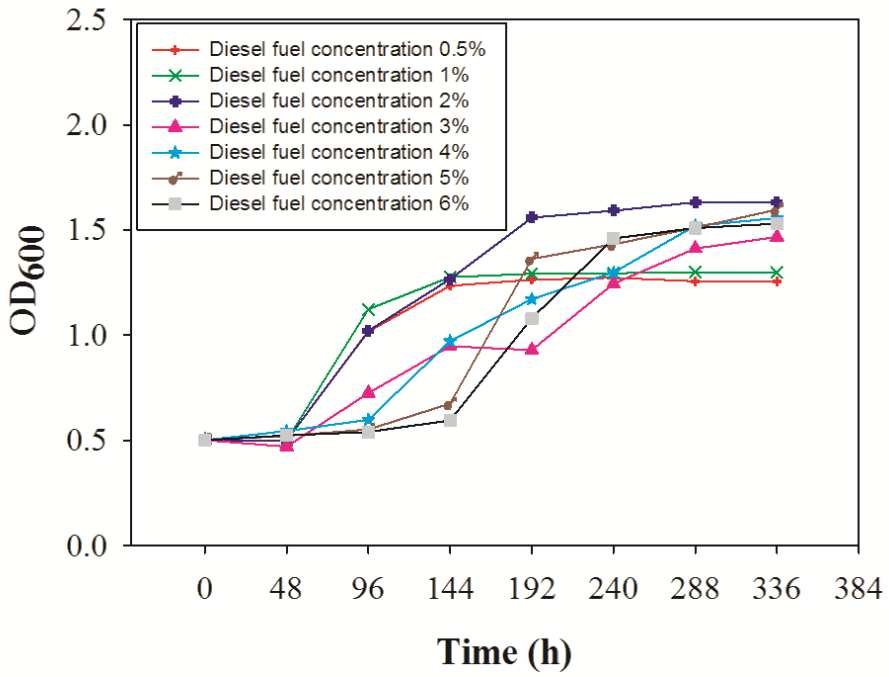


**Figure 6.4** Degradation of different diesel concentration by strain SB53

## 6.3.2 Different temperatures

The growth of the three isolates was investigated at temperatures 18ºC, 28ºC, 38ºC, and 48ºC. The optical density 600 nm ($OD_{600}$) was measured periodically during the treatments and used to determine bacterial growth. Figures 6.5, 6.6, and 6.7 and Table 6.3 show the results. The straight part of the curve in Figure 6.5, tests conducted at temperature 18ºC, represents the lag phase (adaptation time the isolate needed to grow in the diesel fuel). Figure 6.5 shows the isolate AC16 required shorter lag, as AC16 started to grow first as indicated by the increase in the $OD_{600}$. Although the isolate SB53 took loner time for adaptation than AC16, it showed raped growth that exceeded AC16 growth rate after 192 h. SM155 showed slower growth rate compared with the other two isolates. The results reveal that isolate SB53 can tolerate lower temperatures and degraded diesel fuel compared to the other strains.

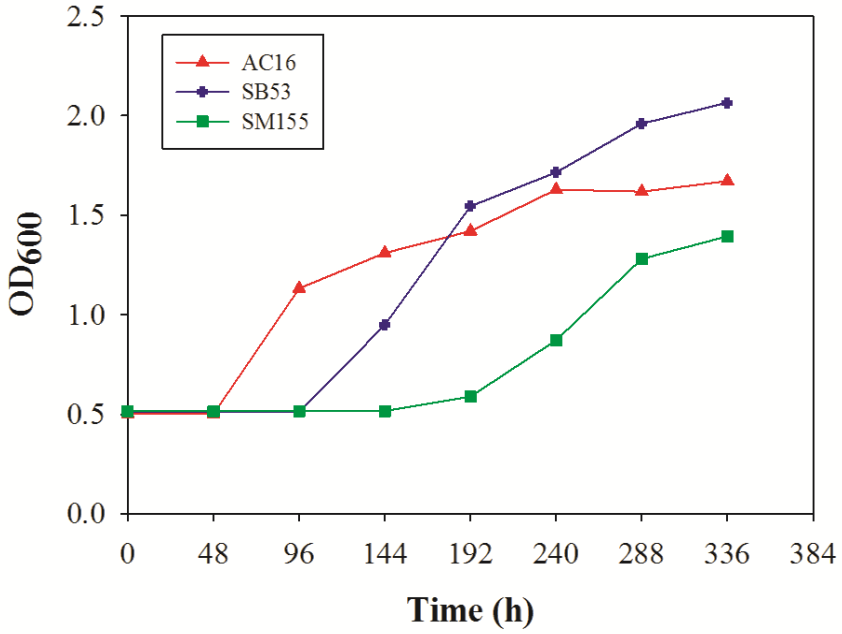


**Figure 6.5** Growth rates of the AC16, SB53, and SM155 at temperature 18$^{o}$C

As shown in Figure 6.6, at temperature 28$^{o}$C, the growth rate of AC16 is higher than the other two isolates. The growth rate of SM155 and SB53 show great similarity in the first ten days after which time the SB53 growths rate is higher than SM155. The test indicated that AC16 can grow quite well at 28$^{o}$C.

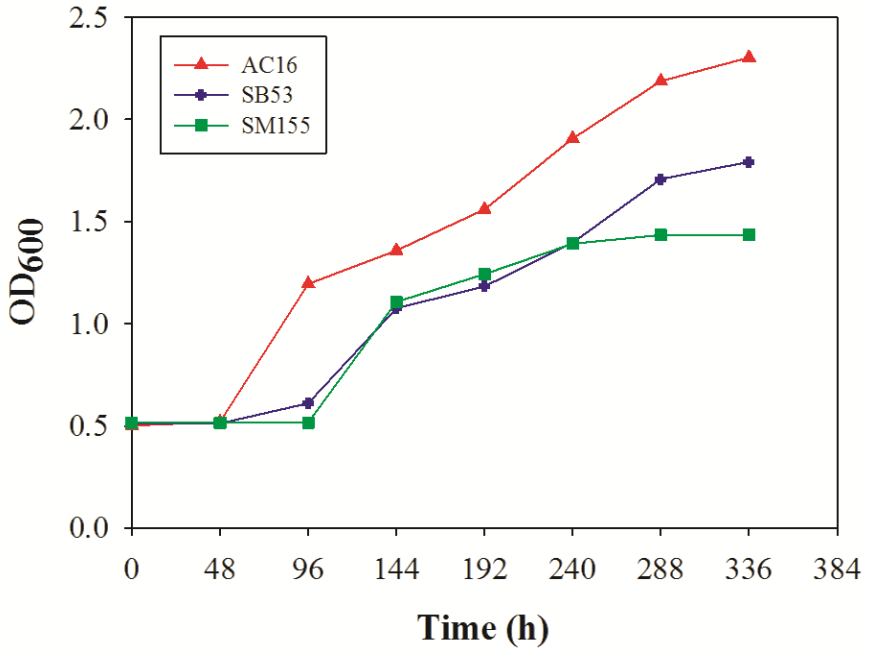


**Figure 6.6** Growth rates of the AC16, SB53, and SM155 at temperature 28ºC

At temperature 38ºC, Figure 6.7 shows that the adaptation phase period was around six days for SM155, ten days for AC16, and twelve days for SB53. The longer lag phase at high temperature can be attribute to the time necessary for bacterial strain to recover from physical damage (Nair 2010). The shorter lag phase for bacterial growth in the test conducted using SM155 indicates that SM155 can recover quickly from the physical damage cause by 38ºC temperature. The results reveal that SM155 can grow and degrade diesel at a temperature of 38ºC better than the other isolates AC16 and SB53.

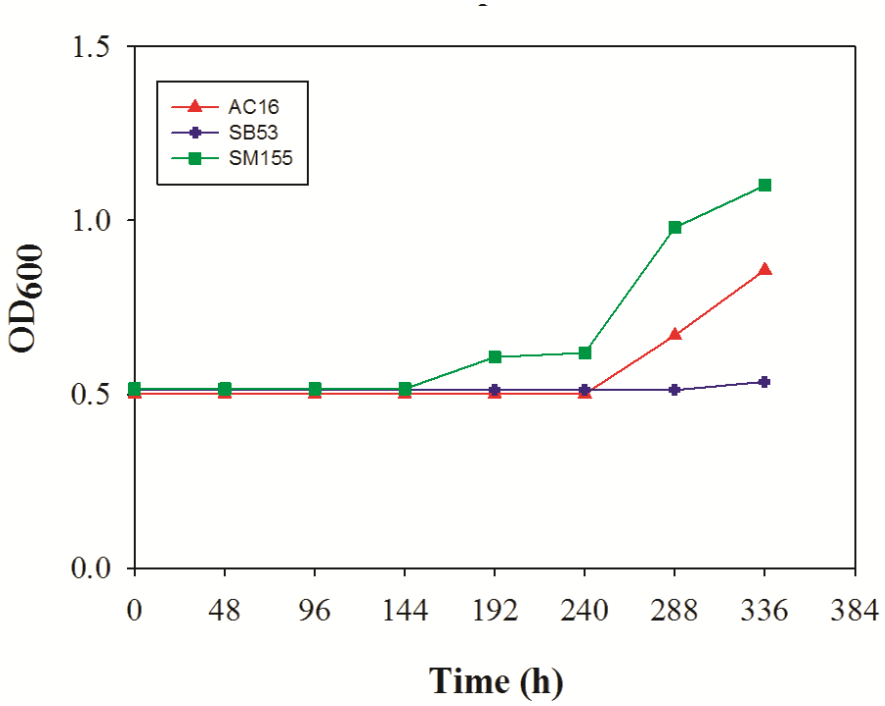


**Figure 6.7** Growth rates of the AC16, SB53, and SM155 at temperature 38$^{o}$C

The results showed at 48$^{o}$C, the three isolates did not grow in the agar medium, which is an indication that the cells did not survive the 48$^{o}$C temperature. The temperature tests were conducted using minimal medium at pH 5.75. Interestingly, the tests revealed that the pH remain relatively unchanged for the tests conducted at temperatures 38$^{o}$C and 48$^{o}$C, while the pH decreased to around 4.5 for the tests conducted at temperature 18$^{o}$C and 28$^{o}$C (see Table 6.3). The results suggested that the bacterial mechanism for temperature adaptation is accompanied by a pH changes at low temperatures between 18 and 28$^{o}$C. The results showed that at temperature 18$^{o}$ C the isolate SB53 degraded diesel better than the other two isolates, whereas at temperature 28$^{o}$ C the isolate AC16 performance was the superior compared to the other isolates. At temperature 38$^{o}$ C, the isolate SM155 can grow better than the other isolates.

**Table 6.3** pH after the temperatures tests conducted with three isolate

| Temperature | pH after the test with isolate AC16 | pH after the test with isolate SB53 | pH after the test with isolate SM155 |
|---|---|---|---|
| 18° C | 4.56 | 4.49 | 4.85 |
| 28° C | 4.69 | 4.59 | 4.88 |
| 38° C | 5.78 | 5.78 | 5.75 |
| 48° C | 5.70 | 5.79 | 5.80 |

### 6.3.3 Different pH

Figure 6.8 shows that the growth curves, as indicated by the $OD_{600}$, of isolates AC16 and SB53 are somewhat similar in the first 6 days. After that the growth rate of AC16 was higher than that of SB53. In the last two days, the growth rate of SB53 exceeded that of AC16. The growth rate of the SM155 was lower than the other two isolates. In the tests conducted at pH 8, the isolate SB53 was faster than the other two isolates in the first four days as shown in Figure 6.9. Isolate AC16 growth rate after five days was higher than the other two isolates. The growth rate of isolate SM155 stabilized after ten days. On the other hand the growth rate of the isolate SB53 continued to increase. The results showed that bacterium CA16, SM155, and SB53 could grow and degrade diesel fuel in the pH range of 6-8. Most heterotrophic bacteria favor neutral pH (Venosa and Zhu 2003) as the pH of the soil has an effluences on the solubility and bioavailability of the contaminant as well as the nutrients. At high pH, cations (for example, calcium, and magnesium), tend to adhere to the soil and become less available, while at low pH the nitrate and chloride are less available (Luo et al. 2012). Table 6.3 shows pH after the tests conducted using different pHs. The table shows that there were no significant changes in pH value after the tests conducted using initial pH 2 and 4. However, significant decreases in the initial pH values were observed in the tests conducted with initial pH 6,8,10, and 12.

Some bacterial strains have the ability to tolerate low pH conditions using internal adaptation mechanisms including the use of proton pumps, production of alkali, the protection or repair of macromolecules, cell membrane changes, induction of pathways by transcriptional regulators, alteration of metabolism, and the role of cell density and cell signaling (Cotter and Hill 2003; Padan et al. 2005; Rousk et al. 2009; Rousk et al. 2011). On the other hand, a shift to an alkaline environment can cause unfavorable conditions for bacteria. The results in this study showed that bacteria did not only survive but that they also grew because of the increase in the optical density ($OD_{600}$) readings. The survival of bacteria is defined as no net increase in viable cells and can be monitored using plate count method (counts of viable cells as colony forming units (CFU))(Davey 2011). The growth of bacteria, typically, is defined as a logarithmic increase in viable cell count and can be monitor using the optical density ($OD_{600}$)(Widdel 2007).

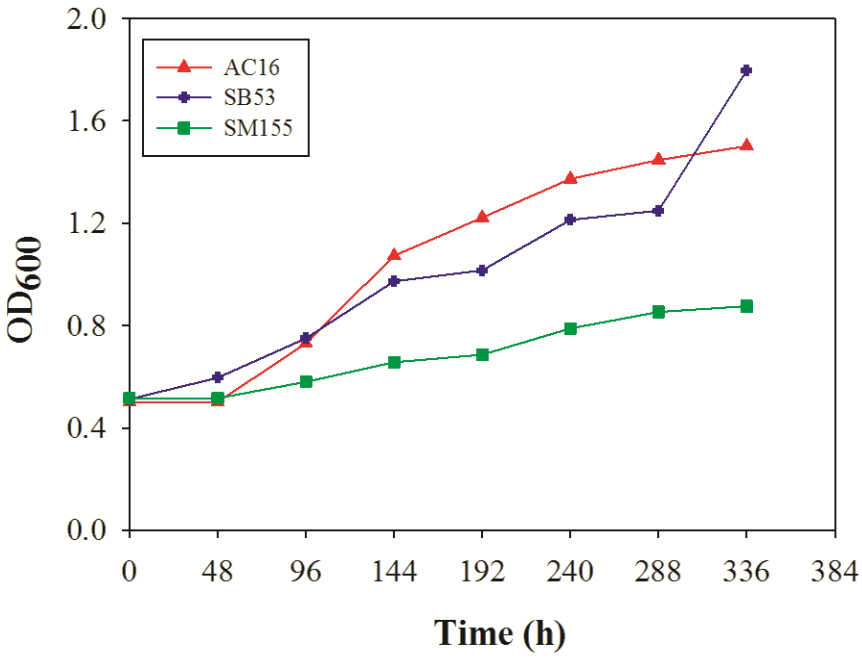


**Figure 6.8** Growth rates of the AC16, SB53, and SM155 at pH 6

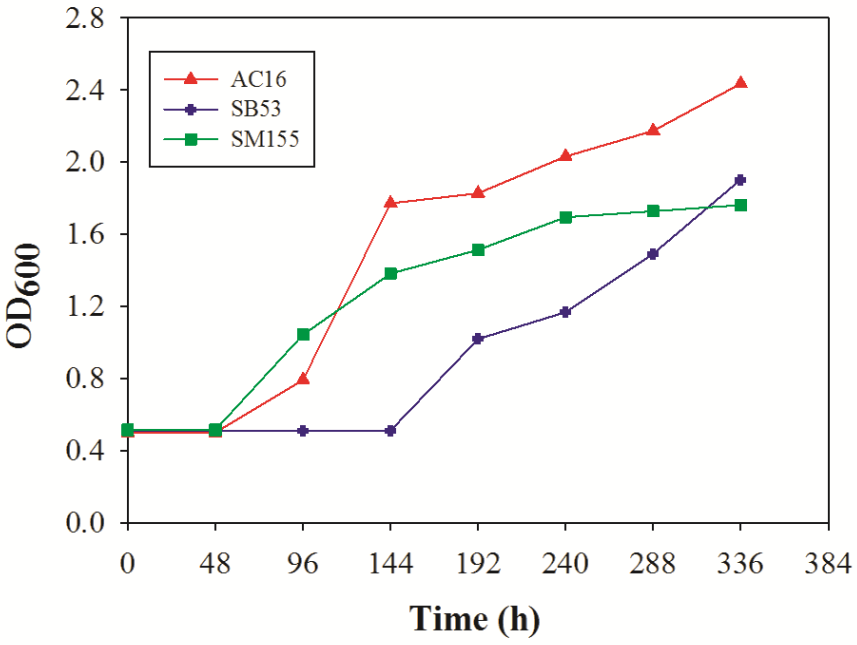


**Figure 6.9** Growth rates of the AC16, SB53, and SM155 at pH 8

**Table 6.4** pH after the tests conducted with three isolate at different pHs

| pH | pH after the test with isolate AC16 | pH after the test with isolate SB53 | pH after the test with isolate SM155 |
|---|---|---|---|
| 2 | 2.1 | 2.3 | 2.4 |
| 4 | 4.5 | 4.5 | 4.2 |
| 6 | 4.8 | 4.8 | 5.5 |
| 8 | 6.0 | 6.0 | 6.5 |
| 10 | 6.8 | 6.6 | 8.3 |
| 12 | 10.0 | 9.3 | 8.0 |

### 6.3.4 Expressed genes and RT-PCR

Table 6.5 shows the results of the PCR. The list shows the genes that were detected in the three isolates. Lipases enzymes Lip A, LipB, and Alk-b2 were detected only on AC16. The genes rubA and 1698/2041 were detected in the three isolates. P450 was detected in SM155 only. Rubredoxin (rubA) is required for n-alkane degradation (Tani et al. 2001). The list of the genes investigated (Table 6.2) were selected based on previous studies (Fierer et al. 2005; Powell et al. 2006; Yergeau et al. 2009; Hassanshahian et al. 2014).

Figures 6.10, 6.11, and 6.12 show the results of the RT-PCR for three isolates after 3 days and 7 days in the tests conducted using diesel fuel and glycerol. Figure 6.10 (a) shows that after 3 days the expression of rubA, in AC16 test conducted with the diesel fuel, is more than double the expression in the test conducted with glycerol. Figure 6.10 (b) shows that after seven days the expression of rubA in the test conducted with glycerol is higher than in the tests conducted with the diesel fuel. Figure 6.11 (a) shows that after 3 days the expression of rubA in the SB53 test conducted with the diesel fuel is three time higher than the expression in the test conducted with glycerol. However, Figure 6.11 (b) shows that after seven days the expression of rubA in the SB53 test conducted with diesel fuel was under the detection limit and in the test conducted with glycerol, it was less than the expression after 7 days (see Figure 6.11 (a)). Figure 6.12 (a) shows that after 3 days the expression of rubA in SM155 test conducted with the diesel fuel is higher than in the test conducted with glycerol, while after seven days the expression of rubA was higher in the tests conducted with glycerol. The results show that the expression of rubA reached its maximum value some time before 7 days. It was not possible to determine when the maximum expression took place because the samples were taken after 3 and 7 days. These findings are in agreement with previous study (Lin et al. 2013). The absence of Lip A and LipB expressions in the three isolates suggests that lipases were not involved in diesel degradation (Singh and Lin 2008; Lin et al. 2013).

RT-PCR products were visualized by gel electrophoresis using 1% TAE Gel stained with ethidium bromide. Figure 6.13 (a) shows that 16S, rubA, P450 were expressed in SM155. Figure 6.13 (b) shows that 16S, rubA, 1698/2041 were expressed in SB53. Figure 6.13 (c) shows that 16S, LipA, rubA, 1698/2041 were expressed in AC16.

**Table 6.5** List of genes

| Gene | AC16 | SB53 | SM155 |
|---|---|---|---|
| 16S | detected | detected | detected |
| LipB | detected | not detected | not detected |
| 1698/2041 | detected | detected | detected |
| LipA | detected | not detected | not detected |
| rubA | detected | detected | detected |
| Alk-b2 | detected | not detected | not detected |
| P450 | not detected | not detected | detected |

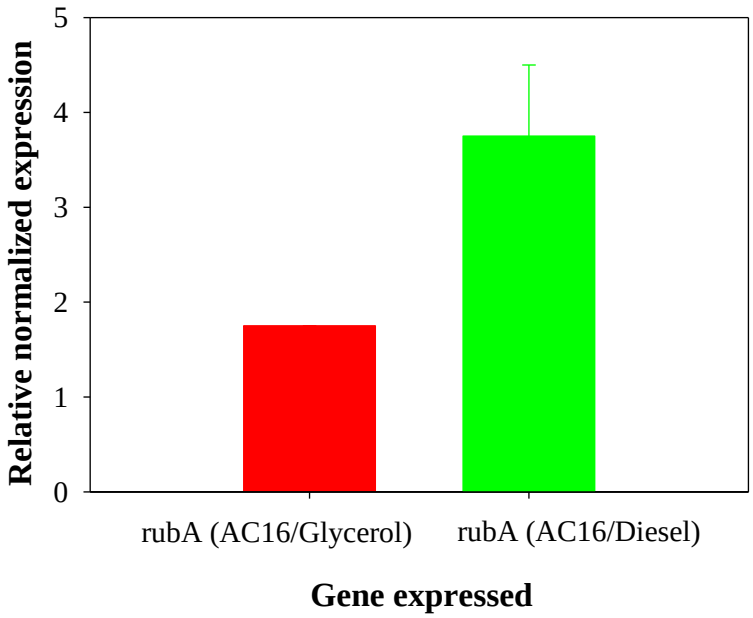


(a)

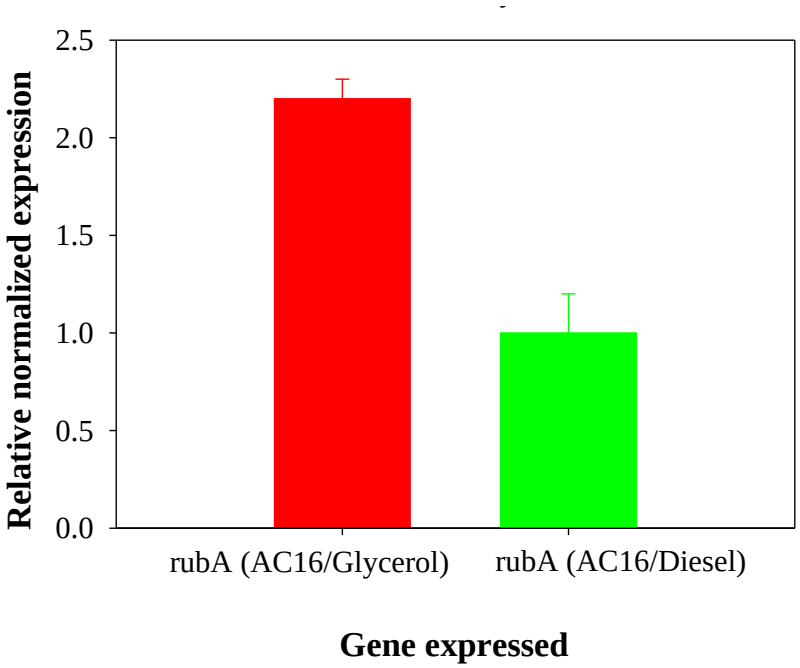


(b)

**Figure 6.10** AC16 gene expression chart (a) after 3 days (b) after 7 days

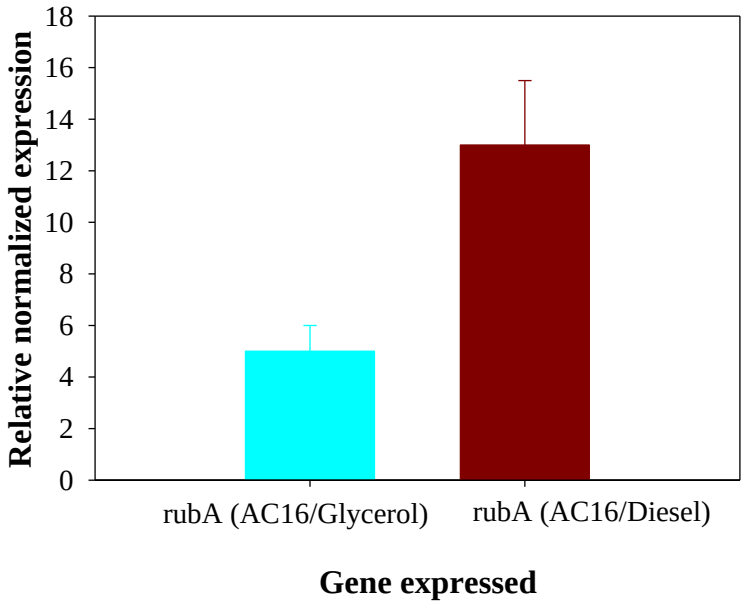


(a)

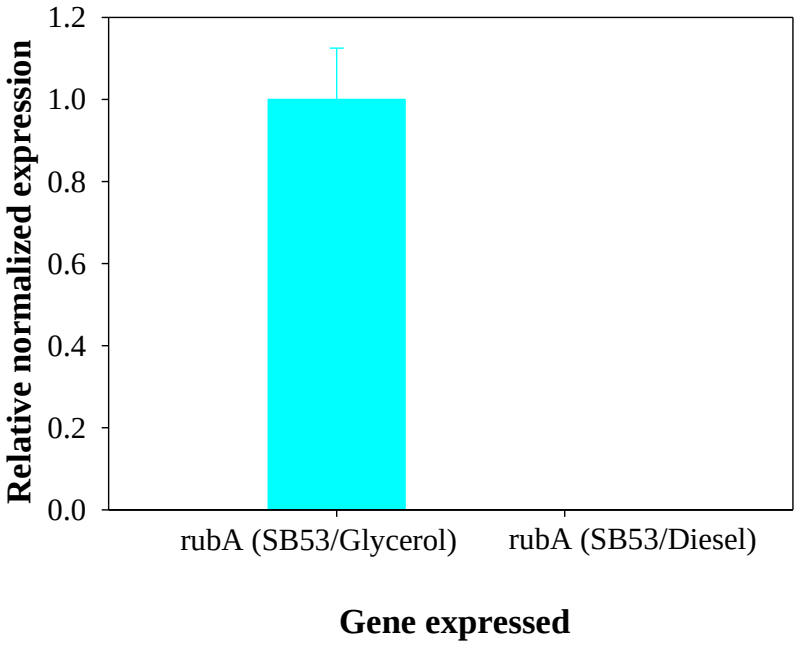


(b)

**Figure 6.11** SB53 gene expression chart (a) after 3 days (b) after 7 days

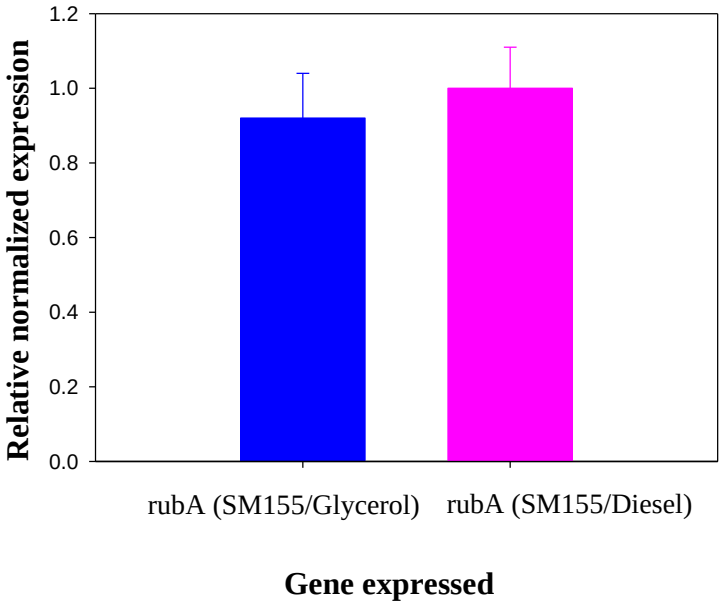


(a)

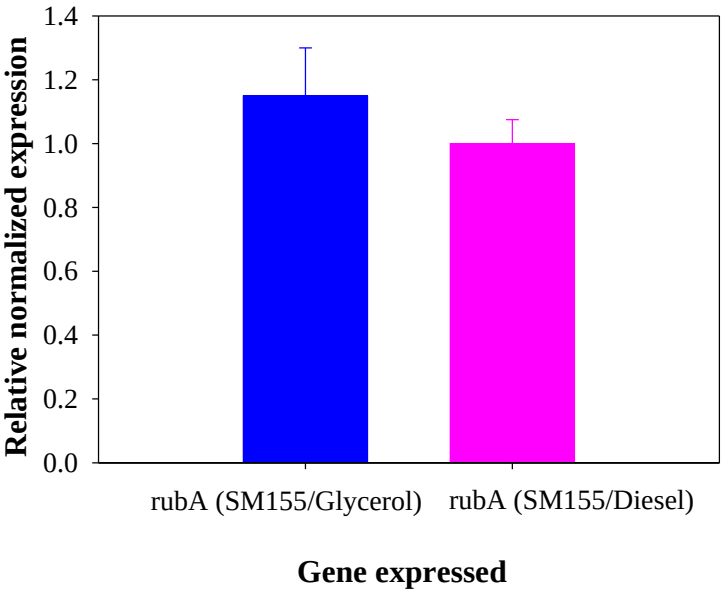


(b)

**Figure 6.12** SM155 gene expression chart (a) after 3 days (b) after 7 days

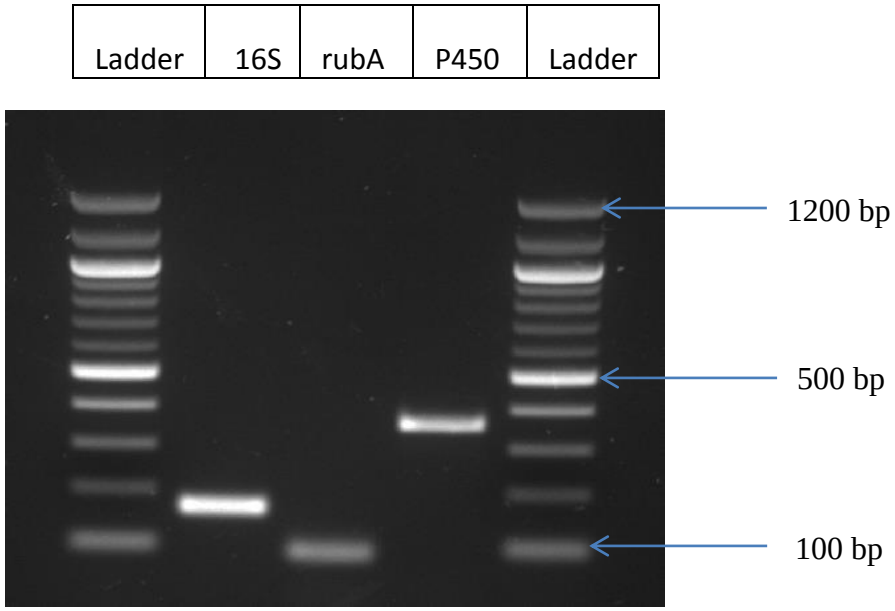


(a) *Sphingobacterium multivorum* SM155 RT-PCR product

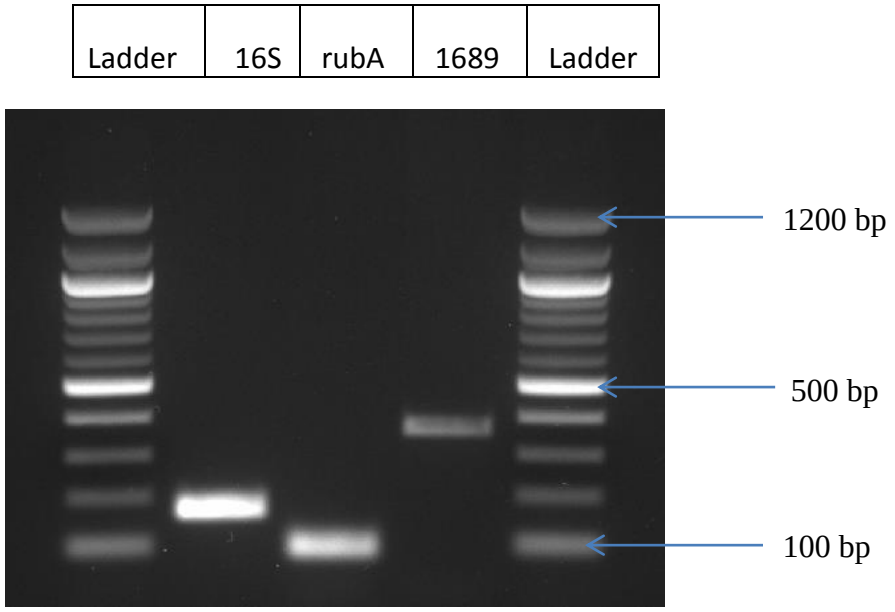


(b) *Sinorhizobium* SB 53RT-PCr product

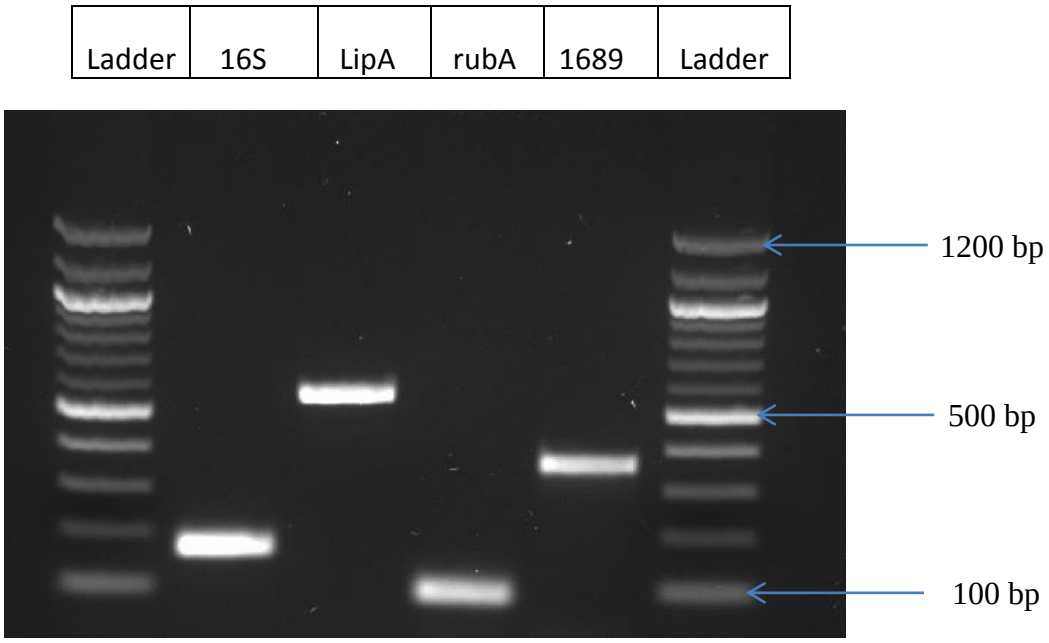


(c) *Acinetobacter calcoaceticus* AC16 RT-PCR product

**Figure 6.13** TR-PCR products for the three isolates

## 6.3.5 Diesel fuel degradation

Figure 6.14 shows the ratio (in percentage) of diesel fuel concentration after the test (C) to the initial concentration ($C_o$= 1 mL diesel/ 50 mL minimal medium). The ratio of the diesel concentrations in the control flasks were around 97%. The reduction in the diesel fuel concentration in the control tests can be attributed to evaporation. The test conducted with the isolates AC16 and SM155 shows the lowest ratio of diesel concentration of 47%. The combination of isolates AC16 and SM155 results in the lowest diesel concentration after the test compared to the other combinations. The result of the second test in which the isolate SM155 combined with SB53 show higher ratio of diesel concentration than the first

test. The combination of the isolates AC16 and SB53 resulted in higher final concentration than the first two tests as shown in Figure 6.14. Combining the three isolates resulted in higher final diesel fuel concentration compared to the first four tests. The results suggest that, in order to achieve high degradation of diesel fuel the combination between of isolates AC16 and SM155 should be used. The results from the RT-PCR gene expression support this finding as rubA was highly expressed in AC16 and SM155 after 3 and 7 days.

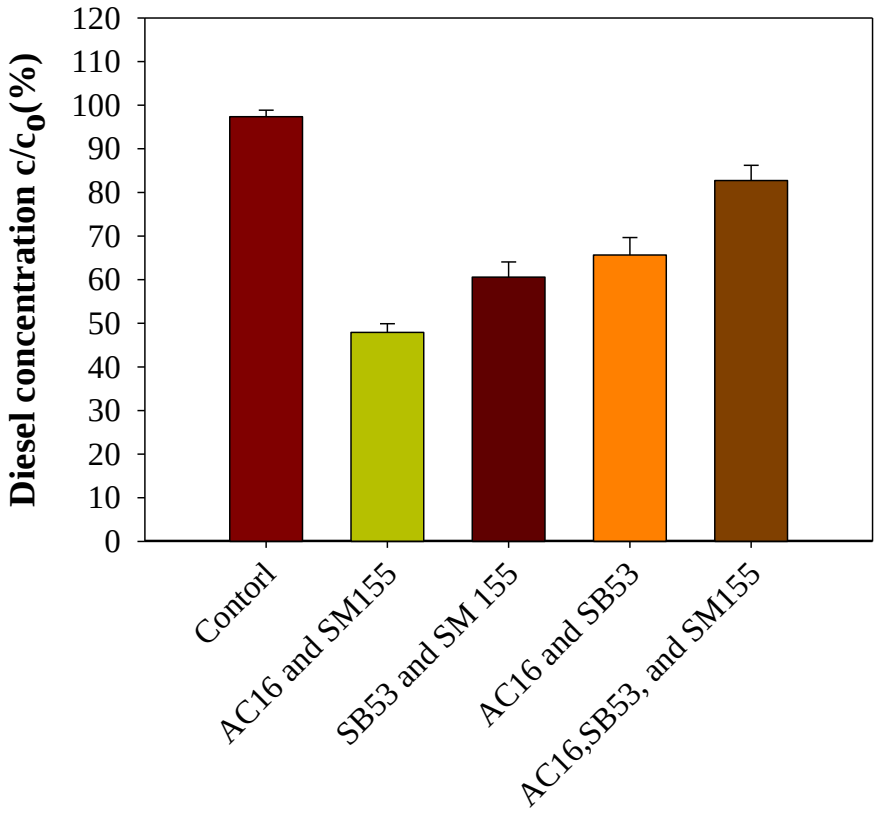


**Figure 6.14** Diesel concentrations in percentage after the tests

### 6.3.6 Phylogenetic tree

The following bacterial 16S rDNA from taxonomically characterized homologues were collected from the Genebank database on NCBI (http:www.ncbi.nlm.nih.gov/genbank) and used for phylogenetic analysis: *Acinetobacter quillouiae* 36A1, *Acinetobacter quillouiae* 36A2, *Acinetobacter quillouiae* 93-32, *Acinetobacter quillouiae* 911-100, *Sphingobacterium multivorum* 911-155 (SM155), *Acinetobacter quillouiae* 911-161, *Acinetobacter quillouiae* 911-173, *Acinetobacter quillouiae* 911-174, *Acinetobacter quillouiae* 911-175, *Acinetobacter quillouiae* 911-181, *Acinetobacter quillouiae* 911-186, *Acinetobacter quillouiae* 911-187, *Acinetobacter quillouiae* 911-195, *Acinetobacter quillouiae* 911-196, *Acinetobacter calcoaceticus* canola16 (AC16), *Sinorhizobiumcorn* 53 (SB53), *Acinetobacter quillouiae* FF1-910, *Acinetobacter quillouiae* FF22, *Acinetobacter calcoaceticus* TC2, *Acinetobacter quillouiae* NBRC110550, *sinorhizobium meliloti* CHW10B, *Sphingobacterium mulivorum nbrc*14087, *Acinetobacter calcoaceticus* strain ATCC 23055, *Acinetobacter calcoaceticus* strain CIP 81.8, *Acinetobacter calcoaceticus* strain LMG 1046, *Acinetobacter calcoaceticus* strain DSM 30006, *Sphingobacterium multivorum* strain NBRC 15339, *Sphingobacterium multivorum* strain NBRC 13310, *Sphingobacterium multivorum* strain NBRC 14983. Multiple alignments were performed using the MAFFT program. A phylogenetic tree based on a comparison of 1500 bases was constructed using the software package MAFFT version 7 (see Figure 6.15). The software uses the neighbor-joining method due to its good balance between accuracy and efficiency. The tree will be useful in outlining the phylogenetic relation among the sequences.

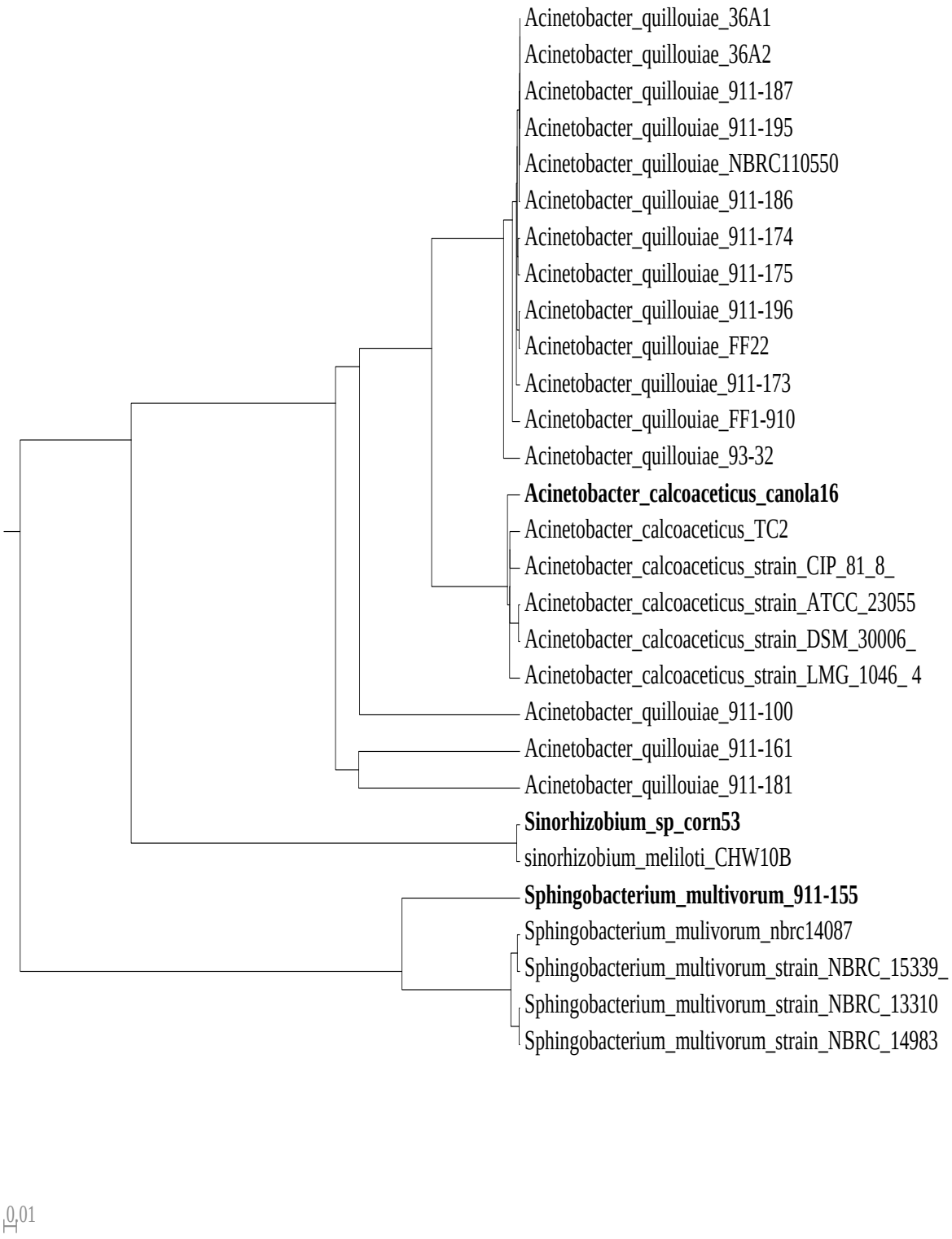


**Figure 6.15** Phylogenetic tree

## 6.4 CONCLUSIONS

In this study, 45 bacterial strains were identified as capable of degrading diesel fuel. However, the growth rates of these strains in agar plates supplemented with diesel fuel vary from strain to another from less than 24 h to more than 4 days. Three isolates were subjected to further characterizations. The results showed that the bacterium CA16, SM155, and SB53, could grow and degrade diesel fuel at a pH range of 6-8. The results reveal a change in the solution pH after the temperature tests, suggesting that the bacterial mechanism for temperature adaptation is accompanied by a pH changes at low temperatures between 18$^{o}$C and 28$^{o}$C. The results showed that at temperature 18$^{o}$C, the isolate SB53 degrade diesel better than the other two isolates, whereas at temperature 28$^{o}$C the isolate AC16 performance was superior to the other isolates. At temperature 38$^{o}$C, the isolate SM155 can grow better than the other isolates. The genes involved in the diesel degradation were identified using PCR and quantified using RT-PCR. RubA was found to be expressed in the three isolates. The results showed that the three isolates can degrade diesel fuel at concentrations of 0.5 to 6%. The isolates can degrade 40% of diesel fuel with initial concentration of 2% (v/v) (in 50 mL minimal medium) after incubation for 14 days. The results of the test conducted with the three isolates combined with each other in a solution with diesel concentration of 17.7 mg/L, showed that the highest degradation of diesel can be achieved when combining AC16 and SM155.

## 6.5 REFERENCES

Bona, C., de Rezende, I. M., Santos, G. D. and de Souza, L. A. (2011). "Effect of soil contaminated by diesel oil on the germination of seeds and the growth of schinus terebinthifolius raddi (Anacardiaceae) seedlings." Brazilian Archives of Biology and Technology, **54**(6): 1379-1387.

Cotter, P. D. and Hill, C. (2003). "Surviving the acid test: Responses of gram-positive bacteria to low pH." Microbiology and Molecular Biology Reviews, **67**(3): 429-+.

Davey, H. M. (2011). "Life, Death, and In-Between: Meanings and Methods in Microbiology." Applied and Environmental Microbiology, **77**(16): 5571-5576.

Fierer, N., Jackson, J. A., Vilgalys, R. and Jackson, R. B. (2005). "Assessment of soil microbial community structure by use of taxon-specific quantitative PCR assays." Applied and Environmental Microbiology, **71**(7): 4117-4120.

Gill, R. T., Harbottle, M. J., Smith, J. W. N. and Thornton, S. F. (2014). "Electrokinetic-enhanced bioremediation of organic contaminants: A review of processes and environmental applications." Chemosphere, **107**: 31-42.

Golgowski, N. (2013). "North Dakota farmer discovers largest oil spill on U.S. soil in the middle of his wheat field." New York Daily News.

Hassanshahian, M., Yakimov, M. M., Denaro, R., Genovese, M. and Cappello, S. (2014). "Using Real-time PCR to assess changes in the crude oil degrading microbial community in contaminated seawater mesocosms." International Biodeterioration & Biodegradation, **93**: 241-248.

Jokiniemi, T., Rossner, H. and Ahokas, J. (2012). "Simple and cost effective method for fuel consumption measurements of agricultural machinery." Agronomy research, **10**(1): 97-107.

Lin, J., Sharma, V. and Toolsi, R. (2013). "Quantitative PCR analysis of diesel degrading genes of Acinetobacter calcoaceticus isolates " African Journal of Microbiology Research, **7**(50): 5613-5624.

Luo, Q., Shen, X. R., Zhang, J. G., Fan, Z. Q. and He, Y. (2012). "Isolation, identification and biodegradation ability of diesel oil degrading Pseudomonas sp strain C7 from bilge water." African Journal of Microbiology Research, **6**(5): 1033-1040.

Nair, A. J. (2010). Principles of biochemistry and genetic engineering, Laxmi Publications Pvt Limited.

Padan, E., Bibi, E., Ito, M. and Krulwich, T. A. (2005). "Alkaline pH homeostasis in bacteria: New insights." Biochimica Et Biophysica Acta-Biomembranes, **1717**(2): 67-88.

Powell, S. M., Ferguson, S. H., Bowman, J. P. and Snape, I. (2006). "Using real-time PCR to assess changes in the hydrocarbon-degrading microbial community in Antarctic soil during bioremediation." Microbial Ecology, **52**(3): 523-532.

Rousk, J., Brookes, P. C. and Baath, E. (2009). "Contrasting soil pH effects on fungal and bacterial growth suggest functional redundancy in carbon mineralization." Applied and Environmental Microbiology, **75**(6): 1589-1596.

Rousk, J., Brookes, P. C. and Baath, E. (2011). "Fungal and bacterial growth responses to N fertilization and pH in the 150-year 'Park Grass' UK grassland experiment." Fems Microbiology Ecology, **76**(1): 89-99.

Singh, C. and Lin, J. (2008). "Isolation and characterization of diesel oil degrading indigenous microrganisms in Kwazulu-Natal, South Africa." African Journal of Microbiology Research, **7**(12): 1927-1932.

Singh, S. N. and Tripathi, R. D. (2007). Environmental bioremediation technologies. New York;Berlin;, Springer.

Sutton, N. B., et al. (2013). "Impact of Long-Term Diesel Contamination on Soil Microbial Community Structure." Applied and Environmental Microbiology, **79**(2): 619-630.

Talley, J. W. (2006). Bioremediation of recalcitrant compounds. Boca Raton, FL, CRC Taylor & Francis.

Tani, A., Ishige, T., Sakai, Y. and Kato, N. (2001). "Gene structures and regulation of the alkane hydroxylase complex in Acinetobacter sp strain M-1." Journal of Bacteriology, **183**(5): 1819-1823.

Transportation-Safety-Board-of-Canada, T. (2014). "Lac-Mégantic runaway train and derailment investigation summary." Transportation Safety Board of Canada

Venosa, A. D. and Zhu, X. Q. (2003). "Biodegradation of crude oil contaminating marine shorelines and freshwater wetlands." Spill Science & Technology Bulletin, **8**(2): 163-178.

Virkutyte, J., Sillanpaa, M. and Latostenmaa, P. (2002). "Electrokinetic soil remediation - critical overview." Science of the Total Environment, **289**(1-3): 97-121.

Whyte, L. G., Smits, T. H. M., Labbe, D., Witholt, B., Greer, C. W. and van Beilen, J. B. (2002). "Gene cloning and characterization of multiple alkane hydroxylase systems in Rhodococcus strains Q15 and NRRL B-16531." Applied and Environmental Microbiology, **68**(12): 5933-5942.

Widdel, F. (2007). "Theory and measurement of bacterial growth." Di dalam Grundpraktikum Mikrobiologie, **4**(11).

Yergeau, E., et al. (2009). "Microarray and Real-Time PCR Analyses of the Responses of High-Arctic Soil Bacteria to Hydrocarbon Pollution and Bioremediation Treatments." Applied and Environmental Microbiology, **75**(19): 6258-6267.

Yeung, A. T. and Gu, Y. Y. (2011). "A review on techniques to enhance electrochemical remediation of contaminated soils." Journal of Hazardous Materials, **195**: 11-29.

Zinkina, J. and Korotayev, A. (2014). Explosive Population Growth in Tropical Africa: Crucial Omission in Development Forecasts-Emerging Risks and Way Out. World Futures. New York, Gordon and Breach Science Publishers S.A

# CHAPTER 7
# SOLAR POWERED ELECTROKINETIC BIOREMEDIATION OF DIESEL FUEL CONTAMINATION[1]

## 7.1 INTRODUCTION

Contamination of soil by diesel fuel is a common environmental challenge. Diesel fuel is classified as hazardous material and when released to the environment can cause serious environmental problems (Kauppi et al. 2011). Different environmental bacteria have been known to use diesel fuel as sole carbon and energy source (Kim et al. 2010; Cerqueira et al. 2012). Many bacteria strains belonging to the genus *Acinetobacter* are known by their ability to degrade diesel fuel. *Acinetobacter haemolyticus* and *Acinetobacter johnsonii* were found to use diesel fuel as sole carbon and energy source (Lee et al. 2012). *Acinetobacter oleivorans* sp. *nov* was identified as an aliphatic hydrocarbon and diesel oil-degrading bacterium (Kang and Park 2010; Kang et al. 2011). *Acinetobacter baumannii* was isolated from soil contaminated with diesel and found to be found to be active in degrading diesel fuel (Palanisamy et al. 2014). *Sphingobacterium* sp. was identified as being capable of degrading diesel fuel (Ebrahimi et al. 2012). *Sinorhizobium* sp. strain was isolated from a contaminated site near a gas station and identified as a crude oil degrading microorganism (Abou-Shanab et al. 2015). Many researchers have concluded that bioremediation of soil contaminated with diesel fuel is feasible (Cyplik et al. 2011; Colla et al. 2014). However, the implementation of bioremediation at contaminated sites has revealed that not all hydrocarbons are degradable by available strains of bacteria. Therefore, there is a need for isolation and characterization of novel strains capable of degrading diesel fuel. In addition, environmental conditions at the contaminated sites may not be favorable for bacterial growth/adaptation, which results in poor degradation. For high yield, bacteria require optimal temperature, moisture content, and pH conditions (Singh and Tripathi 2007).

[1]A version of this chapter has been submitted to Environmental Science and Technology

It is recognized that there will not be a single universal method suitable for remediating all types of soils and contaminants, thus any effective remediation may include implementation of two or more methods (Virkutyte et al., 2002). In many cases, intervention is required to enhance a bioremediation treatment outcome. Electrokinetic enhanced bioremediation is an innovative hybrid technique aimed at accelerating the natural biodegradation of contaminants by increasing the opportunities of interaction between microorganisms and contaminants. Electrokinetics can activate the existing microbial community in the subsurface by delivering nutrients required to promote microbial growth (Acar et al. 1997; Budhu et al. 1997). The technique can also mobilize and precisely deliver new bacteria and their substrates to a contaminated soil (Virkutyte et al. 2002). However, the electrolysis reactions at the electrodes produce high pH near the cathode and low pH in vicinity of the anode. While bacteria can tolerate an environment with a high or low pH value, a pH gradient has a detrimental effect on bacteria (Cotter and Hill 2003; Padan et al. 2005; Krulwich et al. 2011).

Recently, the use of a solar photovoltaic panel to generate power for electrokinetic remediation has gained some interest in the scientific community (Yuan et al. 2009; Hassan et al. 2015; Souza et al. 2016). Solar energy, a renewable energy source with no adverse environmental impact, is a novel power option for electrokinetics and can be economically viable, especially, in remote sites without active power lines. Over the last decade, the initial cost of solar power systems has been declining, and this trend is expected to continue as the price of solar cells decreases and their efficiency increases. The power generated by solar panels varies during the day depending on weather conditions (cloudy sky, rainfall, snow, or clear sky). Also, there could be intervals without electricity at night. The variations in power supply during the day and the zero power intervals cause interruptions in current. However, many studies have shown that the pulsed current results in enhancement of electrokinetic remediation (Hansen et al. 2007; Ryu et al. 2009; Ryu et al. 2010; Jo et al. 2012; Kim et al. 2013).

The use of a solar photovoltaic panel to produce power for an outdoor electrokinetic bioremediation during winter and the effect of low temperature on the process has not been

investigated in the published literature. The applied current in the electrokinetic process results in an increase in temperature in the soil. However, the low temperatures during the winter season cause the soil porewater to freeze. Therefore, the effect of current on soil temperature and the effect of frozen soil on the degradation process need to be investigated.

The present study involved outdoors tests in which electrokinetic bioremediation was used to mitigate soil artificially contaminated with diesel fuel using three novel bacterial strains. A new technique was used to stabilize the pH during the electrokinetic bioremediation. The three novel bacterial strains *Acinetobacter calcoaceticus* (AC16), *Sphingobacterium multivorum* (SM155), and *Sinorhizobiumcorn* (SB53) were isolated from agricultural soil and found to be capable of using diesel fuel as carbon and energy source. The power for electrokinetic bioremediation was provided by a solar photovoltaic panel. The issues and knowledge gaps identified indicate that pursuing the path of solar powered electrokinetic bioremediation would lead to further understanding of contaminated soil bioremediation initiate steps for deploying this new treatment technology.

## 7.2 MATERIALS AND METHODS

### 7.2.1 Soil properties

The soil used in the experiments was obtained from a local site in London, Ontario, Canada. Tests were carried out in accordance with the American Society of Testing and Materials standard procedures to determine the physical and chemical properties of the soil. Tests carried out included analyses for particle-size distribution, Hydrometer, Atterberg limits, specific gravity, cation exchange capacity, and total organic carbon. Most of the tests were carried out in triplicate and the results are shown in Table 7.1. According to the Unified Soil Classification System (USCS), the group symbol of soil is SC and the group name is clayey sand. For the cation exchange capacity test, ammonium acetate and potassium chloride were used as extractants to obtain first the soluble cations and then bound or exchangeable cations. Inductively coupled plasma-optical emission spectroscopy (ICP-

OES, VARIAN, USA) was used to determine the cation concentrations in solution. The method is simple and provides a rapid means to estimate the CEC. A total organic carbon analyzer (TOC-VCPN, SHIMADZU, Kyoto, Japan) was used to determine the organic carbon fraction ($f_{oc}$) in the soil. Soil pH was determined in accordance with the American Society of Testing and Materials Standards procedure g D4972-13 (ASTM D4972-13).

**Table 7.1** Soil physiochemical properties

| Soil property | Measured value |
|---|---|
| Liquid limit | 25 (±2) |
| Plastic limit | 18 (±1) |
| Water content* | 21% |
| Uniformity coefficient ($C_u$) | 5.3 |
| Coefficient of gradation | 1.5 |
| Electrical conductivity | 869 μS/cm |
| pH | 7.0 (±0.1) |
| Cation exchange capacity | 16.75 (±0.10) meq/100 g of soil |
| Organic carbon content ($f_{oc}$) | 2.3% (±0.05) |

The values between the brackets are the range of errors.*Initial water content

## 7.2.2 Experimental apparatus

The experimental equipment consisted of six electrokinetic remediation cells, solar cell panels, Omega-320 data acquisition, an electrokinetic voltage controller (EKVC), two data acquisitions systems, multimeter, and a personal computer. The electrokinetic remediation cell, constructed from clear Plexiglass plates 8 mm in thickness, has inner dimensions of

400 mm × 300 mm × 180 mm (length × width × height), as shown in Figure 7.1. The cell is composed of a soil compartment to accommodate the soil specimen, and two water compartments. Two movable rectangular perforated Plexiglass plates (300 mm × 180 mm) separate the soil compartment from the water compartments. The bottom part of the cell has two rows of small holes located at equal distances to make provisions for five voltage probes used to monitor the voltage gradient across the soil specimen during the test, and five thermocouples to monitor the temperature of the soil during the test. The water compartments houses the electrodes as shown in Figure 7.1. The first water compartment hosts Anode $A1^+$ and Cathode $A2^-$ and the second compartment contains Anode $A2^+$ and Cathode $A1^-$. In the first electrokinetic cell, the electrodes are connected to the solar panel using two electric circuits, electric circuit 1 between Anode $A1^+$ and Cathode $A1^-$, and electric circuit 2 connecting Anode $A2^+$ to Cathode $A2^-$ (in the second and third electrokinetic cells electric circuits 1 was between $B1^+$ and $B1^-$ and $C1^+$ and $C1^-$ and electric circuit 2 connected $B2^+$ to $B2^-$ and $C2^+$ to $C2^-$). The hypothesis was that the coexistence of an anode and a cathode in the same water compartment would result in the hydrogen ions generated at the anode neutralizing the hydroxyl ions produced at the cathode and thereby forming water. The proposed novel configuration is assumed to generate equivalent numbers of hydrogen ions and hydroxide ions that react to form water.

The electrokinetic voltage controller (EKVC) device (Figure 7.2) was designed and fabricated for the purpose of switching the electric potential between the two electric circuits such that at any given time there was only one electric current running through either electric circuit 1 or 2 in the electrokinetic cell. The EKVC took dc input of 70 V and 1 A. It had six output ports and a programmable timer. The output ports were arranged in two sets each with three outputs. For each output port, there were four switched voltage points. Three of the voltage points were used to monitor the voltage distribution across the soil and one to record the electric current. These points were switched to three groups of a four data acquisition points. The voltage distribution profile (at three points) across the soil under treatment and the electric current through the soil were monitored using the voltage points connected to data acquisition terminals. A computer code was written using the

software Labview 2013 to connect the data acquisition terminals with a PC and to record the data. The EKVC alternated the voltage between outputs sets at a set programmable time. The timer can be set to alternate the voltage between the two electric circuits for intervals from thirty seconds to six minutes in thirty second steps. The EKVC was connectable for up to three electrokinetic cells. For instance, EKVC can be connected to electrokinetic cell such that $A1^+$ and $A1^-$ form the first electric circuit and $A2^+$ and $A2^-$ for the second circuit. The EKVC also controls the duration time of the electric current delivered through the electric circuits. In this study the EKVC was set to control the current through the two electric circuits in a complete cycle of nine minutes. First, the current was delivered through the first electric circuit (between anode $A1^+$ and cathode $A1^-$) for three minutes. The current was then delivered through the second electric circuit (between anode $A2^+$ and cathode $A2^-$) for three minutes followed by an off-period of three minutes for both circuits.

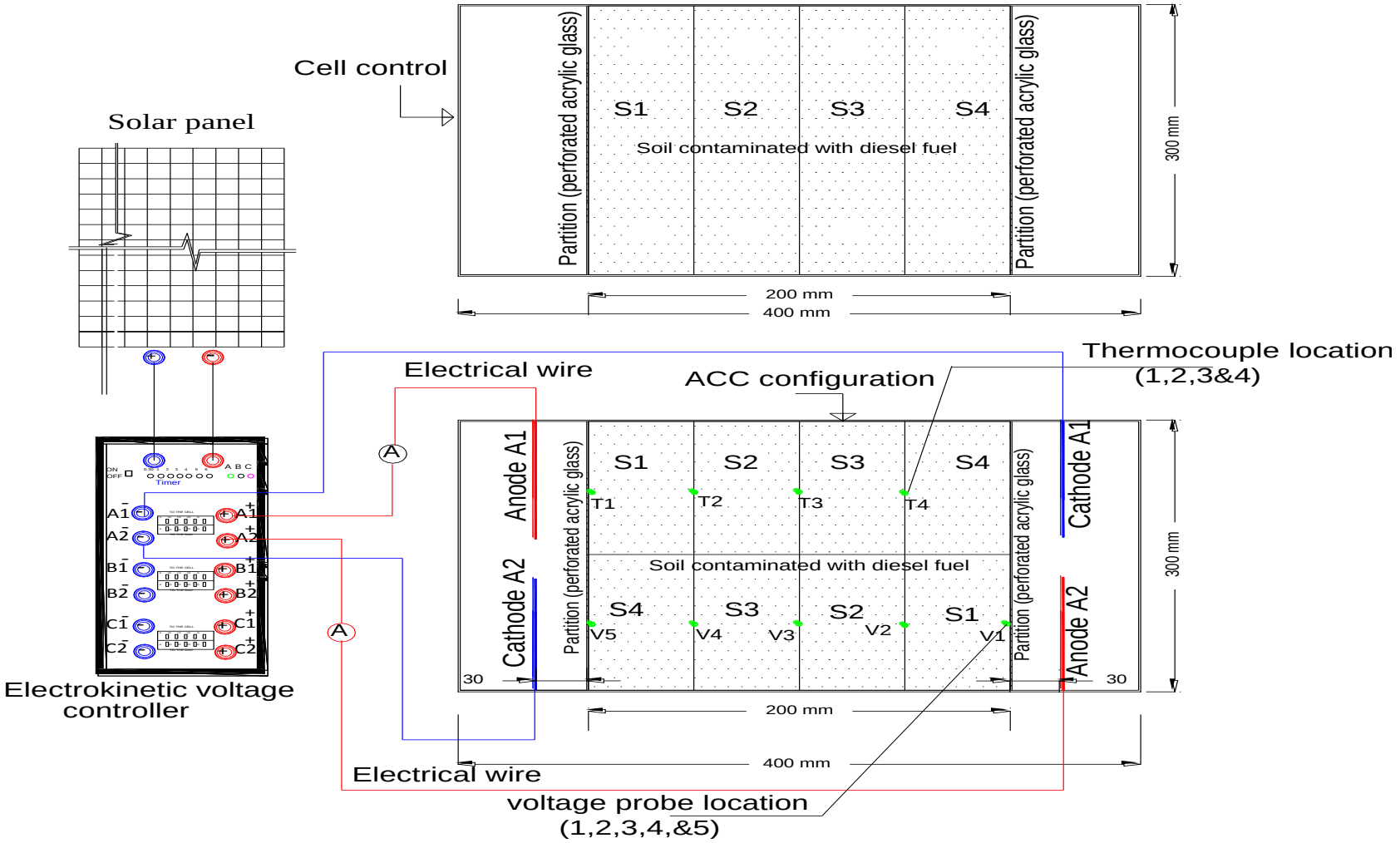


**Figure 7.1** ACC electrokinetic remediation configuration and the control cell


**Figure 7.2** Electrokinetic voltage controller (EKVC)

### 7.2.3 Test procedure

Electrokinetics cells were washed using 70% ethanol and placed in a biosafety cabinet under UV light overnight to kill any microorganisms. Diesel fuel used in the tests was obtained from an above-ground storage tank at the Southern Crop Protection and Food Research Centre, Agriculture and Agri-Food Canada, London, Ontario, Canada. The soil specimen was prepared by thoroughly mixing the soil with the diesel fuel using a mechanical mixer in a ratio of 2 g of diesel fuel/100 g of soil to obtain a concentration of 2% (w/w). The soil was placed into the electrokinetics cell in three layers for a total height of 90 mm. Each layer was tamped using a rectangular Plexiglass plate and a pestle to prevent the entrapment of air pockets and to produce soil specimens with similar densities. In each cell, five voltage probes were connected to EKVC which was connected to a data acquisition system. The temperature of the soil (in the electrokinetics cells) during the test was monitored by four thermocouples connected to Omega data acquisition system for each electrokinetic cell. The electric field from the solar panel was connected to the EKVC, which was connected to the electrodes in the electrokinetic cells. Four reinforced graphite electrodes, each 150 x 120 x 1.5 mm (length × width × thickness), were used in each cell. Two electrodes were placed in each water compartment where one pair of electrodes served as the anodes and the other pair as the cathodes. The two electrodes for each pair were placed 60 mm from each other as shown in Figure 7.1. A geotextile filter situated between the soil sample and the perforated acrylic glass.

Two set of tests were conducted (see Table 7.2). The first set (Cell X, Cell Y, and Cell Z) represents the electrokinetic tests with the two electric circuits and two electrodes in each water compartment configuration. The second set (Cell CX, Cell CY, and Cell CZ) was the control tests conducted without electric field. Electric current, temperature, voltage across the soil, and pH of the water compartments were monitored and recorded during the test. Omega 320 data acquisition had four modules, each module had four channels. Three modules were used to collect temperature data from Cell X, Cell Y, Cell Z, and one module was used to collect voltage data at selected locations in Cell X, Cell Y, Cell Z.

**Table 7.2** Set of tests

| Cell | Soil compartment | Water compartment | Voltage |
|---|---|---|---|
| Cell X | 2% diesel fuel, and 0.85% NaCl | AC16, SB53, SM155 ($OD_{600}$ =1) in minimal medium | Solar power EK |
| Cell Y | 2% diesel fuel, and minimal medium | AC16, SB53, SM155 ($OD_{600}$ =1) in 0.85% NaCl | Solar power EK |
| Cell Z | 2% diesel fuel, AC16, SB53, SM155 ($OD_{600}$ =1) in minimal medium | 0.85% NaCl | Solar power EK |
| Cell CX | 2% diesel fuel, and 0.85% NaCl | AC16, SB53, SM155 ($OD_{600}$ =1) in minimal medium | Control |
| Cell CY | 2% diesel fuel, and minimal medium | AC16, SB53, SM155 ($OD_{600}$ =1) in 0.85% NaCl | Control |
| Cell CZ | 2% diesel fuel, AC16, SB53, SM155 ($OD_{600}$ =1) in minimal medium | 0.85% NaCl | Control |

### 7.2.4 Analysis

At the end of the test, the soil was extruded from the electrokinetic cell and divided into four sections from the anode to the cathode. The soil in each section was tested to determine the water content, pH, nutrients concentration, and diesel fuel concentration. Water content was determined in accordance with ASTM Standards procedure D2216-10 (ASTM, 2010). Tests to measure pH were conducted according to ASTM D4972-13 (ASTM, 2013). A pH-Electrode Sentix 41-3 (WTW-Multi 340i/set) was used to measure the pH.

Samples for diesel fuel concentration analysis were dried under a fume hood. The diesel fuel was extracted from the dry samples by sonication using a 1:1 solution of dichloromethane and acetone. A 10 grams soil sample was sonicated for 2 h using 20 mL of the solvent, followed by replacing the solvent with a fresh solvent and sonicating for another 2 h. The solvent was then replaced again with a fresh solvent, and the sample placed in a table shaker for 24 h. The solvents used in the extraction were combined together (60 mL) and a Kuderna-Danish apparatus was used to reduce the volume of the solvent to approximately 3 mL. Diesel fuel concentrations in soil samples before and after the tests were determined using GC-MS. The GC-MS method used a gas chromatography column DB5-MS (length 40 m, 30 m column and 10 m guard column, internal diameter 250 µm, film thickness 0.25 µm), helium as a carrier gas with 0.8 mL/min flow rate, the temperature of the injection 250$^{o}$C, injected volume of 1 µL, initial temperature of 70$^{o}$C held for 2 min, and then ramped at 5$^{o}$C per min up to 300$^{o}$C and held for 5 min.

# 7.3 RESULTS AND DISCUSSION

## 7.3.1 Applied voltage

The tests were conducted during the winter season with an average daylight of ten hours. The applied voltage fluctuated during the daytime since it was generated by solar panels. Figure 7.3 shows the average voltage generated by a solar panel during the test. The figure shows that the voltage profile would be divided into three segments. The first segment represents an increase in voltage from 7:30 AM to 10:00 AM. The second segment, between 10:00 AM and 3:00 PM, represents a relatively stable voltage. The third segment shows a decrease in voltage between 3:00 PM and 5:50 PM.

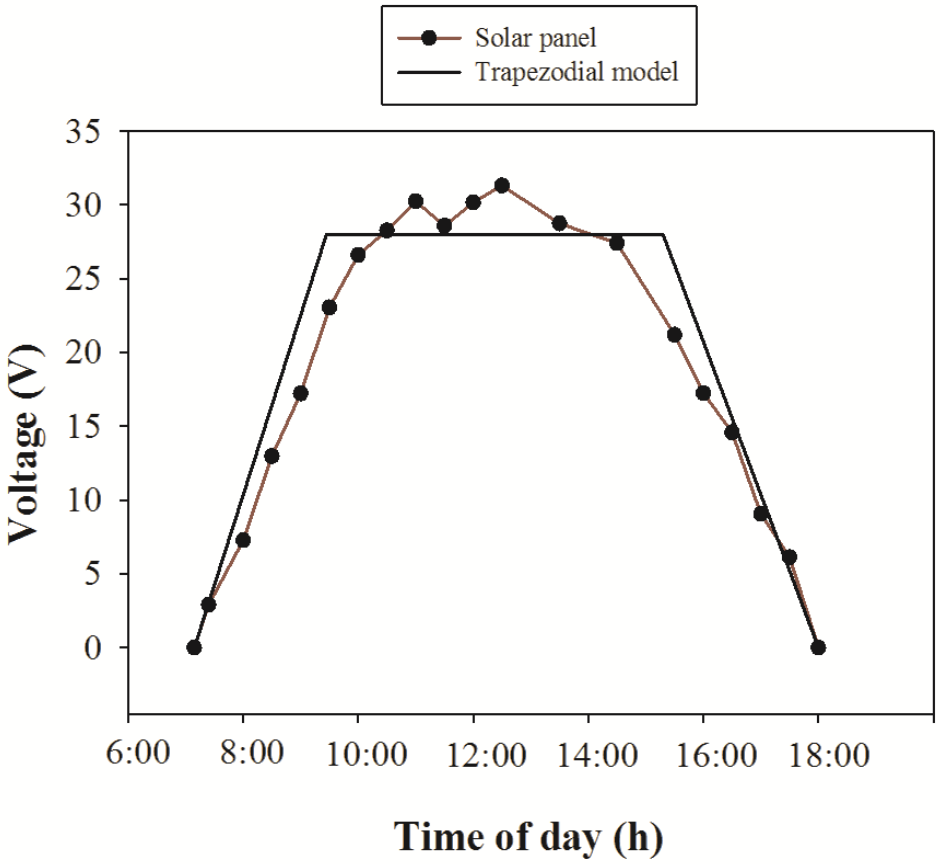


**Figure 7.3** Voltage generated by a solar panel

The profile of the voltage generated by the solar panel shows that solar panels can generate enough power for electrokinetic bioremediation. The distribution of generated voltage as shown in Figure 7.3 is in agreement with trapezoidal model described by Zhang and Smith (2008) where the daylight hours represent the bottom base of the trapezoid and the noon hours represent the upper base of the trapezoid. The height of the trapezoid is the maximum irradiance during the day. The results from this study showed that the power generated by solar energy is not only sufficient for electrokinetic bioremediation, but can also be monitored and evaluated using the trapezoid model.

### 7.3.2 Electric current

The results showed that the electric currents in Cell X, Cell Y, and Cell Z increased rapidly between 7:30 AM and 10:00 AM (see Figure 7.4). Afterward, the currents in the cells continued to increase at a lower rate and reached peak values around 12:30 PM. The currents decreased gradually between 12:30 PM and 4:00 PM and more rapidly between 4:00 PM and 5:30 PM. The current in Cell Z was the highest, and this was expected because the soil specimen was composed of diesel fuel, minimal medium, and the three isolates. The current in Cell Y was less than in Cell Z and this was also directly related to the soil composition (diesel and minimal medium). The lowest current was in Cell X in which the soil contained diesel fuel and 0.85% NaCl.

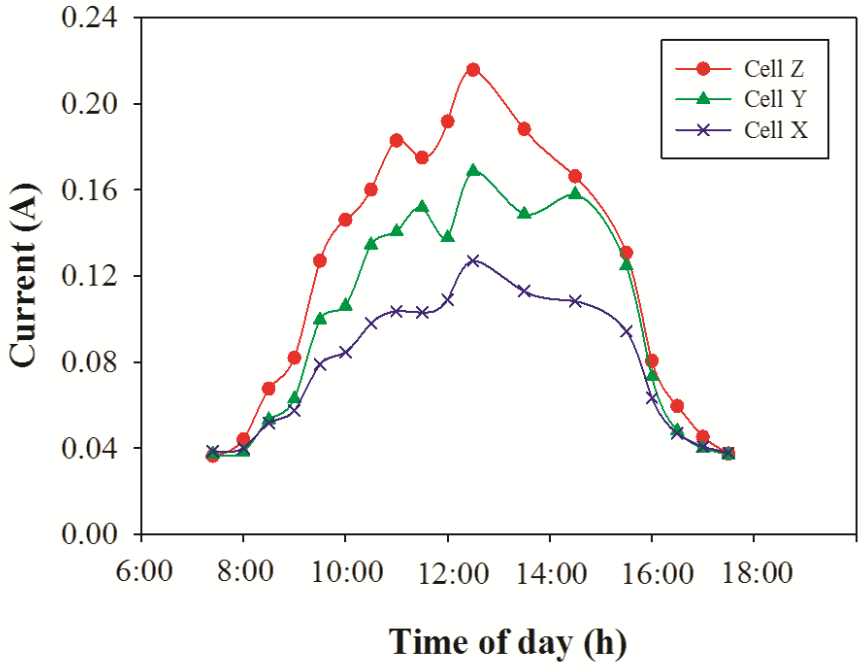


**Figure 7.4** Electric current during the tests

### 7.3.3 Power generated by solar panel

Figure 7.5 shows the average of the power supply from the solar panel during daytime over a period of 55 days in the winter season (December 2015- Feb, 2016). Since power is equivalent to voltage multiplied by the current, the variation in power during the day mimicked the trends in the voltage and electric current. Similar to the electric current, the highest power was found in Cell Z, followed by that of Cell Y, and Cell X, respectively.

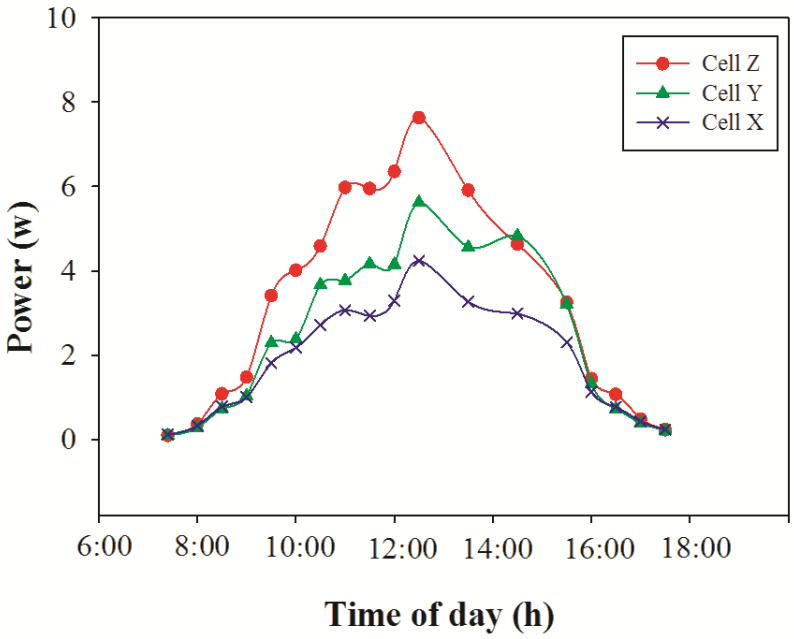


**Figure 7.5** Power generated by solar panel

### 7.3.4 Water content

The average water content in Cells Z, Y, and X prior to the application of the electric field was 21%. Figure 7.6 shows the water content in sections S1 (near the anode) to S4 (near the cathode) along the soil specimens (see Figure 7.1). As seen in Figure 7.6, a slight increase in water content occurred along the soil specimen in Cell Z after electrokinetic treatment. The figure shows that the water content after electrokinetic bioremediation test in Cell Y remained relatively unchanged while a small drop in water content was found after the test in Cell X. However, Figure 7.6 shows that the water content across the soil specimen in the three electrokinetic bioremediation tests (Cells Z, Y and X) remained very close to the initial water content, which demonstrates the effectiveness of the ACC technique in maintaining relatively constant water content in the electrokinetic cells. These results are contrary to the general water content trend in electrokinetic remediation, where a high water content would be expected near the cathode. The high water content near the cathode in electrokinetic remediation is a result of the water produced where the acid and

base fronts, generated by electrolysis reactions at the electrodes, meet. $H^+$ ions are of smaller size than the $OH^-$ ions and accordingly, by electromigration transport, $H^+$ ions would travel a longer distance than $OH^-$ ions. Further, $H^+$ ions also travel by electroosmosis towards the cathode, resulting in an acid-base meeting closer to the cathode (e.g. Narasimhan and Ranjan, 2000; Mohamedelhassan and Shang, 2003). The relative uniformity of water in electrokinetics tests conducted using the ACC technique indicates that the acid front and base front are neutralized in the water compartment. Figure 7.7 shows the water content at the end of the control test was approximately equal to the initial water content. This is to be expected since the control tests were not subjected to an electrical current, but only the effect of ambient temperature that resulted in freeze and thaw cycles.

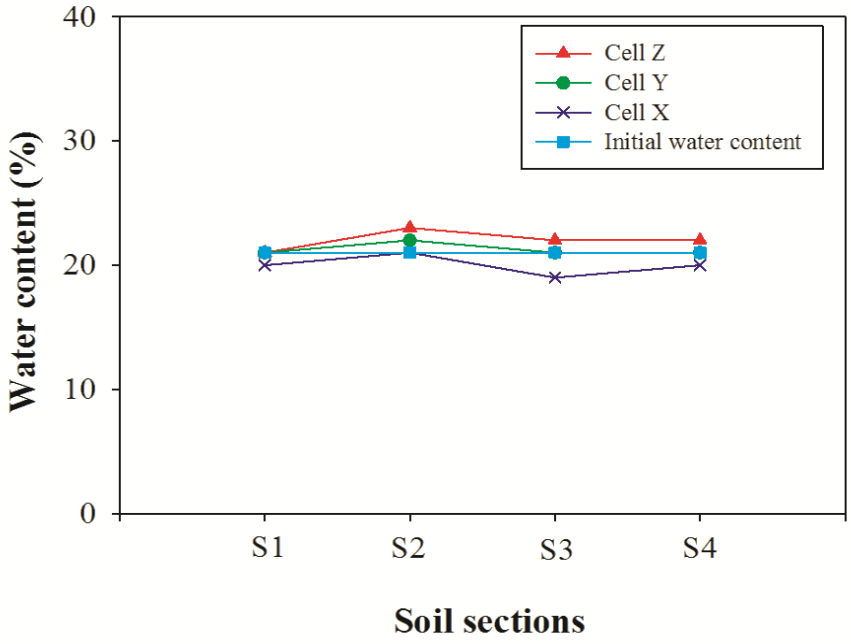


**Figure 7.6** Water content at the end of electrokinetic tests

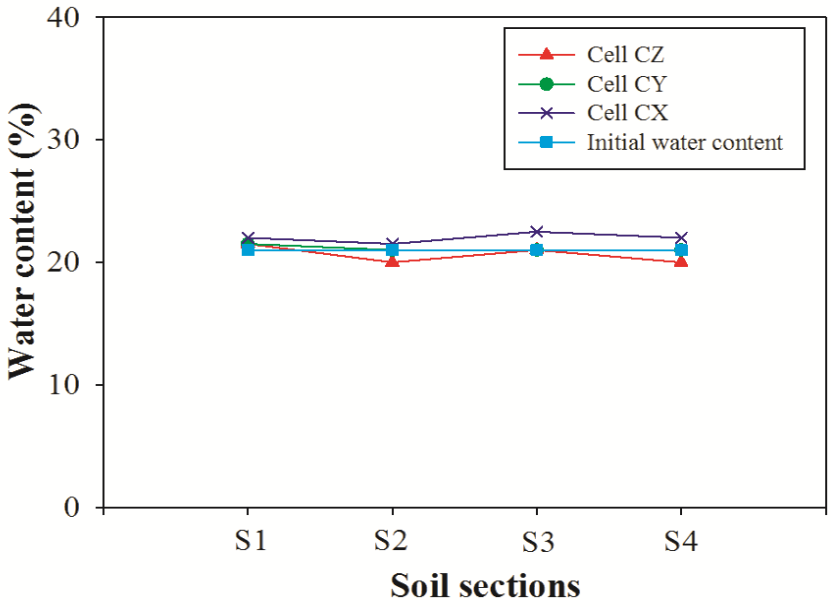


**Figure 7.7** Water content at the end of the control tests

### 7.3.5 Temperature

Figures 7.8, 7.9, and 7.10 present the minimum, median, and high temperatures in Cells Z, Y, and X along with the ambient temperature during the test. Figure 7.8 shows that the minimum temperature in Cell Z was higher than that in Cell Y as a result of the higher current run through Cell Z (see Figure 7.4). Likewise, the temperature in Cell Y was higher than in Cell X. The minimum ambient temperature was lower than the minimum temperatures in Cells Z, Y, and X by 3 to 5$^{o}$C. Figure 7.9 shows the median temperature in Cells Z, Y, and X and the median ambient temperature. The median temperature in Cell Z was slightly higher than the median temperature in Cells Y and X. Figure 7.10 shows the maximum temperature was reported in Cell Z followed by Cells Y and X. The ambient maximum temperature was lower than the maximum temperature in the cells by 3 to7$^{o}$C. The results showed that the electric current increased the temperature of the soil during the tests by 3 to 7$^{o}$C. The change in the outdoor temperature caused the electrolyte solution and the soil in the cells to freeze with temperatures ≤ zero. The electrical resistivity of soil

increases by a factor of 10 as the temperature decreases from +5 to -5ºC (Fortier et al. 1994). Therefore, temperature played an important role in the current produced. Low temperature resulted in low current and vice versa.

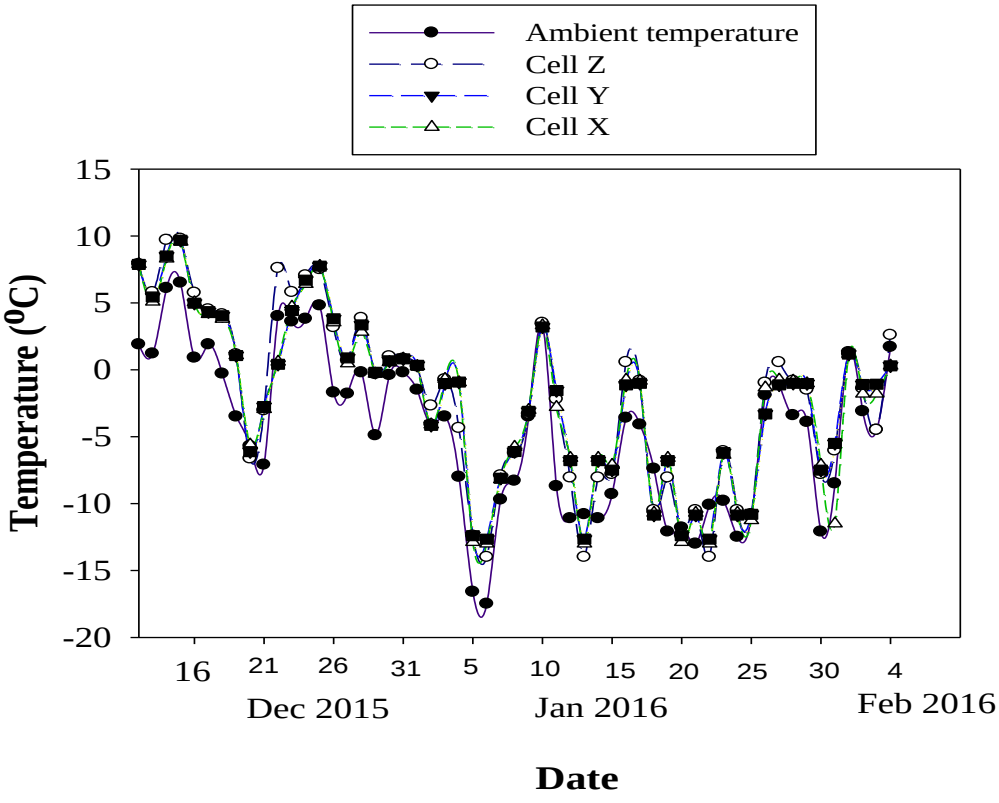


**Figure 7.8** Minimum temperatures during the test

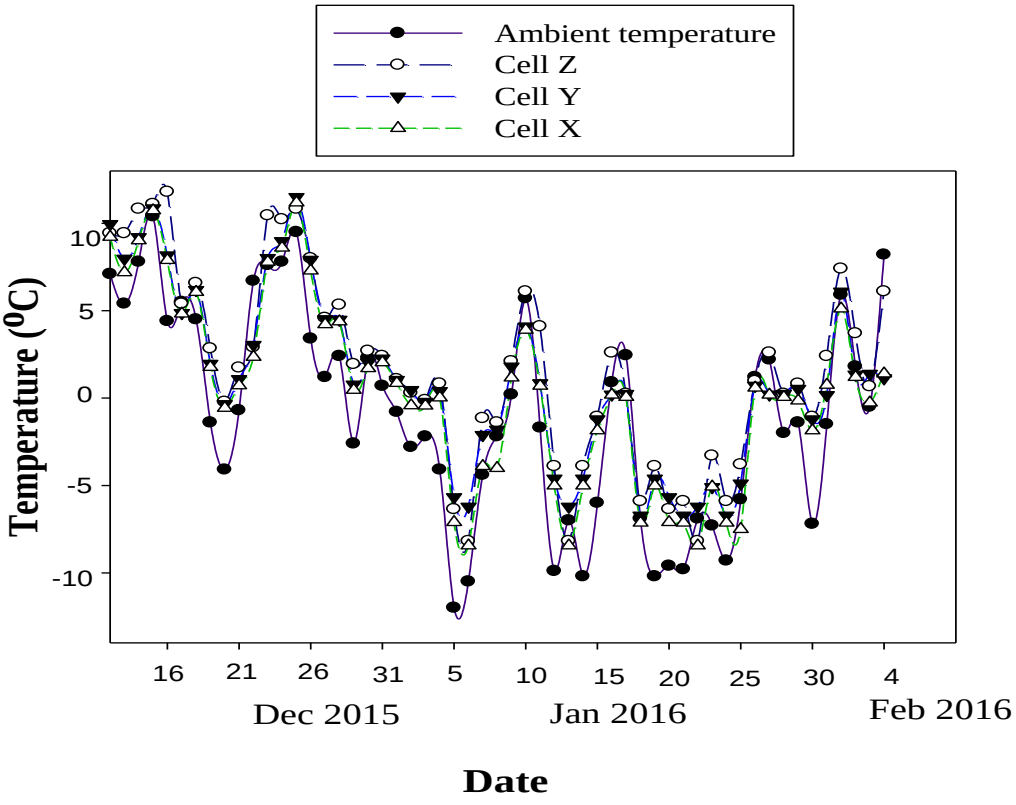


**Figure 7.9** Median temperatures during the test

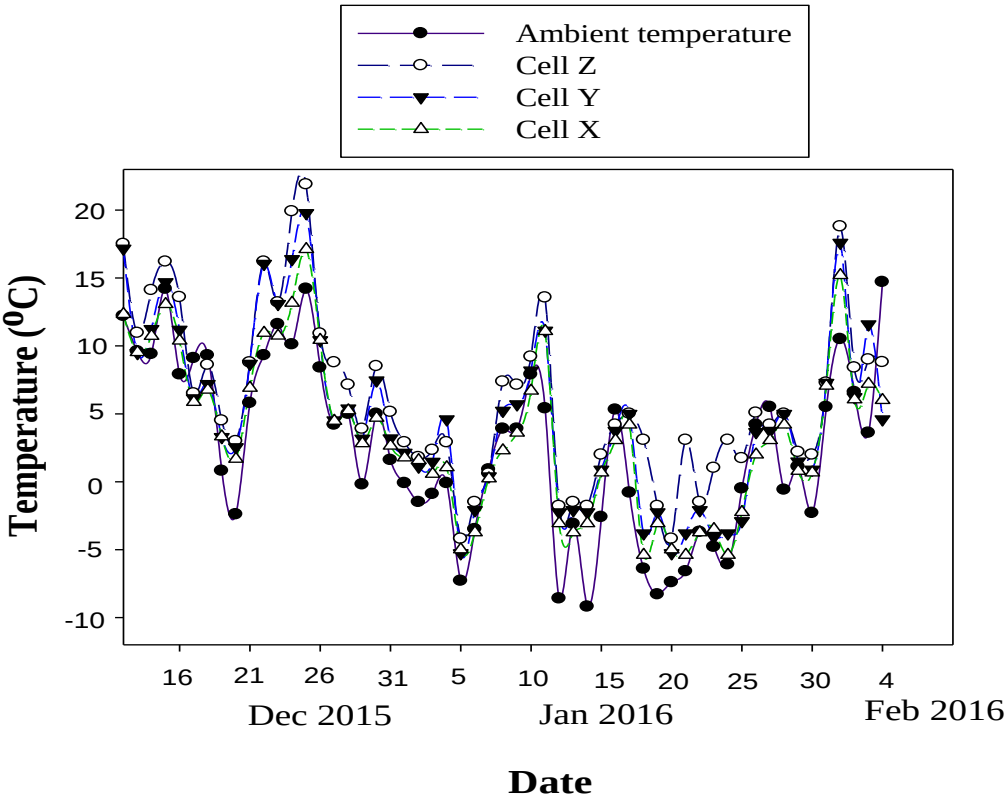


**Figure 7.10** Maximum temperatures during the test

### 7.3.6 pH distribution

Figure 7.11 shows the pH of dried soil after the test in the control cells, Cell CX, Cell CY, and Cell CZ, and the initial soil pH before the test. The initial pH in the soil sample was 7.6. Figure 7.11 shows that the pH values in the control cells were almost similar to the initial pH in the soil (7.6); a small variation in pH (0.1 to 0.3) was observed in Cell CX. Figure 7.12 shows the pH in Cell Z, Cell Y, and Cell X after the test and the initial pH in the soil before the test. The change in the dried soil pH in Cell Z, Cell Y, and Cell X after the test varied between 0.1 and 0.7, compared to the initial pH of the soil. This change in pH was insignificant compared to previous studies that showed, under uncontrolled pH conditions, the pH near the anode dropped to around 2 and increased in the cathode vicinity to 12 (Acar and Alshawabkeh 1993; Virkutyte et al. 2002; Alshawabkeh 2009; Reddy and

Cameselle 2009). The results from the present study indicate the efficiency of the ACC technique in controlling the pH in the soil.

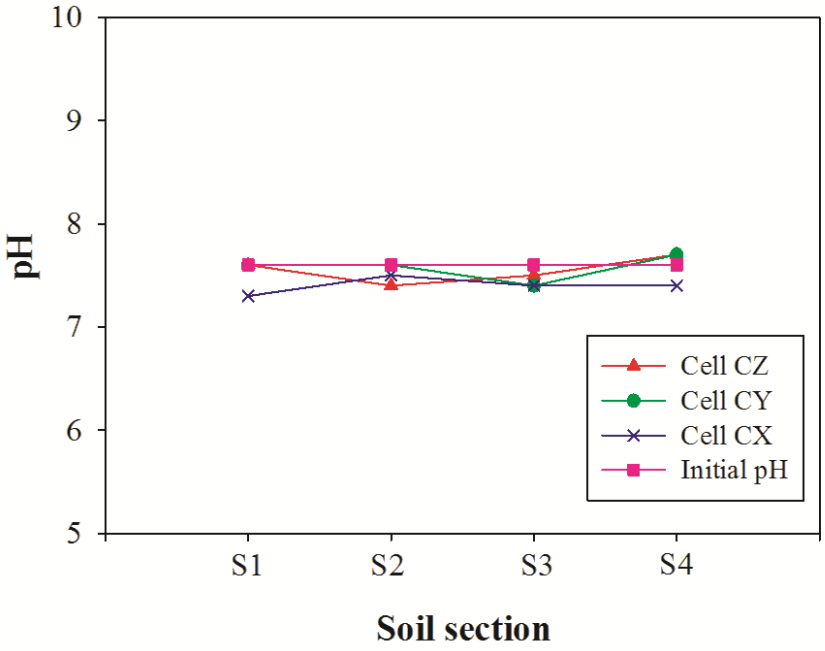


**Figure 7.11** pH after the test in control cells

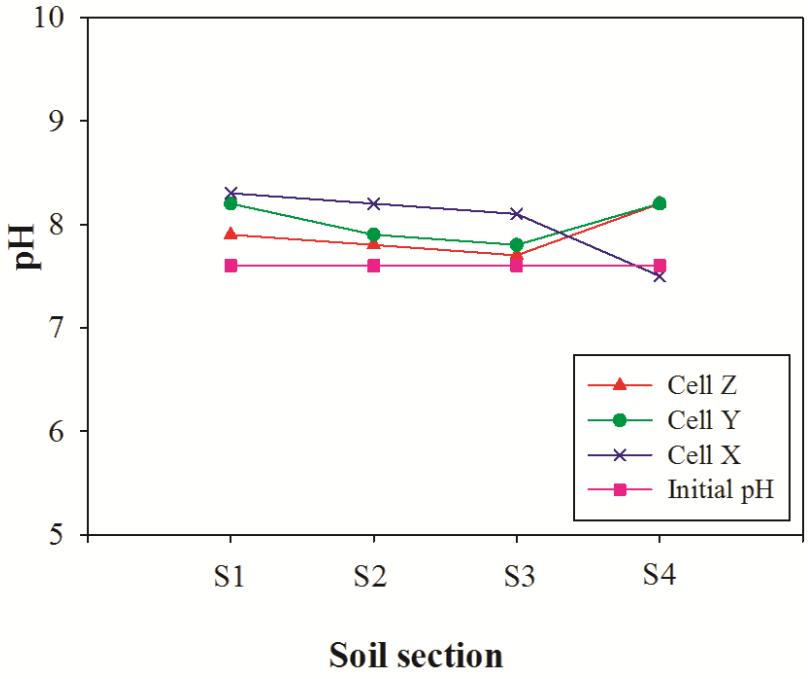


**Figure 7.12** pH after elecrokinetics treatment

## 7.3.7 Voltage gradient

Figures 7.13 to 7.16 show the voltage across Cells Z, Y and X during the tests. In Figure 7.13 the applied voltage from the solar panel was 7.5 V and the voltage in the soil closet to the anode (V1) was 3.8 V (51% of the applied voltage) in the three cells. The profile of the voltage distributions inside the soil in Cells Z and Y were identical except at the location of probe V4. The voltage distribution in Cell X was lower than in Cells Z and Y. The voltage in the soil closet to the cathode (V4) in the three cells was identical and equal to 1.8 V. The high drop in the voltage at the anode side can be attributed to the fact that the anodes were placed in the water compartment and not in direct contact with the soil. The electrodes were placed in the water compartments to allow the hydrogen and hydroxyl ions to neutralize. In this test, the electrokinetic cells were placed outdoors, and this is another factor that can contribute to the high voltage drop at the anode side. The low outdoor temperatures can freez the water in the water compartment, and consequently reduced the

electrical conductivity of the electrolyte solution (Fortier et al. 1994). Visual inspections during the tests revealed that the electrolyte solutions in the water compartments were frozen when the ambient temperature was around zero.

In Figure 7.14 the applied voltage from the solar panel was 16.7 V and the voltage drops in Cell Z, Cell Y, and Cell X was 40%, 47%, and 55%, respectively, of the applied voltage. It was observed that the lower voltage drop in Cell Z compared to the other cells was associated with the higher current run through Cell Z (as shown in Figure 7.4). This high current can result in an increase in temperature in the cell and consequently thaw the electrolyte solution. In Figure 7.15 the applied voltage from the solar panel was 22 V and the voltage drops in Cell Z, Cell Y, and Cell X were 22%, 31%, and 40%, respectively. It was observed that the lower drop in the voltage at the anode side in Cell Z was associated with higher current (as shown in Figure 7.4). Figure 7.16 shows the voltage drops in Cell Z, Cell Y, and Cell X were 21%, 29%, and 39%, respectively. The voltage drops in Figure 7.16 follow the same trend as in Figures 7.14 and 7.15. The general trend for the voltage drop, as shown in Figures 7.13 to 7.16, show that high current is associated with lower voltage drop. Therefore, it can be concluded that there is a correlation between the voltage drop and the current at low temperatures. There were no significant variations in trend of the voltage distribution at the cathode side between the three cells. Previous study showed that under controlled temperatures, desorption mechanism was dominant at the beginning of electrokinetic treatment, and this resulted in an increasing resistance and consequently high voltage drop (Kim and Kim 2001). The results from the present study are in agreement with previous researches that showed electrical potential difference across electrodes increased with an increase in the applied current (Chung and Kang 1999; Alok et al. 2012).

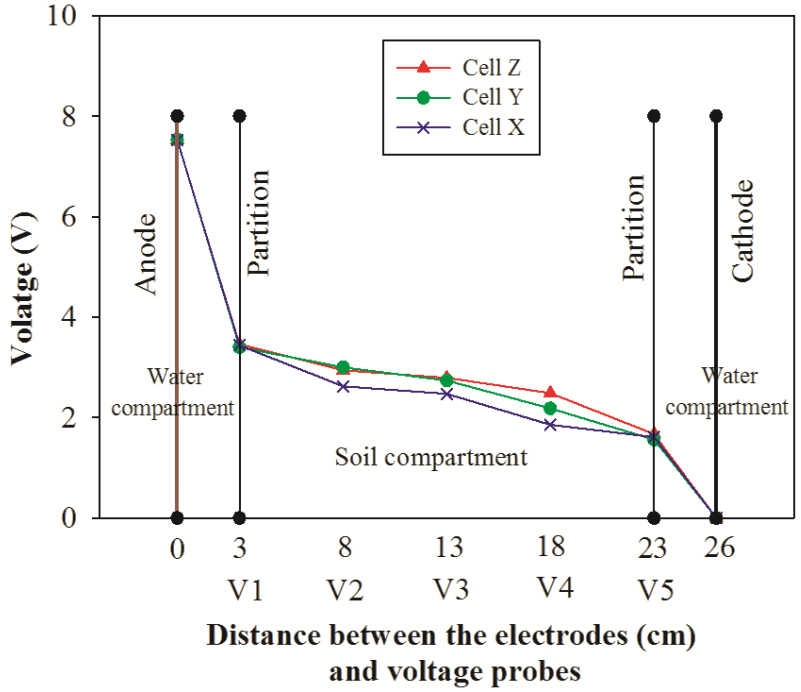


**Figure 7.13** Voltage distribution in the cells at applied voltage 7.5V

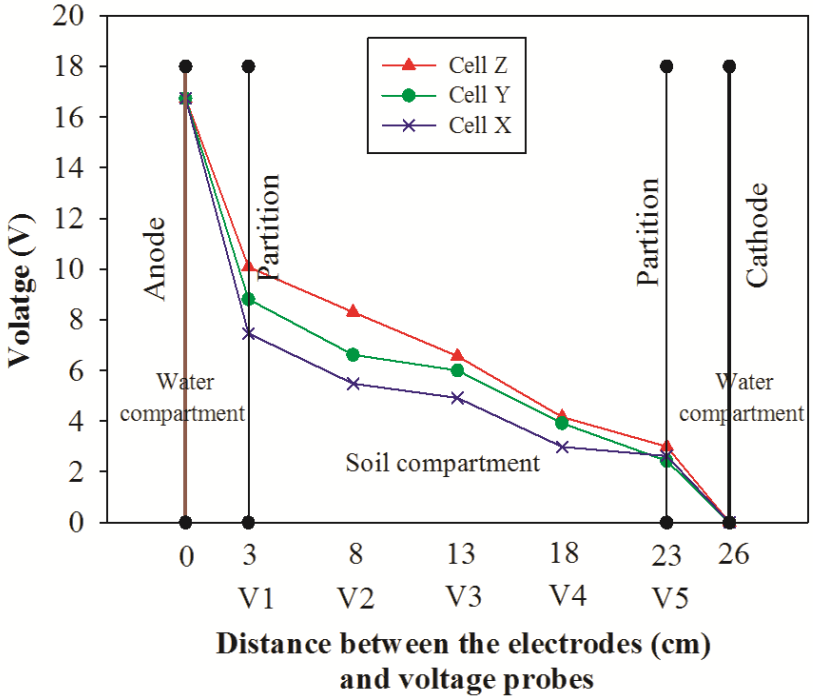


**Figure 7.14** Voltage distribution in the cells at applied voltage 16.0V

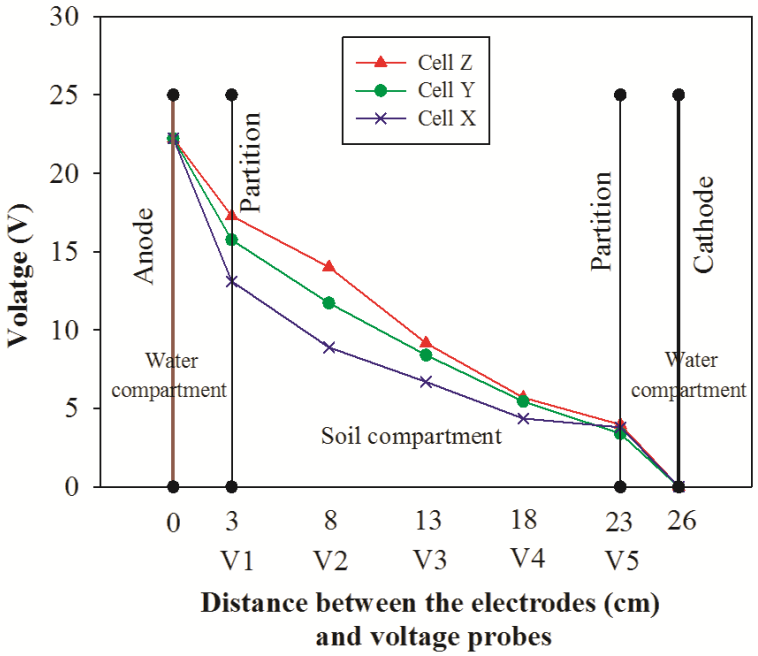


**Figure 7.15** Voltage distribution in the cells at applied voltage 23.0V

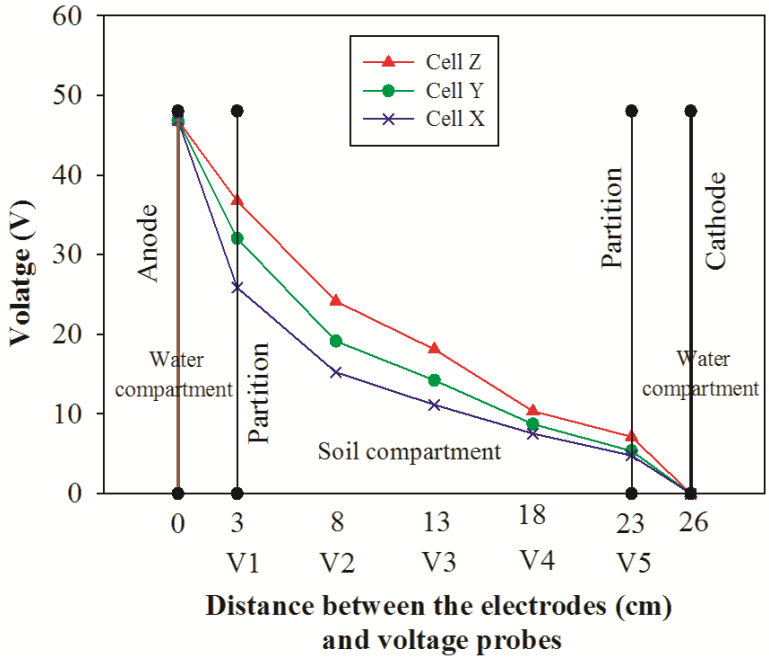


**Figure 7.16** Voltage distribution in the cells at applied voltage 46.0 V

### 7.3.8 Diesel fuel concentration

Figures 7.17 to 7.19 show the ratio (in percentage) of diesel fuel concentration after test C to the initial concentration $C_o$ ($C_o$= 20 mg diesel fuel/g dry soil) in sections S1 to S4 (see Figure 7.1). For Cell Z (electrokinetic enhanced), Figure 7.17 shows that 78%, 75%, 74%, and 75% of the initial diesel fuel remained in S1, S2, S3, and S4, respectively, after the test. This implies that 22%, 25%, 26%, and 25% of the initial diesel fuel was degraded in S1, S2, S3, and S4, respectively. For Cell CZ (control), Figure 7.17 shows that 88%, 89%, 88%, and 87% of the initial diesel fuel remained in S1, S2, S3, and S4 respectively, after the test, that is 12%, 11%, 12%, and 13% of the initial diesel fuel was degraded in S1, S2, S3, and S4. Therefore, the application of electrokinetic bioremediation using the ACC technique resulted in an increase in diesel fuel degradation between 83% and 127% compared to the control. For Cell Y and Cell CY, Figure 7.18 shows that the ratios of diesel fuel after the test in Cell CY (control) were 83%, 84%, 83%, and 82%, in S1, S2, S3 and S4, respectively compared to 78%, 74%, 71%, and 72% of the initial diesel that remained in Cell Y (electrokinetics enhanced). This represents an increase in degradation of 29-61% compared to the control. Figure 7.19 shows that 82%, 85%, 85%, and 86% of initial diesel fuel concentration in Cell X (electrokinetics enhanced) remained in S1, S2, S3, and S4, respectively, after the test. The diesel concentrations in S1, S2, S3, and S4 after the test in Cell CX (control) were 87%, 89%, 90%, and 89%, respectively. This means the degradation in Cell X was 21% to 33% higher than in Cell CX.

In Cell Y where the soil was contaminated with diesel fuel and bacteria were added to the water compartment (see Table 7.2) the degradation was 2-3% higher than in Cell Z, where the soil was contaminated with diesel and bacteria were added to the soil. This may suggest that the ACC technique is efficient in compelling the migration of bacteria into contaminated soil. The results may also suggest that the increase in current increased the diesel fuel degradation as the increase in current increased the temperature in the cell. This may explain the variation in diesel fuel degradation in the cells. No consistent trend of diesel fuel degradation in section S1, S2, S3, and S4 in all cells can be concluded from the tests. This is because the degradation was mainly due to microorganism activity. Also, the

uncontrolled weather conditions, given that the test was conducted outdoors, may have played a role. The results from the present study are in agreement with the previous study by Li et al. (2010) that showed a pollutant removal rate of 45.5% after 100 days of treatment compared with 22% in the test conducted with the bacteria alone. A removal of only 1% was reported in the control test.

Table 7.3 shows the regulatory guidelines for maximum level of total petroleum hydrocarbons in Canada. Fraction refers to the equivalent normal straight-chain hydrocarbon (nC) boiling point ranges (Fraction1: nC6 to nC10, and Fraction2: >nC10 to nC34) (CCME 2008). Diesel fuel compounds are split between fraction 2 and fraction 3. In the present study the initial concentration of diesel fuel was 2 g of diesel fuel/100 g of soil. The test was conducted during the winter season (short day and low temperature) for 55 days. The degradation rate was between 86 mg diesel fuel/ kg soil/ day to 95 mg diesel fuel/ kg soil/ day. Previous study showed diesel fuel degradation of 2.13 – 2.78 g diesel fuel per kg soil per day under controlled conditions (Marquez-Rocha et al. 2001). As shown in Figures 7.17, 7.18, and 7.19, diesel fuel degradation was not high this can be attributed to the fact that the test was conducted during the winter, and the soil and the electrolyte solutions were frozen most of the time. To enhance the degradation, the use of a defrost agent should be considered to melt the electrolyte solution in the water compartments.

**Table 7.3** Maximum total petroleum hydrocarbon (mg/kg) for surface soil

| Land Use | Soil Texture | Fraction 2 | Fraction 3 |
|---|---|---|---|
| Agriculture | Coarse-grained soil | 150 | 300 |
| | Fine-grained soil | 150 | 1300 |
| Residential/Parkland | Coarse-grained soil | 150 | 300 |
| | Fine-grained soil | 150 | 1300 |
| Commercial | Coarse-grained soil | 260 | 1700 |
| | Fine-grained soil | 260 | 2500 |
| Industrial | Coarse-grained soil | 260 | 1700 |
| | Fine-grained soil | 260 | 2500 |

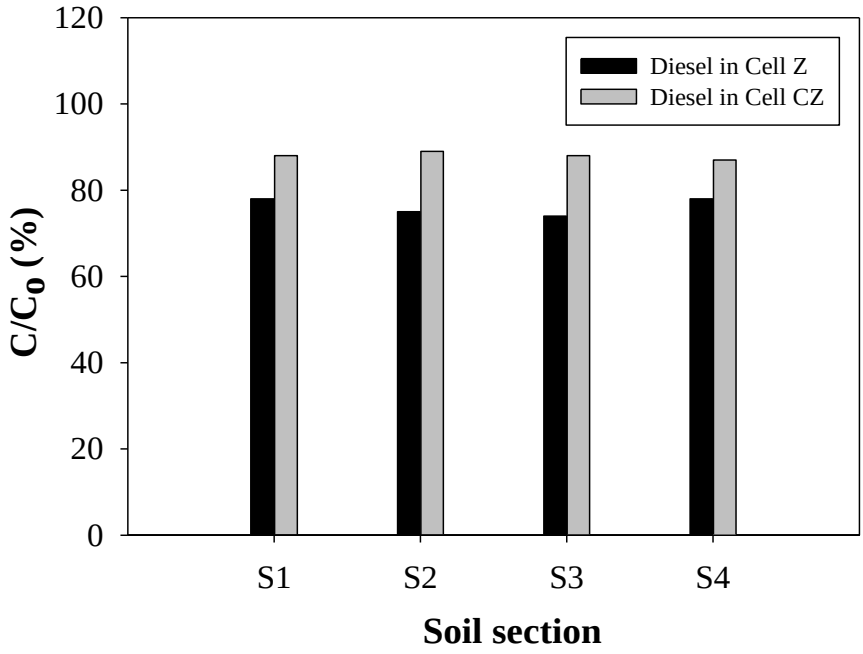


**Figure 7.17** Diesel fuel concentrations in Cell CZ and Cell Z after tests

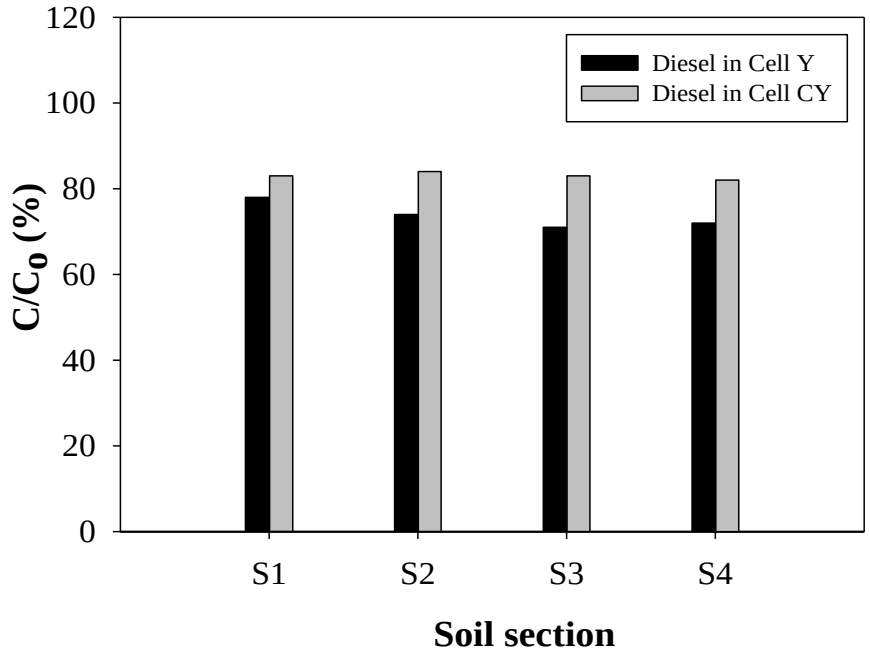


**Figure 7.18** Diesel fuel concentrations in Cell CY and Cell Y after tests

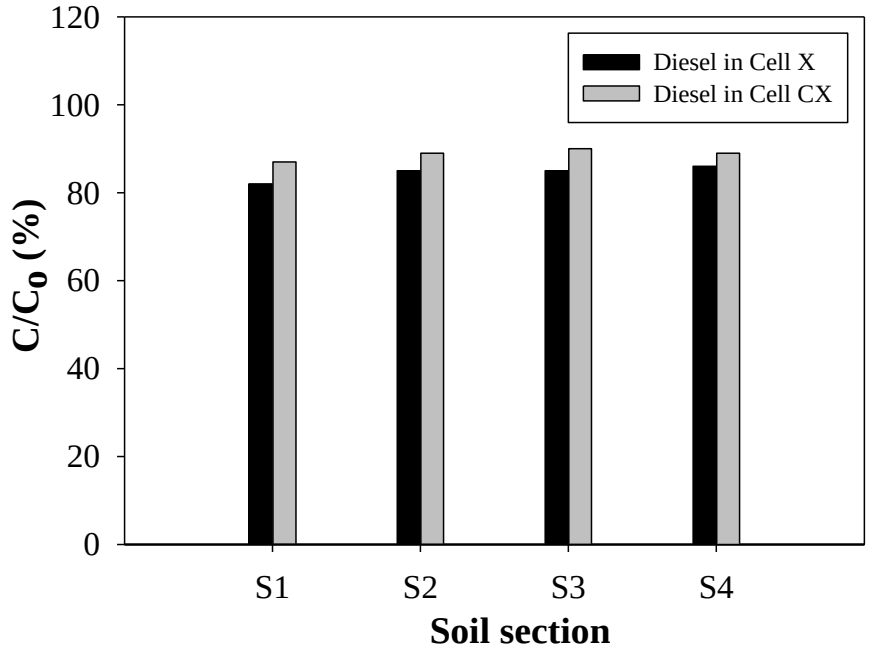


**Figure 7.19** Diesel fuel concentrations in Cell CX and Cell X after tests

## 7.4 CONCLUSIONS

The present study presented results from an outdoor test in which electrokinetic bioremediation, using three novel bacterial strains, was used to clean up soil artificially contaminated with diesel fuel. A new technique was used to stabilize the pH during the electrokinetic bioremediation. The power required for the electrokinetics was supplied by a solar photovoltaic panel. The results showed that solar photovoltaic panel can produce power enough for electro kinetic bioremediation during the winter season. Over the test period, voltages increased from zero, before sun rise, to 30 V at 10:00 AM, followed by a relatively steady voltage during 10:00 AM-3:00 PM, and, finally, a decrease in voltage from 30 V at 3:00 PM to zero volts at sunset. The current produced and the power consumed during the test varied depending on weather conditions. The temperature in the electrokinetic cells was found to be 5-7 $^{o}$C higher than the ambient temperature. The water content and pH of the soil specimen at the end of electrokinetic treatment remained relatively unchanged from initial values. Diesel degradation from electrokinetic bioremediation was 20-30%. The diesel degradation in the control test was 10-12 %.

## 7.5 REFERENCES

Abou-Shanab, R. A. I., Eraky, M., Haddad, A. M., Abdelgaffar, A. R., B. and Salem, A. M. (2015). "Characterization of crude oil degrading bacteria isolated from contaminated soils surrounding gas stations." Proceedings of the 14th International Conference on Environmental Science and Technology, Rhodes, **Greece**: 3-5 September 2015.

Acar, Y. B. and Alshawabkeh, A. N. (1993). "Principles of electrokinetic remediation." Environmental Science & Technology, **27**(13): 2638-2647.

Acar, Y. B., Rabbi, M. F. and Ozsu, E. E. (1997). "Electrokinetic injection of ammonium and sulfate ions into sand and kaolinite beds." Journal of Geotechnical and Geoenvironmental Engineering, **123**(3): 239-249.

Alok, A., Tiwari, R. P. and Singh, R. P. (2012). "Effect Of Ph Of Anolyte In Electrokinetic Remediation Of Cadmium Contaminated Soil " International Journal of Engineering Research & Technology (IJERT), **1**(10).

Alshawabkeh, A. N. (2009). "Electrokinetic Soil Remediation: Challenges and Opportunities." Separation Science and Technology, **44**(10): 2171-2187.

Budhu, M., Rutherford, M., Sills, G. and Rasmussen, W. (1997). "Transport of nitrates through clay using electrokinetics." Journal of Environmental Engineering-Asce, **123**(12): 1251-1253.

Cerqueira, V. S., Hollenbach, E. B., Maboni, F., Camargo, F. A. O., Peralba, M. D. R. and Bento, F. M. (2012). "Bioprospection and selection of bacteria isolated from environments contaminated with petrochemical residues for application in bioremediation." World Journal of Microbiology & Biotechnology, **28**(3): 1203-1222.

Canadian Council of Ministers of the Environment (2008). "Canada-wide srandards for petroleum hydrocarbons (PHC) in soil". http://www.ccme.ca/files/Resources/csm/phc_cws/phc_standard_1.0_e.pdf

Chung, H. I. and Kang, B. H. (1999). "Lead removal from contaminated marine clay by electrokinetic soil decontamination." Engineering Geology, **53**(2): 139-150.

Cotter, P. D. and Hill, C. (2003). "Surviving the acid test: Responses of gram-positive bacteria to low pH." Microbiology and Molecular Biology Reviews, **67**(3): 429-+.

Ebrahimi, M., Sarikhani, M. and Fallah, R. (2012). "Assessment of biodegradation efficiency of some isolated bacteria from oilcontaminated sites in solid and liquid media containing oil-compounds." Int. Res. J. Appl. Basic Sci, **3**(1): 138-147.

Fortier, R., Allard, M. and Seguin, M. K. (1994). "Effect of physical properties of frozen ground on electrical resistivity logging." Cold Regions Science and Technology, **22**(4): 361-384.

Hansen, H. K., Rojo, A. and Ottosen, L. M. (2007). "Electrokinetic remediation of copper mine tailings - Implementing bipolar electrodes." Electrochimica Acta, **52**(10): 3355-3359.

Hassan, I., Mohamedelhassan, E. and Yanful, E. K. (2015). "Solar powered electrokinetic remediation of Cu polluted soil using a novel anode configuration." Electrochimica Acta, **181**: 58-67.

Jo, S. U., Kim, D. H., Yang, J. S. and Baek, K. (2012). "Pulse-enhanced electrokinetic restoration of sulfate-containing saline greenhouse soil." Electrochimica Acta, **86**: 57-62.

Kang, Y. S., Jung, J., Jeon, C. O. and Park, W. (2011). "Acinetobacter oleivorans sp nov Is Capable of Adhering to and Growing on Diesel-Oil." Journal of Microbiology, **49**(1): 29-34.

Kang, Y. S. and Park, W. (2010). "Protection against diesel oil toxicity by sodium chloride-induced exopolysaccharides in Acinetobacter sp strain DR1." Journal of Bioscience and Bioengineering, **109**(2): 118-123.

Kauppi, S., Sinkkonen, A. and Romantschuk, M. (2011). "Enhancing bioremediation of diesel-fuel-contaminated soil in a boreal climate: Comparison of biostimulation and bioaugmentation." International Biodeterioration & Biodegradation, **65**(2): 359-368.

Kim, D. H., Jo, S. U., Yoo, J. C. and Baek, K. (2013). "Ex situ pilot scale electrokinetic restoration of saline soil using pulsed current." Separation and Purification Technology, **120**: 282-288.

Kim, S. H., Han, H. Y., Lee, Y. J., Kim, C. W. and Yang, J. W. (2010). "Effect of electrokinetic remediation on indigenous microbial activity and community within diesel contaminated soil." Science of the Total Environment, **408**(16): 3162-3168.

Kim, S. O. and Kim, K. W. (2001). "Monitoring of electrokinetic removal of heavy metals in tailing-soils using sequential extraction analysis." Journal of Hazardous Materials, **85**(3): 195-211.

Krulwich, T. A., Sachs, G. and Padan, E. (2011). "Molecular aspects of bacterial pH sensing and homeostasis." Nature Reviews Microbiology, **9**(5): 330-343.

Lee, M., Woo, S. G. and Ten, L. N. (2012). "Characterization of novel diesel-degrading strains Acinetobacter haemolyticus MJ01 and Acinetobacter johnsonii MJ4 isolated from oil-contaminated soil." World Journal of Microbiology & Biotechnology, **28**(5): 2057-2067.

Marquez-Rocha, F. J., Hernandez-Rodri, V. and Lamela, M. T. (2001) Biodegradation of diesel oil in soil by a microbial consortium. Water Air and Soil Pollution **128(3-4)**:313-320.

Padan, E., Bibi, E., Ito, M. and Krulwich, T. A. (2005). "Alkaline pH homeostasis in bacteria: New insights." Biochimica Et Biophysica Acta-Biomembranes, **1717**(2): 67-88.

Palanisamy, N., Ramya, J., Kumar, S., Vasanthi, N. S., Chandran, P. and Khan, S. (2014). "Diesel biodegradation capacities of indigenous bacterial species isolated from diesel contaminated soil." Journal of Environmental Health Science and Engineering, **12**.

Reddy, K. R. and Cameselle, C. (2009). Electrochemical remediation technologies for polluted soils, sediments and groundwater. Hoboken, N.J., Wiley**:** xxii, 732 p.

Ryu, B. G., Park, S. W., Baek, K. and Yang, J. S. (2009). "Pulsed Electrokinetic Decontamination of Agricultural Lands around Abandoned Mines Contaminated with Heavy Metals." Separation Science and Technology, **44**(10): 2421-2436.

Ryu, B. G., Yang, J. S., Kim, D. H. and Baek, K. (2010). "Pulsed electrokinetic removal of Cd and Zn from fine-grained soil." Journal of Applied Electrochemistry, **40**(6): 1039-1047.

Singh, S. N. and Tripathi, R. D. (2007). Environmental bioremediation technologies. New York;Berlin;, Springer.

Souza, F. L., SaÃ©z, C., Llanos, J., Lanza, M. R. V., CaÃ±izares, P. and Rodrigo, M. A. (2016). "Solar-powered electrokinetic remediation for the treatment of soil polluted with the herbicide 2,4-D." Electrochimica Acta, **190**: 371-377.

Virkutyte, J., Sillanpaa, M. and Latostenmaa, P. (2002). "Electrokinetic soil remediation - critical overview." Science of the Total Environment, **289**(1-3): 97-121.

Yuan, S. H., Zheng, Z. H., Chen, J. and Lu, X. H. (2009). "Use of solar cell in electrokinetic remediation of cadmium-contaminated soil." Journal of Hazardous Materials, **162**(2-3): 1583-1587.

# CHAPTER 8
# COMPLETE GENOME SEQUENCE OF *Arthrobacter* sp. LS16[1]

## 8.1 INTRODUCTION

*Arthrobacter* sp. are soil associated, Gram-positive, obligate aerobes with high survivability that are commonly isolated around the world (Hagedorn and Holt 1975; Mongodin et al. 2006). Previous studies have indicated that Arthrobacter are capable of degrading a variety of chemical compounds. Various strains of *Arthrobacter sp*. have been identified as capable of degrading atrazine, as well as utilizing phenanthrene, fluorine, dibenzothiophene, or carbizole as a sole carbon and energy source (Casellas et al. 1997; Samanta et al. 1999; Seo et al. 2006; Seo et al. 2009; Vandera et al. 2015; Sagarkar et al. 2016). Additionally, individual strains that have been previously shown to degrade a range of phenolic-derived compounds are resistant to desiccation, making them desirable for bioremediation (Pieper and Reineke 2000; Unell et al. 2008; Vikram et al. 2012). The ability of *Arthrobacter* species to degrade a wide range of chemical compounds including pesticides, herbicides and petroleum-derived hydrocarbons can be attributed to their adaptable genome, which can survive under severe conditions (Mongodin et al. 2006). A study in Canadian high arctic showed that *Arthorbacter* sp. can grow at temperatures below $0^oC$ (Bliss 1977). In general, it has been shown that *Arthrobacter* sp. can grow in temperatures between $-6^oC$ - $40^oC$ (Ganzert et al. 2011; Arora and Jain 2013) and pH ranges of 4 - 9.5 (Husserl et al. 2010; Ganzert et al. 2011).

*Arthrobacter* sp. LS16 (here forth, LS16) used in this study, was isolated from agricultural soils based on its ability to metabolize lignosulphonate, otherwise known as black liquor, a common side-product of sulfite pulping. The whole genome sequence reported here will allow for better understanding of the genetic basis of these traits.

[1]A version of this chapter has been published in the Genome Announcement

# 8.2 MATERIAL AND METHODS

## 8.2.1 Amplification of 16S DNA

A single bacterial colony was inoculated into 2.5 mL of 1/5 broth (the broth consists of nutrient broth: potatodextrise: tryptic soy (NPT) in the ratio of 2g: 5g: 6g) grown for 24 h at 37°C with shaking at 200 rpm. Cells were collected by centrifugation of 1.5 mL culture at 13000 rpm for 5 minutes and bacterial genomic DNA was isolated using a Sigma-Aldrich GenElute Bacterial Genomic DNA Kit (Product No. NA2120) following the manufacturers protocol. PCR amplification of an approximately 1,500 base pair sequence of the bacterial 16S rDNA gene was performed with primers 8F (5'-AGAGTTTGATCCTGGCTCAG-3') and 1492R (5'-GGTTACCTTGTTACGACTT-3'). Each 50 µL PCR mixture contained 1X PCR buffer, 2.0 mM $MgCl_2$, 200 µM dNTPs, 1.5 units Taq, and 2.5 µM of each primer, 1 µL (50 ng) of genomic DNA as template and ultrapure water (from Sigma). The PCR reaction was carried out with the Bio-Rad Thermal Cycler: one initial denaturation cycle at 95 ºC for 5 min, followed by 30 cycles of denaturation for 30 s at 94°C, annealing for 45 s at 57°C, and extension for 60 s at 72°C, with the final overall extension for 10 min at 72ºC. The 16S PCR products were purified by using QIAquick PCR purification kit (Qiagen).

## 8.2.2 Library preparation and sequencing

The DNA (PCR product) was assessed for quantity and quality using NanoDrop spectroscopy and agarose gel electrophoresis. A library with an approximate insert size of 500-600 bp was prepared for sequencing using NexteraXT DNA sample preparation kit according to the manufacturer's protocol. The generated library was used as a template for a limited cycle PCR using Nextera primers, the resulting library was purified and the quality was evaluated using an Agilent 2100 Bioanalyzer and qPCR. The final library loaded onto the Illumina MiSeq Sequencer at 10pmol and PE 2x300 bp runs were performed. LS16 genome was sequenced using 2x300 bp paired-end chemistry generating 7.62 million read pairs representing 100X coverage of the LS16 genome. Read pairs were

trimmed resulting in a 94X coverage library and the reads were assembled *de novo* and scaffolded using SPAdes (K-mer values of 21, 33, 55, 77, 99, and 127) resulting in a draft assembly of 33 contigs (Bankevich et al. 2012).

### 8.2.3 Scaffolding of draft genome

A previously completed genome closely related to LS16 draft genome facilitated scaffolding of the LS16 draft genome. To identify the most closely related, completed genome to LS16, Basic Local Alignment Search Tool (BLAST) was used to compare LS16 draft genome against the National Center for Biotechnology Information (NCBI) nucleotide sequence database. The comparison revealed that *A. arilaitensis* RE117 is the most closely related completed genome to the LS16 draft genome (Monnet et al. 2010). Previously completed genome closely related to a newly obtained draft genome is known as a reference genome.

The 33 contigs contained within the draft genome do not represent the true genetic structure and are arranged and numbered by descending base pair size. Mauve is a software tool that can reorder contigs in a draft genome by utilized a user provided reference genome. The LS16 draft genome was aligned using the progressive Mauve contig reordering algorithm against the completely sequenced genome of *A. arilaitensis* RE117 which showed the highest nucleotide-level similarity to LS16 (Darling et al. 2010; Darling et al. 2011). Directional orientation of the draft genome contigs were confirmed by comparisons against the reference genome using BLAST.

### 8.2.4 Gap closure

The gaps in the LS16 draft genome were identified through Mauve alignments against the complete genome *A. arilaitensis* RE117. Primer-BLAST (based off of the Primer3 software) was used to design the primers to close the gaps (Ye et al. 2012). In the primer design, the provision is made to hybridize 250-305 bp from the ends of the contigs flanking the gap along with the gap product. The forward and reverse primers were designed to be similar in the GC% content and melting temperature, and minimized self-complementarity.

LS16 genomic DNA was used as the target sequence for amplification of gaps between contigs. PCR reactions for amplification of contigs gaps were carried out with the Bio-Rad Thermal Cycler: one initial denaturation cycle at 95 ºC for 1 min, followed by 40 cycles of denaturation for 30 s at 95 °C, varied annealing temperature dependent on $T_m$ of the primers pair for 45 s, and extension for 300 s at 72 °C, with a terminal extension for 20 min at 72 ºC. Each 50 µL PCR mixture contained 1X PCR buffer, 2.0 mM MgCl2, 200 µM dNTPs, 1.5 units Phusion® Taq polymerase, and 2.5 µM of each primer, 1 uL (50 ng) of genomic DNA as template and Ultrapure® DNase and Rnase-free Water (from Sigma).

## 8.2.5 Genome annotation

National Center for Biotechnology Information (NCBI) Prokaryotic Genome Automatic Annotation Pipeline (PGAAP) was used for annotation of the complete LS16 genome (Besemer et al. 2001; Angiuoli et al. 2008).

## 8.2.6 Characterization of LS16

### 8.2.6.1 Growth curve

LS16 was streaked onto LB agar (LB agar consists of 10g tryptone, 5g yeast extract, 10 g NaCl, and 15 agar per liter of $dH_2O$) plate and incubated for 24 h at 28ºC to determine the growth rate of LS16. A single colony was picked and grown in LB broth in a 15 mL plastic tube, the plastic tube was placed in a rotary wheel and incubated for 24 h at 28ºC. 3 mL of culture was used to inoculate 500 mL of LB broth. The bottle was incubated with shaking for 48 h at 28ºC. The resulting culture was transferred to 50 mL tubes and centrifuged at 170 rpm. The supernatant was discarded and cell pellets were washed twice with 0.85% NaCl to remove residual nutrients. The washed pellets were re-suspended and standardized to an $OD_{600}$ of 0.1 in minimal medium (The minimal medium consists of $NH_4SO_4$- 1 g/L, $KH_2PO_4$ - 0.5 g/L, $K_2HPO4$ - 0.5 g/L, $MgSO_4$- 0.1 g/L, NaCl - 5 g/L, $CaCL_2$ - 0.1 g/L, and MSN- 1 g/L) with glycerol as a sole carbon source (0.3% Glycerol v/v). The final solution

was incubated in a wheel at room temperature for 10 days. The $OD_{600}$ was monitored and recorded periodically.

### 8.2.6.2 Growth at different temperatures

The growth of LS16 at different temperatures was investigated. An inoculum of an $OD_{600}$= 0.1 was prepared as described above. Glycerol was used as a sole carbon source (0.3% Glycerol v/v). The final solution placed in four incubator shakers. The temperatures in the shakers were adjusted to 12ºC, 22ºC, 32ºC, and 42ºC. The $OD_{600}$ of the solutions in the shakers were monitored and recorded periodically.

### 8.2.6.3 Growth at different pH

The growth of LS16 at different pH was investigated. Minimal medium, 300mL, was prepared and distributed equally in six 250 flasks (50 mL in each flask). The pHs of the solutions in the flasks were adjusted to pH of 2, 4, 6, 8, 10, and 12, then autoclaved. LS16 pellets were prepared as describe above. The solutions in the flasks were adjusted to $OD_{600}$ of 0.1 using the pellets. Glycerol was used as sole carbon source (0.3% Glycerol v/v). The flasks were placed in a shaker at room temperature. The $OD_{600}$ of the solutions in the shakers were monitored and recorded periodically.

### 8.2.6.4 Biodegradation

The ability of LS16 to degrade Phenanthrene, Fluorine, Atrazine, Carbezole, and Dibezothiophene (DBT) was investigated. Minimal medium solution, 250mL, of an $OD_{600}$= 0.1 was prepared using LS16 pellets as described above and distributed equally in six 250 flasks (50 mL in each flask). Stock solutions of 50 mg/L concentration of Phenanthrene, Fluorine, Atrazine, Carbezole, and Dibezothiophene (DBT) were prepared using Dimethyl sulfoxide (DMSO) as solvent. Phenanthrene, Fluorine, Atrazine,

Carbezole, and Dibezothiophene (DBT) were added into the flasks at concentrations of 100 mg/L suing the stock solution.

## 8.3 RESULTS AND DISCUSSION

### 8.3.1 Sequencing (draft genome)

LS16 genome was sequenced using 2x300 bp paired-end chemistry generating 7.62 million read pairs representing 100X coverage of the LS16 genome. Read pairs were trimmed resulting in a 94X coverage library and the reads were assembled *de novo* and scaffolded using SPAdes (K-mer values of 21, 33, 55, 77, 99, and 127) resulting in a draft assembly of 33 contigs. This assembly had the largest contig size of 798 kb, $N_{50}$ length of 347 kb, and total genome size of 3.85 Mb. The draft genome provides the majority of the genetic information contained in the contigs but does not provide important spatial information and may miss various novel or unique sequences. The draft genome was aligned with the reference genome of *A. arilaitensis* RE117 using the positional alignment software Mauve. Various contigs were not identified in the Mauve alignment, as shown in Figure 8.1, missing contigs included 18, 20, 21, 24, 25, 27, 28, 29, 30, 31, 32, and 33.

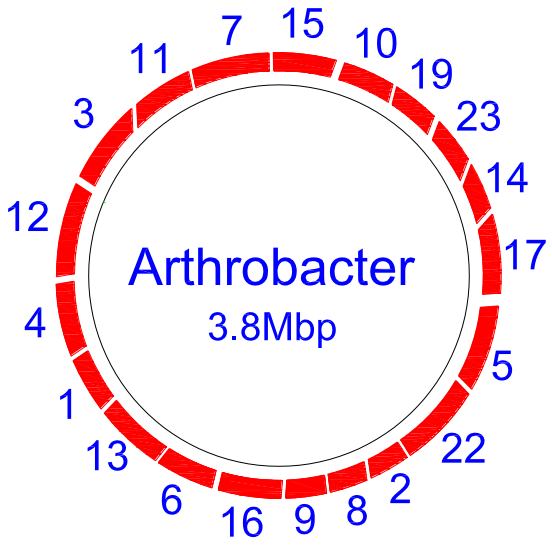


**Figure 8.1** Mauve generated alignment of LS16 genome against the *A. arilaitensis* RE117 reference genome. Red bars represent draft contigs superimposed onto the most likely location identified via the contig reorder tool using progresiveMauve. Various contigs are absent from the alignment, likely representing areas of unique or novel sequence. Contig size is not drawn to scale.

## 8.3.2 Genome Finishing

Finishing of the contig gaps (identifying gaps in the true genome sequence and sequencing and assembling the sequence) was performed using Long and Accurate-PCR across gaps with primers complementary to protein coding sequences flanking the 5' and 3' ends of contigs followed by Sanger sequencing and primer walking where necessary as described previously (Eastman and Yuan 2015). Figures 8.2-8.5 show the contigs gaps assembly. The genome of LS16 consists of a single circular replicon of 3 851 242 base pairs, with a G + C content of 64.32 % and no extra-chromosomal plasmids. Annotation was completed using the NCBI Prokaryote Genome Annotation Pipeline (Besemer et al. 2001; Angiuoli et al. 2008; Gao and Zhang 2008). Annotation revealed 3551 genes, 3255 CDS, 209 pseudo

genes, 1 ncRNA, 31 frameshifted genes, 67 tRNAs loci and 19 rRNAs genes, which is in accordance with other completely sequenced *Arthrobacter* sp. genomes.

The whole genome nucleotide sequence of *Arthrobacter* sp. LS16 has been deposited in GenBank under the accession no. CP012171. The version described in this study is the first version CP012171.00.

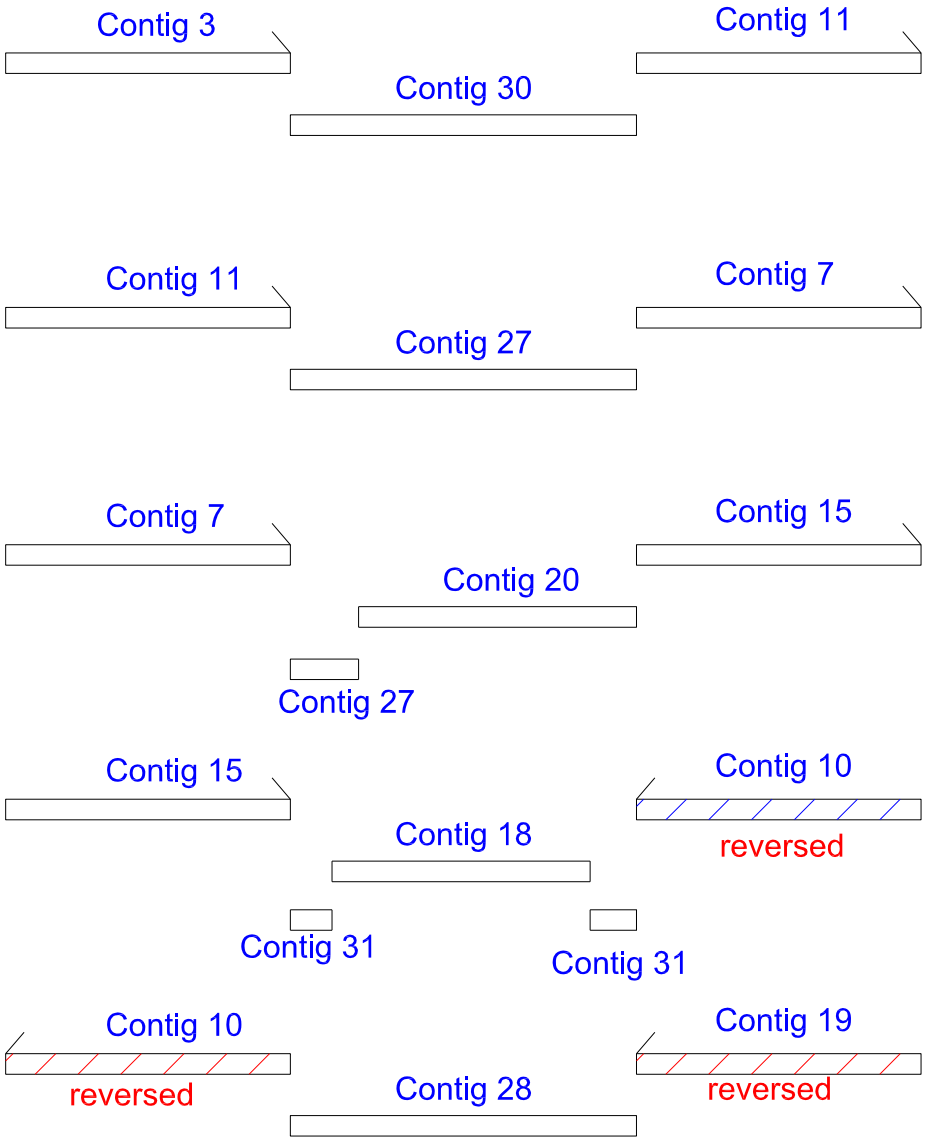


**Figure 8.2** Assembly of LS16 genome between Contig 3 to contig 19

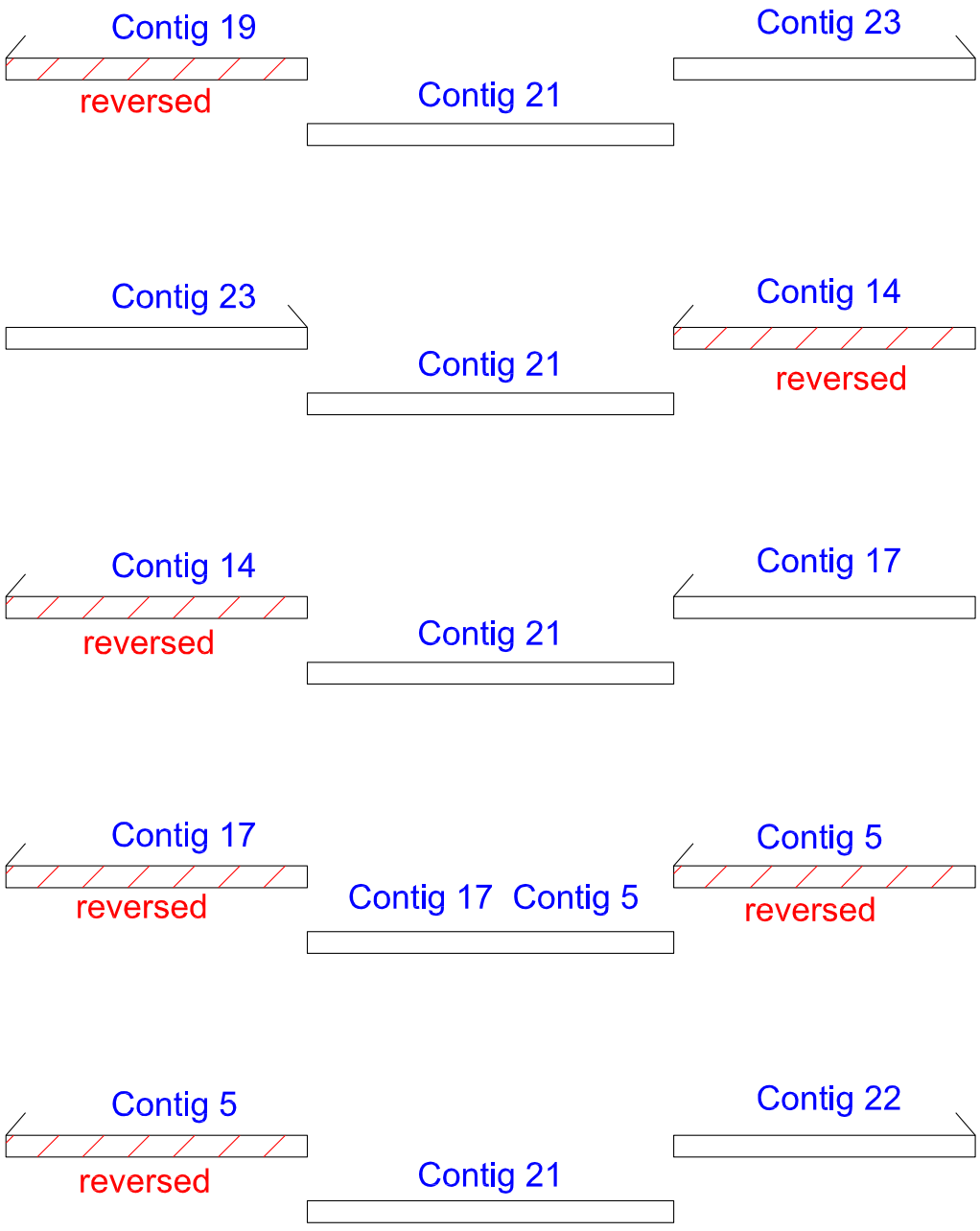


**Figure 8.3** Assembly of LS16 genome between Contig 19 to contig 22

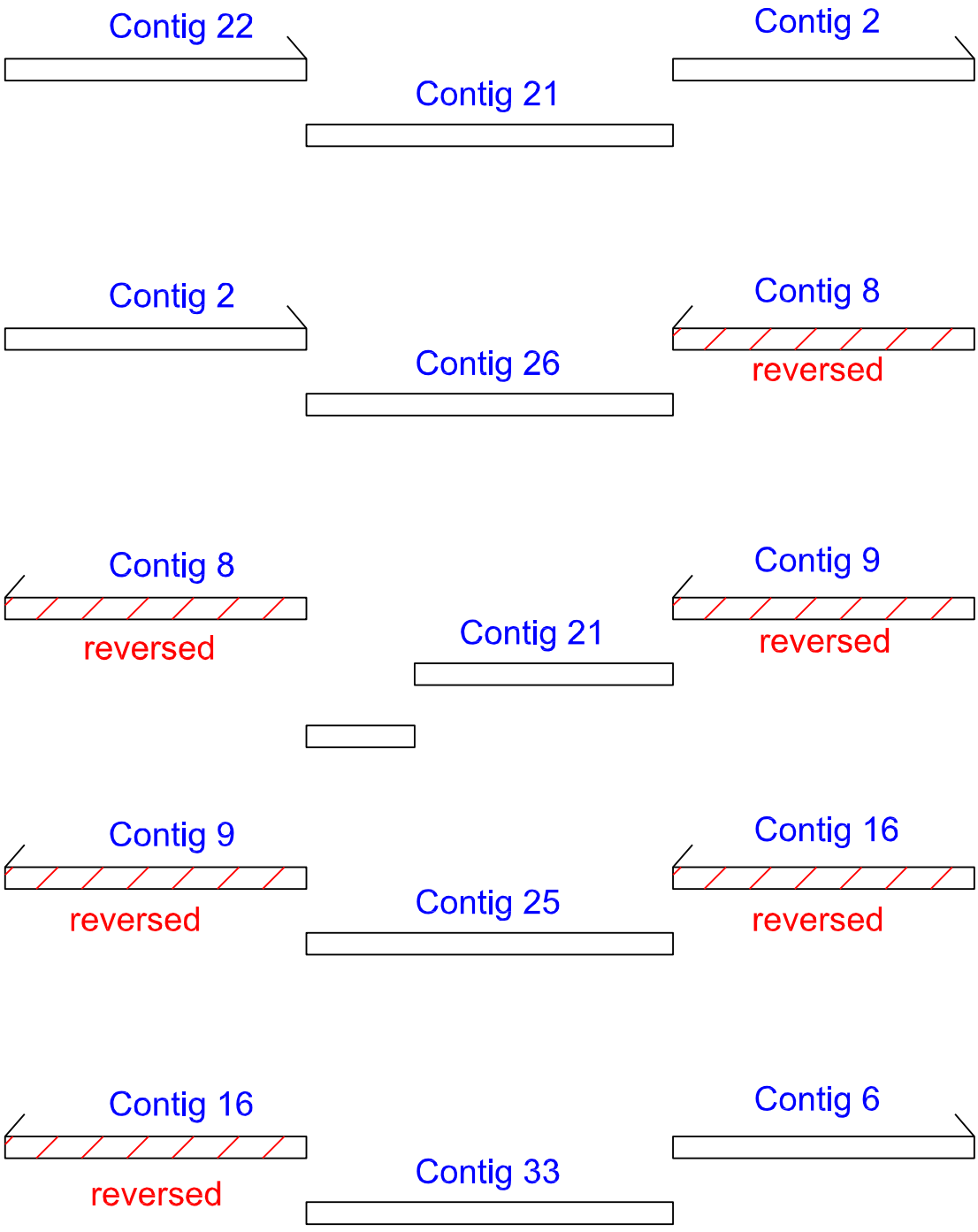


**Figure 8.4** Assembly of LS16 genome between Contig 22 to contig 6

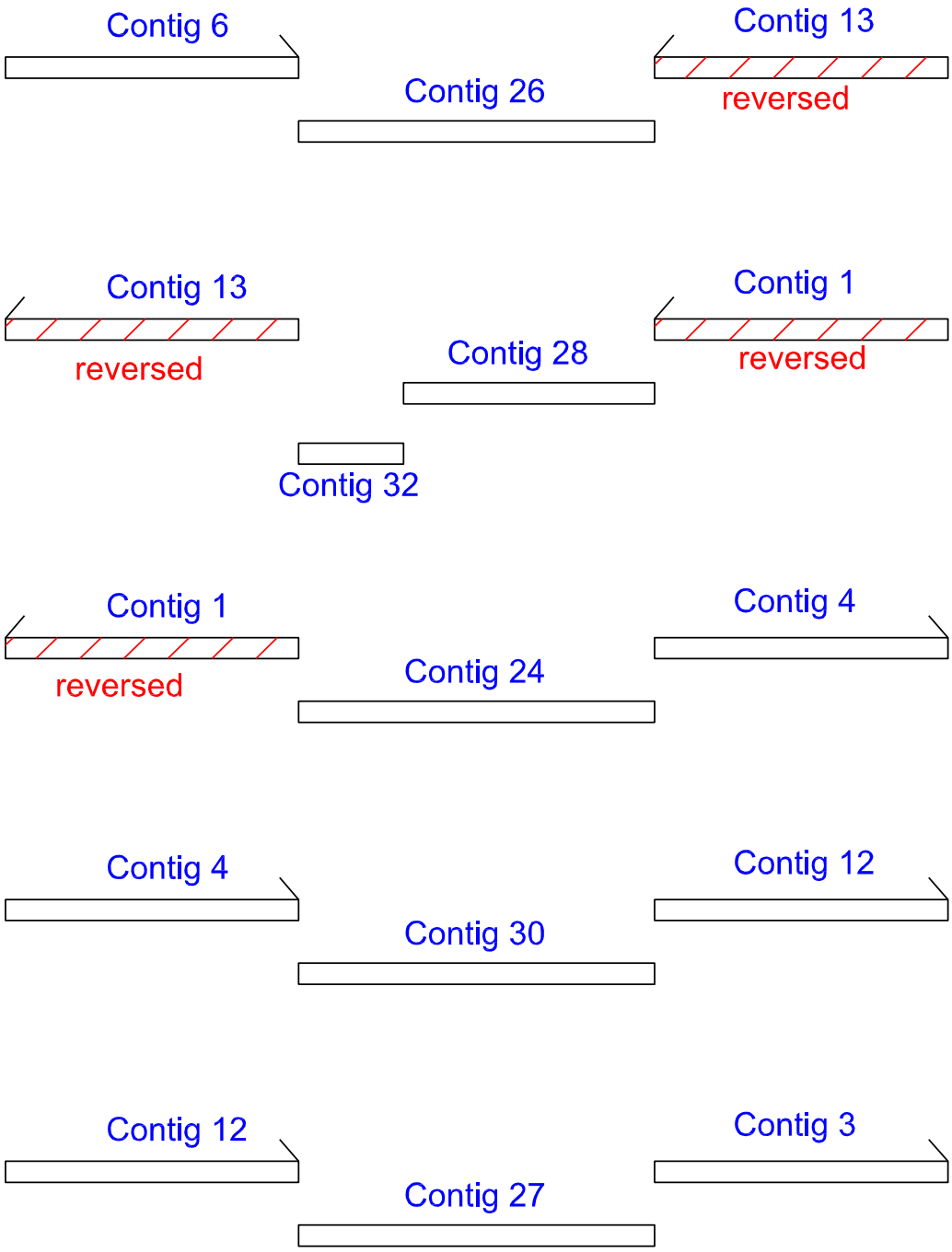


**Figure 8.5** Assembly of LS16 genome between Contig 6 to contig 3

### 8.3.3 Growth curve

Figure 8.6 shows the growth rate of LS16. The exponential phase corresponded to time zero and 24 h, followed by post-exponential phase from 24 h to 48 h, where the growth rate was less rapid. By 48 h cells had entered the stationary phase where cell death was equal to cell growth which continued until the end of the test.

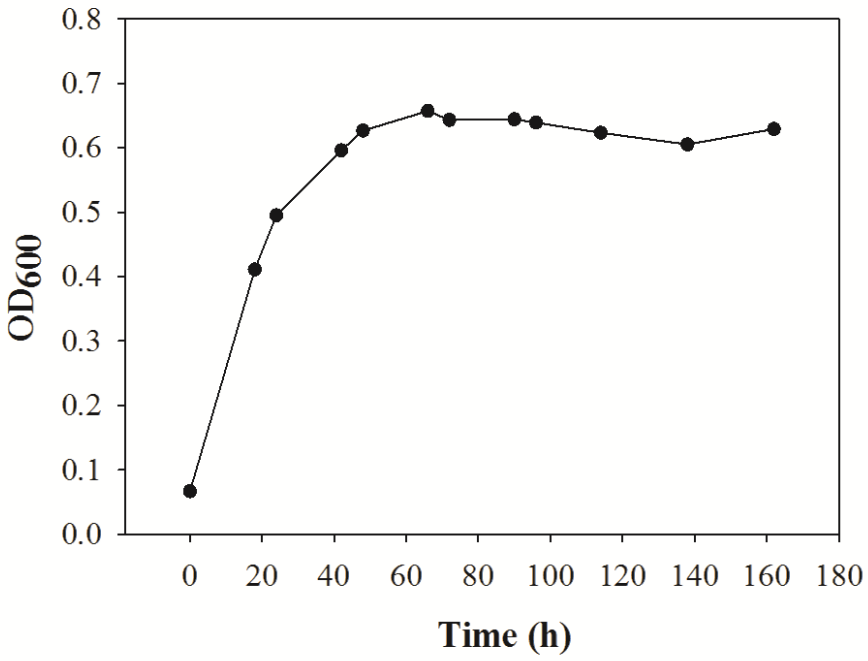


**Figure 8.6** LS 16 growth curve

### 8.3.4 Growth at different temperatures

Figure 8.7 shows the growth of LS16 at different temperatures 12, 22, 32, and 42ºC. The figure shows that at low temperature LS16 growths increased gradually in the first seven days. After that the growth increased more rapidly. At temperature 22º C, the growth occurred rapidly in the first 48 h and then stabilized until the end of the test. At temperature 32º C the growth profile increased rapidly in the first 24 h and then increased less rapidly until the end of the test. The test conducted at 32ºC showed the highest growth curve for

LS16. In the test conducted at 42°C, the growth rate increased rapidly for the first 48 h and then less rapidly until the end of the test. Previous studies showed that *Arthrobacter* sp. can grow at temperatures between -6 and 40°C (Ganzert et al. 2011; Arora and Jain 2013). In this study, the results showed that LS16 can grow in temperatures between 12°C and 42°C and the optimum growth temperature for LS16 is 32°C.

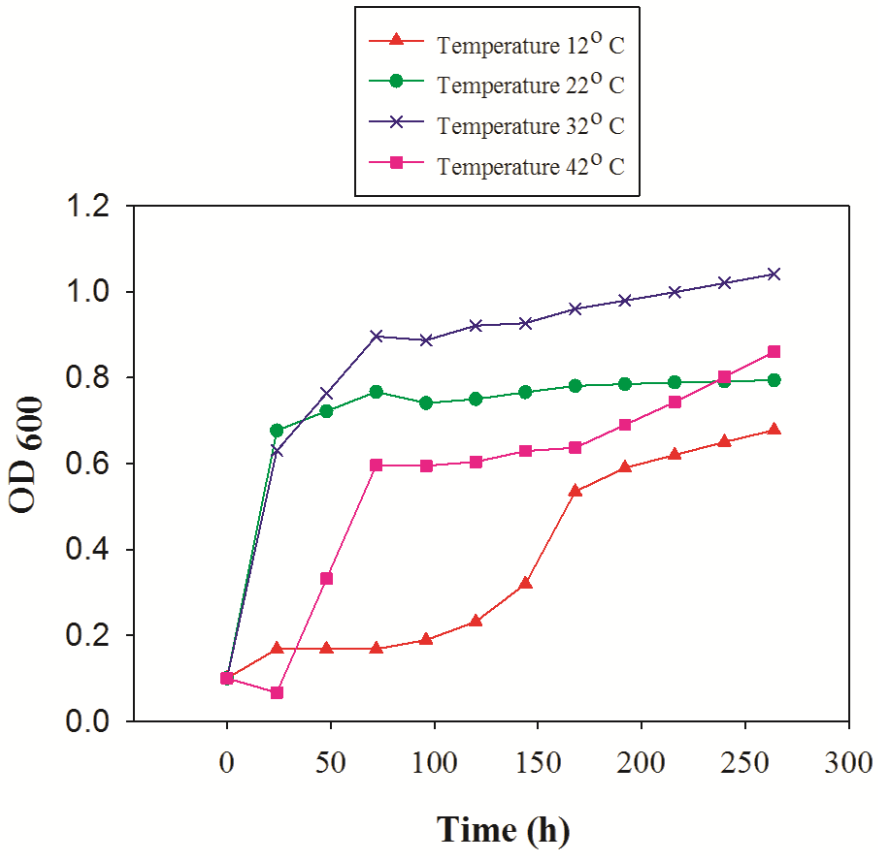


**Figure 8.7** LS16 growths at different temperatures

## 8.3.5 Growth at different pH

LS16 was grown at different pH values (2-12) to investigate pH effect on growth. There was no growth reported at pH 2, pH4, and pH12. Figure 8.8 shows the growth of LS16 at pH 6, 8, and 10. The growth profile of LS16 at pH 6 increased in the first 24 h and then

increased gradually until the end of the test. At pH 8, the figure shows rapid increase in growth rate in the first week and then stabilized to the end of the test. At pH 10, the growth rate continued to increase rapidly until day nine, and stabilized afterwards. The test conducted at pH 10 shows the best results for LS16. *Arthrobacter* has previously been shown to be capable of growing at pH values between 4 and 10 (Ganzert et al. 2011; Arora and Jain 2013). The results from the present study show no growth occurred below pH 6 and at pH 12. The optimum pH was found to be 10. However, the pH values at the end of the test are similar to the initial pH at low pH (pH 2 and 4) and differ significantly from the initial pHs at the higher pH values (pH 6,8,10, and 12) (see Table 8.1).

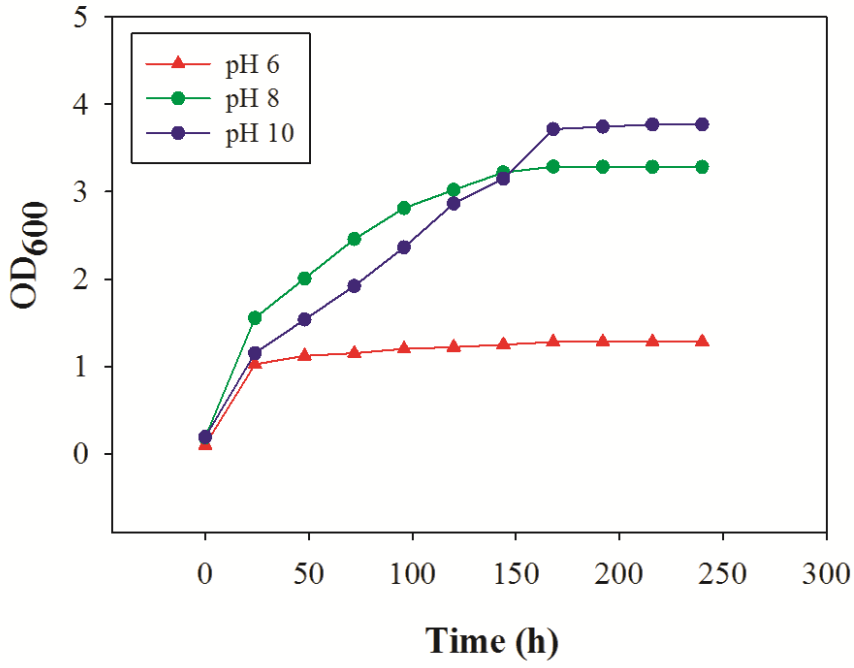


**Figure 8.8 LS16** growth curve at different pHs

**Table 8.1** Initial and final pHs

| | | | | | | |
|---|---|---|---|---|---|---|
| Initial pH | 2 | 4 | 6 | 8 | 10 | 12 |
| Final pH | 2 | 4.16 | 4.5 | 5.35 | 6.99 | 9.16 |

### 8.3.6 Biodegradation

Figure 8.9 shows the $OD_{600}$ of LS16 during the tests. Five different compounds were tested including phenanthrene, fluorine, dibenzothiophene (DBT), carbazole, and atrazine. The results show an increase in the optical density of all the compounds, except for fluorine, indicating a growth of LS16. The increase in the optical density is low and this is to be expected as low degrading rate is normally associated with hydrocarbon degradation.

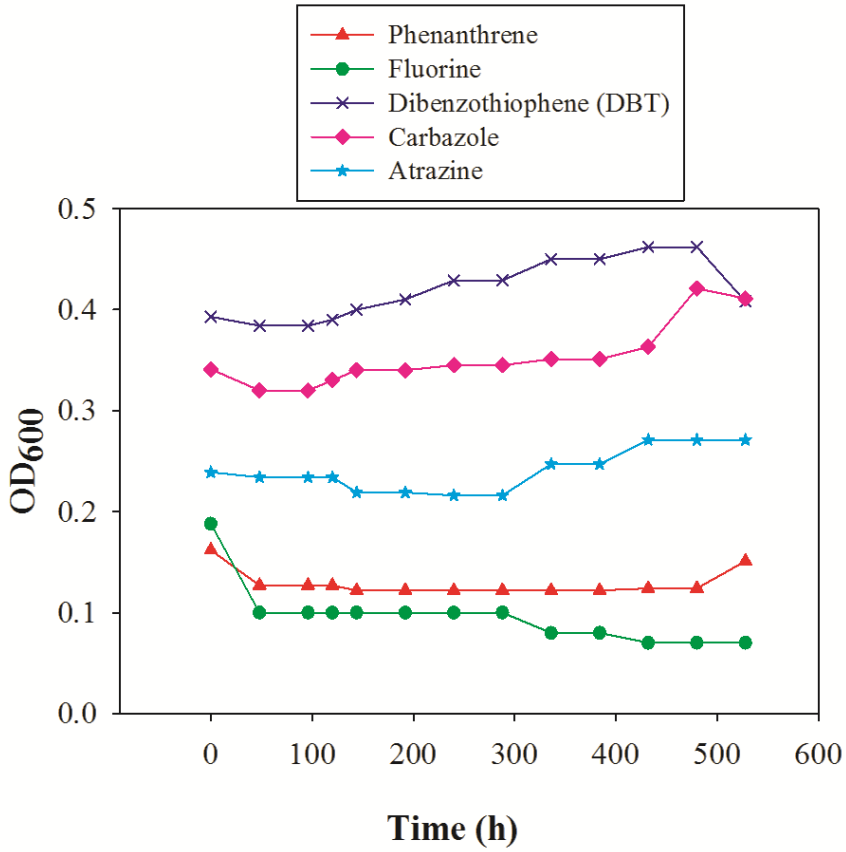


**Figure 8.9** Degradation curve for LS16

## 8.4 CONCLUSIONS

The complete genomic sequence of the bacterium *Arthrobacter* sp. LS16 is presented. LS16 genome consists of a single circular chromosome of 3.85 Mb with no identified extrachromosomal plasmid. LS16 demonstrates various characteristics amicable to industrial applications including metabolism of lignin-derived and phenolic compounds, robust growth at high pH, and bioremediation of soils contaminated with hydrocarbons. In-

depth analysis of the *Arthrobacter* sp. LS16 genome will further our understanding of the underlying mechanisms guiding genetic modification of pathways to enhance bioremediation traits. The optimum growth conditions for LS16 are pH 10 and temperature 32$^{o}$ C. The results indicated that LS16 can degrade phenanthrene, carbazole, atrazine, and dibenzothiophene.

## 8.5 REFRENCES

Angiuoli, S. V., et al. (2008). "Toward an online repository of Standard Operating Procedures (SOPs) for (Meta) genomic annotation." Omics-a Journal of Integrative Biology, **12**(2): 137-141.

Arora, P. K. and Jain, R. K. (2013). "Arthrobacter nitrophenolicus sp nov a new 2-chloro-4-nitrophenol degrading bacterium isolated from contaminated soil." 3 Biotech, **3**(1): 29-32.

Bankevich, A., et al. (2012). "SPAdes: A New Genome Assembly Algorithm and Its Applications to Single-Cell Sequencing." Journal of Computational Biology, **19**(5): 455-477.

Besemer, J., Lomsadze, A. and Borodovsky, M. (2001). "GeneMarkS: a self-training method for prediction of gene starts in microbial genomes. Implications for finding sequence motifs in regulatory regions." Nucleic Acids Research, **29**(12): 2607-2618.

Bliss, L. C. (1977). Truelove Lowland, Devon Island, Canada : a high arctic ecosystem. Edmonton, University of Alberta Press.

Casellas, M., Grifoll, M., Bayona, J. M. and Solanas, A. M. (1997). "New metabolites in the degradation of fluorene by Arthrobacter sp strain F101." Applied and Environmental Microbiology, **63**(3): 819-826.

Darling, A. E., Mau, B. and Perna, N. T. (2010). "progressiveMauve: Multiple Genome Alignment with Gene Gain, Loss and Rearrangement." Plos One, **5**(6).

Darling, A. E., Tritt, A., Eisen, J. A. and Facciotti, M. T. (2011). "Mauve Assembly Metrics." Bioinformatics, **27**(19): 2756-2757.

Eastman, A. W. and Yuan, Z. C. (2015). "Development and validation of an rDNA operon based primer walking strategy applicable to de novo bacterial genome finishing." Frontiers in Microbiology, **5**.

Ganzert, L., Bajerski, F., Mangelsdorf, K., Lipski, A. and Wagner, D. (2011). "Arthrobacter livingstonensis sp. nov. and Arthrobacter cryotolerans sp. nov., salt-tolerant and psychrotolerant species from Antarctic soil." International Journal of Systematic and Evolutionary Microbiology, **61**: 979-984.

Gao, F. and Zhang, C. T. (2008). "Ori-Finder: A web-based system for finding oriCs in unannotated bacterial genomes." Bmc Bioinformatics, **9**.

Hagedorn, C. and Holt, J. G. (1975). "A nutritional and taxonomic survey of Arthrobacter soil isolates." Can J Microbiol, **21**(3): 353-61.

Husserl, J., Spain, J. C. and Hughes, J. B. (2010). "Growth of Arthrobacter sp Strain JBH1 on Nitroglycerin as the Sole Source of Carbon and Nitrogen." Applied and Environmental Microbiology, **76**(5): 1689-1691.

Mongodin, E. F., et al. (2006). "Secrets of soil survival revealed by the genome sequence of Arthrobacter aurescens TC1." Plos Genetics, **2**(12): 2094-2106.

Monnet, C., et al. (2010). "The Arthrobacter arilaitensis Re117 Genome Sequence Reveals Its Genetic Adaptation to the Surface of Cheese." Plos One, **5**(11).

Pieper, D. H. and Reineke, W. (2000). "Engineering bacteria for bioremediation." Current Opinion in Biotechnology, **11**(3): 262-270.

Sagarkar, S., Bhardwaj, P., Storck, V., Devers-Lamrani, M., Martin-Laurent, F. and Kapley, A. (2016). "s-triazine degrading bacterial isolate Arthrobacter sp AK-YN10, a candidate for bioaugmentation of atrazine contaminated soil." Applied Microbiology and Biotechnology, **100**(2): 903-913.

Samanta, S. K., Chakraborti, A. K. and Jain, R. K. (1999). "Degradation of phenanthrene by different bacteria: evidence for novel transformation sequences involving the formation of 1-naphthol." Applied Microbiology and Biotechnology, **53**(1): 98-107.

Seo, J. S., Keum, Y. S., Cho, I. K. and Li, Q. X. (2006). "Degradation of dibenzothiophene and carbazole by Arthrobacter sp P1-1." International Biodeterioration & Biodegradation, **58**(1): 36-43.

Seo, J. S., Keum, Y. S. and Li, Q. X. (2009). "Bacterial Degradation of Aromatic Compounds." International Journal of Environmental Research and Public Health, **6**(1): 278-309.

Unell, M., Nordin, K., Jernberg, C., Stenstrom, J. and Jansson, J. K. (2008). "Degradation of mixtures of phenolic compounds by Arthrobacter chlorophenolicus A6." Biodegradation, **19**(4): 495-505.

Vandera, E., Samiotaki, M., Parapouli, M., Panayotou, G. and Koukkou, A. I. (2015). "Comparative proteomic analysis of Arthrobacter phenanthreniuorans Sphe3 on phenanthrene, phthalate and glucose." Journal of Proteomics, **113**: 73-89.

Vikram, S., Kumar, S., Subramanian, S. and Raghava, G. P. S. (2012). "Draft Genome Sequence of the Nitrophenol-Degrading Actinomycete Rhodococcus imtechensis RKJ300." Journal of Bacteriology, **194**(13): 3543-3543.

Ye, J., Coulouris, G., Zaretskaya, I., Cutcutache, I., Rozen, S. and Madden, T. L. (2012). "Primer-BLAST: A tool to design target-specific primers for polymerase chain reaction." Bmc Bioinformatics, **13**.

# CHAPTER 9
# SUMMARY CONCLUSIONS AND RECOMMENDATIONS FOR FUTURE RESEARCH

## 9.1 SUMMARY

This thesis presents the enhancement of electrokinetic bioremediation. Laboratory experiments and outdoor experiments were conducted in the study.

Sorption isotherm tests were conducted using six phenanthrene solution with concentrations from 300 to 800 μg/L. Following sorption tests, desorption tests were carried out using phenanthrene-free solution. In addition, two test series were performed to compare phenanthrene desorption by hydraulic and electroosmotic flows at room temperature. A fixed wall hydraulic permeameter apparatus was used to generate a hydraulic flow rate of $1.4 \times 10^{-3}$ mL/s at a pressure of 260 kPa, while a low level current density (0.3-0.43 mA/cm$^2$) was applied to generate electroosmotic flow rate equivalent to the hydraulic flow. The power required and phenanthrene concentrations in effluent samples after desorption by electroosmotic and hydraulic flows were determined.

A novel electrode configuration technique to stabilize soil pH during electrokinetic bioremediation process was investigated. The novel configuration employs an anode and a cathode placed side by side at each end of the soil under treatment (an anode and a cathode in the same compartment at each end) in the electrokinetic cell. Six electrokinetics cells were used to carry out two different sets of tests (novel configuration and conventional configuration) in triplicates. Tests using the novel configuration technique, termed anode-cathode-compartment (ACC), were performed along with control tests that were carried out using conventional anode-cathode (CAC) configuration. In the ACC technique, the anode and the cathode in the compartment were connected to the oppositely charged electrode in the other compartment via two electric circuits across the cell. An innovative

device (Electrokinetic voltage controller, EKVC) was designed, and used to switch the current between the two electric circuits. The ACC setup was designed to allow the hydrogen ions generated at the anode to be neutralized by the hydroxyl ions formed at the cathode. Solution of sodium nitrate, $NaNO_3$ (1 g/L), was used as a model compound (added in the water compartment) to investigate and compare the efficacy of ACC and CAC configurations in delivering nitrate (i.e. nutrients). Voltage across the soil specimen, electric current, and pH of water in the electrode compartments were monitored during the test. Water content, pH, and nitrate concentration were determined across the soil specimen after the test.

A solar panel was used to generate power for the electrokinetic bioremediation of soil contaminated with phenanthrene. Kaolinite, used as the test soil, was artificially contaminated with phenanthrene to a concentration of 2 mg per g of dry soil. *Mycobacterium pallens* sp. at a concentration of $10^8$ colony forming units per mL was used as the microorganism to degrade phenanthrene. Electrokinetics was used to deliver nutrients to the microorganisms. Tests were carried out in four different cells: Cell X (uncontaminated soil), Cell A (soil, phenanthrene, bacteria, and nutrients), Cell B (soil, phenanthrene, and nutrients), Cell C (soil, phenanthrene). In addition, four control experiments were conducted without electric current. ACC technique was used for the test to keep the pH of the soil and water unchanged.

Three hundred bacterial strains were isolated from agricultural soil and characterized according to their ability to degrade diesel fuel. Forty five strains were able to use diesel fuel as sole carbon and energy source. Three distinct strains designated as AC16, SM155, and SB53, were selected and subjected to further investigation, including ability to grow in liquid medium at different diesel fuel concentrations, identification of functional genes, and ability to grow at different temperatures and pH. The three isolates AC16, SM155, and SB53 were identified as *Acintobacter calcoaceticus*16, *Sphingobacterium multivorum*155,

and *Sinorhizobium* sp. B53, respectively, based on their 16S rDNA. The three strains were found to be capable of using diesel fuel as carbon and energy source

Electrokinetic bioremediation outdoor tests were conducted to rehabilitate soil contaminated with diesel fuel. The tests were conducted using the three distinct bacterial strains. ACC configuration was used for the electrokinetic bioremediation tests. The tests were carried out in outdoors for 55 days using six electrokinetic remediation cells. Voltage generated by the solar panel, current passed through the electrokinetic cells, and the temperatures of the soil specimens in the electrokinetic remediation cells were monitored and recorded periodically during the course of the tests. The pH, water content, and diesel fuel concentration were determined at the end of the tests.

Arthrobacter sp. LS16 used in this study was isolated from agricultural soils based on its ability to metabolize lignosulphonate a common side-product of sulfite pulping. The whole genome sequence is completed. LS16 was characterized for the ability to grow at different pH and temperatures and to degrade phenanthrene, carbazole, atrazine, and dibenzothiophene.

## 9.2 CONCLUSIONS

**Chapter 3**

- The phenanthrene concentration in effluent samples after desorption by electroosmotic flow was found to be three to four times the concentration after desorption by hydraulic flow.

- The power required in the hydraulic flow test was three orders of magnitude higher than the consumed power in the electrokinetic flow test. These results

showed that phenanthrene desorption by electroosmotic flow is more efficient than by hydraulic flow

**Chapter 4**

- In the novel configuration (ACC), the pH at both water compartments was between 7.2-7.8.
- After test with ACC, pH across the soil specimen remained close to the initial pH.
- Very little variation was found in the water content across the soil at the end of the test with ACC
- Relatively uniform nitrate concentration was reported across the soil between the electrodes at the end of the tests with ACC.
- The ACC configuration has a potential to enhance the outcome and promote the use of electrokinetic bioremediation in mitigating contaminated soils.

**Chapter 5**

- The results showed that solar photovoltaic panels can generate enough power for electrokinetic bioremediation
- The current generated in the cell is directly related to the composition of the soil in the electrokinetic cell. The highest current was generated in the cell containing phenanthrene, bacteria and nutrients (0.6A), followed by the cell containing phenanthrene and nutrients (0.4A). The lowest current (0.14A) was generated in the cell that contained only phenanthrene.
- There was an 8-18$^{o}$C increase in temperature with respect to ambient temperature in the electrokinetic cells.
- The highest phenanthrene degradation after electrokinetic was 50% compared to a maximum degradation of 22% in the control test.

**Chapter 6**

- The results showed that the isolate AC16, SM155, and SB53 can grow at temperature between 18$^{o}$C and 38$^{o}$C whereas temperature 48$^{o}$C has detrimental effect on three isolates.
- The isolates grow better at pH between 6 and 8, while there was no grow at pH 2 and pH 12.
- Reverse transcription polymerase chain reaction (RT-PCR) results showed that the gene RubA was found to be expressed in the three isolates.
- The three isolates can degrade diesel fuel at concentrations between 0.5 to 6%. The isolates can degrade 40% of diesel fuel with initial concentration of 2% (v/v) in 50 mL minimal medium, after incubation for 14 days.
- The results of showed that, at diesel fuel concentration of 2% (v/v), the highest degradation of diesel fuel can be achieved when combining AC16 and SM155.

**Chapter 7**

- The results showed that solar photovoltaic panel can produce power enough for electrokinetic bioremediation during the winter season.
- Over the test period, the voltages increased from zero before sun rise to 30 V at 10:00 AM, followed by relatively stabilize period between 10:00 Am and 3:00 PM. The voltage then started to decrease from 30 V and dropped to zero volts by sun set.
- The current produced and the power consumed during the period of the test varied depending on the weather conditions.
- The temperatures in the electrokinetic cells were found to be higher by 5-7$^{o}$C than the ambient temperature.
- The water content and the pH in the soil specimen at the end of the tests were maintained relatively unchanged from the initial values.

- The diesel degradations in the soil after electrokinetic bioremediation were 20-30%, compared to 10-12% in the control test.

**Chapter 8**

- Complete genome of *Arthrobacter* LS16 was deposited in the National center for biotechnology information (NCBI).
- LS16 demonstrates various characteristics amicable to industrial applications including metabolism of lignin-derived and phenolic compounds, robust growth at high pH, and bioremediation of soils contaminated with hydrocarbons.
- The optimum growth conditions for LS16 are pH 10 and temperature 32$^{o}$ C.
- The results indicated that LS16 can degrade phenanthrene, carbazole, atrazine, and dibenzothiophene.

## 9.3 RECOMMENDATIONS FOR FUTURE RESEARCH

The results obtained from the present study provide insight on use of electroosmotic flow for desorption of phenanthrene, the stabilization of pH during the electrokinetic bioremediation, the use of solar panel to generate power for electrokinetic bioremediation, and the isolation of new strains capable of degrading diesel fuel. However, further research is definitely necessary to expand knowledge related to electrokinetic bioremediation and to make use of the results from this study to enhance the degradation process.

- A number of factors can influence desorption by electroosmotic flow, including the type of contaminant, temperature, and type of soil. Further investigations should be conducted to study the effect of these factors on desorption by electroosmotic flow.
- The effect of the use of different electrode material in the ACC technique, the relation between the size of the water compartment and the rate of the switch of the electric circuits, the distance of the electrode from the soil, and the distance between the electrodes. The effect of these components should be investigated.

- A pilot tests using ACC to stabilize pH during electrokinetic bioremediation should be conducted to provide practical results for a large contaminated soil scale.
- Investigation of new ways to reduce the voltage drop between the electrodes and soil under treatment using antifreeze compound.
- Isolation and characterization of new strains capable of degrading petroleum hydrocarbons.
- The effect of the electric current in microorganisms' intracellular components/activities and the in bacterial RNA should be investigated.
- Application of the ACC technique using electrokinetic bioremediation to mitigate soil contaminated with crude oil should be investigated.
- Numerical modeling methods for migration of bacteria and nutrients during electrokinetic bioremediation should be conducted.

# Appendices A

This appendix provides additional information to show the setup of fixed wall hydraulic test and electrokinetic desorption tests presented in Chapter 3

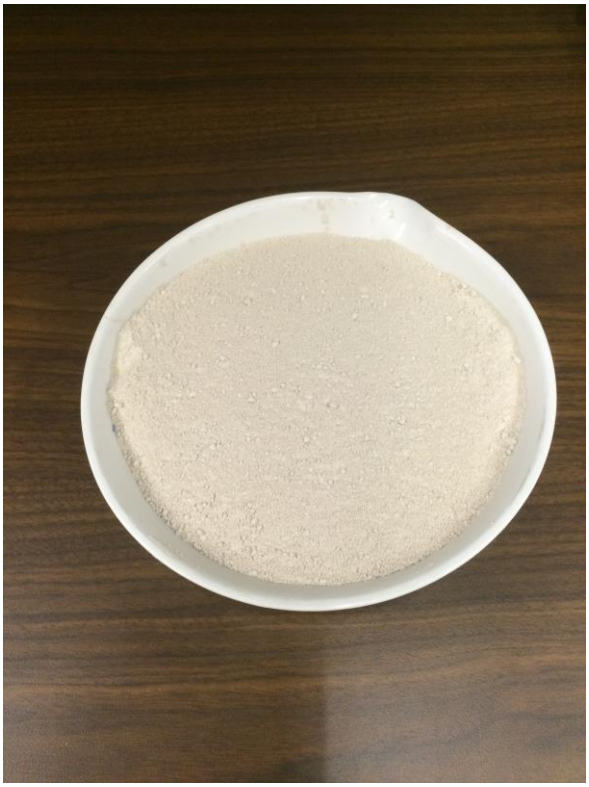

**Figure A. 1** Clay soil **(**kaolinite) used in the tests

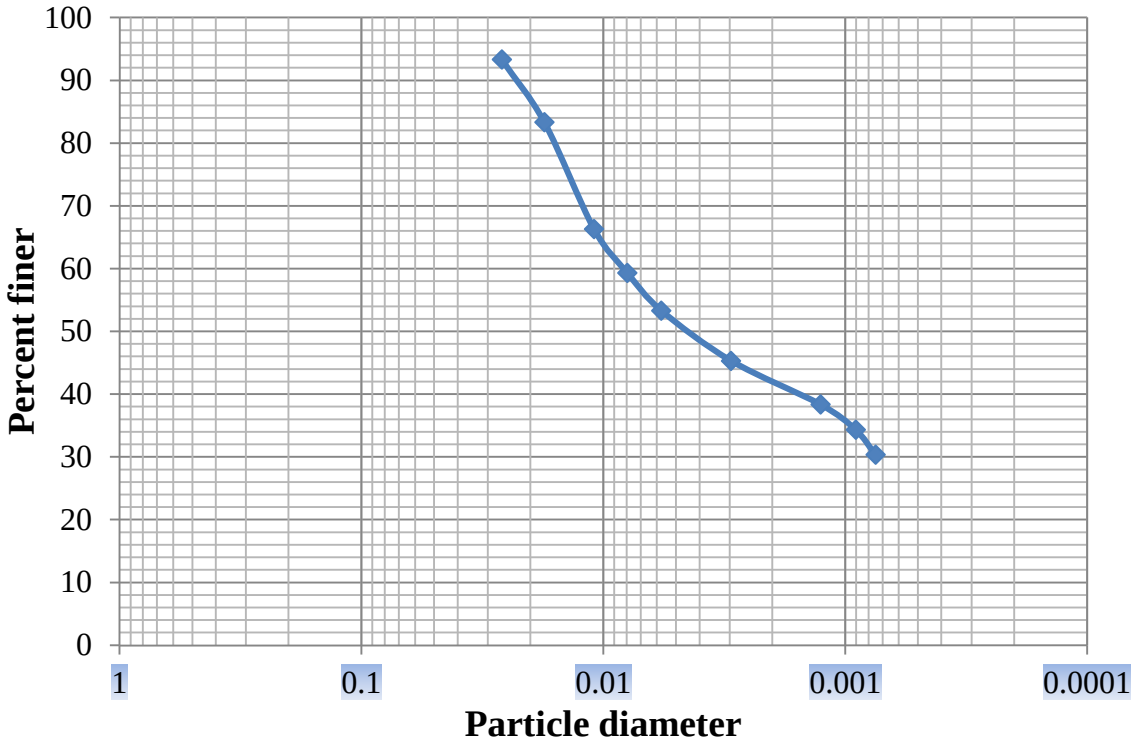


**Figure A. 2** Particle-size distribution curve (Hydrometer test)

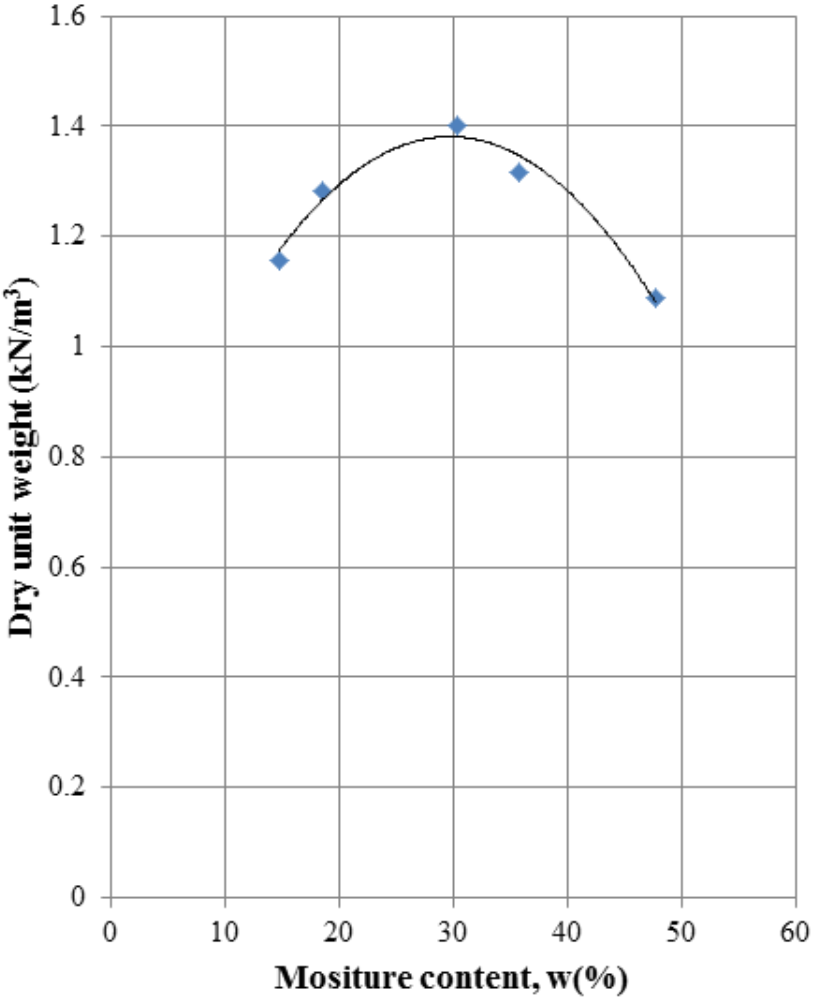


**Figure A. 3** Modified proctor test


**Figure A. 4** Photo showing electrokinetics apparatus used in desorption by electroosmotic flow tests

**Figure A. 5** Photo showing fixed wall permeameter apparatus used in desorption by hydraulic flow

**Table A.1** Desorption tests (Phenanthrene initial concentration 500mg/kg)

| Pore volume | Electroosmotic flow | Hydraulic flow |
|---|---|---|
| 1 | 15.1246 | 7.4668 |
| 2 | 26.3498 | 12.7133 |
| 3 | 29.6087 | 17.8068 |
| Total removal | 71.0831 | 37.9869 |

**Table A.2** Desorption tests (Phenanthrene initial concentration 1000mg/kg)

| Pore volume | Electroosmotic flow | Hydraulic flow |
|---|---|---|
| 1 | 25.2413 | 9.5254 |
| 2 | 30.3469 | 14.1249 |
| 3 | 30.9092 | 20.7006 |
| Total removal | 86.4974 | 44.3509 |

**TableA.3** Desorption tests (Phenanthrene initial concentration 2000mg/kg)

| Pore volume | Electroosmotic flow | Hydraulic flow |
|---|---|---|
| 1 | 37.0626 | 12.6897 |
| 2 | 36.5612 | 17.3128 |
| 3 | 37.3383 | 19.0773 |
| Total removal | 110.9621 | 49.0798 |

**TableA.4** Desorption tests (Phenanthrene initial concentration 3000mg/kg)

| Pore volume | Electroosmotic flow | Hydraulic flow |
|---|---|---|
| 1 | 42.0647 | 17.6127 |
| 2 | 34.6119 | 16.6246 |
| 3 | 33.7929 | 17.9539 |
| Total removal | 110.4695 | 52.1912 |

**TableA.5** Desorption tests (Phenanthrene initial concentration 4000mg/kg)

| Pore volume | Electroosmotic flow | Hydraulic flow |
|---|---|---|
| 1 | 62.4089 | 14.9718 |
| 2 | 52.0654 | 18.2068 |
| 3 | 63.8665 | 19.8536 |
| Total removal | 178.3408 | 53.0322 |

**Table A.6** Desorption tests (Phenanthrene initial concentration 5000mg/kg)

| Pore volume | Electroosmotic flow | Hydraulic flow |
|---|---|---|
| 1 | 69.7022 | 20.7477 |
| 2 | 58.1073 | 22.3945 |
| 3 | 62.8963 | 23.3003 |
| Total removal | 190.7058 | 66.4425 |

# Appendices B

This appendix provides additional information to show the setup electrokinetic bioremediation tests for phenanthrene presented in Chapter 5

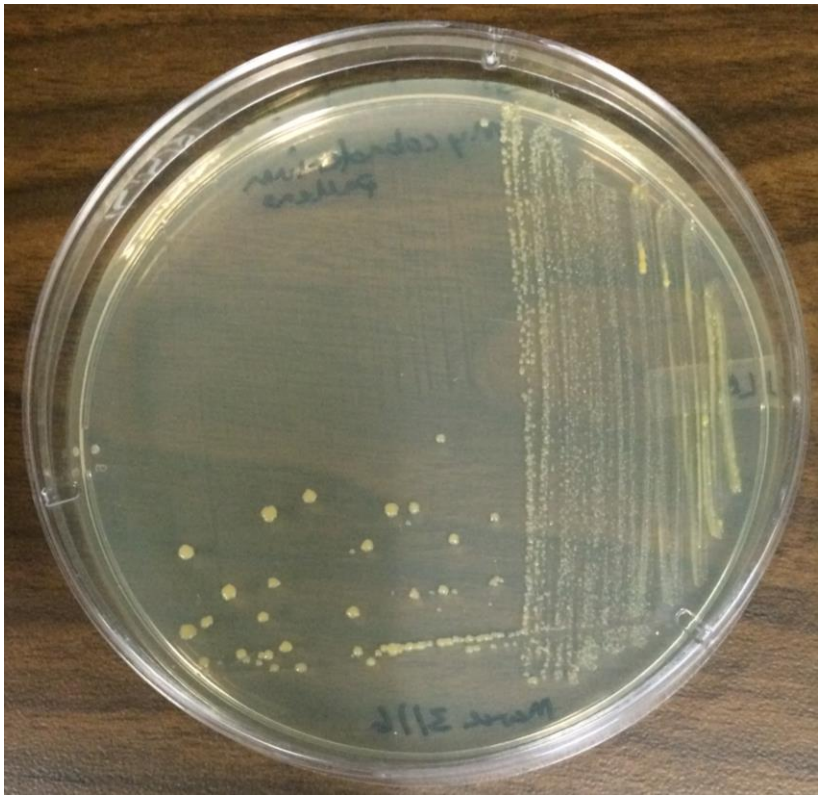

**Figure B. 1** Photo showing *Mycobacterium pallens* used in phenanthrene degradation test

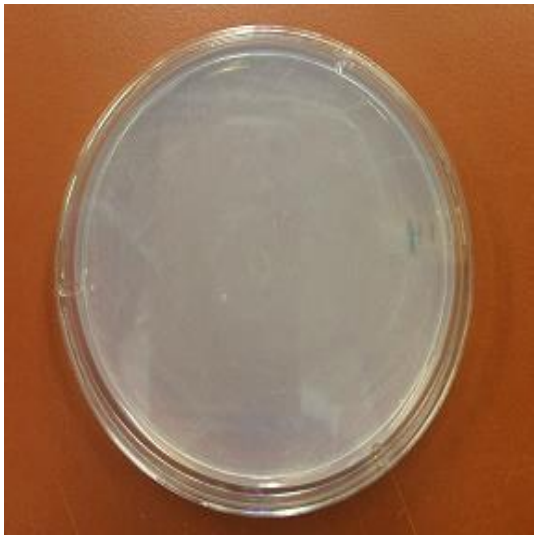

Phenanthrene layer and *Mycobacterium pallens* (20µL) in center of Petri plate at the beginning of the test

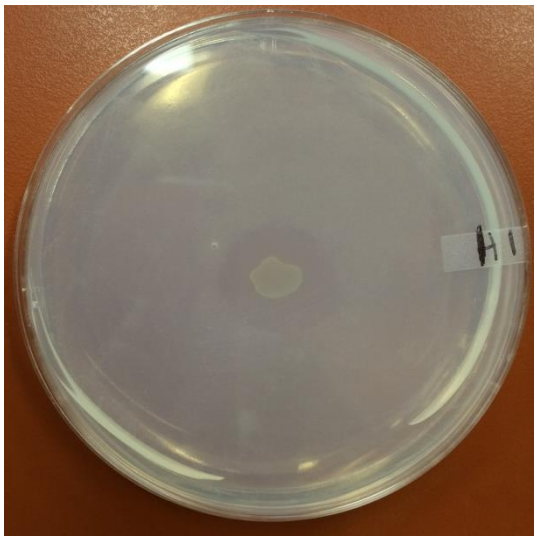

Clearing zone around *Mycobacterium pallens* after two weeks

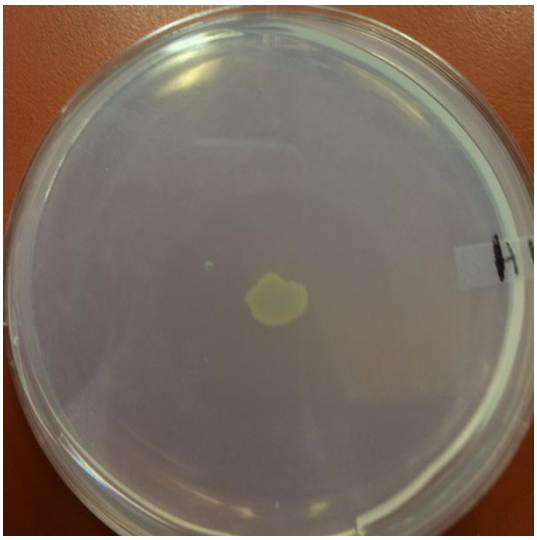

Clearing zone around *Mycobacterium pallens* after five weeks

**Figure B. 2** Photos showing Phenanthrene degradation by *Mycobacterium pallens*


**Figure B. 3** Photo showing the outdoors test setup (solar panel, two cabinets) used in phenanthrene degradation test


**Figure B. 4** Photo showing the outdoors test setup (PC, Electrokinetic cells) used in phenanthrene degradation test

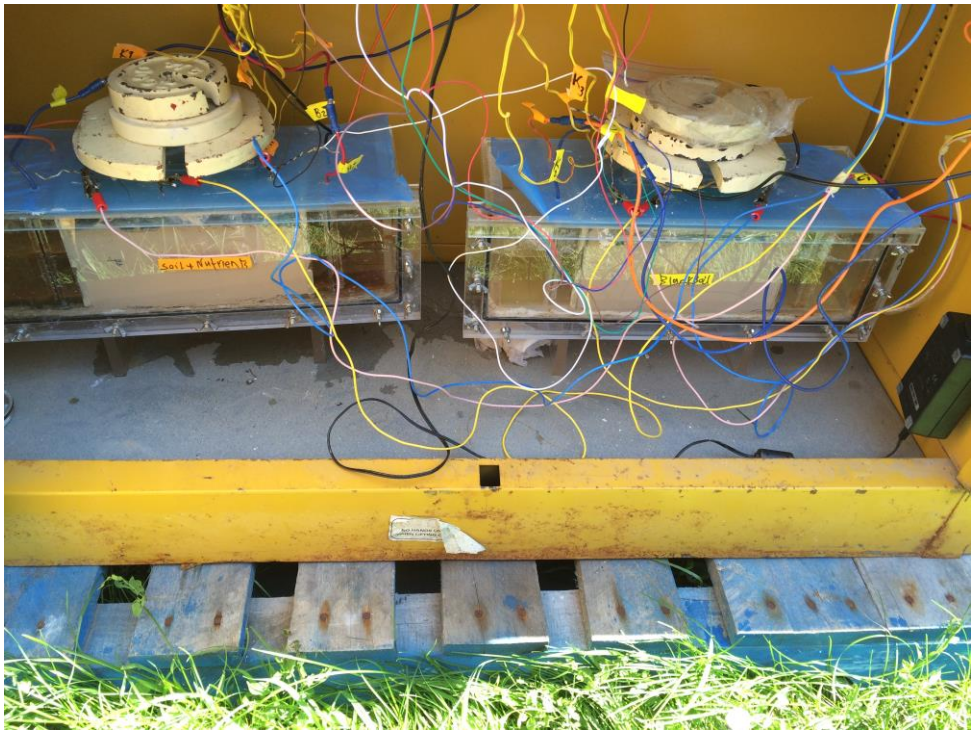


**Figure B. 5** Photo showing the outdoors test setup (Electrokinetic cells)

used in phenanthrene degradation test

# Appendices C

This appendix provides additional information to show the setup electrokinetic bioremediation tests for phenanthrene presented in Chapter 6

**Table C. 1** List of bacterial strains isolated and characterized based on their ability to degrade diesel fuel

| Isolate code | BLAST results (closest strain) | Growth in diesel fuel |
|---|---|---|
| Canola Lignin 16 | Acinetobacter calcoaceticus 100% | less than 24 h |
| Canola Ligin 2 | | less than 24 h |
| 10.7-218 | | less than 24 h |
| CO2-11 | | less than 24 h |
| Corn Lignin 9 | | less than 24 h |
| Corn Lignin 10 | | less than 24 h |
| Corn Lignin 8 | | less than 24 h |
| FF CO2 36A2 | Acinetobacter quillouiae 100% | less than 24 h |
| 1 | | less than 24 h |
| 2 | | less than 24 h |
| 911-91 | | Grow between 24-48 h |
| 911-94 | | Grow between 24-48 h |
| 911-103 | | Grow between 24-48 h |
| 911-122 | | Grow between 24-48 h |
| 911-173 | Acinetobacter quillouiae 99% | Grow between 24-48 h |
| FF1:910 | Acinetobacter quillouiae 100% | Grow between 24-48 h |
| FF CO2 36A | | Grow between 24-48 h |
| FF CO2 36A1 | Acinetobacter quillouiae 100% | Grow between 24-48 h |
| FF lig 14-2 | | Grow between 24-48 h |
| 3 | | Grow between 24-48 h |
| 911-100 | Acinetobacter quillouiae 88% | Grow around 48 h |
| 911-113 | | Grow around 48 h |

**Table C. 2** List of the bacterial strain ( Cont'd)

| | | |
|---|---|---|
| 911-119 | | Grow around 48 h |
| 911-152 | Bacterium JNMFL/Acinetobacter | Grow around 48 h |
| 911-155 | Sphingobacterium multivorum 89% | Grow around 48 h |
| 911-186 | Acinetobacter quillouiae 100% | Grow around 48 h |
| 9-3-32 | Acinetobacter | Grow around 48 h |
| FF lig 22 | Acinetobacter quillouiae 100% | Grow around 48 h |
| 911-99 | | Grow after 48 h |
| 911-154 | | Grow after 48 h |
| Corn53 | Sinorhizobium 100% | Grow after 48 h |
| 911-161 | Acinetobacter quillouiae 84% | Grow after 48 h |
| 911-174 | Acinetobacter quillouiae 100% | Grow after 48 h |
| 911-175 | Acinetobacter quillouiae 100% | Grow after 48 h |
| 911-181 | Acinetobacter quillouiae 80% | Grow after 48 h |
| 911-187 | Acinetobacter quillouiae 100% | Grow after 48 h |
| 911-195 | Acinetobacter quillouiae 100% | Grow after 48 h |
| 911-196 | Acinetobacter quillouiae 100% | Grow after 48 h |
| FF1:911 | | Grow after 48 h |
| Corn lignin 69 | | Grow after 48 h |
| p. MACTRANS Ba 141 | | Grow after 48 h |
| 10.7-207 | | Grow after 48 h |
| BS 13933 | | Grow after 48 h |
| 911-129 | | Grow after 48 h |
| 911-90 | | Grow after 48 h |

**Figure C. 1** *Sinorhizobium* SB 53

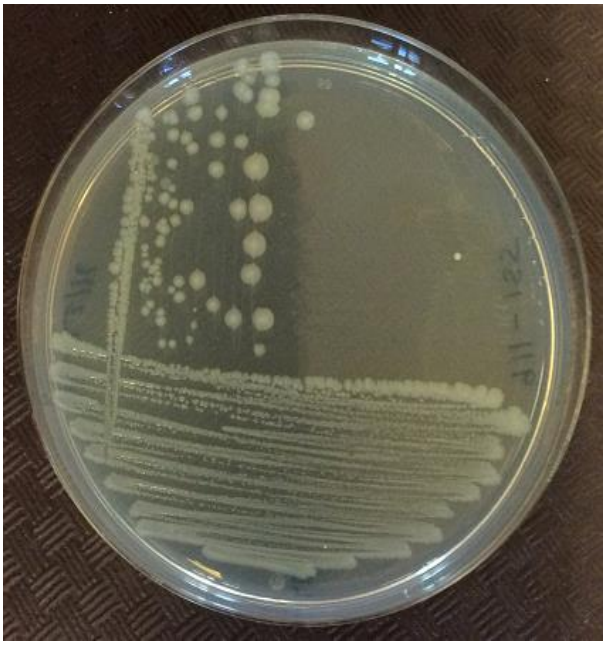

**Figure C. 2** *Sphingobacterium multivorum* SM155

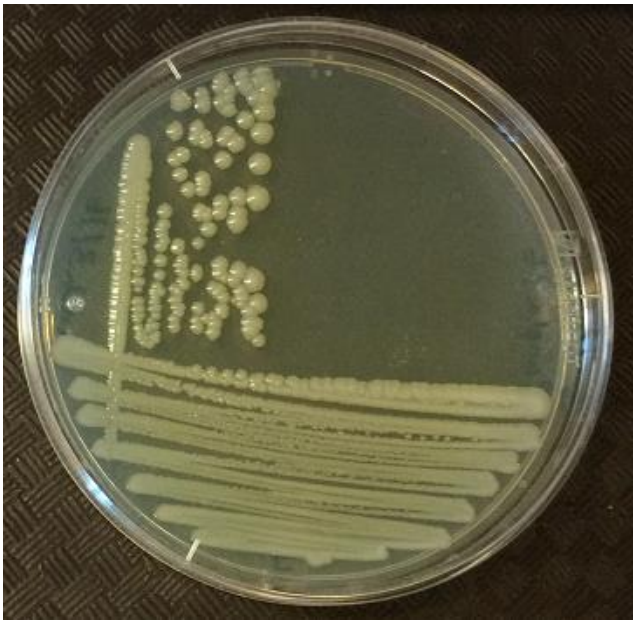

**Figure C. 3** *Acinetobacter calcoaceticus* AC16

# Appendices D

This appendix provides additional information to show the setup electrokinetic bioremediation tests for phenanthrene presented in Chapter 7

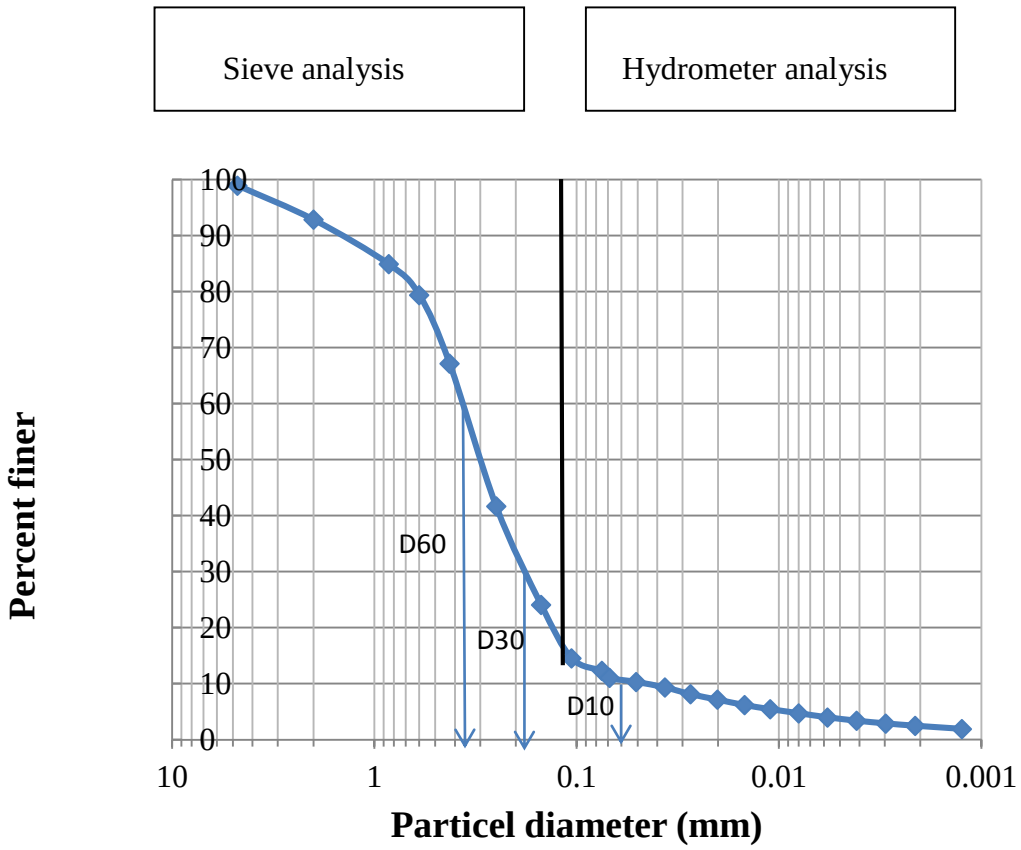


**Figure D. 1** Particle-size distribution curve (Sieve analysis and Hydrometer analysis)

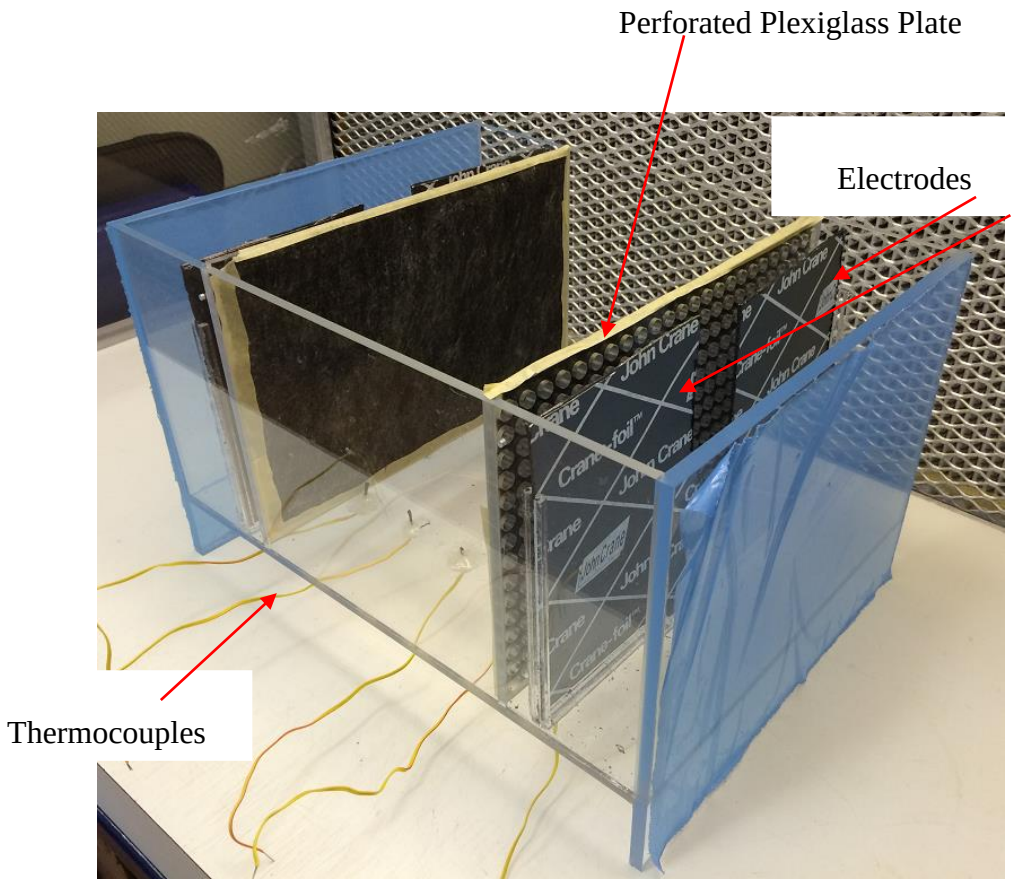


**Figure D. 2** Electrokinetic cell used in the diesel fuel degradation tests

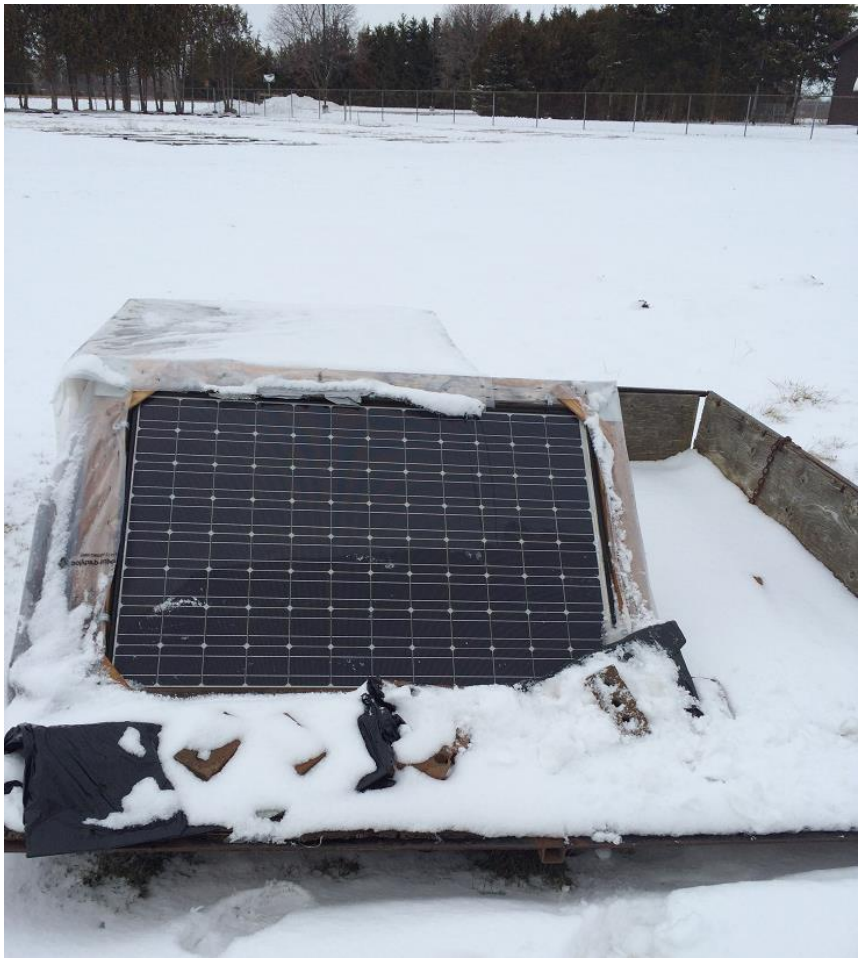

**Figure D. 3** Solar panel orientation during the winter


**Figure D. 4** Photo showing equipment used in the diesel degradation test

# Appendices E

This appendix provides additional information to show the setup electrokinetic bioremediation tests for phenanthrene presented in Chapter 8

**Figure E. 1** *Arthrobacter* LS16

# Curriculum Vitae

**Name:** Ikrema Hassan

**Post-secondary Education and Degrees:**

University of Khartoum
Khartoum, Sudan
1987-1993 B.Sc.

University of Khartoum
Khartoum, Sudan
1999-2001 MSc

Lakehead University
Thunder Bay, Ontario, Canada
2009-2011 MSc.

The University of Western Ontario
London, Ontario, Canada
2011-2016 Ph.D.

**Honours and Awards:**

L.G. Soderman Award
2014

**Related Work Experience**

Teaching Assistant
Lakehead University
2009-2011
Teaching Assistant
The University of Western Ontario
2011-2015

**Publications:**

**Hassan**, I., E. Mohamedelhasan (2014). "Sorption, Desorption, Remediation, and Fertility characteristics of clay soil." Journal of Civil Engineering and Architecture, **8**: 1274-1284.

**Hassan**, I., A. W. Eastman, B. Weselowski, E. Mohamedelhassan, E. K. Yanful and Z.-C. Yuan (2016a). "Complete Genome Sequence of Arthrobacter sp. Strain LS16,

Isolated from Agricultural Soils with Potential for Applications in Bioremediation and Bioproducts." Genome announcements **4**(1) e01586-15.

**Hassan**, I. and E. Mohamedelhassan (2012). "Electrokinetic Remediation with Solar Power for a Homogeneous Soft Clay Contaminated with Copper." International Journal of Environmental Pollution and Remediation (IJEPR) **1**(Issue 1): 67-74.

**Hassan**, I., E. Mohamedelhassan and E. K. Yanful (2015a). "Solar powered electrokinetic remediation of Cu polluted soil using a novel anode configuration." Electrochimica Acta, **181**: 58-67.

**Hassan**, I., E. Mohamedelhassan, E. K. Yanful and Z.-C. Yuan (2015b). "Sorption of phenanthrene by kaolin and efficacy of hydraulic versus electroosmotic flow to stimulate desorption." Journal of Environmental Chemical Engineering, **3**(4, Part A): 2301-2310.

**Hassan**, I., E. Mohamedelhassan, E. K. E. Yanful and Z.-C. Yuan (2016b). "A Review Article: Electrokinetic Bioremediation Current Knowledge and New Prospects." Advances in Microbiology, **6**(1): 57-75.

**Hassan**, I. and E. Mohamedelhassan (2011). "Integrated solar electrokinetics remediation of clay soil with innovative anode configurations." Proceedings of the international conference on environmental pollution and remediation: Paper 148.